

**Wettability and Oil Recovery by Imbibition and Viscous
Displacement from Fractured and Heterogeneous Carbonates**

Final Report
07/18/2002 – 01/17/2006

Norman R. Morrow, Co-Principle Investigator
Chemical & Petroleum Engineering
University of Wyoming
Jill Buckley, Co-Principle Investigator
New Mexico Petroleum Recovery Research Center
New Mexico Institute of Mining and Technology

April 2006

DE-FC26-02NT15344

Submitted by:
Chemical & Petroleum Engineering
University of Wyoming
Dept. 3295, 1000 E. University Ave
Laramie, WY 82071

Disclaimer

This report was prepared as an account of work sponsored by an agency of the United States Government. Neither the United States Government nor any agency thereof, nor any of their employees, makes any warranty, express or implied, or assumes any legal liability or responsibility for the accuracy, completeness, or usefulness of any information, apparatus, product, or process disclosed, or represents that its use would not infringe privately owned rights. Reference herein to any specific commercial product, process, or service by trade name, trademark, manufacturer, or otherwise does not necessarily constitute or imply its endorsement, recommendation, or favoring by the United States Government or any agency thereof. The views and opinions of authors expressed herein do not necessarily state or reflect those of the United States Government or any agency thereof.

ABSTRACT

About one-half of U.S. oil reserves are held in carbonate formations. The remaining oil in carbonate reservoirs is regarded as the major domestic target for improved oil recovery. Carbonate reservoirs are often fractured and have great complexity even at the core scale. Formation evaluation and prediction is often subject to great uncertainty. This study addresses quantification of crude oil/brine/rock interactions and the impact of reservoir heterogeneity on oil recovery by spontaneous imbibition and viscous displacement from pore to field scale.

Wettability-alteration characteristics of crude oils were measured at calcite and dolomite surfaces and related to the properties of the crude oils through asphaltene content, acid and base numbers, and refractive index. Oil recovery was investigated for a selection of limestones and dolomites that cover over three orders of magnitude in permeability and a factor of four variation in porosity. Wettability control was achieved by adsorption from crude oils obtained from producing carbonate reservoirs. The induced wettability states were compared with those measured for reservoir cores. The prepared cores were used to investigate oil recovery by spontaneous imbibition and viscous displacement. The results of imbibition tests were used in wettability characterization and to develop mass transfer functions for application in reservoir simulation of fractured carbonates. Studies of viscous displacement in carbonates focused on the unexpected but repeatedly observed sensitivity of oil recovery to injection rate. The main variables were pore structure, mobility ratio, and wettability. The potential for improved oil recovery from rate-sensitive carbonate reservoirs by increased injection pressure, increased injectivity, decreased well spacing or reduction of interfacial tension was evaluated.

TABLE OF CONTENTS

ABSTRACT	iii
List of Tables	vii
List of Figures	viii
Introduction	1
Executive Summary	1
Task 1	2
Introduction.....	2
Contact Angle Measurements	3
Wettability Alteration of Carbonate Rock	4
Solid Surfaces	4
Brine.....	4
Oil Components	5
Aging Temperature and Aging Time	5
AFM Observations.....	6
Experimental Materials and Methods	6
Materials and their Preparation.....	6
Experimental Methods.....	7
Results and Discussion	10
Surface Properties of Calcite	10
AFM Images	11
Contact Angles of Crude Oil/Brine/Calcite Ensembles.....	12
Task 1 Appendix	36
Task 2:	53
Part I: Rock Selection and Characterization	53
Introduction.....	53
Sample Selection and Analysis	54
Rock Sample Selection	54
Rock Characterization.....	54
Results and Discussion	56
Gambier Limestone.....	56
Edwards (Garden City) Limestone	57
Whitestone Upper Zone Limestone	57
Lueders Limestone.....	58
Whitestone Lower Zone Limestone.....	58
Fort Riley Limestone	59
BET and CEC	59
Water Adsorption/Desorption Isotherms and BJH Analysis	59
Part II: Wettability Control	72
Introduction.....	72
Experiments	73
Results and Discussion	73
Wettability Alteration	73
Stability of Induced Wetting for Limestones.....	75
Correlation of Viscosity Ratio for MXW-F Cores	75

Crude oil.....	76
Task 3:	88
Part I: Very Strongly Water-Wet (VSWW) Imbibition.....	88
Introduction.....	88
Experiments	89
Six Limestones.....	89
Scaling of VSWW Imbibition.....	89
Results and Discussion	89
Spontaneous Imbibition of Clean Mineral Oil for Six Limestone Rocks.....	89
VSWW Correlation.....	90
Part II: The Effect of Different Crude Oil/Brine/Rock (COBR)	108
Combinations on Wettability through Spontaneous Imbibition	108
Introduction.....	108
Experimental Materials and Procedures	109
Cores	109
Crude Oil.....	110
Crude Oil with Reduced Solvency (CO/Reduced Solvency)	110
Brine.....	110
Mineral Oil.....	110
Oil/Brine Interfacial Tension	110
Establishment of Initial Water Saturations Prior to Aging	110
Aging in and Replacement of the Crude Oil and CO/Reduced Solvency	111
Spontaneous Imbibition	111
Amott Indices.....	111
Results and Discussion	111
Comparison of Imbibition by Limestone and Sandstone MXW Cores	112
Comparison of Imbibition for Limestone and Sandstone MXW-F Cores.....	113
Amott Indices.....	114
Part III: Oil Recovery by Spontaneous Imbibition before and after Wettability	
Alteration of Three Carbonate Rocks by A Moderately Asphaltic Crude Oil.....	124
Introduction.....	124
Experimental	125
Rock Characterization.....	125
Cores	125
Brine.....	126
Crude Oil.....	126
Mineral Oils	127
Intermediate Solvent	127
Core Preparation	127
Spontaneous Imbibition	128
Amott Indices.....	128
Results and Discussion	128
VSWW Imbibition.....	129
Comparison of Imbibition for Different Rock Types	129
Spontaneous Imbibition of Oil by Gambier Cores – Cottonwood and Minnelusa	
Crudes	130

MXW Imbibition	130
MXW-F and MXW-DF Imbibition	130
Induction Time.....	130
Oil Recovery	131
Oil Wetness of Carbonate Rocks	131
Model Limestone	131
Task 4:	140
Introduction.....	140
Experiments	141
Rock Characterization.....	141
Rocks.....	142
Crude Oil.....	143
Brine.....	143
Mineral Oil.....	143
Oil/Brine Interfacial Tension	143
Core Preparation	143
Waterflood	144
Pore Casts.....	144
Results and Discussion	144
Oil Recovery for VSWW Cores	144
High PV Waterfloods of MXW Cores	145
2PV Waterfloods.....	146
Sensitivity of Residual Oil to Flood Rate	148
Conclusions	162
Task1.....	162
Task 3.....	163
Task 4.....	165
References	166

List of Tables

Table 1.1 Crude oil properties.....	27
Table 1.2 Brine composition and pH.....	30
Table 1.3 Thickness of organic coatings on oil-treated calcite surface.....	30
Table 1.4 Contact angles measured in adhesion tests using a captive drop of crude oil under one of three different brines. All units are degrees, \pm indicates one standard deviation for the measurements in the preceding column.....	30
Table 1.5 Correlations of water-advancing contact angles with oil properties.....	32
Table A1. Summary of adhesion data measured with brine, a captive drop of crude oil, and clean calcite (contact time 2-15 min).....	47
Table A2. Contact angles on cleaved calcite after aging in crude oil (initially dry or wet with the same aqueous phase as that used to float off bulk oil).....	53
Table 2.1 Synthetic brine composition.....	87
Table 2.2 Selected properties of crude oil samples.....	87
Table 2.3 Gambier and Edwards (GC) cores tested for the effect of initial water saturation.	
Table 2.4 Edwards (GC) cores tested for the effect of aging time for Cottonwood crude oil.....	88
Table 2.5 Gambier and Edwards (GC) MXW-F cores tested for wetting stability and the effect of oil phase viscosity	89
Table 3.1 Synthetic brine composition.....	104
Table 3.2 Edwards (GC) cores tested with different mineral oil viscosities.....	105
Table 3.3 Edwards (GC) cores tested for the effect of variation in core length ($\mu_o = 3.8\text{cP}$).	
Table 3.4 Edwards (GC) and Berea 90 sandstone cores tested for correlation of different boundary conditions.....	106
Table 3.5 Minnelusa crude oil.....	124
Table 3.6 Cottonwood crude oil.....	125
Table 3.7 Selected properties of sandstone and limestone cores.....	125
Table 3.8 Selected properties of crude oil samples.....	125
Table 3.9 Synthetic brine composition.....	126
Table 3.10 Amott Indices.....	126
Table 3.11 Selected properties of three rocks.....	143
Table 3.12 Cores.....	143
Table 3.13 Synthetic brine composition.....	144
Table 4.1 Selected properties of sandstone and limestone cores.....	160
Table 4.2 Core properties.....	161
Table 4.3 Selected properties of crude oil samples.....	162
Table 4.3 Selected properties of crude oil samples.....	162
Table 4.4 Synthetic brine composition.....	162
Table 4.5 Composition of epoxy resin and hardener for pore casts.....	163

List of Figures

Fig. 1.1 Definition of contact angle.....	33
Fig. 1.2 Scheme for separating crude oil into saturate, aromatic, resin and asphaltene (SARA) components	33
Fig. 1.3 Section view of a calcite surface aged in E-1XD-00crude oil	34
Figure 1.4 Section view of a calcite surface aged in Tensleep crude oil	34
Fig. 1.5. Contact angle measured by flooding method changes with observation time..	35
Fig. 1.6 Calcite surface with oil drops after being flooded with DDW (surface was pre-equilibrated with DDW, then aged in Uwyo-M-04 for 24 h).....	35
Fig. 1.7 Evolution of pH of unbuffered brines in contact with calcite powder (0.5g calcite in 20ml brine).....	36
Fig. 1.8 Zeta potential of calcite powder varies with pH of 0.01M brine.....	36
Fig. 1.9 3 $\mu\text{m} \times 3 \mu\text{m}$ AFM height image of clean calcite surface under air.....	37
Fig. 1.10 AFM image of calcite exposed first to (0.1M NaCl) brine then aged for 2 days and 21 days in E-1XD-00 crude oil (deflection image in water).....	37
Fig. 1.11 AFM image of calcite exposed first to (0.1M NaCl) brine then aged for 2 days and 21 days in Tensleep crude oil (deflection image in water).....	38
Fig. 1.12 AFM images of calcite exposed first to 0.1M NaCl brine then aged for 2 days and 21days in crude oil (C-F-03) (Deflection images in water).....	38
Fig. 1.13 AFM images of calcite exposed first to 0.1M NaCl brine then aged for 21days in crude oil (LB-03) (Deflection images in water).....	39
Fig. 1.14 AFM image of calcite exposed first to 0.1M NaCl brine then aged for 2 days in E-1XD-00 (deflection image).....	39
Fig. 1.15 AFM image of calcite exposed first to 0.1M NaCl brine then aged for 2 days in C-F-03 asphaltenes solution (In deflection image).....	40
Fig. 1.16 Advancing contact angles between brine and crude oil on initially clean calcite. Results are shown for five oils and three different brine compositions. Replicate experiments with oils E-1XD-00 and LB-03 and the \pm one standard deviation error bars indicate the extent of scatter in the results.....	40
Fig. 1.17 Advancing contact angle of oil drops on pre-equilibrate calcite surface in pH=8.0 buffer.....	41
Fig. 1.18 Advancing contact angle of oil drops on pre-equilibrated calcite surfaces in brines with monovalent and divalent cations.....	41
Fig. 1.19 Contact angles of oil drops on calcite surfaces pre-equilibrated in 0.1M NaCl grouped according to the amount of asphaltene in each crude oil.....	42
Fig. 1.20 Comparison of water advancing contact angles measured by the flooding method for calcite surfaces that were pre-wetted with similar surfaces that were dry when submerged in crude oil. All samples were aged for one day in crude oil at ambient conditions.	43
Fig. 1.21 Contact angles by the flooding method on polished marble and freshly cleaved Iceland spar surfaces pre-wetted with DDW and aged for one day in crude oil.....	43
Fig. 1.22 Contact angles by the flooding method for selected oils.....	44
Fig. 1.23 Contact angles on selected oil-treated calcite samples after removal of oil by rinsing with toluene. All samples were pre-wetted with 0.1M NaCl.....	44

Fig. 1.24 Comparison of contact angles between decane and DDW on surfaces aged for 12 days in crude oil. Contact angles were measured after removal of crude oil by rinsing with toluene.....	45
Fig. 1.25 Comparison of contact angles between decane and DDW on surfaces aged for 12 days in crude oil at either 25 or 60°C. Contact angles were measured after removal of crude oil by rinsing with toluene.....	45
Fig. 1.26 Comparison of contact angles between decane and DDW on surfaces aged for 12 days in crude oil or in their maltenes. Contact angles were measured after removal of crude oil by rinsing with toluene.....	46
Fig. 2.1 Thin section of Canadian #2 limestone rock sample.....	71
Fig. 2.2 Thin sections of Gambier limestone.....	72
Fig. 2.3 SEM micrographs of Gambier limestone.....	72
Fig. 2.4 Thin sections of Edwards (GC) limestone.....	73
Fig. 2.5 SEM micrographs of Edwards (GC) limestone.....	73
Fig. 2.6 Pore size distribution of Edwards (GC) limestone.....	74
Fig. 2.7 Thin sections of Whitestone UZ limestone.....	75
Fig. 2.8 SEM micrographs of Whitestone UZ limestone.....	75
Fig. 2.9 Mercury injection for Whitestone UZ and Edwards (GC) limestones.....	76
Fig. 2.10 Pore size distribution of Whitestone UZ limestones.....	76
Fig. 2.11 Thin sections of Lueders limestone.....	77
Fig. 2.12 SEM Micrographs of Lueders limestone.....	77
Fig. 2.13 Thin sections of Whitestone LZ limestone.....	78
Fig. 2.14 SEM micrographs of Whitestone LZ limestone.....	78
Fig. 2.15 Thin sections of Fort Riley limestone.....	79
Fig. 2.16 SEM micrographs of Fort Riley limestone.....	80
Fig. 2.17 BET surface area and CEC comparison of selected limestones and a Berea sandstone.....	81
Fig. 2.18 Percentage of micro- and meso-porosity for all tested limestone rocks from water adsorption/desorption isotherms (Fischer <i>et al.</i> , 2005).....	82
Fig. 2.19 Adsorbed volume versus relative pressure for five selected limestones from BJH analysis.....	82
Fig. 2.20 Example of reproducibility of imbibition behavior for wettability alteration of duplicate core plugs.....	90
Fig. 2.21 The effect of crude oil composition on wettability alteration.....	91
Fig. 2.22 The effect of initial water saturation on wettability alteration.....	92
Fig. 2.23 The effect of aging time and initial water saturation on wettability alteration.....	93
Fig. 2.24 Tests of stability of the induced wettability state for MXW-F wetting for five values of mineral oil viscosity.....	95
Fig. 2.25 Oil recovery vs. imbibition time for MXW-F Gambier and Edwards (GC) cores with different mineral oil viscosities.....	97
Fig. 2.26 Oil recovery versus dimensionless time for MXW-F Gambier and Edwards (C) cores with variation in viscosity of the probe mineral oil.....	98
Fig. 3.1 Spontaneous imbibition behavior of six selected limestones.....	108
Fig. 3.2 Vugs in Whitestone LZ Cores (1.5" diameter core).....	108
Fig. 3.3 Spontaneous imbibition behavior of VSWW Edwards (GC) AFO cores with different probe oil viscosities.....	110

Fig. 3.4 Spontaneous imbibition behavior of VSWW Edwards (GC) cores of different lengths.....	112
Fig. 3.4 Spontaneous imbibition behavior of VSWW Edwards (GC) cores of different lengths.....	113
Fig. 3.5 Correlated VSWW Edwards (GC) spontaneous imbibition for different core lengths and probe oil viscosities and fit to Aronofsky <i>et al.</i> (1958) equation.....	113
Fig. 3.6 Different boundary conditions, flow regimes, and characteristic length.....	114
Fig. 3.7 Spontaneous imbibition behavior of VSWW Edwards (GC) cores with different boundary conditions.....	116
Fig. 3.8 Spontaneous imbibition behavior of VSWW Berea 90 cores with different boundary conditions.....	118
Fig. 3.9 Thin section and SEM photos and recovery of crude oil from MXW limestone and sandstone by spontaneous imbibition.....	129
Fig. 3.10 Recovery of crude oil from MXW (CO/reduced solvency) limestone and sandstone by spontaneous imbibition.....	131
Fig. 3.11 Recovery of mineral oil from MXW-F, MXW-F (CO/reduced solvency), and MXW-DF limestone and sandstone by spontaneous imbibition.	134
Fig. 3.12 Thin section and SEM photos.....	145
Fig. 3.13 (a) Scaled VSWW imbibition results for the three limestones and Berea sandstone, and (b) comparison with range of normalized results for a variety of rock types.....	146
Fig. 3.14 Comparison of spontaneous imbibition for two grainstones with MXW, MXW-F, and MXW-DF wetting states induced by Cottonwood crude oil.....	147
Fig. 3.15 Comparisons of (a) spontaneous imbibition of brine for Gambier cores with MXW, MXW-F, and MXW-DF wetting states induced by Cottonwood crude oil (Tie <i>et al.</i> , 2003) and (b) spontaneous imbibition of oil after forced displacement (MXW-DF for Gambier and Minnelusa crude oil is included).....	148
Fig. 3.16 Comparison of recovery of oil with VSWW for (a) MXW, (b) MXW-F, (c) MXW-DF by spontaneous imbibition for three carbonate rocks, and (d) total oil recovery (spontaneous imbibition plus forced displacement) versus Amott-Harvey wettability index. (WW – water-wet, WWW – weakly water-wet, NW – neutral wet, WOW – weakly oil-wet, IW – intermediate wetting, OW – oil-wet (Cueic, 1991)) (* Tie <i>et al.</i> , 2003).....	150
Fig. 4.1 Thin section and SEM.....	163
Fig. 4.2 Mercury injection and pore structure.....	164
Fig. 4.3 Waterflood residual saturation for VSWW Edwards (GC) and Whitestone UZ rocks (BT: Breakthrough, R: oil recovery, R* : oil recovery at lowest flooding rate)...	165
Fig. 4.4 Waterflood residual saturation for MXW Edwards (GC) and Whitestone UZ rocks.....	165
Fig. 4.5 Waterflood residual saturation for Edwards (GC) and Whitestone UZ rocks with VSWW and MXW wetting states.....	166
Fig. 4.6 Waterflood residual saturation for Edwards (GC), Whitestone UZ, and Gambier limestone for various rates (2PV at each rate): (a) MXW, (b) MXW-F, and (c) MXW-DF wetting states.....	168

Fig. 4.7 Waterflood residual saturation vs capillary number (2PV injected at each rate) for MXW, MXW-F, and MXW-DF wetting states: (a) Edwards (GC), (b) Whitestone UZ, and (c) Gambier limestones.....169

Fig. 4.8 Comparison of total oil recovery (spontaneous imbibition plus forced displacement) versus Amott-Harvey wettability index (Tie and Morrow, 2005). (WW – water-wet, WWW – weakly water-wet, NW – neutral wet, WOW – weakly oil-wet, IW – intermediate wetting, OW – oil-wet (Cuiec, 1991)).....170

Fig. 4.9 Relative reduction in residual oil saturation with increase in capillary number for all tested samples at all the tested wetting states. (R_{os}^* - residual oil at lowest flood rate).....171

Fig. 4.10 Pore casts for the three tested limestones.....172

Introduction

About one-half of U.S. oil reserves are held in carbonate rocks. Formation evaluation and prediction of oil recovery from carbonate reservoirs are recognized areas of need for research. The oil left in heterogeneous carbonate reservoirs is regarded as the major target for additional oil recovery from domestic reservoirs. Carbonate reservoirs are often fractured and have great complexity even at the core scale. Several examples of unexpected sensitivity to rate of oil production have been reported for heterogeneous carbonates. This study was focused on quantification of crude oil/brine/rock interactions and the impact of reservoir heterogeneity on oil recovery by spontaneous imbibition and viscous displacement from pore to field scale.

The objectives of this project were:

1. To relate wettability alteration on carbonate surfaces by adsorption from crude oil to the chemical properties of the oil.
2. To develop methods of wettability control for a selection of carbonate rocks by adsorption from crude oil and to test the stability of adsorbed states.
3. To measure oil recovery and characterize wettability by spontaneous imbibition measurements for strongly water-wet carbonate rocks and for the same rocks after systematic changes in wettability induced by adsorption from crude oil. Variables include sample size, shape, boundary conditions, initial saturations and oil/brine viscosity ratios. Results were correlated to provide a means of measurement of wettability from imbibition rate and to provide mass transfer functions for reservoir simulation of recovery from fractured reservoirs.
4. To investigate the sensitivity of oil recovery to rate of viscous displacement from heterogeneous carbonate rocks for both very strongly water-wet and a range of mixed wet conditions with emphasis on differentiating between mobility ratio, end effects, and the influence of pore structure and wettability.

Executive Summary

This report presents the first comprehensive study of the effect of pore structure and wettability on recovery of oil from carbonate rocks by waterflooding and spontaneous imbibition. Reservoir carbonate rocks are notoriously difficult to clean to a very strongly water-wet condition that is needed as a reference state and a starting point for preparation of restored state cores. This problem has been overcome by identification of suitable outcrop carbonates which are initially very strongly water wet and can be obtained in the large enough quantity for parametric studies of the factors which determine oil recovery from carbonate reservoirs.

The first part of the report presents basic studies of the alteration of carbonate surfaces by adsorption from crude oil using three approaches of surface preparation. Atomic force microscopy is used to determine the thickness and character of the adsorbed organic layers. Wetting changes are assessed from contact angle measurements. Clear differences were obtained for different types of crude oil as characterized by asphaltene content, acid

and base numbers and other properties. Differences with variation in brine composition were less consistent.

The second task concerned selection and characterization of limestone rocks. Five grainstones and one boundstone were studied in detail. Despite wide variations in pore structure, scanning electron micrographs indicated that all of the pore walls were covered by calcite crystals. Thus compared to clastic rocks, the complications arising from complex pore geometry are somewhat compensated by relative simplification of the surface mineralogy. The rocks can be obtained at low cost and three in particular may become industry standards for carbonate studies comparable to the way Berea sandstone has served as a widely used model for sandstone.

Under the third task, extensive results are presented on the spontaneous imbibition behavior of the outcrop core samples and how it is altered by changing the carbonate rock to a mixed-wet state by adsorption from crude oil in the presence of connate water. Distinct patterns of wettability alteration were observed for a particular crude oil/brine combination. As reported previously for sandstones, oil recovery tended to pass through a maximum, when the core was slightly on the water-wet side, of neutral wettability. Commonly used methods of core preparation after adsorption are shown to have drastic effect on recovery behavior by both spontaneous imbibition and waterflooding. These results had immediate impact on industry core analysis protocol.

The final task concerns rate sensitivity of waterflood recoveries at capillary numbers much lower than observed for sandstones. For all three of the limestones selected for this study, some degree of rate sensitivity was observed for both strongly water-wet and mixed-wet conditions. For the two grainstones, the rock that had been identified as heterogeneous from petrophysical measurements exhibited the greater rate sensitivity. The greatest rate sensitivity was obtained for the boundstone. Inspection of pore casts indicated that differences in rate sensitivity could be attributed to distinct differences in pore structure. The grainstone that exhibited the least sensitivity to rate showed the largest sensitivity of waterflood residual oil to wettability. For this rock, change from water wet to mixed wet almost doubled the waterflood recovery. The difference is ascribed to recovery of oil from moldic pores that remain filled with oil under strongly water-wet conditions.

Task 1: *Wettability alteration at carbonate surfaces*

Jill Buckley and Xiaotao Sun, PRRC, New Mexico Tech

Introduction

In this study we investigated wetting behavior of carbonate minerals. The goal of the study was to gain a better understanding of the chemical mechanism of the wettability alteration process in a crude oil/brine/rock (COBR) system. The wetting condition was determined by measuring the contact angles of crude oil on a clean mineral surface in aqueous phase or of aqueous phase on an oil-aged rock surface. Numerous crude oil samples with different chemical properties were studied using different methods of

exposure, brine compositions, aging times, and other relevant variables. Oil-treated calcite surfaces were also investigated using atomic force microscopy.

Contact Angle Measurements

Wettability is the ability of a fluid to wet a solid surface in the presence of a second fluid. For pure compounds, the definition of contact angle in terms of the interfacial tensions of the three phases is given by Young's equation:

$$\sigma_{os} = \sigma_{ws} + \sigma_{ow} \cos \theta_{ow} \quad (1.1)$$

where σ (dyne/cm) is the surface or interfacial energy between oil and solid (os), water and solid (ws), and oil and water (ow) interfaces, and θ (degrees) represents the contact angle at the oil-water-solid interface measured through the water phase as shown in Fig. 1.1.

Contact angle is a thermodynamic property and is essentially single-valued for a specific combination of solid and two pure fluids. In a crude oil, brine, and rock system, each phase is a complex mixture; the contact angle is usually not single-valued. The water-advancing angle is normally different from the water-receding angle. Hysteresis is very common due to surface contamination, heterogeneity in chemical composition, surface roughness, and static and dynamic interface properties. Nevertheless, history-dependent contact angle measurements provide a convenient method to quantify the wettability of smooth mineral surfaces that have been in contact with immiscible oleic and aqueous liquids.

In this work, three different approaches to characterization of carbonate surface wetting in the presence of crude oil and brine have been extensively tested and compared. In the first test we use a clean surface, submerged in brine. A drop of crude oil is formed and pressed against the surface for a short period of time, then withdrawn. In previous work on silicate surfaces (e.g., Buckley *et al.*, 1998; Liu and Buckley, 1999) this procedure has been referred to as an adhesion test, but receding and advancing contact angles can be measured in cases where the contact line is not pinned.

A second method was developed to avoid the problem of contact line pinning. Clean surfaces are pre-wetted with selected brines, then aged for longer periods of time in crude oil. Changes in surface properties can be assessed after the sample has been removed from crude oil and rinsed with a solvent such as toluene, which does not precipitate asphaltenes. After rinsing, the surface can be examined by contact angle measurements, both advancing and receding, with probe fluids (usually decane and distilled water) and by atomic force microscopy (AFM) imaging (Lord and Buckley, 2002).

Hirasaki and Zhang (2004) suggested a third approach in which the clean, pre-wetted surface is submerged in oil. After some aging period, the oil is floated off the surface by addition of brine, leaving drops of oil on the surface. Water advancing contact angles can be measured for the remaining drops of oil.

It is not expected that these three different methods will give the same results. Rather they are intended to complement one another and to fill in different pieces of the wettability puzzle. All three methods require extremely smooth surfaces in order to give reproducible results, a condition that can be very difficult to fulfill with natural materials.

Wettability Alteration of Carbonate Rock

Many factors can affect reservoir wetting, including the components of crude oil, brine composition, rock, aging time, and temperature. The effects of these variables, either individually or in combination, can be very difficult to predict for complex crude oil, brine, and rock systems.

Solid Surfaces

Calcite, marble, lithographic limestone, and chalk have been used in previous studies as representatives of carbonate rock to study wettability alteration (a few examples include Standnes and Austad, 2000a; Hirasaki and Zhang, 2004; Seethepalli *et al.*, 2004; Goddard *et al.*, 2005; Gomari *et al.*, 2006).

Carbonates are quite reactive; metal ions in brine can affect dissolution rate and organic compounds are readily adsorbed (e.g., Morse, 1986). Surface electrical properties of calcite dispersed in an aqueous solution have been studied using a number of different electrokinetic methods (Somasundaran and Agar, 1967; Thompson and Pownall, 1989; Pierre *et al.*, 1990; Moulin and Roques, 2003) and flotation techniques (Somasundaran and Agar, 1967). Results are not entirely consistent; zeta potential varies in absolute values and sign. Strand *et al.* (2006) found that relative concentration of Ca^{2+} and SO_4^{2-} appeared to have a significant effect on the surface charge of chalk, and therefore suggested that both are potential determining ions. Hirasaki and Zhang (2003) reported that the surface charge of the calcite becomes more negative with the presence of NaCO_3 and NaHCO_3 in the brine. Moulin and Roques (2003) reviewed work on zeta potential of calcite and concluded that disparate results are due to differences in the measurement conditions and the nature of the potential determining ions. It is generally accepted that ions such as Ca^{2+} and CO_3^{2-} are the potential determining ions and that the isoelectric point of calcite is around pH 8 to 10. In a carbonate reservoir where the pH of the brine is near neutral, the carbonate reservoir normally would be positively charged.

Brine

Stability of water films of nanometer thickness on the rock surface, which are controlled by surface charge on the water/solid and water/oil interfaces, affects wetting alteration of the minerals in COBR systems (Hirasaki, 1990). Buckley *et al.* (1998) observed that the presence of water promoted wetting alteration of silicate surfaces that were pre-equilibrated in NaCl solutions with low pH and low ionic strength before aging in an asphaltic crude oil. Conversely, pre-equilibration in an NaCl brine with high pH and high ionic strength established a stable water film that inhibited wetting alteration by the same crude oil. The presence of an aqueous phase on calcite significantly affects the adsorption of organic acids (Madsen and Lind, 1997; Legens *et al.*, 1998).

Oil Components

SARA Fractions. Crude oils differ markedly in their chemical composition. Most of the components in crude oils are hydrocarbons; only a small fraction consists of polar constituents. Some polar components can adsorb on mineral surfaces and alter their wetting properties. The extent to which specific components partition to the oil/water and oil/rock interfaces can vary with oil composition. With respect to understanding wettability alteration, it is useful to separate crude oil into four fractions: saturates, aromatics, resins, and asphaltenes (SARA), as shown in Fig. 1.2.

Resins and asphaltenes are the most polar oil fractions, containing the material that most directly affect reservoir wetting. The effects of asphaltenes on wetting can differ depending on the composition of the rest of the oil (Al-Maamari and Buckley, 2003). Aromatics and resins are good asphaltene solvents, whereas saturates are non-solvents for asphaltenes.

Acidic and Basic Oil Components. Polar functional groups concentrated in the asphaltenes and resins exhibit both acidic and basic characteristics. The interfacial tension (IFT) between an oil and an aqueous phase correlates with asphaltene content of the oil and with measures of acidic and basic properties (Fan and Buckley, 2005). Acid and base numbers, measured by nonaqueous potentiometric titration (ASTM-D664-89 and ASTM-D2896-88), reported in units of mg KOH/g of oil, are used to quantify the amounts of the soluble acids and bases in a crude oil.

According to Thomas *et al.* (1993a and b), carboxylic acids adsorb almost irreversibly onto carbonate minerals, making the carbonate surface oil-wet. However, the literature regarding correlations between the wetting condition and the acid content of crude oils is not all in agreement. Shedid and Ghannom (2004) reported a decrease in contact angle with an increase in acid number based on data for three crude oils. Goddard and Tang (2005) found that among four types of acids, naphthenic acids with greater hydrophobic character produced the highest percentage of oil-wet calcite powder.

Compared with acids, basic components in crude oils have received much less attention. Dubey and Doe (1993) showed a high degree of non-water-wetness of silicates could be attributed to a high base number, assuming the base number was measured accurately. Although acids are more likely to interact with carbonate surfaces, neglecting the presence of basic components that may compete for interactions with crude oil acids may help to account for some of the discrepancies in the literature.

Aging Temperature and Aging Time

Reports of the effect of aging temperature on wettability alteration by exposure of crude oil to smooth mineral surfaces do not agree. Higher advancing angles on glass surface were obtained at higher temperature (Liu and Buckley, 1997). Xie *et al.* (1997) reported that wax may deposit when the temperature drops below the wax appearance temperature. The receding contact angles measured by Lichaa *et al.* (1993) on smooth calcite surfaces displayed a steady decline with increasing temperature for three different rock-fluid systems. In a study of the effect of acids on wetting condition of chalk cores,

Zhang and Austad (2005) reported that the temperature was not a very important parameter over the 40 to 120°C range.

Increase in aging time may result in decrease in water-wetness on smooth mineral surfaces, depending on the preparation of the sample. Liu and Buckley (1997) found that more oil-wet conditions were obtained as the aging time increased and that adsorption of crude oil components on pre-wetted glass surfaces is strongly time-dependent. The wetting alteration of a dry surface was insensitive to the aging time and temperature.

AFM Observations

The AFM technique—optimized for the study of soft material in a variety of fluid environments—can be used to observe micron- and nanometer-scale changes in the topography of mineral surfaces after exposure to crude oil. Images can be produced in air or in a fluid such as decane or water. Lord and Buckley (2002) used AFM to describe film and aggregate morphology on crude oil-treated mica surfaces in an aqueous or oleic media. The films displayed different characteristics for asphaltene solutions than for the parent crudes. Force measurements between a crude oil drop and mica surface have also been reported (Basu and Sharma, 1996). Mica surfaces that are molecularly smooth have been widely used as a substrate for AFM imaging. In this study AFM will be used to investigate the suitability of calcite for use in similar experiments.

Experimental Materials and Methods

Materials and their Preparation

Calcite Samples

Iceland spar (CaCO_3 , Ward's Natural Science) was used as a model surface in this study. Prior to treatment, calcite crystals were cleaved carefully into approximately 1x2 cm pieces with smooth surfaces. Care was taken at all times to handle calcite samples only by their edges so that the freshly cleaved surfaces were not contaminated. All the samples were soaked in de-ionized distilled water in a container that was shaken in an ultrasonic bath for a few minutes to remove debris from the surfaces. Each sample then was removed from the container, rinsed with distilled water, put into a new container, and aged in de-ionized water again. This procedure was repeated several times until the water remained clear.

Before being used in contact angle measurement, the samples were rinsed with distilled water, dried in air, and then equilibrated with the appropriate aqueous solutions.

Powdered samples of the same material were used to measure zeta potential. A piece of calcite was ground with a mortar and pestle, soaked in the selected brine, shaken, then allowed to settle for at least 4 hours before being used in the zeta potential measurements. Only the upper layer of clear liquid was taken for tests.

Samples used for AFM imaging were examined microscopically to ensure that they were free of large dents or steps. Very stringent sample selection is needed since the AFM has a working distance that is limited to about 1 μ .

Crude Oils

Seventy-one crude oil samples were chosen from the population of the CO-Wet database for this study. The choice of oils was mainly based on chemical properties including asphaltene content, acid number, and base number, as well as physical properties including viscosity and API gravity. All oil samples were used as received without further treatment. Properties of the crude oils are listed in Table 1.1.

Hydrocarbon and Solvents

Toluene used to rinse surfaces without precipitating asphaltenes was HPLC grade and was used as received.

The purity of decane used as probe fluid in contact angle measurements is A.R grade and was further purified by passing it through a column containing silica gel (grade 62, 60 – 200 mesh, Aldrich, Milwaukee, WI) and alumina (80 – 200 mesh, Fisher Scientific). The silica gel and alumina were dried at 200°C in an oven for 8 hours before use to remove any sorbed water.

All solvents used for cleaning the quartz cell and glassware cleaning, including isopropyl alcohol, acetone, toluene, hydrochloric acid, and ammonium hydroxide, were 99%+ grade (Fisher Scientific) and were used as received.

Aqueous Solutions

Ultrapure water was used to prepare all aqueous solutions. Distilled water was deionized by passing through Milli-Q cartridge filters (Millipore, Bedford, MA) and then redistilled in an all-glass system prior to use. Water so treated is referred to either as double-distilled water or DDW. The pH of the DDW was 6.5 – 6.8.

Brines were prepared from DDW and A.R. grade chemicals to obtain the desired pH and ion concentrations. The pH values of brines were measured with a Corning model 240 pH Meter with a Corning combination electrode.

Brine compositions and pH values are listed in Table 1.2

Experimental Methods

Atomic Force Microscopy

Pieces of calcite were soaked in brine overnight then aged in crude oil for either two or 21 days. The samples were removed from the crude oil and rinsed with toluene to remove surplus oil until there was no visible oil adhering on the surface. The samples were then thoroughly air dried and mounted onto an AFM magnetic puck using a small amount of Super Glue Gel.

The AFM samples were imaged at ambient temperature in contact mode in air or under a fluid (decane or water) using methods described by Lord and Buckley (2002). The AFM used was a NanoScope IIIA (Veeco Instruments, Santa Barbara, CA), and the probes used were Olympus Oxide-Sharpended Silicon Nitride (Model OTR4-35, 100- μm cantilever, Veeco Instruments, Santa Barbara, CA).

Both height and deflection signal images were captured during the contact mode scanning. As Lord and Buckley (2002) point out “On soft surfaces, however, the deflection signal produced by reducing the sensitivity of the feedback control system while monitoring the position of the cantilever can produce much more detailed images.” It is also important to minimize the imaging force during scanning, especially imaging in air. Images on the clean calcite show that the calcite is easily scraped even when using a very pliable cantilever (Si_3N_4). The force is greatly damped in fluid.

At least two different regions were imaged on each sample to ensure that those selected for analysis were representative. Regions imaged for each sample also need to be selected carefully to avoid extremely rough areas.

Section analysis, an offline function that plots the height or deflection signal from an AFM scan along an arbitrary line chosen by the user, was used to evaluate coating thickness from images in which a hole was visible, exposing the substrate. Both section analyses shown here (Figs. 1.3 and 1.4) are height signals. The triangular cursors can be moved along the section to mark average film height and the height of the substrate in the hole. Vertical distance between the cursors is calculated automatically. Note the smoother substrate surface in the hole.

In some cases it was necessary to add some toluene to the decane used for imaging to soften the surface so that a hole could be made. The addition of toluene causes swelling that increases the measured thickness a few percent.

Amount of Asphaltene in Oil

The asphaltene content in a crude oil was determined by mixing one part of crude oil with 40 parts of n-heptane. The oil and precipitant were mixed thoroughly and allowed to equilibrate for 2 days. The mixture was then filtered through 0.22 μm filters (cellulose acetate, Corning Separation Division) according to a standard procedure described in detail by Wang (2000).

Interfacial Tension Measurement

The pendant drop method was used to measure the interfacial tension between varying concentrations of brine and an oil drop using an OCA20 pendant drop apparatus with SCA20 software (DataPhysics Instruments GmbH, Germany). With this apparatus, a pendant drop of oil was formed with a microsyringe suspended in a bath of the brine. The shape of the drop was fitted to the Young-Laplace equation to calculate the interfacial tension. The microsyringe was bent into the shape of a J so the drop could “hang” upward.

The protocol of interfacial tension measurement was as described by Buckley and Fan (2005). A steel needle with an outer diameter of 0.91 mm was used and the oil drop volumes were around 8 μ L. Drops were aged in the surrounding solution for up to 2000s, the final IFTs were recorded as an average after the values were nearly constant.

Maltene Preparation

After removal by filtration of the n-C₇ asphaltenes from a mixture of crude oil and n-heptane, maltenes were recovered by evaporation of n-heptane from the filtered solution using a BUCHI – RE 111 rotavapor. The mixture was placed in a flask in a water bath at a temperature of from 30°C to 50°C and evacuated with a vacuum pump. The evaporated heptane was collected in a cold trap. Evaporation continued until visible heptane production ceased and weight loss was less than 0.5 g between repeated weighings.

Asphaltene Solutions

The recovered asphaltenes were used to prepare asphaltene solutions for calcite treatment in AFM experiments. Toluene was added to the asphaltenes to produce 2.5% solutions and the mixtures were shaken in an ultrasonic bath for at least 10 min.

Captive Drop Method for Contact Angle Measurements

Contact angles on clean calcite surfaces were measured using the captive drop method (Gaudin *et al.*, 1963) with a drop of crude oil under brine. The captive drop method was also used for oil-treated surfaces after rinsing with toluene, with decane and DDW serving as probe fluids. All measurements were carried out at room temperature.

For experiments on a clean calcite surface, a crude oil drop was produced by a Gilmont pipette. The drop was allowed to remain motionless on the surface for 2 to 15 minutes before the receding angle measurement was taken. Then the oil was drawn back into the pipette slowly until the contact line moved. After another 2 to 15 minutes, the advancing angle was recorded. All contact angles reported are based on an average of four to six measurements on a single piece of calcite.

For oil-treated calcite surfaces, contact angles (water-advancing and water-receding angles) between water and decane were measured by using the same procedure. The contact angles were measured using a Data Physics OCA20 pendant drop apparatus with SCA20 software. The reported data are an average of at least four measurements on a single piece of calcite, with two samples for each aging condition.

Contact Angle Measurements by the “Flooding” Method

In this study, “flooding” describes the injection of brine to remove oil by buoyancy from a smooth calcite surface, as described by Hirasaki and Zhang (2003).

The procedure used to produce oil-treated surfaces and to measure contact angles by flooding is the following:

- 1) Cleave and clean the samples as described above.
- 2) Age in selected brine for one day (or air dry if sample is to be used dry).

- 3) Remove the sample from the brine, drain excess brine by touching an edge against a Kimwipe.
- 4) Age in crude oil for desired period in a quartz glass cell.
- 5) Inject about 20 ml of brine at a rate of about 1 ml/min.
- 6) Seal the cell with cling film; avoid vibration.
- 7) Record the contact angles of oil drops on the top surface of the calcite until the contact angle values are constant.

A small amount of the flooding medium was injected before the sample was aged in crude oil in order to prevent oil from attaching to the cell bottom during the flooding with brine.

Fig. 1.5 shows a typical contact angle result. The angle initially decreases then approaches a constant value.

There are advantages to this method compared to the captive drop method. The sequence of fluid exposures is analogous to the actual experience of reservoir rock in waterflooding. It overcomes the problems of short-term contact between the oil and the surface of rocks in an adhesion test and the possibility of over washing by the toluene in an adsorption test.

A problem with this method of measurement is that the surface of the calcite has rough areas and steps that may dominate the contact angle observations. The oil drops that form after waterflooding vary widely in size and contact angles. Figure 1.6 shows a calcite surface with oil drops of different size (not all of which are in focus in this picture) after the sample was aged in Uwyo-M-04 crude oil for one day then flooded with distilled water. The sizes of oil drops varied from 0.01 to 0.1 mm, and the range of contact angles was 78 to 108°.

For captive drop measurements, it is relatively easy to select smooth areas on the substrate for contact angle measurements. To reduce uncertainty of the results, each flooding contact angle was measured from both front and side views for all the oil drops and recorded as an average plus standard deviation. The reproducibility of the flooding method is usually poorer than that of the captive drop method.

Results and Discussion

Surface Properties of Calcite

A series of brines was employed to study the effect of composition as well as pH of the brines on the surface charge of calcite. Since the calcite acts as a buffer, almost all the brines tested without buffering changed within a few days to a pH of 8 to 9, regardless of the initial pH, as shown in Fig. 1.7.

Zeta potential measurements were performed on ground calcite powder suspended in brine solutions, by using a Delsa 440SX zeta potential analyzer (Beckman Coulter

Corporation, Germany). The zeta potential of the calcite powder changes with pH of brine for $[\text{Na}^+] = 0.01\text{M}$ (Fig. 1.8). Zeta potential was near zero when the pH of the brine was around 8 to 10.

AFM Images

Clean Calcite

The image of clean calcite provides a basis for comparison with oil-treated calcite surfaces. Fig. 1.9 is an image of clean calcite scanned using AFM under air. As shown on the left, linear steps and small dents are often encountered on calcite surfaces. A surface analysis (right box) of an arbitrarily selected rectangular area (the black solid line in the left image) shows that the roughness of the surface is only 1.7nm. Although it is not molecularly smooth like peeled mica, and often is far from smooth, it may still be possible to find relatively smooth parts of cleaved calcite surfaces. Adsorption of crude oil components produced rougher surfaces that can be distinguished from bare calcite

Oil Treated Calcite

The AFM images of the oil-treated calcite are organized according to the surface treatments, with comparisons of different crude oils, different imaging media, and varying aging times.

There is diversity in the appearance of surface features resulting from exposure to different crude oils. Usually there are continuous coatings with some irregularly shaped particles on the surface.

Crude Oil Aging Time

a. E-1XD-00

A stable coating was detected after a longer aging time for the treated calcite surface in crude oil E-1XD-00 (Fig. 1.10). It was easy to scrape a hole on the treated surface after two days, but not for the sample aged for 21 days.

b. Tensleep

Similar observations apply to the calcite surface aged in Tensleep crude oil. More stable coating was detected after a longer aging time (Fig. 1.11b). It was easy to scrape a hole on the treated surface after two days, but not for the sample aged for 21 days.

c. C-F-03

As shown in Fig. 1.12, all the coatings on calcite surfaces after aging in C-F-03 crude oil disintegrated readily.

d. LB-03

The coating on calcite surface after aging in crude oil LB-03 is disrupted, but it is more stable and dense than that for C-F-03, as shown in Fig. 1.13.

Imaging media

Fig. 1.14 shows the difference between scanning in air and scanning under water for a surface aged in E-1XD-00 crude for 2 days. In water, the surface was covered with a layer of rough coating. However, the coating was easily scraped away in air. Mostly substrate was revealed after the second scan as shown in Fig. 1.14b, which implies that the bond between the calcite and adsorbed materials in air is weak.

The adsorption of extracted asphaltenes was also investigated by AFM (Fig. 1.15). A calcite sample was aged in C-F-03 asphaltene solution for 2 days, then washed with toluene, air dried, and observed by AFM. The substrate was visible during the first scan when imaged under air while the film was intact in water. Again, the deposits are more stable in the presence of water.

The approximate depth of the film can be determined by performing a section analysis. Normally, the substrates were evenly covered with a continuous film through which the substrate was not visible. In some cases, a small area of the film could be scraped off by increasing the force of the tip. If the adsorbed film is too stable to permit scraping, toluene can be added to the imaging medium to swell the film and weaken it, after which it can be scraped for thickness analysis. The results of section analysis are listed in the Table 1.3.

Even allowing for the effect of toluene on the coating, there is a significant change in the thickness of the coatings with aging time. The coatings are thicker and more stable after a longer aging time.

Contact Angles of Crude Oil/Brine/Calcite Ensembles

Crude oil Captive Drops on Clean Calcite (Adhesion-Type Experiments)

The effect of brine compositions (including pH and concentrations of various ions) were studied by measuring the contact angles of crude oil drops on calcite surfaces submerged in these brines. Oil drops remained on the calcite surface for 2 to 15 min before the receding and advancing angle were measured. A complete list of adhesion measurements is given in the Appendix, Table A1. Varying the contact time from two to 15 minutes did not produce any noticeable trends in the resulting contact angles.

Contact angles for five crude oils selected from the results in Table A1 are shown in Fig. 1.16. For crude oils E-1XD-00 and LB-03, three replicate experiments are shown with each of the three brine compositions. Error bars are one standard deviation each in the plus and minus directions. While there is a great deal of scatter in the results of these tests, it is clear that one oil, E-1XD-00, consistently has much higher contact angles than any of the other oils. This is true regardless of brine composition. In fact we see no consistent trends with brine composition in any of these results.

Three crude oils tested with pH 8 buffered brines of different total ionic concentration are shown in Fig. 1.17. Again, there is no consistent trend with brine strength and the differences mainly appear to reflect differences between the crude oils.

A comparison between brines with monovalent and divalent cations is shown in Fig. 1.18. Divalent cations include Mg^{2+} and Ca^{2+} and the monovalent ions are Na^+ and K^+ . The brine concentrations are all 0.1M. In some cases there are dramatic differences between brines with monovalent and divalent cations (the monovalent-cation brines sometimes produce much more oil-wet conditions), but in most cases the differences between crude oils appear to dominate over differences in brine composition.

A comparison of 34 crude oils contacted with calcite that was pre-equilibrated with 0.1M NaCl is shown in Fig. 1.19. The oils have been divided into three groups: oils with less than 1% asphaltene, oils with 1-4% asphaltenes, and oils with more than 4% asphaltene. The oils with the highest amounts of asphaltenes have the lowest contact angles in adhesion tests with 0.1M NaCl, while some of the highest angles are found for the oils with the least asphaltenes. Similar comparisons with 0.1M $NaHCO_3$ and synthetic seawater, SSW, as the aqueous phase also show low contact angles for the high asphaltene group, but there is less difference between the low and intermediate groups.

Contact Angles Measured by Oil Drops Remaining after Flootation of Oil (Flooding Method)

Three data tables in the Appendix (Tables A2-A4) summarize details of the measurements made on carbonate surfaces aged in crude oil either wet or dry. The bulk oil was floated off the surface by injection of brine to simulate a waterflood. Table A2 has results for freshly cleaved calcite surfaces, the calcite surfaces in Table A3 were polished, and Table A4 summarizes measurements on polished marble surfaces.

Aging time in oil varied from one hour to five months, but by far the most experiments were for surfaces aged for one day or less. Replicate experiments with LB-03 crude oil in which dry calcite was aged for 28 days followed by flooding with 0.1M NaCl illustrate a problem frequently encountered with long-term aging experiments. The averages of water advancing angles on four separately aged pieces of calcite were 94° , 160° , 165° , and 180° . The occurrence of very oil-wet observations, with a layer of oil covering the entire surface and no contact angles measurable, increased with aging times of one day or more. It is not clear whether these observations should be interpreted as complete oil-wetting or whether, in light of the replicates, these are samples for which we fail to float off enough oil to allow measurements on the oil remaining.

Figure 1.20 shows a suite of tests with 51 crude oils. All calcite surfaces were freshly cleaved and aged for one day in crude oil before the flooding test. Whether the surfaces were pre-equilibrated with distilled water or were aged dry, results are clearly correlated. Probably the small amount of water covering the vial bottom to prevent attachment of the oil explains why these pairs of test show similar results. It is interesting to note, however, that wet and dry tests with maltenes replacing crude oils (designated in the Appendix tables by the suffix “-m”) are not correlated.

Results of contact angles measured by this flooding method show even more scatter than those assessed by other methods. Drops of different sizes can have very different contact angles (Hirasaki and Zhang, 2003). Drops may form preferentially on rough patches,

contributing to additional scatter in the results. The existence of drops, their size, and their number cannot be controlled in these experiments. Comparisons of the many duplicate experiments in Table A2 show that the results are not reproducible, despite efforts to select very smooth surfaces. Polishing does not appear to improve reproducibility. Measurements with marble as a substrate are compared to the Iceland spar in Fig. 1.21. In some cases, water advancing angles are lower and in others higher on marble. Replicate experiments on Iceland spar illustrate the difficulty in reproducing results. Contact angles measured by the flooding method for the set of oils in Fig. 1.16 are shown in Fig. 1.22 as a function of aging time in oil.

Wetting Alteration by Adsorption

Measurement of advancing angles between the crude oil drops and calcite in brine, has a number of drawbacks. The contact line is often pinned and exhibits substantial hysteresis. There is also the problem that contact times are short. The floatation or flooding method overcomes the problem of short exposure times, but it may accentuate the effect of roughness. Evaluation of the adsorption of the oil on the surface of a calcite sample after the bulk crude oil has been removed by rinsing with a solvent provides an alternate method to probe the interactions in COBR systems that has been used extensively for wetting tests of silicate surfaces. The extent of wetting alteration by adsorption of crude oil components can be assessed using contact angles of probe fluids under either water-advancing or water-receding conditions.

After exposure, samples were rinsed with toluene to remove bulk crude oil. Decane and DDW were used as the probe fluids for all contact angle measurements on the oil treated samples. A complete summary of measurements and results is given in the Appendix in Table A5. Results of adsorption of crude oil, measured with decane and DDW after removal of crude by rinsing with toluene is shown in Fig. 1.23 for the suite of oils that were shown in Figs. 1.16 (adhesion tests) and 1.22 (flooding tests). Typical error bars (plus or minus one standard deviation) are shown for LB-03. In measurements with all three methods, exposure to the E-1XD-00 crude oil gives the highest contact angles; Minnelusa-02 produces relatively low water-advancing angles. In Table 1.4 the effects of three different brine compositions are compared for 27 crude oils.

In Fig. 1.24 results are compared for dry and pre-wetted calcite samples aged for 12 days in this same group of oils. Differences between samples aged dry or pre-wetted with DDW, 0.1M NaCl or 0.1M NaHCO₃ show that little difference can be attributed to brine. Far more difference is observed from one crude oil to another.

The effects of raising the temperature during crude oil aging are shown in Fig. 1.25. There is as much difference between replicate experiments at one temperature as there is between the experiments at 25 and 60°C. Higher temperature aging results are either higher or lower than the ambient conditions tests, depending on the oil.

The effect of removing asphaltenes by mixing oils with n-heptane and recovering the maltenes is shown in Fig. 1.26. In most cases, the resulting contact angles are lower, although the change is small. For Minnelusa-02, the most asphaltic of the oils tested, the

maltene-treated calcite had slightly higher water-advancing angles than did calcite treated with the crude oil.

Correlation of Contact Angles with Crude Oil Properties

The strongest influence on wetting of calcite appears to be the identity of the crude oil. Using data in the CO-Wet database (Buckley and Wang, 2002), Yang *et al.* (2003) showed that contact angles between decane and DDW on mica correlated with crude oil chemical properties (mica surfaces, aged for 21 days in crude oil, crude oil removed by rinsing with toluene). The physical and chemical properties tested are those shown in Table 1.1, including density (or API gravity), viscosity (and log of the viscosity), average molecular weight, RI, P_{RI} (the RI of a mixture in which the first asphaltenes can be observed microscopically), acid and base numbers, amounts of SARA fractions, and isoelectric point (IEP).

For tests on mica, two buffered brine compositions were used: {pH4, 0.01M NaCl} which often produces unstable water films and {pH8, 1M NaCl} which is more likely to produce stable water films. There were no single variables that produced significant linear correlations; the best was $R^2=0.24$ between amount of asphaltene and θ_{A8} , the water-advancing contact angle for the mica surface pre-wetted with {pH8, 1M NaCl} buffer. Most single-variable, linear correlation coefficients were less than 0.1. Better correlations were obtained with combinations of variables, although the restriction that relationships must be linear is probably unnecessarily restrictive. A positive correlation means that higher values of a given variable are correlated to higher values of θ_A , whereas variables with negative correlations have the opposite effect.

The mica results showed different correlations depending on the brine composition. For θ_{A4} , there was a positive correlation with amount of asphaltene and a negative relationship with the amount of resins, producing an overall R^2 of only 0.33. The p values (probability that a variable has been included in the multiple regression in error) were less than 0.0002, suggesting that the relationships are real, but the results are very scattered. The correlation for θ_{A8} was completely different. The amount of asphaltene was negatively correlated, as was the base# to acid# ratio, B/A, giving an overall value of R^2 of 0.41. The B/A p-value was 0.06, making inclusion of this variable somewhat doubtful.

For calcite, no strong trends with brine composition were observed. Different correlations emerge, depending on how the contact angles were measured, as shown in Table 1.5. In all three cases, there is a measure of the heavy ends (asphaltene amount or average MW) that correlates negatively with contact angle. It is possible that the kinetics of adsorption are slower for heavier oil components. All p-values are less than 0.03. In terms of R^2 , the results are comparable to or better than those obtained on mica.

Table 1.1 Crude oil properties

Crude Oil	°API Gravity (°)	avg MW (Daltons)	RI at 20°C	P _{RI} (RI units)	n-C ₇ asph (%)	ρ at 20°C (g/cm ³)	μ at 20°C (cP)	Acid# (mg KOH/g oil)	Base #	IEP (pH units)	Saturates (%)	Aromatics (%)	Resins (%)	n-C ₆ asph (%)
A-95	25.2	236	1.5128	1.4513	8.7	0.8956	41.2	0.24	2.20	5.0	51.0	20.5	19.7	8.8
C-A2-00	22.7	306	1.5146	1.4368	4.3	0.9142	127.8	1.28	5.64	5.3	58.1	11.9	23.4	6.6
C-Ab-04	20.8	419	1.5253	1.4242	2.5	0.9266	377.1	1.68	2.17	5.0	58.8	22.2	16.4	2.7
C-AG-03	40.3	141	1.4535		0.1	0.8543	1.9	0.08	0.50	5.7	82.5	12.5	4.5	0.5
C-B2-01	36.3	196	1.4732	1.4260	1.3	0.8380	6.5	0.50	2.67	5.4	68.5	17.5	12.7	1.3
C-BF-1A-04	26.4		1.5047	1.4352										
C-Cap-04	18.6	420	1.5205	1.4152	0.6	0.9402	746.0	2.62	1.97	4.5	62.4	21.0	15.9	0.7
C-CM2-02	17.2	386	1.5324		3.0	0.9479	3954.0	2.18	5.46	5.0				
C-F-03	29.5	282	1.4973	1.4403	6.0	0.8755	22.1	0.16	1.52	3.9	61.7	18.4	13.5	6.5
C-F2-03	27.9	335	1.4993	1.4397	2.0	0.8847	28.6	0.70	1.32	3.8	63.2	17.9	16.2	2.7
C-GC-T1-03	31.1		1.4875		4.6	0.8671	17.0	0.03	1.69	5.2				
C-GC-T2-03	31.6	248	1.4899		9.6	0.8647	16.8			5.2	62.5	17.2	14.4	5.9
C-GGC-00	29.2	222	1.4951	1.3943	0.3	0.8774	16.7	1.49	0.94	4.1	64.9	21.7	13.2	0.3
C-HM-01	21.9	304	1.5187		9.6	0.9192	294.0	0.08	4.31	5.3	58.1	13.6	18.9	9.4
C-K-01	18.9	319	1.5287	1.4320	3.5	0.9374	396.0	2.44	5.19	4.8	52.8	19.0	24.8	3.3
C-K2-02	18.9	328	1.5295		3.2	0.9375	375.5	2.66	5.06	5.0				
C-Kb-02	19.0	330	1.5292		3.0	0.9370	367.0	2.55	5.66	4.0				
C-Lb-01	31.7	241	1.4858		1.6	0.8640	22.6	0.05	2.50	5.4	72.0	14.9	10.9	2.2
C-LH-99	22.6	268	1.5137	1.4231	2.8	0.9161	89.6	1.90	6.05	4.4	49.5	21.5	25.6	3.4
Cottonwood-03	26.4	262	1.5044	1.4412	2.5	0.8929	26.1	0.04	1.87	3.6	57.9	22.7	16.5	2.9
C-R-00	31.1	235	1.4851	1.4440	1.9	0.8673	19.1	0.25	0.49	3.9	70.6	16.3	11.4	1.6
C-R-01	31.1	254	1.4846	1.4446	1.3	0.8674	17.8		0.40	4.0	70.6	15.0	12.9	1.6
C-T-01	26.2	280	1.5052	1.4628	9.8	0.8945	97.6	0.38	1.87	3.8	60.6	17.0	11.6	10.8
C-T-02	34.2	214	1.4807	1.4211	1.4	0.8511	9.4	0.01	1.30	4.0	61.1	22.8	14.6	1.6
C-WB-03	22.6	357	1.5118	1.4421	0.9	0.9150	70.1	1.45	2.70	5.1	69.0	19.6	11.1	0.4
DS-P-01	30.6	241	1.4881		2.0	0.8695	16.5	0.31	1.51	4.8	69.7	16.7	13.0	0.6

Crude Oil	°API Gravity (°)	avg MW (Daltons)	RI at 20°C	P _{RI} (RI units)	n-C ₇ asph (%)	ρ at 20°C (g/cm ³)	μ at 20°C (cP)	Acid# (mg KOH/g oil)	Base #	IEP (pH units)	Saturates (%)	Aromatics (%)	Resins (%)	n-C ₆ asph (%)
E-1XD-00	22.3	287	1.5141	1.4336	2.5	0.9165	137.4	1.56	2.98	5.0	64.1	18.5	15.3	2.2
E-1XFR-01	40	179	1.4667	1.4039	0.3	0.8223	3.7	0.16	0.65	4.3	70.6	21.5	7.6	0.3
E-1XO-00	21.9	264	1.5139	1.4142	0.8	0.9191	15.3	3.42	2.57	5.1	57.8	22.1	19.4	0.7
E-1XR-00	29.2	218	1.4913	1.4071	0.3	0.8777	22.1	0.54	2.02	4.9	71.6	17.6	10.4	0.4
E-2XR-00	25.4	235	1.5040	1.4274	1.3	0.8983	47.0	0.91	2.46	5.1	65.7	18.4	14.9	1.1
E-8XFR-01	38.6	189	1.4676	1.4020	0.3	0.8290	4.7	1.03	0.74	3.8	70.9	19.7	9.1	0.4
E-BL-00	31.3	213	1.4896	1.4395	3.6	0.8651	23.4	0.17	1.33	5.0	66.3	21.2	9.5	3.0
EJ-G-03	43.4	154	1.4530		0.3	0.8061	2.1	0.18	0.66	5.4	83.1	15.2	1.4	0.3
E-S1XCA-01	23.2	298	1.5123	1.4626	2.1	0.9115	80.6	0.48	3.42	4.8	60.7	19.1	18.3	2.0
E-S1XG-01	33.3	237	1.4841	1.4681	0.5	0.8554	9.6	0.14	1.57	5.0	68.7	19.8	11.0	0.4
E-S1XL-01	33.5	220	1.4800	1.4088	0.4	0.8543	10.3	0.48	1.83	5.1	71.5	19.3	8.9	0.3
E-S3XR-01	30	251	1.4907	1.4238	0.9	0.8732	19.8	0.23	2.03	5.1	68.5	16.4	14.5	0.6
Gulfaks-96	27.1	245	1.4930		0.4	0.8827	15.8	0.24	1.19	3.8	63.3	25.5	10.9	0.2
Lagrove	41.3	168	1.4659	1.4530	3.4	0.8109	4.6	0.29	0.65	3.6	59.4	24.9	10.2	5.5
LB-03	30.6	244	1.4848	1.4362	0.1	0.8699	13.1	1.57	0.59	4.2	70.1	17.6	12.0	0.3
Mars-97	28.5	258	1.4952	1.4298	1.9	0.8804	27.6	0.37	1.79	3.4	57.2	22.5	17.3	3.0
Mars-P	16.5	309	1.5384	1.4262	4.8	0.9524	481.0	3.92	2.30	2.3	38.4	29.8	25.8	6.0
Minnelusa-02	24.3	264	1.5138		8.6	0.9050	60.5	0.01	2.01	4.6	58.0	20.2	13.9	7.9
Minnelusa-03	24.5	332	1.5201		7.2	0.9039	58.1	0.12	1.71	4.4	58.5	19.8	12.7	9.1
MY3-02	28	245	1.4955		1.0	0.8842	21.7	0.20	1.17	3.4	61.9	24.8	12.2	1.1
MY4-02	28.1	244	1.4943		1.0	0.8835	21.6	0.22	1.23	3.4	65.3	23.7	9.9	1.1
SQ-95	37.2	213	1.4769	1.4166	1.3	0.8409	5.8	0.17	0.62	3.8	65.2	18.3	13.9	2.6
Steen-NM-1	22.3	279	1.5288	1.4683	11.0		223.0	0.26	2.93	5.5	56.0	18.9	13.7	11.4
Steen-NM-2	28.5	265	1.4939	1.4620	1.6	0.8815	23.3		1.53		66.8	19.0	12.2	2.0
Steen-OLEOD	20	325	1.5331	1.4262										
Tensleep	31.2	271	1.4877	1.4438	3.2	0.8684	21.6	0.16	0.96	3.9	69.3	16.0	9.4	5.3
Tensleep-99	31.1	270	1.4906	1.4428	4.1	0.8685	18.7	0.10	1.03	4.0	64.0	19.8	12.9	3.2

Crude Oil	°API Gravity (°)	avg MW (Daltons)	RI at 20°C	P _{RI} (RI units)	n-C ₇ asph (%)	ρ at 20°C (g/cm ³)	μ at 20°C (cP)	Acid# (mg KOH/g oil)	Base #	IEP (pH units)	Saturates (%)	Aromatics (%)	Resins (%)	n-C ₆ asph (%)
T-VJ487-05-1	28.4	300	1.5015		3.6	0.8820	20.6		2.01		64.1	19.4	11.4	5.2
T-VJ488-05-1	30.2	310	1.4898		0.4	0.8717	15.5		1.77		68.5	19.6	11.6	0.3
UNAM	23.65	265	1.5080	0.0000	0.5	0.9066	44.3	1.40	2.60					
Uwyo-E-04	24.7	312	1.5112	1.4657	2.8	0.9025	38.5	0.16	1.82	4.7	60.3	24.5	12.0	3.2
Uwyo-M-04	21.9	347	1.5194	1.4469	7.0	0.9189	89.7	1.46	2.49	4.7	60.1	21.5	12.1	6.3
Ventura-Rice	31.15		1.4900	1.4500	5.7	0.8714	15.0	0.31	4.73	4.7				
W-Az-03	32.8	268	1.4797		1.2	0.8581	24.2	0.19	1.45	4.9	75.1	12.3	11.6	1.0
W-Ch-03	32.8	252	1.4781		0.8	0.8584	16.8	0.11	1.29	5.1	74.9	12.5	12.1	0.5
W-Da-03	32.1	263	1.4891	1.4153	2.1	0.8618	33.7	0.76	3.27	6.8	63.0	16.2	18.3	2.5
W-Lo-03	28.1	251	1.4964	1.4217	1.7	0.8836	17.8	0.39	0.94	4.9	61.3	20.6	16.2	1.9
W-Mi-01	37.9	195	1.4736	1.4242	0.2	0.8354	4.4		0.19	5.1	76.4	17.5	5.7	0.4
W-Mr-03	30.1	237	1.4912	1.4274	0.8	0.8724	10.4		1.00	5.0	62.0	25.2	11.9	1.0
W-Pc-03	25.8	281	1.5050	1.4412	4.4	0.8963	47.5	0.43	1.65	3.8	55.0	19.6	20.9	4.5
W-Sc-03	27.4	285	1.4971	1.4120	1.8	0.8875	42.4	0.40	1.74	4.8	66.5	17.8	14.1	1.6
W-Sch-04	18.6	380	1.5310	1.4233	1.9	0.9394	535.5	0.67	3.02	4.0	52.4	20.9	23.9	2.8
W-Sk-04	32.9	235	1.4824	1.4309	0.4	0.8574	10.7	0.07	0.83	5.6	69.8	20.7	8.9	0.6
W-TH-05	31.8	300	1.4885	1.4619		0.8632	13.5	0.18	1.37	9.3	70.1	15.3	11.8	2.8
W-Ur-01	30.9	235	1.4931	1.4202	2.0	0.8699	16.4	0.20	1.45	3.6	55.3	24.7	17.8	2.1

Note: Oil properties are from CO-Wet database. (Buckley and Wang, 2002).

Table 1.2 Brine composition and pH

Brine	NaCl (g/L)	CaCl ₂ *2H ₂ O (g/L)	MgCl ₂ *6H ₂ O (g/L)	Na ₂ SO ₄ (g/L)	Na ₂ HPO ₄ (g/L)	NaH ₂ PO ₄ (g/L)	NaHCO ₃ (g/L)	pH
DDW								6.8
{8, 0.01} buffer					0.6211	0.0318		8
{8, 0.1} buffer					6.211	0.3179		8
{8, 1} buffer	47.04				13.44	0.6359		8
0.1M CaCl ₂		14.70						5.7
0.1M NaCl	5.844							6.6
0.1M NaHCO ₃							8.401	8.0
SSW	24.00	1.47	10.64	3.20				

Table 1.3 Thickness of organic coatings on oil-treated calcite surface

Crude Oil	Coating thickness (nm)		Comments
	aged 2days	aged 21days	
C-F-03	-	-	coating disintegrates
Tensleep	25	50	estimate from hole
E-1XD-00	38	170	toluene used to scrape hole
LB-03	-	108	estimate from hole

Table 1.4 Contact angles measured in adhesion tests using a captive drop of crude oil under one of three different brines. All units are degrees, ± indicates one standard deviation for the measurements in the preceding column

crude oil	0.1M NaCl				0.1M NaHCO ₃				SSW			
	θ _A	±	θ _R	±	θ _A	±	θ _R	±	θ _A	±	θ _R	±
A-95	85	11	47	16	71	14	34	8	77	18	46	13
C-Ab-04	81	16	38	6	80	22	43	12	59	15	41	3
C-AG-03	98	28	40	8	50	24	41	13	106	30	45	13
C-Cap-04	66	23	45	8	60	14	46	4	48	12	41	7
C-CM2-02	26	8	26	5	61	12	26	6				
C-F-03	23	4	20	5	41	17	33	12				
C-F2-03	91	32	55	6	94	16	57	7	86	21	57	10
C-K-01	101	19	67	14	72	17	40	6	105	17	55	13
Cottonwood-03	84	16	36	6					70	27	34	5
C-T-03	110	23	58	16	70	27	47	18	73	25	38	7
E-1XD-00	103	10	47	15	124	10	28	5	107	15	50	10
E-1XD-00 (repeat)	119	13	35	8	106	5	38	4	135	10	41	14
E-1XD-00 (repeat)	123	12	49	10	127	12	37	21	114	11	52	9

crude oil	0.1M NaCl				0.1M NaHCO ₃				SSW			
	θ_A	\pm	θ_R	\pm	θ_A	\pm	θ_R	\pm	θ_A	\pm	θ_R	\pm
E-1XD-00 (repeat)					121	21	36	12				
E-1XR-00	106	6	36	7	82	15	32	9	92	11	39	5
E-2XR-00	133	17	40	5	121	10	34	20	131	15	47	26
E-8XFR-01	141	13	71	22	125	25	51	21	83	41	48	19
E-BL-00	65	22	27	7	30	12	24	6	54	9	32	5
E-S1XCA-01	97	15	36	11					125	22	30	16
E-S1XG-01	46	12	22	4	33	11	32	15	51	14	31	5
E-S1XG-01 (repeat)	100	17	43	8								
E-S1XL-01	73	8	23	2	114	19	39	7	79	25	39	9
E-S1XL-01 (repeat)	64	21	42	12								
E-S3XR-01	106	12	40	6	37	7	31	8	69	16	39	8
Gullfaks-96	104	15	45	8	109	10	63	7	107	18	50	10
Lagrove	56	25	57	15					59	9	44	15
LB-03	68	8	42	7	64	4	42	6	49	8	36	5
LB-03 (repeat)	23	4	20	5	77	16	36	7	34	4	34	6
LB-03 (repeat)	58	5	31	9	64	4	42	6				
LB-03 (repeat)					50	10	31	11				
Mars-97	120	13	46	12	124	7	39	12	91	19	41	7
Minnelusa-02	46	4	30	5	24	4	21	5	33	6	29	4
Minnelusa-03	48	13	44	7	32	6	31	5	35	5	34	4
SQ-95	70	10	45	8	64	20	54	18	101	29	53	7
SQ-95 (repeat)					85	15	46	8				
SQ-95 (repeat)					91	17	39	9				
Tensleep	112	13	67	13	96	36	48	18				
Tensleep (repeat)	90	14	43	9	94	13	19	2				
Tensleep (repeat)	91	9	45	8								

Table 1.5 Correlations of water-advancing contact angles with oil properties

measurement method	variable	sign	number of samples	R ²
Adhesion ¹	n-C ₇ asph.wt%	-	40	0.35
	viscosity at 20°C	-		
	base #	+		
Flooding ²	MW	-	40	0.44
	A ₈ (contact angle on mica with {pH8,1M NaCl})	+		
Adsorption ³	MW	-	19	0.47
	acid #	+		

¹surfaces submerged in 0.1M NaCl

²surfaces pre-wetted with DDW, aged in crude oil for 1 day at ambient conditions

³surfaces pre-wetted with 0.1M NaCl, aged in crude oil for 12 days, rinsed with toluene

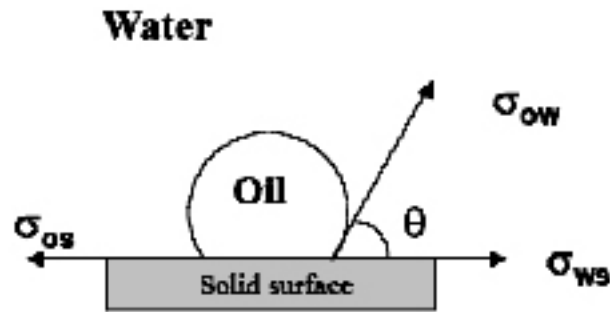


Fig. 1.1 Definition of contact angle.

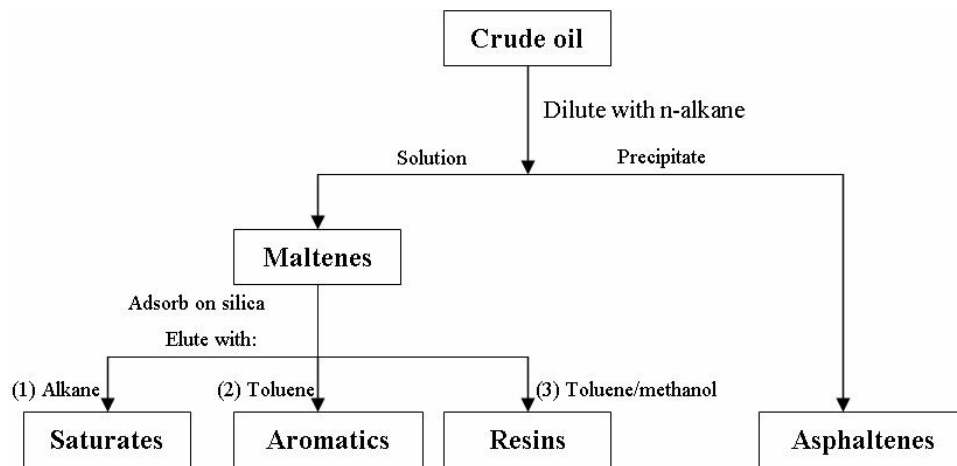
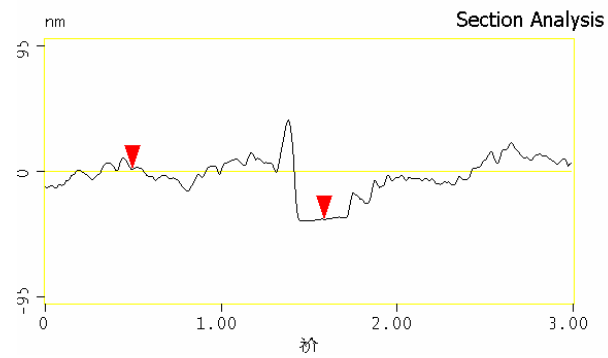
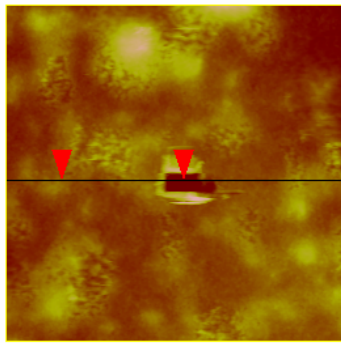


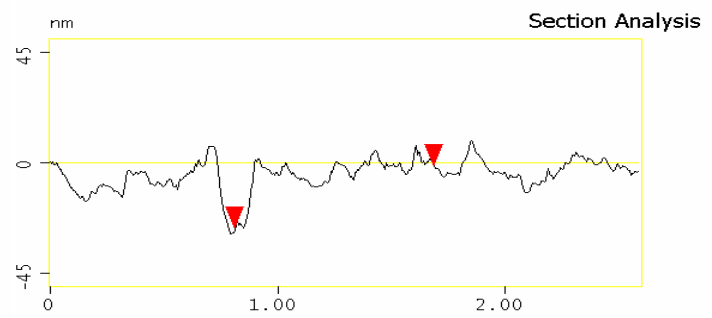
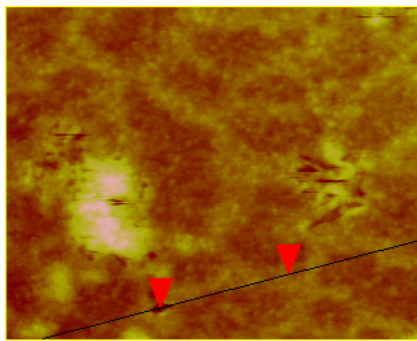
Fig. 1.2 Scheme for separating crude oil into saturate, aromatic, resin and asphaltene (SARA) components



c-010.043

Surface distance	1.152 nm
Horiz distance(L)	1.090 nm
Vert distance	38.362 nm
Angle	2.016 °

Fig. 1.3 Section view of a calcite surface aged in E-1XD-00crude oil



er500450.100

Surface distance	902.25 nm
Horiz distance(L)	875.58 nm
Vert distance	25.413 nm
Angle	1.662 °

Figure 1.4 Section view of a calcite surface aged in Tensleep crude oil

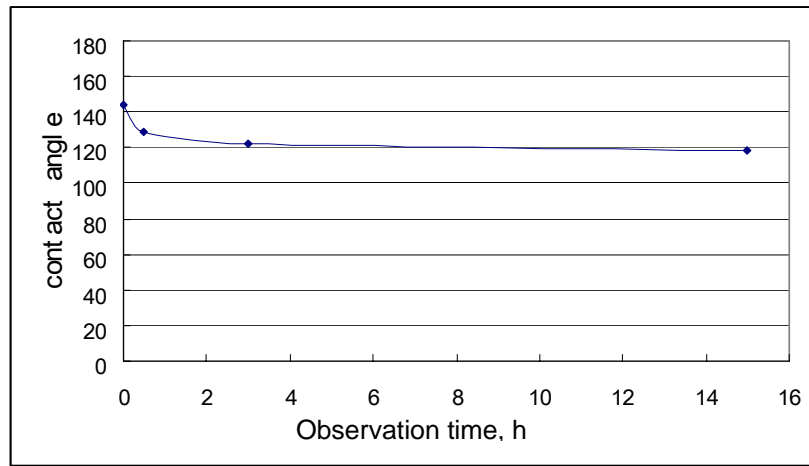


Fig. 1.5. Contact angle measured by flooding method changes with observation time



Fig. 1.6 Calcite surface with oil drops after being flooded with DDW (surface was pre-equilibrated with DDW, then aged in Uwyo-M-04 for 24 h).

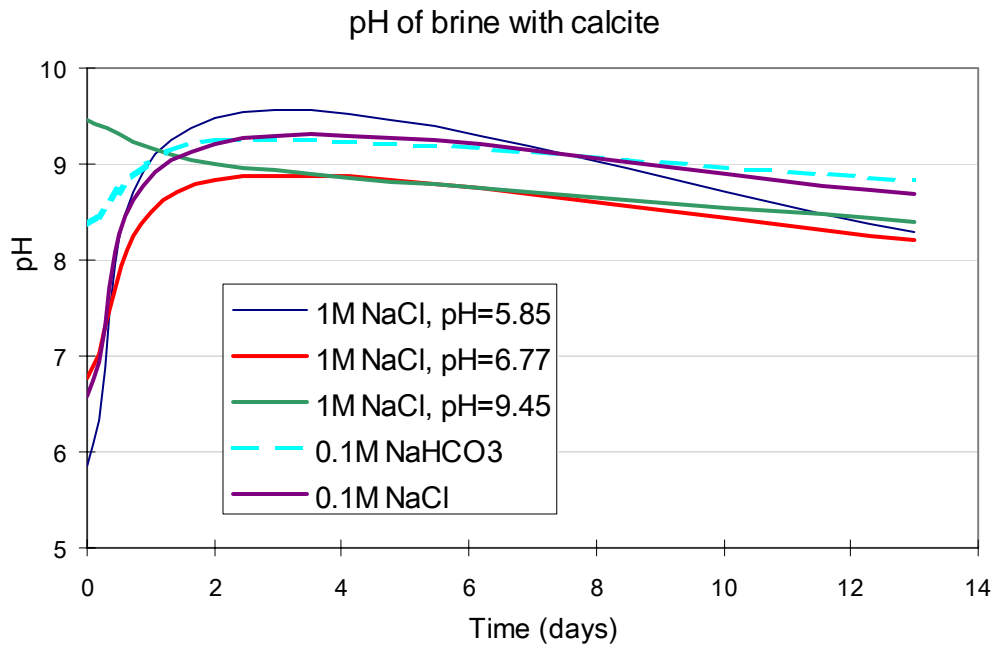


Fig. 1.7 Evolution of pH of unbuffered brines in contact with calcite powder (0.5g calcite in 20ml brine)

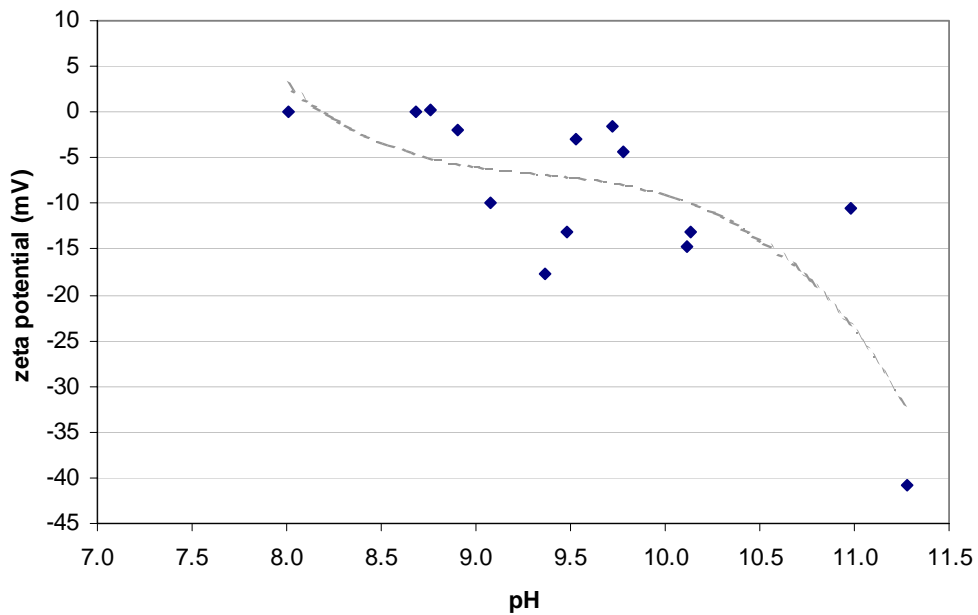


Fig. 1.8 Zeta potential of calcite powder varies with pH of 0.01M brine

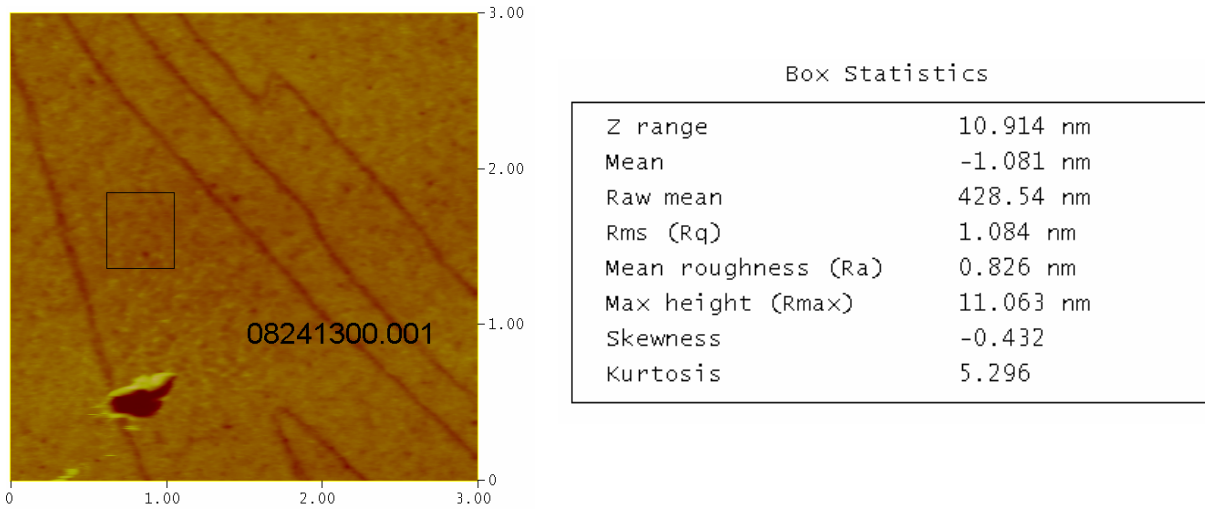
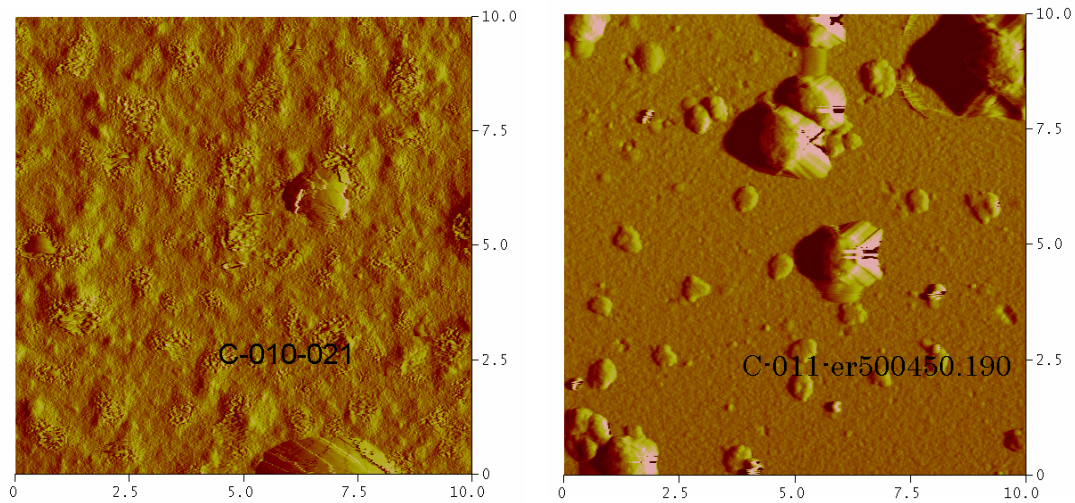


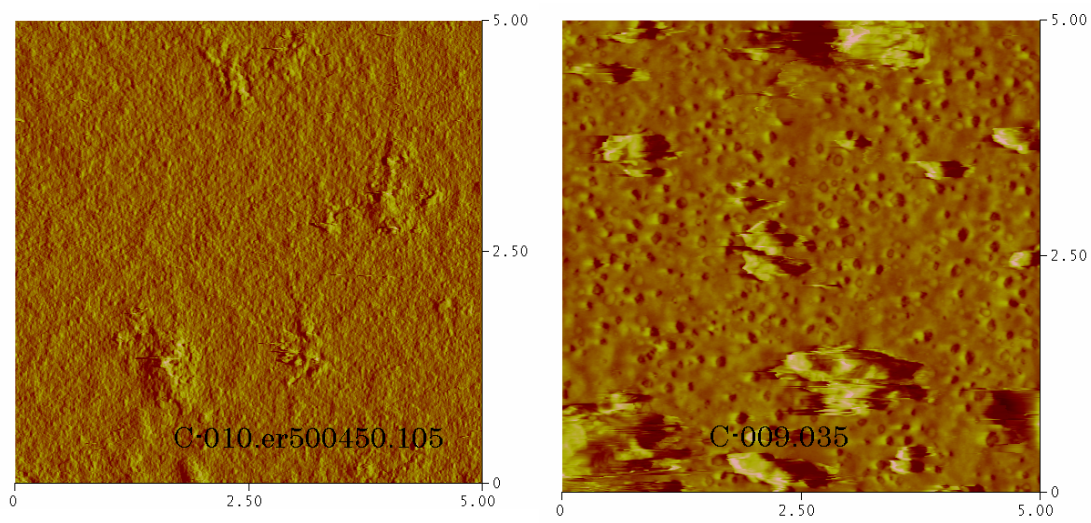
Fig. 1.9 3 μm × 3 μm AFM height image of clean calcite surface under air



a. After 2 days

b. After 21 days

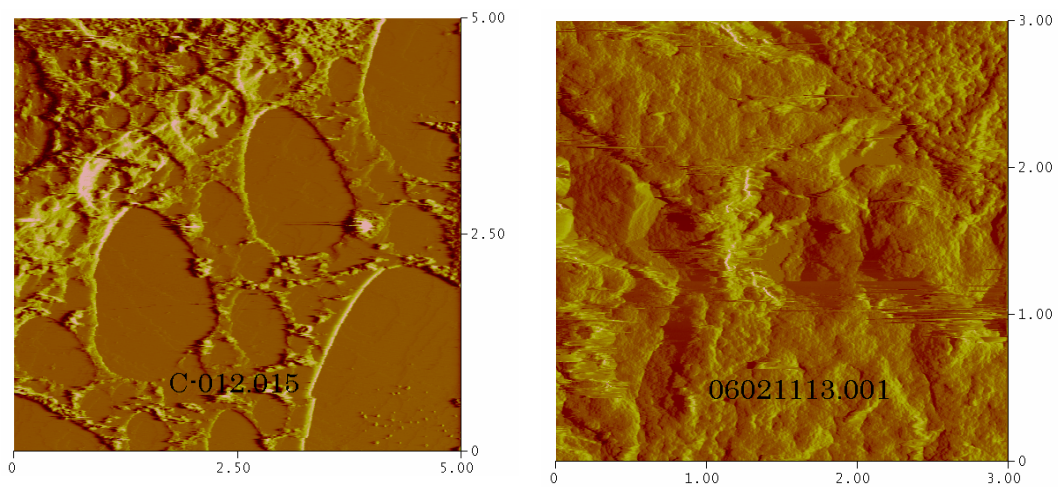
Fig. 1.10 AFM image of calcite exposed first to (0.1M NaCl) brine then aged for 2 days and 21 days in E-1XD-00 crude oil (deflection image in water)



a. After 2 days

b. After 21days

Fig. 1.11 AFM image of calcite exposed first to (0.1M NaCl) brine then aged for 2 days and 21 days in Tensleep crude oil (deflection image in water)



a. After 2 days

b. After 21days

Fig. 1.12 AFM images of calcite exposed first to 0.1M NaCl brine then aged for 2 days and 21days in crude oil (C-F-03) (Deflection images in water)

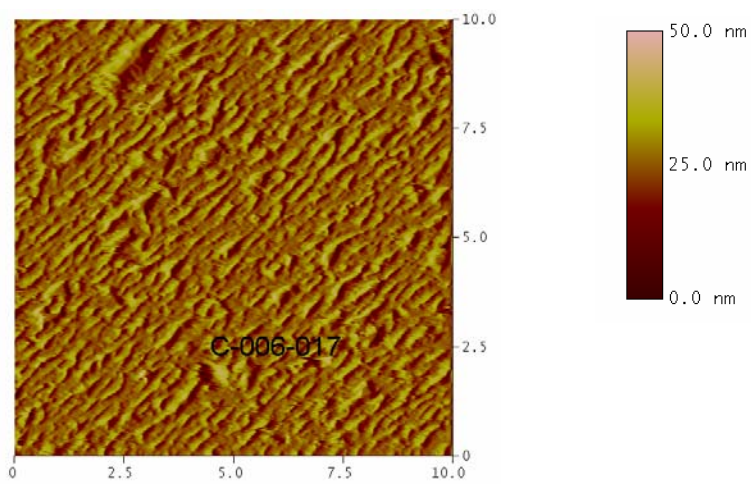
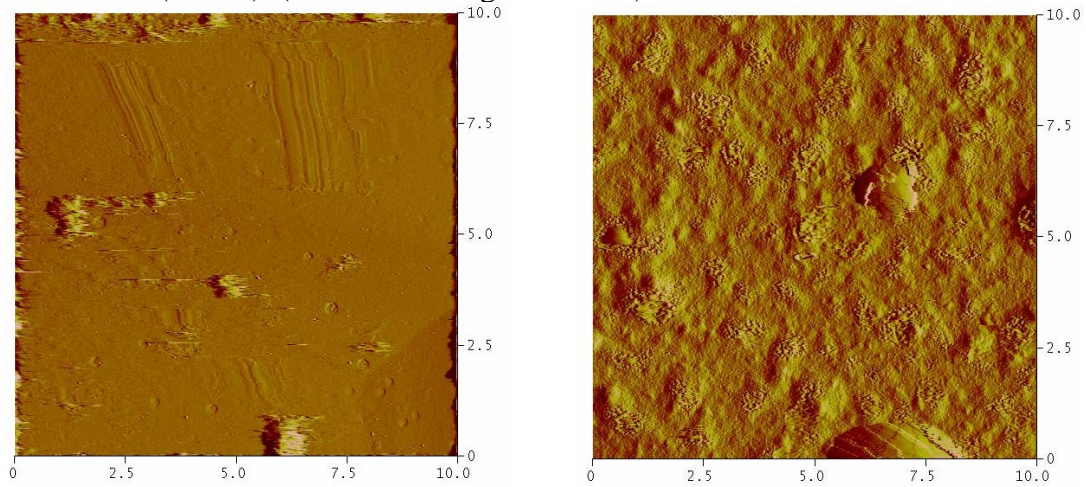


Fig. 1.13 AFM images of calcite exposed first to 0.1M NaCl brine then aged for 21 days in crude oil (LB-03) (Deflection images in water)



a. Imaged in air

b. Imaged in DDW

Fig. 1.14 AFM image of calcite exposed first to 0.1M NaCl brine then aged for 2 days in E-1XD-00 (deflection image)

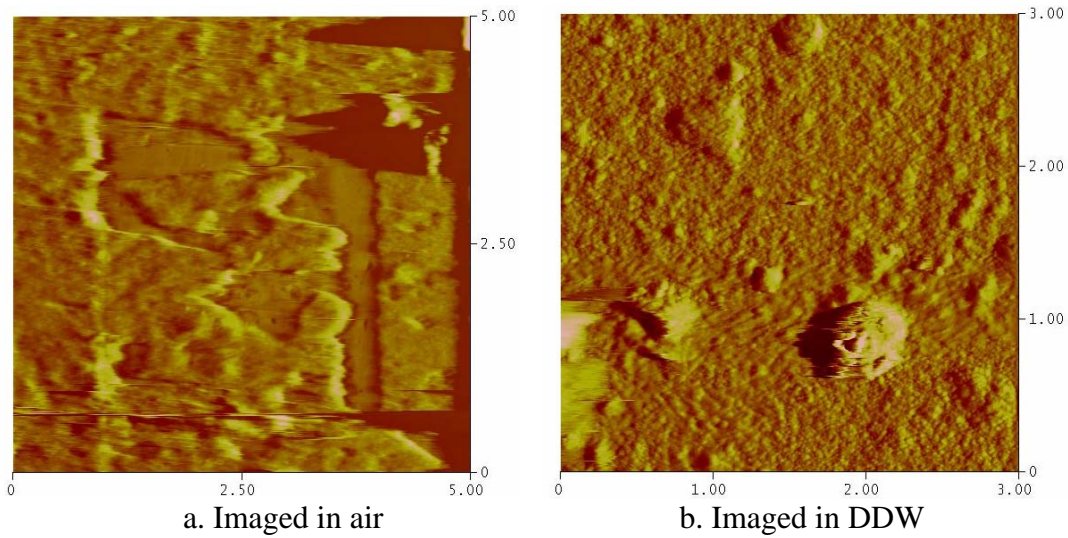


Fig. 1.15 AFM image of calcite exposed first to 0.1M NaCl brine then aged for 2 days in C-F-03 asphaltenes solution (In deflection image)

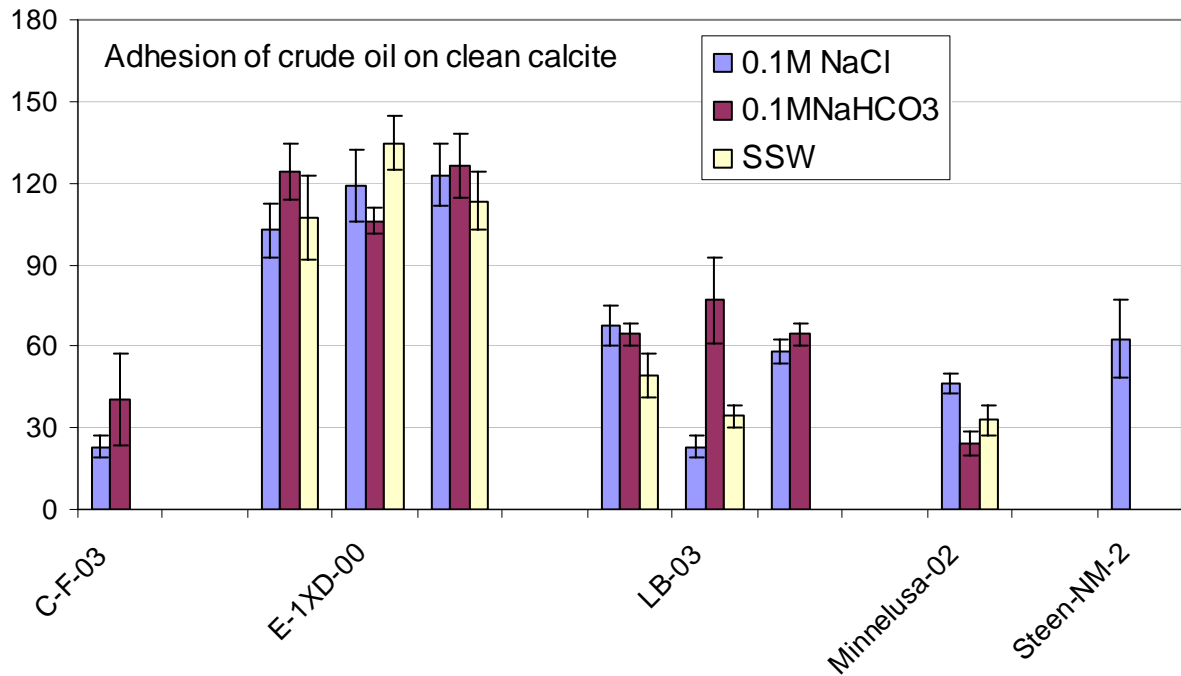


Fig. 1.16 Advancing contact angles between brine and crude oil on initially clean calcite. Results are shown for five oils and three different brine compositions. Replicate experiments with oils E-1XD-00 and LB-03 and the \pm one standard deviation error bars indicate the extent of scatter in the results.

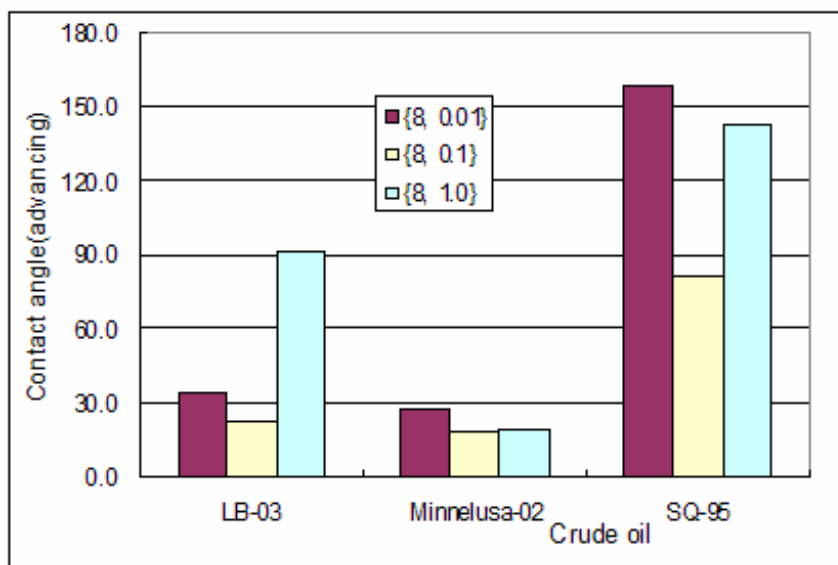


Fig. 1.17 Advancing contact angle of oil drops on pre-equilibrated calcite surface in pH=8.0 buffer

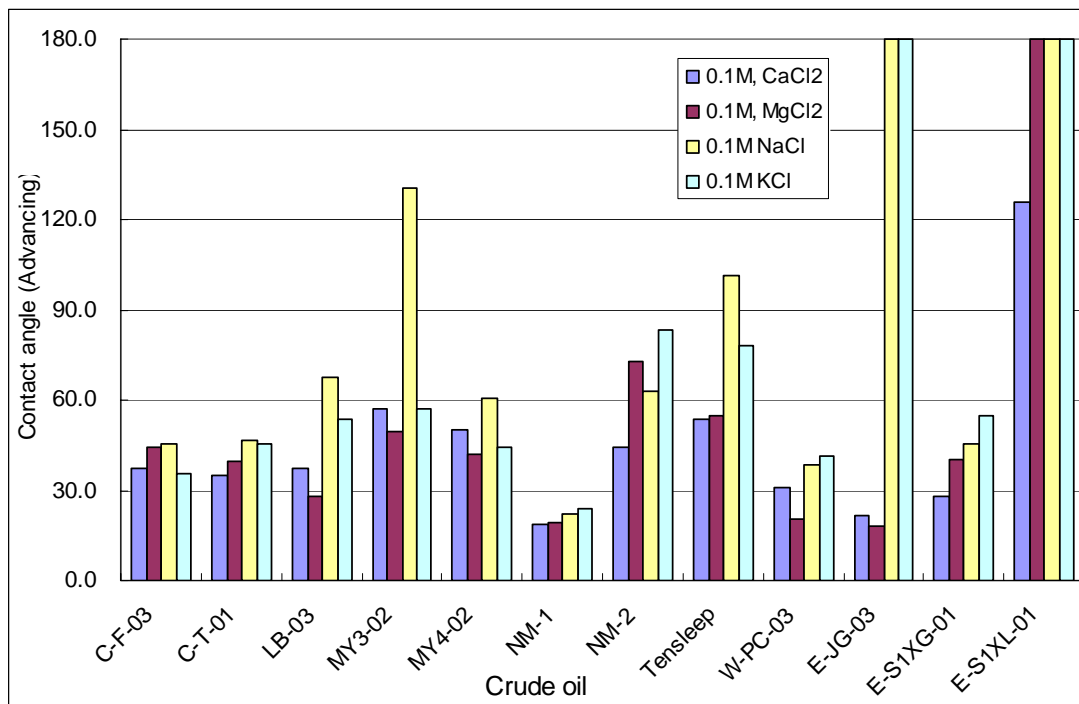


Fig. 1.18 Advancing contact angle of oil drops on pre-equilibrated calcite surfaces in brines with monovalent and divalent cations.

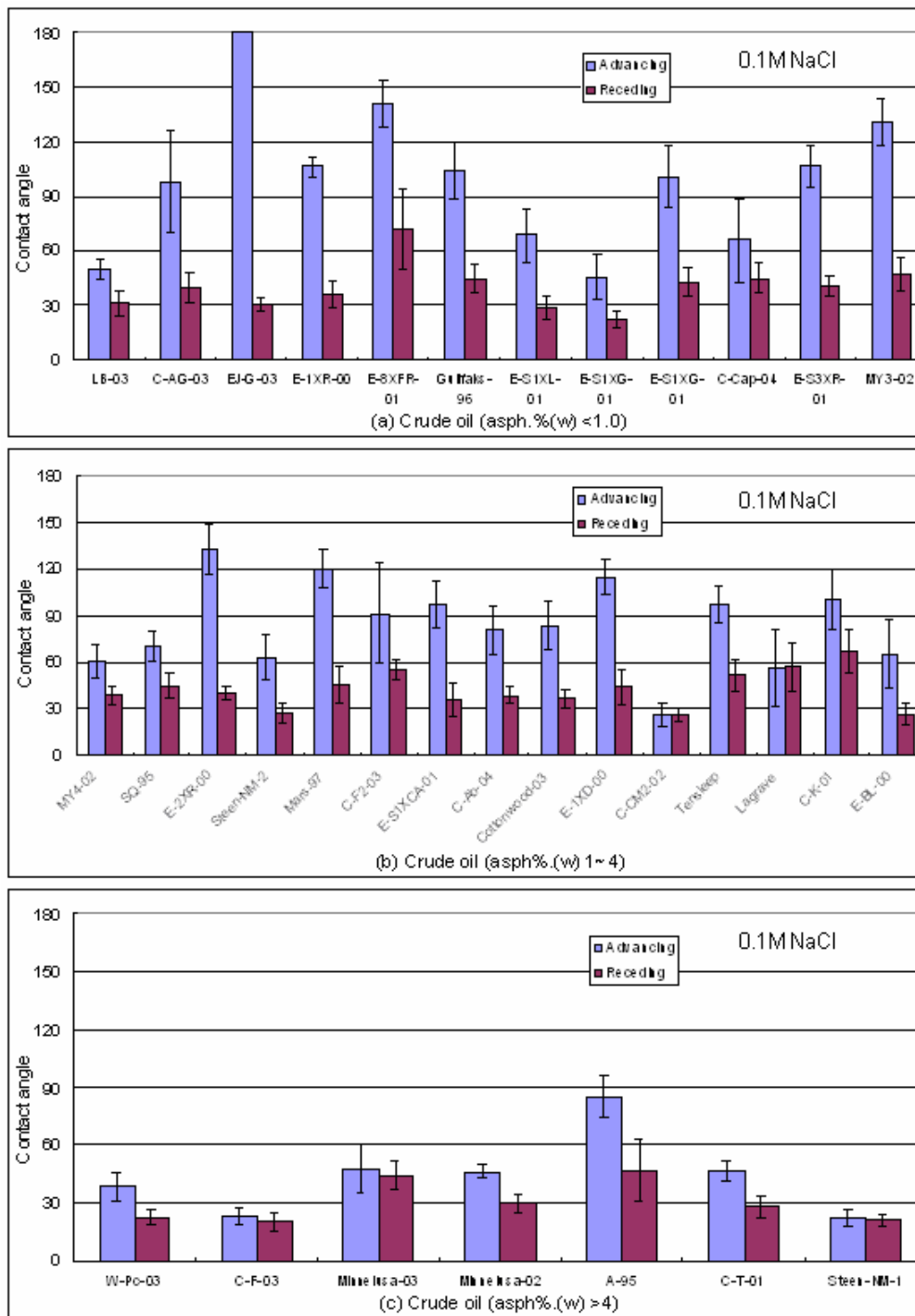


Fig. 1.19 Contact angles of oil drops on calcite surfaces pre-equilibrated in 0.1M NaCl grouped according to the amount of asphaltene in each crude oil.

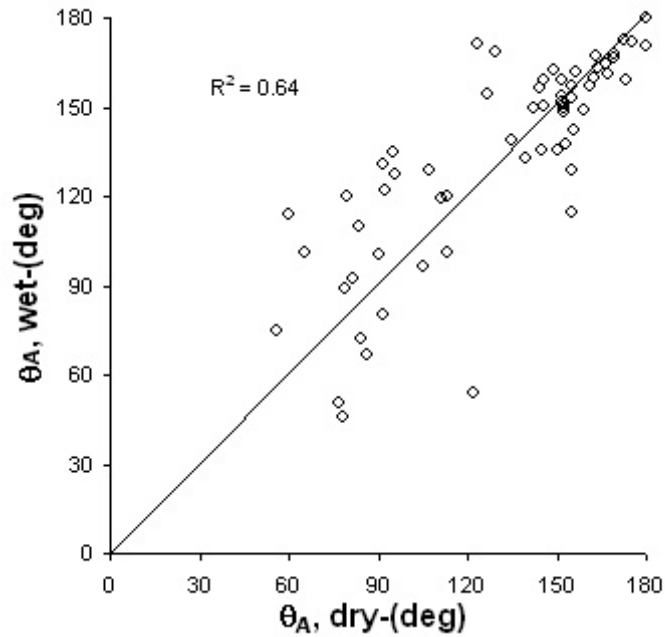


Fig. 1.20 Comparison of water advancing contact angles measured by the flooding method for calcite surfaces that were pre-wetted with similar surfaces that were dry when submerged in crude oil. All samples were aged for one day in crude oil at ambient conditions.

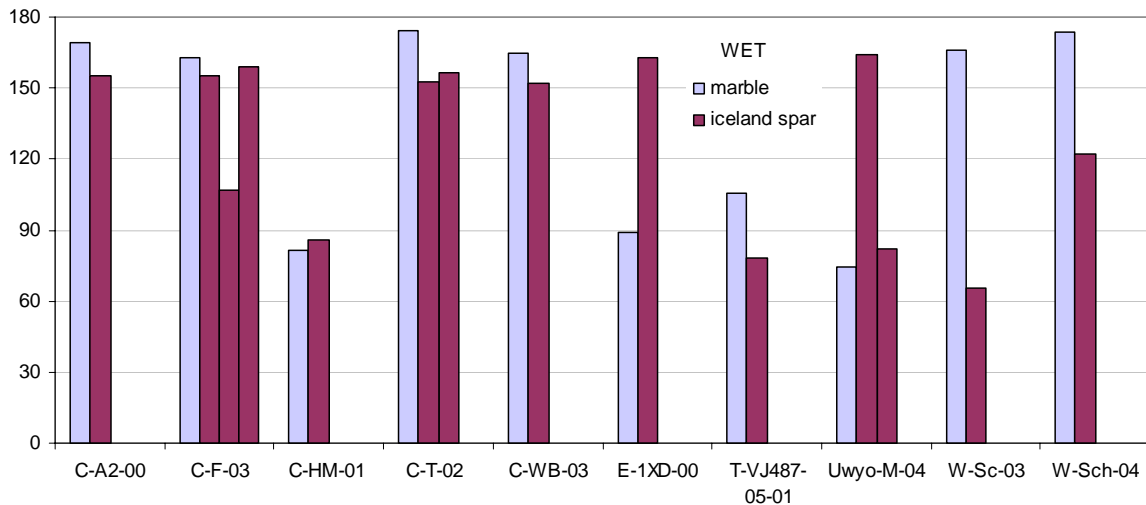


Fig. 1.21 Contact angles by the flooding method on polished marble and freshly cleaved Iceland spar surfaces pre-wetted with DDW and aged for one day in crude oil.

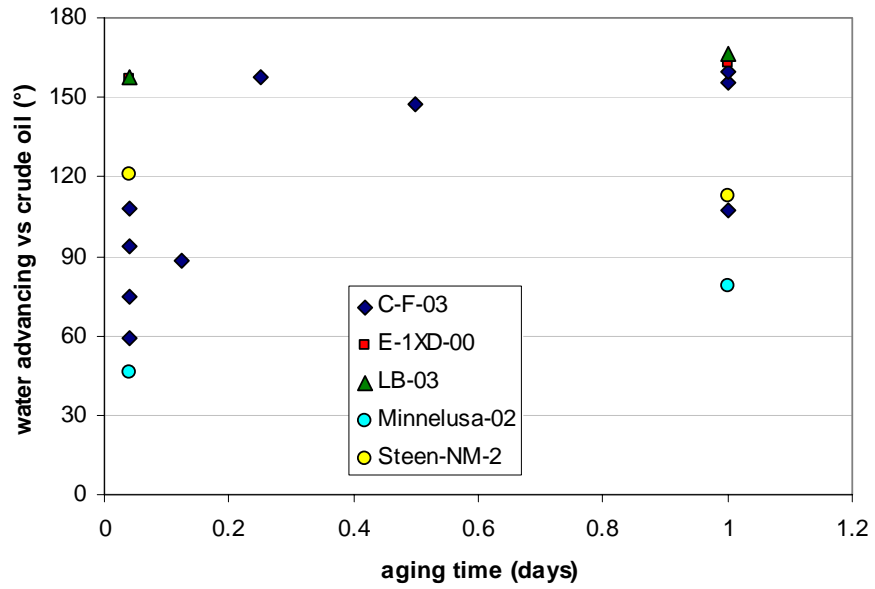


Fig. 1.22 Contact angles by the flooding method for selected oils.

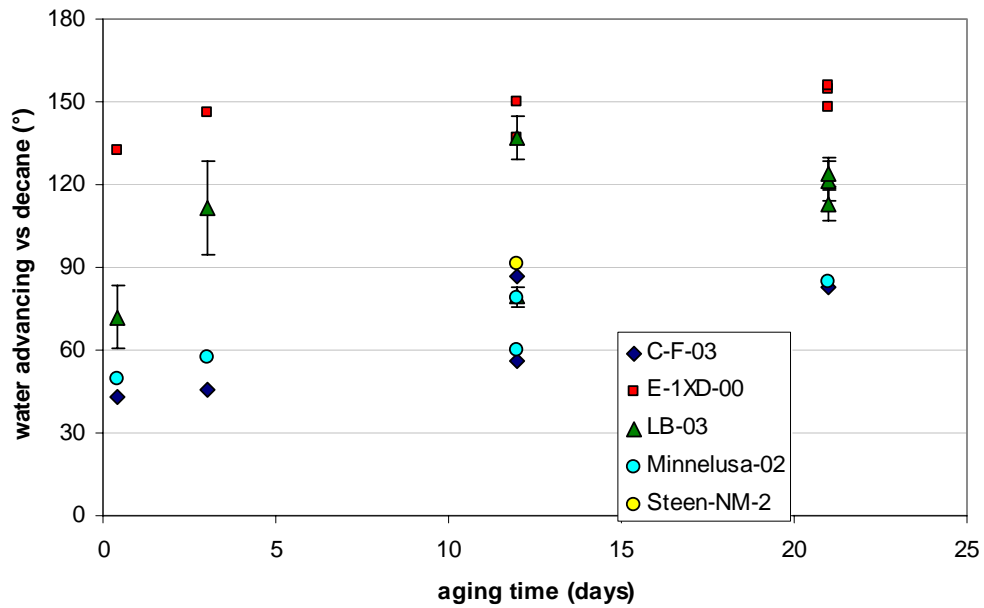


Fig. 1.23 Contact angles on selected oil-treated calcite samples after removal of oil by rinsing with toluene. All samples were pre-wetted with 0.1M NaCl.

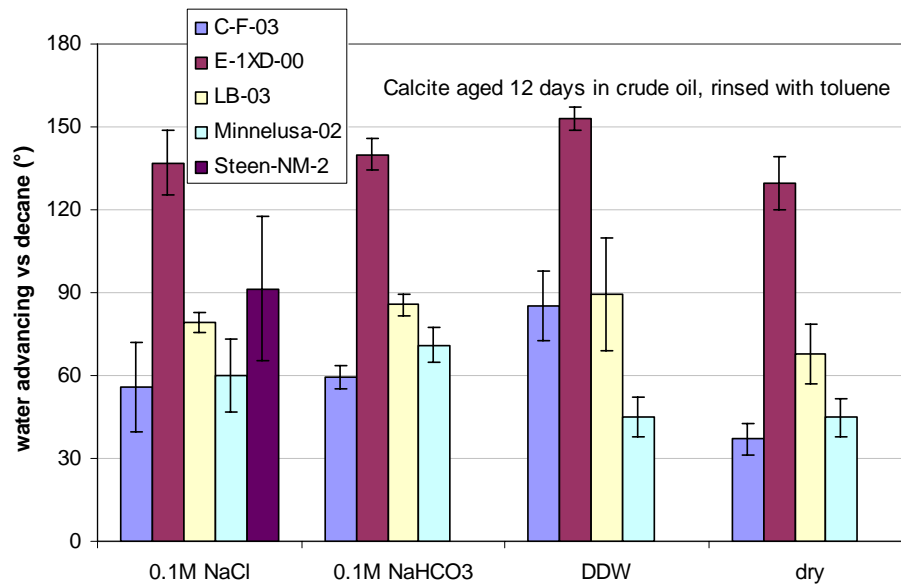


Fig. 1.24 Comparison of contact angles between decane and DDW on surfaces aged for 12 days in crude oil. Contact angles were measured after removal of crude oil by rinsing with toluene.

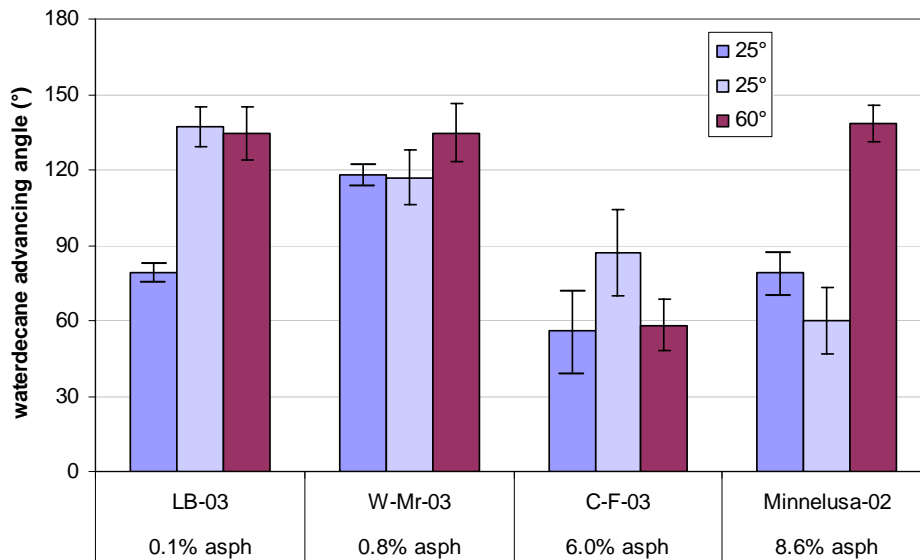


Fig. 1.25 Comparison of contact angles between decane and DDW on surfaces aged for 12 days in crude oil at either 25 or 60°C. Contact angles were measured after removal of crude oil by rinsing with toluene.

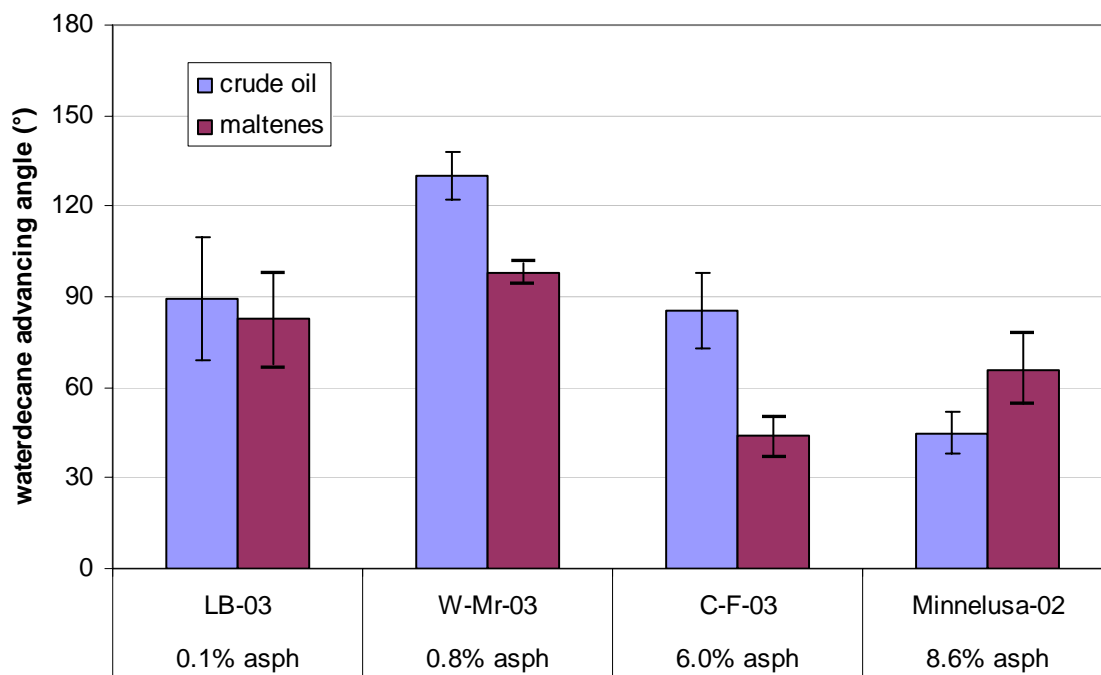


Fig. 1.26 Comparison of contact angles between decane and DDW on surfaces aged for 12 days in crude oil or in their maltenes. Contact angles were measured after removal of crude oil by rinsing with toluene.

Task 1 Appendix

Table A1. Summary of adhesion data measured with brine, a captive drop of crude oil, and clean calcite (contact time 2-15 min).

Crude Oil	Aqueous Phase	θ_A (deg)	<i>Std dev</i> θ_A (deg)	θ_R (deg)	<i>Std dev</i> θ_R (deg)
A-95	0.1M NaCl	85	11	47	16
A-95	0.1M NaHCO ₃	71	14	34	8
A-95	SSW	77	18	46	13
C-Ab-04	0.1M NaCl	81	16	38	6
C-Ab-04	0.1M NaHCO ₃	80	22	43	12
C-Ab-04	SSW	59	15	41	3
C-AG-03	0.1M NaCl	98	28	40	8
C-AG-03	0.1M NaHCO ₃	50	24	41	13
C-AG-03	SSW	106	30	45	13
C-Cap-04	0.1M NaCl	66	23	45	8
C-Cap-04	0.1M NaHCO ₃	60	14	46	4
C-Cap-04	SSW	48	12	41	7
C-CM2-02	0.1M KHCO ₃	90	3	37	6
C-CM2-02	0.1M NaCl	26	8	26	5
C-CM2-02	0.1M NaHCO ₃	61	12	26	6
C-F-03	0.1M CaCl ₂	37	7	21	4
C-F-03	0.1M KCl	36	10	21	3
C-F-03	0.1M KCl	36	10	21	3
C-F-03	0.1M MgCl ₂	26	7	20	4
C-F-03	0.1M MgCl ₂	44	14	24	3
C-F-03	0.1M NaCl	23	4	20	5
C-F-03	0.1M NaHCO ₃	41	17	33	12
C-F2-03	0.1M NaCl	91	32	55	6
C-F2-03	0.1M NaHCO ₃	94	16	57	7
C-F2-03	SSW	86	21	57	10
C-K-01	0.1M NaCl	101	19	67	14
C-K-01	0.1M NaHCO ₃	72	17	40	6
C-K-01	SSW	105	17	55	13
C-K2-02	0.1M NaHCO ₃	88	10	50	13
C-Kb-02	0.1M CaCl ₂			39	3

Crude Oil	Aqueous Phase	θ_A (deg)	<i>Std dev</i> θ_A (deg)	θ_R (deg)	<i>Std dev</i> θ_R (deg)
C-Kb-02	0.1M KHCO3	117	20	60	9
C-Kb-02	0.1M NaHCO3			29	5
Cottonwood-03	0.1M NaCl	84	16	36	6
Cottonwood-03	dist H2O	69	12	28	5
Cottonwood-03	SSW	70	27	34	5
Cottonwood-03	Ubergen	52	11	31	5
C-T-01	0.1M CaCl2	35	6	24	5
C-T-01	0.1M KCl	45	11	24	2
C-T-01	0.1M MgCl2	40	7	26	6
C-T-01	0.1M NaCl	47	5	28	6
C-T-03	0.1M NaCl	110	23	58	16
C-T-03	0.1M NaHCO3	70	27	47	18
C-T-03	SSW	73	25	38	7
E-1XD-00	0.1M NaCl	103	10	47	15
E-1XD-00	0.1M NaCl	119	13	35	8
E-1XD-00	0.1M NaCl	123	12	49	10
E-1XD-00	0.1M NaHCO3	124	10	28	5
E-1XD-00	0.1M NaHCO3	106	5	38	4
E-1XD-00	0.1M NaHCO3	127	12	37	21
E-1XD-00	0.1M NaHCO3	121	21	36	12
E-1XD-00	SSW	107	15	50	10
E-1XD-00	SSW	135	10	41	14
E-1XD-00	SSW	114	11	52	9
E-1XR-00	0.1M NaCl	106	6	36	7
E-1XR-00	0.1M NaHCO3	82	15	32	9
E-1XR-00	SSW	92	11	39	5
E-1XR-00	Ubergen	92	7	35	9
E-2XR-00	0.1M NaCl	133	17	40	5
E-2XR-00	0.1M NaHCO3	121	10	34	20
E-2XR-00	SSW	131	15	47	26
E-8XFR-01	0.1M NaCl	141	13	71	22
E-8XFR-01	0.1M NaHCO3	125	25	51	21
E-8XFR-01	SSW	83	41	48	19
E-BL-00	0.1M NaCl	65	22	27	7
E-BL-00	0.1M NaHCO3	30	12	24	6
E-BL-00	SSW	54	9	32	5
EJ-G-03	0.1M CaCl2	21	5	19	4

Crude Oil	Aqueous Phase	θ_A (deg)	<i>Std dev</i> θ_A (deg)	θ_R (deg)	<i>Std dev</i> θ_R (deg)
EJ-G-03	0.1M KCl			25	5
EJ-G-03	0.1M MgCl ₂	18	5	20	6
EJ-G-03	0.1M NaCl			31	4
E-S1XCA-01	0.1M NaCl	97	15	36	11
E-S1XCA-01	SSW	125	22	30	16
E-S1XG-01	0.1M CaCl ₂	28	4	21	3
E-S1XG-01	0.1M KCl	55	10	26	2
E-S1XG-01	0.1M MgCl ₂	40	10	21	4
E-S1XG-01	0.1M NaCl	46	12	22	4
E-S1XG-01	0.1M NaCl	100	17	43	8
E-S1XG-01	0.1M NaHCO ₃	33	11	32	15
E-S1XG-01	SSW	51	14	31	5
E-S1XL-01	0.1M CaCl ₂	85	14	24	2
E-S1XL-01	0.1M CaCl ₂	126	16	20	2
E-S1XL-01	0.1M MgCl ₂			17	3
E-S1XL-01	0.1M NaCl	73	8	23	2
E-S1XL-01	0.1M NaCl			22	4
E-S1XL-01	0.1M NaCl	64	21	42	12
E-S1XL-01	0.1M NaHCO ₃	114	19	39	7
E-S1XL-01	SSW	79	25	39	9
E-S3XR-01	0.1M NaCl	106	12	40	6
E-S3XR-01	0.1M NaHCO ₃	37	7	31	8
E-S3XR-01	SSW	69	16	39	8
Gullfaks-96	0.1M NaCl	104	15	45	8
Gullfaks-96	0.1M NaHCO ₃	109	10	63	7
Gullfaks-96	SSW	107	18	50	10
Gullfaks-96	Ubergen	89	8	46	17
Laggrave	0.1M NaCl	56	25	57	15
Laggrave	SSW	59	9	44	15
LB-03	{8, 0.01}	34	9	21	6
LB-03	{8, 0.1}	23	7	24	7
LB-03	{8, 1.0}	91	24	48	5
LB-03	0.1M CaCl ₂	52	12	35	4
LB-03	0.1M CaCl ₂	37	7	21	4
LB-03	0.1M KCl	54	5	31	4
LB-03	0.1M MgCl ₂	28	7	26	6
LB-03	0.1M NaCl	68	8	42	7

Crude Oil	Aqueous Phase	θ_A (deg)	<i>Std dev</i> θ_A (deg)	θ_R (deg)	<i>Std dev</i> θ_R (deg)
LB-03	0.1M NaCl	23	4	20	5
LB-03	0.1M NaCl	58	5	31	9
LB-03	0.1M NaHCO ₃	64	4	42	6
LB-03	0.1M NaHCO ₃	77	16	36	7
LB-03	0.1M NaHCO ₃	64	4	42	6
LB-03	0.1M NaHCO ₃	50	10	31	11
LB-03	SSW	49	8	36	5
LB-03	SSW	34	4	34	6
LB-03	Ubergen	54	7	34	7
Mars-97	0.1M NaCl	120	13	46	12
Mars-97	0.1M NaHCO ₃	124	7	39	12
Mars-97	SSW	91	19	41	7
Minnelusa-02	{10, 1.0}	53	9	42	4
Minnelusa-02	{11, 0.01}	19	3	19	2
Minnelusa-02	{6, 0.01}	23	5	23	4
Minnelusa-02	{6, 1.0}	65	7	43	7
Minnelusa-02	{7, 0.01}	22	5	20	3
Minnelusa-02	{8, 0.01}	28	4	29	7
Minnelusa-02	{8, 0.01}	17	2	19	3
Minnelusa-02	{8, 0.1}	18	3	18	3
Minnelusa-02	{8, 1.0}	59	7	32	5
Minnelusa-02	{8, 1.0}	19	3	21	5
Minnelusa-02	0.1M CaCl ₂	27	4	23	4
Minnelusa-02	0.1M NaCl	46	4	30	5
Minnelusa-02	0.1M NaHCO ₃	24	4	21	5
Minnelusa-02	SSW	33	6	29	4
Minnelusa-03	0.1M NaCl	48	13	44	7
Minnelusa-03	0.1M NaHCO ₃	32	6	31	5
Minnelusa-03	SSW	35	5	34	4
Minnesula-02	{8, 0.1}	18	3	18	3
Minnesula-02	0.1M NaHCO ₃	24	4	21	5
MY3-02	0.1M CaCl ₂	57	10	42	5
MY3-02	0.1M KCl	57	8	40	5
MY3-02	0.1M MgCl ₂	50	9	31	5
MY3-02	0.1M NaCl	131	13	47	9
MY4-02	0.1M CaCl ₂	50	7	32	3
MY4-02	0.1M KCl	44	11	37	4

Crude Oil	Aqueous Phase	θ_A (deg)	<i>Std dev</i> θ_A (deg)	θ_R (deg)	<i>Std dev</i> θ_R (deg)
MY4-02	0.1M MgCl2	42	18	31	6
MY4-02	0.1M NaCl	60	11	39	6
nC10	dist H2O	18	4	18	2
nC10	dist H2O	21	5	18	4
SQ-95	{10, 0.01}	64	6	27	8
SQ-95	{11, 0.01}	121	10	31	6
SQ-95	{6, 0.01}	44	7	23	3
SQ-95	{7, 0.01}	46	8	27	9
SQ-95	{8, 0.01}	76	14	28	9
SQ-95	{8, 0.01}-24h	159	5	17	2
SQ-95	{8, 0.01}-48h	18	4	16	3
SQ-95	{8, 0.01}-48h	59	11	22	4
SQ-95	{8, 0.01}-72h	18	3	16	2
SQ-95	{8, 0.1}	82	24	42	9
SQ-95	{8, 1.0}	144	10	76	12
SQ-95	{9, 0.01}	64	13	31	3
SQ-95	0.1M CaCl2	55	10	36	5
SQ-95	0.1M NaCl	70	10	45	8
SQ-95	0.1M NaHCO3	64	20	54	18
SQ-95	0.1M NaHCO3	85	15	46	8
SQ-95	0.1M NaHCO3	91	17	39	9
SQ-95	0.1M NaHCO3+ 0.005M Na2SO4	136	20	49	5
SQ-95	0.1M NaHCO3+ 0.01M Na2SO4	121	19	50	6
SQ-95	0.1M NaHCO3+ 0.005M Na2SO4	105	16	48	10
SQ-95	0.1M NaHCO3+ 0.01M Na2SO4	128	11	58	13
SQ-95	0.1M NaHCO3-24h	91	17	39	9
SQ-95	0.1M NaHCO-348h	119	25	48	8
SQ-95	SSW	101	29	53	7
Steen-NM-1	0.1M CaCl2	19	4	18	2
Steen-NM-1	0.1M KCl	24	3	23	3
Steen-NM-1	0.1M MgCl2	19	3	20	4
Steen-NM-1	0.1M NaCl	22	5	21	3
Steen-NM-2	0.1M CaCl2	45	8	27	5
Steen-NM-2	0.1M KCl	84	24	34	9
Steen-NM-2	0.1M MgCl2	73	3	38	4

Crude Oil	Aqueous Phase	θ_A (deg)	<i>Std dev θ_A</i> (deg)	θ_R (deg)	<i>Std dev θ_R</i> (deg)
Steen-NM-2	0.1M NaCl	63	14	27	6
Tensleep	0.1M KCl	78	9	37	6
Tensleep	0.1M MgCl ₂	55	6	33	7
Tensleep	0.1M NaCl	112	13	67	13
Tensleep	0.1M NaCl	90	14	43	9
Tensleep	0.1M NaCl	91	9	45	8
Tensleep	0.1M NaHCO ₃	96	36	48	18
Tensleep	0.1M NaHCO ₃	94	13	19	2
Ventura-Rice	0.1M NaHCO ₃	20	4	26	6
W-Pc-03	0.1M CaCl ₂	31	4	23	4
W-Pc-03	0.1M KCl	42	7	23	3
W-Pc-03	0.1M KCl	47	12	24	5
W-Pc-03	0.1M MgCl ₂	20	5	19	4
W-Pc-03	0.1M NaCl	38	8	22	4

Table A2. Contact angles on cleaved calcite after aging in crude oil (initially dry or wet with the same aqueous phase as that used to float off bulk oil).

Crude Oil	x = Initially Dry	Aging in Oil (days)	Aqueous Phase	Time after Flooding (hr)	θ_A (deg)	Std dev θ_A (deg)	drop size (mm)
C-A2-00	x	0.04	dist H2O	24	156	6	
C-A2-00		0.04	dist H2O	24	155	4	
C-A2-00	x	1	dist H2O	24	155	3	
C-A2-00		1	dist H2O	24	157	6	
C-Ab-01	x	0.04	dist H2O	24	136	4	
C-Ab-01		0.04	dist H2O	24	116	8	
C-Ab-01	x	1	dist H2O	24	105	14	
C-Ab-01		1	dist H2O	24	97	23	
C-AG-03	x	0.04	dist H2O	24	166		
C-AG-03		0.04	dist H2O	24	167		
C-AG-03	x	1	dist H2O	24	175		
C-AG-03		1	dist H2O	24	172		
C-B2-01	x	0.04	dist H2O	24	156		
C-B2-01		0.04	dist H2O	24	137		
C-B2-01	x	1	dist H2O	24	151		
C-B2-01		1	dist H2O	24	136	13	
C-BF-1A-04	x	0.04	dist H2O	24	134	15	
C-BF-1A-04		0.04	dist H2O	24	124	8	
C-BF-1A-04	x	1	dist H2O	24	92	6	
C-BF-1A-04		1	dist H2O	24	131	9	
C-Cap-04		0.04	dist H2O	24	117		
C-Cap-04	x	0.04	dist H2O	24	87		
C-Cap-04		1	dist H2O	24	80		
C-Cap-04	x	1	dist H2O	24	92		
C-CM2-02		6	0.1M NaHCO3	24	133	3	
C-CM2-02		0.04	dist H2O	24	106	2	
C-CM2-02	x	0.04	dist H2O	24	119	1	
C-CM2-02		1	dist H2O	24	101	12	
C-CM2-02	x	1	dist H2O	24	90	13	
C-F-03		0.125	0.00033M CaCl2	0.5	111		

Crude Oil	x = Initially Dry	Aging in Oil (days)	Aqueous Phase	Time after Flooding (hr)	θ_A (deg)	Std dev θ_A (deg)	drop size (mm)
C-F-03		0.125	0.00033M CaCl ₂	3	129		
C-F-03		0.125	0.001 M NaHCO ₃	0.5	64		0.3
C-F-03		0.125	0.001 M NaHCO ₃	0.5	71		<0.1
C-F-03		0.04	0.01M CaCl ₂	3	20		
C-F-03		0.04	0.01M CaCl ₂	0.5	103		
C-F-03		0.125	0.01M CaCl ₂	24	0		
C-F-03		0.125	0.01M CaCl ₂	24	70		
C-F-03		0.5	0.01M CaCl ₂	8	120		
C-F-03		0.04	0.01M NaCl	24	79		1.5
C-F-03	x	0.04	0.01M NaCl	24	65		2.5
C-F-03		0.125	0.01M NaCl	3	103		
C-F-03		0.125	0.01M NaCl	0.5	108		
C-F-03		21	0.1M MgCl ₂	24	172		
C-F-03		21	0.1M NaCl	24	160		
C-F-03		28	0.1M NaCl	24	156		3.5
C-F-03		0.04	1.0M CaCl ₂	3	27		
C-F-03		0.04	1.0M CaCl ₂	0.5	56		
C-F-03		0.125	1.0M CaCl ₂	24	84		
C-F-03		0.125	1.0M CaCl ₂	24	107		
C-F-03		0.5	1.0M CaCl ₂	24	88		
C-F-03		0.5	1.0M CaCl ₂	8	110		
C-F-03		0.04	1.0M NaHCO ₃	0.5	29		<0.1
C-F-03		0.125	1.0M NaHCO ₃	0.5	61		1.8
C-F-03		0.42	1.0M NaHCO ₃	3	108		2
C-F-03		0.04	dist H ₂ O	24	86		0.7
C-F-03	x	0.04	dist H ₂ O	24	94		3.3
C-F-03	x	0.04	dist H ₂ O	24	75	5	
C-F-03		0.04	dist H ₂ O	24	103	14	
C-F-03	x	0.04	dist H ₂ O	24	59		1.8

Crude Oil	x = Initially Dry	Aging in Oil (days)	Aqueous Phase	Time after Flooding (hr)	θ_A (deg)	Std dev θ_A (deg)	drop size (mm)
C-F-03	x	0.04	dist H2O	24	108		1.3
C-F-03		0.125	dist H2O	24	132		
C-F-03	x	0.125	dist H2O	24	89		
C-F-03		0.25	dist H2O	24	124		6.0
C-F-03	x	0.25	dist H2O	24	158		5.1
C-F-03		0.5	dist H2O	24	150		5.4
C-F-03	x	0.5	dist H2O	24	147		5.4
C-F-03		1	dist H2O	24	114	16	
C-F-03		1	dist H2O	24	129	16	
C-F-03		1	dist H2O	24	149		7.8
C-F-03	x	1	dist H2O	24	155	6	
C-F-03	x	1	dist H2O	24	107	19	
C-F-03	x	1	dist H2O	24	159		8.0
C-F-03		0.04	NaCl, 1.0M	0.5	86		1.2
C-F-03		0.125	NaCl, 1.0M	3	137		3.5
C-F-03		0.42	NaCl, 1.0M	3	120		2.0
C-F-03-maltene	x	1	dist H2O	24	35	1	
C-F-03-maltene	x	1	dist H2O	24	94	12	
C-F-03-maltene		1	dist H2O	24	115	15	
C-F-03-maltene		1	dist H2O	24	49	6	
C-GC-T1-03	x	0.04	dist H2O	24	69	13	
C-GC-T1-03		0.04	dist H2O	24	85	9	
C-GC-T1-03	x	1	dist H2O	24	92	11	
C-GC-T1-03		1	dist H2O	24	122	28	
C-GC-T2-03	x	0.04	dist H2O	24	67		
C-GC-T2-03		0.04	dist H2O	24	68		
C-GC-T2-03	x	1	dist H2O	24	155		
C-GC-T2-03		1	dist H2O	24	153		
C-GGC-00	x	0.04	dist H2O	24	168		
C-GGC-00		0.04	dist H2O	24	114		
C-GGC-00	x	1	dist H2O	24	135		
C-GGC-00		1	dist H2O	24	139		
C-HM-01	x	0.04	dist H2O	24	51		
C-HM-01		0.04	dist H2O	24	50		

Crude Oil	x = Initially Dry	Aging in Oil (days)	Aqueous Phase	Time after Flooding (hr)	θ_A (deg)	Std dev θ_A (deg)	drop size (mm)
C-HM-01	x	1	dist H2O	24	86		
C-HM-01		1	dist H2O	24	67		
C-K2-02	x	0.04	dist H2O	24	85	4	
C-K2-02		0.04	dist H2O	24	135	14	
C-K2-02		1	dist H2O	24	120	6	
C-K2-02	x	1	dist H2O	24	80	12	
C-Kb-02		6	0.1M NaHCO3	24	146		
C-Kb-02		6	0.1M NaHCO3	24	139		
C-Lb-01	x	0.04	dist H2O	24	120		
C-Lb-01		0.04	dist H2O	24	61		
C-Lb-01	x	1	dist H2O	24	152		
C-Lb-01		1	dist H2O	24	152		
C-LH-99	x	0.04	dist H2O	24	80		
C-LH-99		0.04	dist H2O	24	67		
C-LH-99	x	1	dist H2O	24	95		
C-LH-99		1	dist H2O	24	135		
C-R-00		0.04	dist H2O	24	161	2	
C-R-00		0.04	dist H2O	24	140		
C-R-00	x	0.04	dist H2O	24	100	11	
C-R-00	x	0.04	dist H2O	24	119		
C-R-00	x	1	dist H2O	24	173		
C-R-00	x	1	dist H2O	24	156	2	
C-R-00		1	dist H2O	24	159	7	
C-R-00		1	dist H2O	24	142	2	
C-R-01		0.04	dist H2O	24	114		
C-R-01	x	0.04	dist H2O	24	123		
C-R-01	x	1	dist H2O	24	152		
C-R-01		1	dist H2O	24	159		
C-T-02	x	0.04	dist H2O	24	156	12	
C-T-02		0.04	dist H2O	24	153		
C-T-02		0.04	dist H2O	24	135	10	
C-T-02	x	0.04	dist H2O	24	171		
C-T-02	x	1	dist H2O	24	152		

Crude Oil	x = Initially Dry	Aging in Oil (days)	Aqueous Phase	Time after Flooding (hr)	θ_A (deg)	Std dev θ_A (deg)	drop size (mm)
C-T-02	x	1	dist H2O	24	157	8	
C-T-02		1	dist H2O	24	150		
C-T-02		1	dist H2O	24	162	2	
C-WB-03	x	0.04	dist H2O	24	103		
C-WB-03		0.04	dist H2O	24	89		
C-WB-03	x	1	dist H2O	24	152		
C-WB-03		1	dist H2O	24	154		
DS-P-01	x	0.04	dist H2O	24	129		
DS-P-01		0.04	dist H2O	24	119		
DS-P-01	x	1	dist H2O	24	146		
DS-P-01		1	dist H2O	24	159		
E-1XD-00		56	0.1M NaCl	24	151		
E-1XD-00	x	0.04	dist H2O	24	157		
E-1XD-00		0.04	dist H2O	24	149		
E-1XD-00	x	1	dist H2O	24	163		
E-1XD-00		1	dist H2O	24	167		
E-1XFR-01	x	0.04	dist H2O	24	172		
E-1XFR-01		0.04	dist H2O	24	173	2	
E-1XFR-01	x	1	dist H2O	24	167		
E-1XFR-01		1	dist H2O	24	161		
E-1XO-00	x	0.04	dist H2O	24	130		
E-1XO-00		0.04	dist H2O	24	111		
E-1XO-00	x	1	dist H2O	24	145		
E-1XO-00		1	dist H2O	24	136		
E-1XR-00		0.04	dist H2O	24	152	12	
E-1XR-00	x	0.04	dist H2O	24	146	9	
E-1XR-00	x	1	dist H2O	24	163	1	
E-1XR-00		1	dist H2O	24	160	4	
E-2XR-00	x	0.04	dist H2O	24	119	9	
E-2XR-00		0.04	dist H2O	24	167	6	
E-2XR-00	x	1	dist H2O	24	129	2	
E-2XR-00		1	dist H2O	24	168	3	
E-8XFR-01	x	0.04	dist H2O	24	174	2	
E-8XFR-01		0.04	dist H2O	24	168	7	

Crude Oil	x = Initially Dry	Aging in Oil (days)	Aqueous Phase	Time after Flooding (hr)	θ_A (deg)	Std dev θ_A (deg)	drop size (mm)
E-8XFR-01	x	1	dist H2O	24	169	4	
E-8XFR-01		1	dist H2O	24	168	1	
E-BL-00		0.04	dist H2O	24	116	7	
E-BL-00	x	0.04	dist H2O	24	127	10	
E-BL-00		1	dist H2O	24	150	5	
E-BL-00	x	1	dist H2O	24	142	6	
EJ-G-03		21	0.1M CaCl2	24	170		
EJ-G-03		21	0.1M KCl	24	180		
EJ-G-03		7	0.1M MgCl2	24	137		
EJ-G-03		7	0.1M NaCl	24	180		
E-S1XCA-01	x	0.04	dist H2O	24	170	2	
E-S1XCA-01		0.04	dist H2O	24	168	2	
E-S1XCA-01		1	dist H2O	24	157	7	
E-S1XCA-01	x	1	dist H2O	24	161	7	
E-S1XG-01		0.04	dist H2O	24	130	14	
E-S1XG-01	x	0.04	dist H2O	24	154	9	
E-S1XG-01		1	dist H2O	24	151	11	
E-S1XG-01	x	1	dist H2O	24	146	9	
E-S1XL-01		21	0.1M MgCl2	24	172		
E-S3XR-01	x	0.04	dist H2O	24	120	7	
E-S3XR-01		0.04	dist H2O	24	123	11	
E-S3XR-01	x	1	dist H2O	24	153	5	
E-S3XR-01		1	dist H2O	24	148	8	
LB-03		28	0.1M NaCl	24	180		
LB-03		28	0.1M NaCl	24	94		0.4
LB-03		28	0.1M NaCl	24	165		2.2
LB-03		28	0.1M NaCl	24	160		1.6
LB-03		21	0.1M NaHCO3	24	86		
LB-03		21	0.1M NaHCO3	24	86		1.0
LB-03		21	0.1M NaHCO3	24	156		
LB-03		21	0.1M NaHCO3	24	151		3.0
LB-03	x	0.04	dist H2O	24	157		

Crude Oil	x = Initially Dry	Aging in Oil (days)	Aqueous Phase	Time after Flooding (hr)	θ_A (deg)	Std dev θ_A (deg)	drop size (mm)
LB-03		0.04	dist H2O	24	134		
LB-03	x	1	dist H2O	24	166		
LB-03		1	dist H2O	24	165		
LB-03-maltene	x	1	dist H2O	24	154	3	
LB-03-maltene		1	dist H2O	24	103	0	
Mars-P		0.04	dist H2O	24	77		
Mars-P	x	0.04	dist H2O	24	90		
Mars-P		1	dist H2O	24	101		
Mars-P	x	1	dist H2O	24	113		
Minnelusa-02		0.04	0.1M NaCl	24	34		0.3
Minnelusa-02		0.04	0.1M NaCl	24	90		0.7
Minnelusa-02		0.04	0.1M NaCl	24	105	17	0.5
Minnelusa-02		0.04	0.1M NaCl	24	98		0.8
Minnelusa-02		0.04	0.1M NaHCO3	24	23	2	0.1
Minnelusa-02		0.04	0.1M NaHCO3	24	34		0.5
Minnelusa-02		1	0.1M NaHCO3	24	43	10	
Minnelusa-02	x	0.04	dist H2O	24	46		
Minnelusa-02		0.04	dist H2O	24	56		
Minnelusa-02		0.25	dist H2O	24	158		
Minnelusa-02		0.25	dist H2O	24	106		
Minnelusa-02		0.5	dist H2O	24	175		
Minnelusa-02		1	dist H2O	24	108	3	0.6
Minnelusa-02		1	dist H2O	24	78	0	0.5
Minnelusa-02		1	dist H2O	24	91	0	2.5
Minnelusa-02		1	dist H2O	24	77		
Minnelusa-02	x	1	dist H2O	24	79		
Minnelusa-02		3	dist H2O	24	180		
Minnelusa-02-m	x	1	dist H2O	24	56	1	
Minnelusa-02-m		1	dist H2O	24	103	10	
SQ-95		0.04	{10, 0.01}	24	103	1	
SQ-95		0.125	{10, 0.01}	24	143	10	
SQ-95		0.04	{7, 0.01}	24	100	6	
SQ-95		0.04	{9, 0.01}	24	95	21	

Crude Oil	x = Initially Dry	Aging in Oil (days)	Aqueous Phase	Time after Flooding (hr)	θ_A (deg)	Std dev θ_A (deg)	drop size (mm)
SQ-95		0.125	{9, 0.01}	24	117	6	
SQ-95		1	{9, 0.01}	24	99	4	
SQ-95		150	0.001M Na ₂ CO ₃	24	170	3	
SQ-95		150	0.01M Na ₂ CO ₃	24	180		
SQ-95		150	0.01M Na ₂ CO ₃	24	159		
SQ-95		150	0.1M Na ₂ CO ₃	24	180		
SQ-95	x	0.04	dist H ₂ O	24	108	6	
SQ-95	x	1	dist H ₂ O	24	123	8	
SQ-95		1	dist H ₂ O	24	172		
Steen-NM-1		0.04	dist H ₂ O	24	101		
Steen-NM-1	x	0.04	dist H ₂ O	24	50		
Steen-NM-1		1	dist H ₂ O	24	128		
Steen-NM-1	x	1	dist H ₂ O	24	96		
Steen-NM-2	x	0.04	dist H ₂ O	24	121		
Steen-NM-2		0.04	dist H ₂ O	24	94		
Steen-NM-2	x	1	dist H ₂ O	24	113		
Steen-NM-2		1	dist H ₂ O	24	120		
Steen-OLEOD	x	0.04	dist H ₂ O	24	57		
Steen-OLEOD		0.04	dist H ₂ O	24	59		
Steen-OLEOD	x	1	dist H ₂ O	24	56		
Steen-OLEOD		1	dist H ₂ O	24	75		
Tensleep-99	x	0.04	dist H ₂ O	24	98	1	
Tensleep-99		0.04	dist H ₂ O	24	98	25	
Tensleep-99		1	dist H ₂ O	24	155	13	
Tensleep-99	x	1	dist H ₂ O	24	127	3	
T-VJ487-05-01-m	x	1	dist H ₂ O	24	79		
T-VJ487-05-01-m		1	dist H ₂ O	24	51	11	
T-VJ487-05-1		0.04	dist H ₂ O	24	45		
T-VJ487-05-1	x	0.04	dist H ₂ O	24	39		
T-VJ487-05-1		1	dist H ₂ O	24	46		
T-VJ487-05-1	x	1	dist H ₂ O	24	78		
T-VJ488-05-01-m	x	1	dist H ₂ O	24	120	15	

Crude Oil	x = Initially Dry	Aging in Oil (days)	Aqueous Phase	Time after Flooding (hr)	θ_A (deg)	Std dev θ_A (deg)	drop size (mm)
T-VJ488-05-01-m		1	dist H2O	24	136	8	
T-VJ488-05-1		0.04	dist H2O	24	49		
T-VJ488-05-1	x	0.04	dist H2O	24	58		
T-VJ488-05-1		1	dist H2O	24	72		
T-VJ488-05-1	x	1	dist H2O	24	84		
UNAM	x	0.04	dist H2O	24	119	13	
UNAM		0.04	dist H2O	24	161	4	
UNAM	x	1	dist H2O	24	145	8	
UNAM		1	dist H2O	24	156	3	
Uwyo-E-04		0.04	dist H2O	24	87	10	
Uwyo-E-04	x	0.04	dist H2O	24	34	4	
Uwyo-E-04	x	1	dist H2O	24	60	10	
Uwyo-E-04		1	dist H2O	24	114	15	
Uwyo-E-04-m		1	dist H2O	24	108	10	
Uwyo-E-04-m	x	1	dist H2O	24	75	10	
Uwyo-M-04	x	0.04	dist H2O	24	68	19	
Uwyo-M-04		0.04	dist H2O	24	97	12	
Uwyo-M-04	x	1	dist H2O	24	164	3	
Uwyo-M-04		1	dist H2O	24	163	4	
Uwyo-M-04	x	1	dist H2O	24	82	4	
Uwyo-M-04		1	dist H2O	24	92	13	
Uwyo-M-04-m	x	1	dist H2O	24	81	24	
Uwyo-M-04-m	x	1	dist H2O	24	113	5	
Uwyo-M-04-m		1	dist H2O	24	94	5	
Uwyo-M-04-m		1	dist H2O	24	99	12	
W-Az-03	x	0.04	dist H2O	24	164	4	
W-Az-03		0.04	dist H2O	24	145	4	
W-Az-03		1	dist H2O	24	133	18	
W-Az-03	x	1	none	24	139	6	
W-Ch-03		0.04	dist H2O	24	93	4	
W-Ch-03	x	0.04	dist H2O	24	92	4	
W-Ch-03		1	dist H2O	24	137	13	
W-Ch-03	x	1	none	24	153	3	
W-Da-03	x	0.04	dist H2O	24	162	4	

Crude Oil	x = Initially Dry	Aging in Oil (days)	Aqueous Phase	Time after Flooding (hr)	θ_A (deg)	Std dev θ_A (deg)	drop size (mm)
W-Da-03		0.04	dist H2O	24	125	5	
W-Da-03	x	1	dist H2O	24	149	5	
W-Da-03		1	dist H2O	24	162	6	
W-Lo-03		0.04	dist H2O	24	66	5	
W-Lo-03		0.04	dist H2O	24	115	10	
W-Lo-03	x	0.04	dist H2O	24	78	6	
W-Lo-03	x	0.04	dist H2O	24	78		
W-Lo-03		1	dist H2O	24	119	9	
W-Lo-03		1	dist H2O	24			
W-Lo-03		1	dist H2O	24	110	7	
W-Lo-03		1	dist H2O	24	129		
W-Lo-03	x	1	dist H2O	24	111	10	
W-Lo-03	x	1	dist H2O	24	108	5	
W-Lo-03	x	1	dist H2O	24	83	26	
W-Lo-03	x	1	dist H2O	24	155		
W-Mi-01	x	0.04	dist H2O	24	180		
W-Mi-01		0.04	dist H2O	24	168		
W-Mi-01	x	1	dist H2O	24	173		
W-Mi-01		1	dist H2O	24	173		
W-Mr-03	x	0.04	dist H2O	24	146		
W-Mr-03		0.04	dist H2O	24	114		
W-Mr-03	x	1	dist H2O	24	180		
W-Mr-03		1	dist H2O	24	180		
W-Mr-03-m	x	1	dist H2O	24	164	2	
W-Mr-03-m		1	dist H2O	24	164	6	
W-Pc-03		0.04	dist H2O	24	83	7	
W-Pc-03	x	0.04	dist H2O	24	82	7	
W-Pc-03		1	dist H2O	24	151	6	
W-Pc-03	x	1	dist H2O	24	153	15	
W-Sc-03	x	0.04	dist H2O	24	85	5	
W-Sc-03		0.04	dist H2O	24	89	18	
W-Sc-03	x	1	dist H2O	24	65	10	
W-Sc-03		1	dist H2O	24	101	25	
W-Sch-04		0.04	dist H2O	24	105	19	

Crude Oil	x = Initially Dry	Aging in Oil (days)	Aqueous Phase	Time after Flooding (hr)	θ_A (deg)	Std dev θ_A (deg)	drop size (mm)
W-Sch-04	x	0.04	dist H2O	24	81	9	
W-Sch-04	x	1	dist H2O	24	122	4	
W-Sch-04		1	dist H2O	24	54	4	
W-Sk-04	x	0.04	dist H2O	24	151		
W-Sk-04		0.04	dist H2O	24	124		
W-Sk-04	x	1	dist H2O	24	169		
W-Sk-04		1	dist H2O	24	166		
W-TH-05	x	0.04	dist H2O	24	60		
W-TH-05		0.04	dist H2O	24	47		
W-TH-05	x	1	dist H2O	24	77		
W-TH-05		1	dist H2O	24	51		
W-Ur-01	x	0.04	dist H2O	24	163		
W-Ur-01		0.04	dist H2O	24	155		
W-Ur-01	x	1	dist H2O	24	180		
W-Ur-01		1	dist H2O	24	171		

Task 2: *Rock selection and wettability control*

Hongguang Tie and Norman R. Morrow, Chemical and Petroleum Engineering,
University of Wyoming

Part I: Rock Selection and Characterization

Six outcrop limestone rocks that span four orders of magnitude in permeability and vary by a factor of three in porosity were selected from a range of available outcrop carbonates. Selected rocks were characterized by thin section microscopy, scanning electron microscopy (SEM), BET surface area, cation exchange capacity (CEC), mercury injection, BJH analysis, water adsorption/desorption isotherms, and laboratory measurements of porosity and permeability. Three of the selected rocks were classified as homogeneous and the others as heterogeneous on the basis of variation in permeability of $1\frac{1}{2}''(D)\times 2\frac{1}{2}''(L)$ cores cut from $12''\times 12''\times 6''$ blocks. Combined data from the selected characterization methods provided comprehensive petrophysical description of the selected limestones. Thin section and SEM analyses showed huge differences in pore size, shape, throat aperture distribution, structure, and origin among the tested limestone rocks. The rock surfaces, however, all appeared to be covered by calcite crystals. Three rocks, two homogeneous and one heterogeneous, were selected for study of wetting alteration and oil recovery behavior.

Introduction

Wettability and oil recovery related research on carbonate rocks has been hampered by the lack of a widely accepted model rock. Unlike sandstones, carbonates normally exhibit higher degrees of heterogeneity even at the core scale. During deposition, carbonate sediments normally have about 40 to 70% porosity (Choquette and Pray, 1970). This porosity is called the primary porosity with interparticle pores usually being dominant. Depending on the origin of the sediments, intraparticle porosity can also be abundant. Extensive diagenetic changes significantly alter the size, shape, and structure of pores in carbonates. Normally, cementation, mechanical and chemical compaction, and dolomitization reduce the porosity, while dissolution and fracturing enhance or create porosity (Moore, 1989). Cementation and dissolution are generally two of the most important processes. Through diagenesis, reduction in carbonate porosities to below 30% is common for typical ancient carbonates (Halley, 1987) and the types of porosity can vary widely. Identification of different types of porosity is usually achieved by thin section and SEM analyses. However, visual estimation of porosity and permeability through thin sections does not always provide satisfactory results due to the nature of carbonate pore system. Laboratory core analysis measurements are also required.

In wettability studies, having rock samples at a very strongly water-wet wetting state provides an important starting point and reference state. Reservoir carbonates, which are commonly oil-wet or intermediate-wet, however, are almost impossible to clean to a strongly water-wet condition without causing change in pore structure (Cuiec *et al.*, 1979; Gant and Anderson, 1988). One major advantage of working with outcrop rocks is that they are typically, although not always, very strongly water-wet.

Two outcrop carbonate rocks, Indiana limestone and Baker dolomite, have been used previously in oil recovery research. However, Churcher *et al.* (1991) reported that Indiana limestone showed large variations in both porosity (12.1 to 21.1%) and permeability (4 to 57 mD) for the three tested samples. The two Baker dolomite samples, other than showing porosity difference, appeared to have thin layers of organic acids absorbed on the rock surfaces. Boneau and Clampitt (1977) performed Amott-Harvey wettability index measurement on a selection of Baker dolomite samples and obtained values ranging from 0.41 to 0.69. Very strongly water-wet rocks would have an index of unity. Churcher *et al.* (1991) obtained comparable values of Amott Index to water and recommended extraction with a chloroform/methanol mixture for Baker dolomite samples to obtain uniform wetting before using them in flow experiments but did not test this recommendation.

In this work, six readily available limestone outcrop rocks were selected for petrophysical characterization through thin section, SEM, BET surface area, cation exchange capacity (CEC) measurements, mercury injection, BJH analysis, water adsorption/desorption isotherms, and porosity and permeability measurements. Three of the limestones provided wide variation in permeability, porosity, pore type and size distribution and were selected for detailed studies of wettability and oil recovery.

Sample Selection and Analysis

Rock Sample Selection

A wide range of outcrop carbonate rock samples collected from the U.S., Canada, and Australia, were prescreened for further study. Selection of rocks was based on pre-characterization results. Six limestone rocks, Gambier, Edwards (Garden City), Whitestone Upper Zone, Lueders, Whitestone Lower Zone, and Fort Riley, were chosen for detailed analysis.

Rock Characterization

All the selected outcrop carbonates were characterized by a set of petrophysical analyses and measurements.

Thin Section

A thin section is prepared by impregnation of a rock sample with epoxy resin. It is a thin slice of rock of about 28 μ thickness (at this thickness, the quartz crystals become clear through transmitted light under a petrographic microscope) with all pore spaces filled with colored resin, usually blue. Thin section analysis is one of the most powerful tools in analyzing rock mineralogy, composition, texture, and pore sizes and their distribution with respect to each other. Thin section analysis requires the use of a petrographic microscope at various magnifications.

Scanning Electron Microscopy (SEM)

SEM is capable of providing detailed information on 3D rock structure at magnifications much higher than the limitation set by the wavelength of light for optical microscopes. SEM uses high energy electron beams to map 3D structure. Freshly broken rock surfaces are usually examined. With the aid of SEM technology, small structures such as the

location and form of clay minerals in a sandstone rock can be investigated in detail. In carbonate rocks SEM micrographs can be used to examine detailed fossil structures and fine intraparticle porosity.

BET Surface Area

BET surface area (Brunauer *et al.*, 1938), i.e., total surface area, is based on surface adsorption of gas and is usually measured with N₂. It can also be obtained using other gases such as helium or krypton but results will vary with molecular size. It has been reported that BET surface areas measured using krypton are about 30% lower than using nitrogen (Brantley and Mellot, 2000). BET surface areas can provide useful indications of the microstructure of rocks.

Cation Exchange Capacity

CEC is the quantity of positively charged ions that a clay mineral or similar material can accommodate on its surface. It is usually expressed as milliequivalent (meq) per 100g. During measurement, cations are usually replaced by ammonium acetate at a pH of 7.0. The concentration of displaced cations is then determined by atomic absorption spectrophotometry. CEC values are important in determination of the volume of clay in shaly sands (Bassiouni, 1994). The volume of clay plays an essential role in the correction of porosity obtained through spontaneous potential (SP), gamma ray, and neutron density logs. The CEC on carbonate samples was measured to confirm the lack of clays.

Mercury Injection Capillary Pressure Analysis

Mercury injection is a standard analytical method for characterization of porous materials. In mercury injection capillary pressure analysis, non-wetting phase (clean mercury) is injected into an evacuated and cleaned/dried rock sample at pressure increments up to 60,000 psi. The volume of mercury injected at each pressure increment is recorded up to the maximum value of the tests. If no further injection is achieved by raising the pressure it is usually assumed that 100% mercury saturation has been achieved. The injection process can be reversed to obtain a non-wetting phase imbibition curve but the measured capillary imbibition pressures are highly sensitive to contact angle. In the petroleum industry, mercury injection capillary pressure analysis provides important information on evaluation of reservoir lithologies, cap rock sealing capacity, and intra-formational and fault seals. Raw data obtained through mercury injection is used to obtain pore-throat aperture size distributions (meso- (2.1 nm to 53 nm) to macro-pores (>53 nm)).

BJH Adsorption Isotherms

BJH analysis (Barrett *et al.*, 1951) is used to obtain pore size in the micro- (<2.1 nm) to meso- range from nitrogen adsorption isotherms measured at -196°C. The theory is based on a model of the porous medium as a collection of cylindrical pores. The interpretation also assumes a hemispherical liquid-vapor meniscus and a well-defined surface tension.

Water Adsorption/Desorption Isotherms

Water adsorption/desorption isotherms for materials such as soils are often obtained with use of sulphuric acid to control humidity of closed chambers. Fischer *et al.* (2005)

developed a safer and highly reliable approach to control humidity by substituting sulphuric acid, which is highly corrosive and requires special care in handling, by glycerol. Results obtained by surface adsorption and capillary condensation give reliable estimation of pore size distributions in the micro- to meso- range.

Porosity and Permeability Measurements

Porosity and permeability from the reservoir engineering perspective are the two most important parameters of oil and gas reservoirs. Porosity is usually obtained through vacuum saturation with liquid, usually brine or oil. Permeability can be measured to either gas, usually N₂, or to a liquid such as brine or oil. Gas permeability measurements using N₂ were made for all of the core samples used in the present work unless otherwise specified.

Results and Discussion

Over ten outcrop carbonates were selected for laboratory characterization. Petrophysical analysis showed that some of the samples did not meet the experimental needs due to various reasons. For example, the Canadian #2 sample was too porous, and the grains were too loosely packed (Fig. 2.1) to maintain mechanical stability in laboratory measurements. After careful consideration of the petrophysical properties of the available outcrop limestones, six were chosen for wettability and oil recovery research. Among the selected limestones, three were found to be homogeneous at the core scale, Gambier, Edwards (Garden City), and Lueders limestones, and the others, Whitestone Upper Zone, Whitestone Lower Zone, and Fort Riley limestones, were heterogeneous. Determination of homogeneity/heterogeneity was based on permeability measurements on cores cut from 12"×12"×6" blocks. Five of the selected rocks are traditionally used as building stone and are readily available at low cost. Among the six selected limestone rocks, Gambier, Edwards (Garden City), and Whitestone Upper Zone limestones, were chosen for detailed studies of wettability alteration and oil recovery behavior through spontaneous imbibition and viscous displacement studies.

Gambier Limestone

Gambier limestone is a very high porosity and permeability outcrop carbonate rock quarried from Mount Gambier, Australia. The rock is of Oligocene-age and is classified as a reef boundstone according to Dunham's carbonate rock classification (Dunham, 1962). Thin sections showed that the main components of this rock are well-preserved coral fossil fragments at various orientations (Fig. 2.2). Coarse sparry calcite crystals can also be identified. SEM micrographs revealed the 3D structure of the coral fossils; there was abundant porosity given by chambers within the fossils (Fig. 2.3). Although the pore structures are complicated, the pore linings are pure calcite crystals. The porosity of this limestone rock is composed of two types: intraparticle (pores inside the fossil fragments) and interparticle (pores between the fossil fragments). In the absence of cementation and mechanical compaction, both intraparticle and interparticle porosities are highly preserved. The coral reef chambers in each fossil even featured separate values of drainage entry pressures based on two-phase epoxy displacement techniques (S. Seth, 2005, personal communication). Laboratory measured porosity was around 54% for the tested samples and permeability about 4000 mD. Such high values of porosity and

permeability greatly reduce the amount of time needed for spontaneous imbibition experiments and make the rock particularly easy to work with, especially at wetting states other than strongly water-wet. On the other hand, because of the high porosity and permeability and the early stage of formation, this rock is far removed from most of the wide variety of rocks types that make up carbonate reservoirs. Mercury injection data is not yet available. The percentage of micro- to meso-pores is about 0.5% from water adsorption/desorption analysis (Fischer *et al.*, 2005).

Edwards (Garden City) Limestone

Edwards (Garden City), abbreviated as Edwards (GC), is a limestone rock that has been widely used as a building stone. It is also referred to as West Texas Crème/Cream, Cedar Hill Cream, and Valencia Ivory. Several famous buildings, such as the San Angelo Fine Arts Museum, San Angelo, Texas, and the St. Stephens Catholic Church, Midland, Texas, are built primarily with this rock. Edwards (GC) is quarried from a member of the Edwards Formation near Garden City, Texas. Because the Edwards limestone can be found in outcrop on numerous locations across Texas, it is identified by the name of the formation plus the city. The Edwards is a grainstone (Dunham, 1962) that contains well-sorted fossil shells cemented by sparry calcite (Fig. 2.4). The porosity of this rock includes intraparticle, moldic, and a minor amount of intercrystal porosities. Interparticle porosity is almost completely diminished through cementation with blocky calcite cement (Choquette and Pray, 1970; James and Choquette, 1984; Choquette and James, 1987; Scholle and Ulmer-Scholle, 2003). In classification aligned to reservoir engineering, much of the pore space is vugular and includes both touching and separate vugs (Lucia, 1983 and 1995). Very little porosity can be detected inside the fossil shells and between the calcite crystals indicating a lack of microporosity. It can be seen from the SEM micrographs (Fig. 2.5) that the internal surfaces of the rock are all occupied by calcite crystals of various sizes. These observations indicate that the rock surface chemistry should be relatively simple even though the rock surfaces are rough. Results from water adsorption/desorption isotherms (Fischer *et al.*, 2005) and BJH analysis (Fig. 2.19) demonstrated a low percentage of pore throats in the micro- to meso- range. SEM photos also revealed pore bodies of size 200 to 300 μ in diameter connected by about 5 μ channels (Fig. 2.5). Pore throat size distribution from the combined results of mercury injection and BJH analysis indicate that the highest frequency of pore sizes is around 5 μ , which confirms the interpretation of SEM micrographs (Fig. 2.6). (The double distribution peaks seen in the pore size distribution plot are probably an artifact of the mercury injection experiments, because it coincides with the pressure at which the injection cell was changed.) It can be seen that Edwards (GC) rock has a relatively narrow throat size distribution with almost all pores in the range of 0.1 to 10 μ and most in the 1 to 10 μ range. The huge difference between the sizes of pore bodies and throats results in an aspect ratio in the range of 50 to 60.

Whitestone Upper Zone Limestone

Whitestone Upper Zone limestone, abbreviated as Whitestone UZ, is quarried from the upper bench of the Whitestone Member of the Lower Cretaceous Walnut Formation, Texas. It is also known as Texas Crème/Cream building stone. This rock is a grainstone (Dunham, 1962) and contains mostly well-sorted fossil shells cemented by sparry calcite

(Fig. 2.7). Standard petrophysical properties indicate Whitestone UZ is distinctly heterogeneous within a single 12"×12"×6" block and from one block to another even at the core scale. Cores obtained from one block show air permeability variation from <1 mD to >30 mD and porosity variation from 18.9% to 26.4%. Two types of porosities are dominant in this rock: moldic and intercrystal (Figs. 2.7 and 2.8). It can be seen from the SEM photomicrographs that although the pores in Whitestone UZ may be of smaller dimensions and more complicated shapes, there appear to be more connections between individual pores. The aspect ratio is much smaller due to the smaller pore sizes. As for the two homogeneous limestones discussed above, the internal pore surfaces of Whitestone UZ are lined with calcite crystals. Therefore, although the three selected limestone rocks have higher degrees of complexity in pore size, shape, and connections, unlike most sandstones, they have simpler surface chemistry.

Comparison of mercury injection capillary pressure curves for Whitestone UZ and Edwards (GC) (Fig. 2.9) showed that Whitestone UZ has an entry pressure of about an order of magnitude higher than Edwards (GC) indicating much smaller pores. Unlike Edwards (GC) limestone, Whitestone UZ did not exhibit a plateau in the mid-saturation range. The higher slope for Whitestone UZ relative to that for Edwards (GC) indicates a wider distribution of pore sizes. Pore size distribution obtained through a combination of results from mercury injection and BJH analysis showed that Whitestone UZ has pore sizes in the range from 10 nm to about 2 μ , with peaks at 300 nm and 1 μ (Fig. 2.10). Water adsorption/desorption isotherms showed more than 2% micro- to meso-porosity in Whitestone UZ as compared to 0.5% for the Edwards (GC) limestone (Fischer *et al.*, 2005).

Lueders Limestone

Lueders limestone rock is quarried from the Permian Lueders Formation. In the building stone business, it is referred to as Texas Lueders. From thin sections, this rock is a grainstone (Dunham, 1962) that contains shell fragments, pellets and calcite cements (Fig. 2.11). It has complex pore structure. Moldic pores that formed by dissolution of fossil fragments are dominant in this rock. Local changes in porosity can be easily identified from thin sections, but the overall measurements of permeability show only minimal variations from core to core for one 12"×12"×6" block. The measured N₂ permeability is about 2 mD. This rock is of grayish color and is composed almost completely of calcite minerals. As for the three limestone rocks already discussed, the internal surfaces of the pores are lined by calcite crystals of various sizes (Fig. 2.12).

Whitestone Lower Zone Limestone

Whitestone Lower Zone, or Whitestone LZ, also referred to as Texas Shell as a building stone, is a limestone rock quarried from the lower bench of the Whitestone Member of the Lower Cretaceous Walnut Formation. In the geological setting, this rock is about 10 to 15 ft below the Whitestone Upper Zone limestone. To the naked eye, Whitestone LZ appears to be heterogeneous because of cavernous holes as big as several centimeters that clearly originated from fossils. However, these large vugs are not well connected because all the measured gas permeability values are well below 10 mD, and most are less than 1 mD. From thin section, it can be seen that this grainstone rock consists of poorly sorted

fossil shells and pellets cemented by sparry calcite (Fig. 2.13). Both moldic and intercrystal pores are present. Intercrystal pores probably result from incomplete cementation of deposited fossil shells and incomplete filling of these shells by sparry calcite. Calcite crystals of various sizes cover pore walls and infill some of the fossilized shells. Intercrystal pores are usually surrounded by larger sized calcite crystals. The calcite crystal size increases from the edge of the nearby grain to the wall of an intercrystal pore (Fig. 2.14).

Fort Riley Limestone

Fort Riley limestone is a grainstone quarried from the Permian Fort Riley Member of the Barneston Formation. It is also known as Silverdale Kansas building stone. Thin section photos showed three types of porosities: intraparticle, moldic, and intercrystal with the first two being dominant (Fig. 2.15). Fossil shells and sparry calcite crystals can be easily identified. SEM micrographs revealed irregularly shaped pores with surfaces coated by calcite crystals of different sizes (Fig. 2.16). Details of a fossil shell surface can be seen in Fig. 2.16 (bottom).

BET and CEC

Comparisons of BET surface area and CEC are presented in Fig. 2.17. Results for a Berea sandstone sample (Berea 500 of about 500 mD in permeability) are also listed for comparison.

Rock surface area is essential to wetting alteration through adsorption from crude oil. Among all the tested limestone samples, Edwards (GC) has the lowest BET surface area, while Fort Riley has the highest. Gambier, Whitestone UZ, and Lueders exhibit slightly higher BET surface area values than Berea 500 sandstone sample due to the presence of micro-pores and the abundance of high surface area tiny calcite crystals on the pore walls. For Edwards (GC), which has the simplest pore structure and least amount of micro- to meso-porosity among all the tested limestones, low BET surface area is expected. The presence of vugs, shell dissolution pores, and about 1% micro- to meso-porosity cause Whitestone LZ to have slightly lower BET surface area than the Berea sandstone sample. Fort Riley limestone, which has the highest percentage of small pores (<53nm), about 4.4%, and more complicated pore structures, gives the highest BET surface area (1.639 m²/g) (Fig. 2.18). A second Fort Riley sample had an even higher BET surface area, (3.133 m²/g).

All the tested limestone rock samples demonstrated lower CEC values comparing to the Berea sandstone sample indicating the lack of clays. The homogeneous Edwards (GC) and Lueders limestone samples showed the lowest CEC values. This is attributed to the high content of crystallized calcite minerals in the two limestone rocks. The relatively high CEC values for Fort Riley and Gambier limestones are possibly caused by the presence of small amount of clay minerals on the fossil surfaces.

Water Adsorption/Desorption Isotherms and BJH Analysis

Results from water adsorption/desorption isotherms and BJH analysis are compared in Figs. 2.18 and 2.19. Two of the three selected homogeneous limestones, Gambier and

Edwards (GC), have micro- plus meso-porosity of around 0.5%. The percentages of micro-pores and micro- plus meso-pores increase from Whitestone UZ, to Lueders, to Fort Riley limestones. This, to some extent, reflects the increased complexity in pore structure of the three rocks. Comparison of the amount of N₂ adsorbed in BJH analysis versus the relative pressure is given in Fig. 2.19. Edwards (GC) and Fort Riley give clearly different behavior, having the lowest and highest adsorbed amount respectively over the whole range of tested relative pressures. These two rocks exhibit extreme difference in comparison of micro- to meso-porosity (Fig. 2.18). The other three rocks, Gambier, Whitestone UZ, and Lueders, showed comparable adsorption behavior.

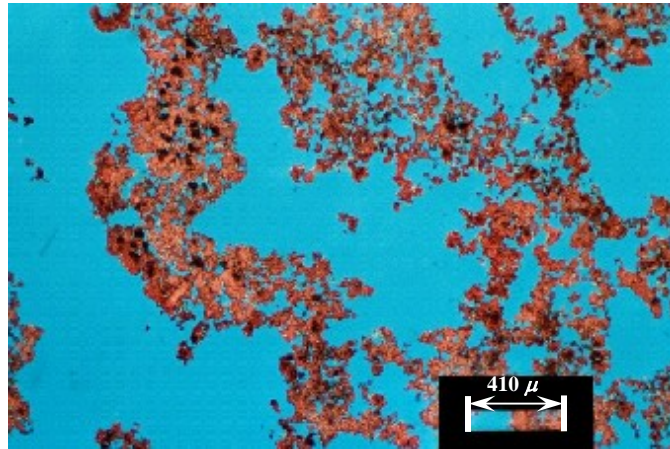


Fig. 2.1 Thin section of Canadian #2 limestone rock sample

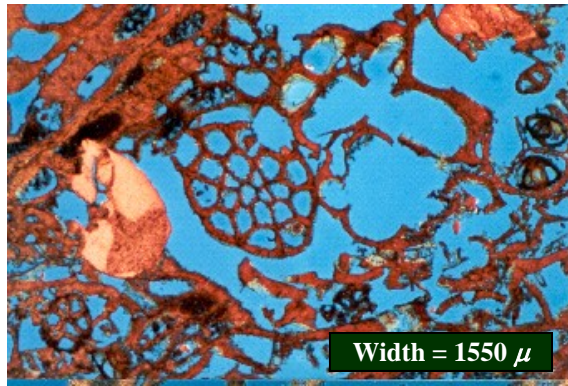
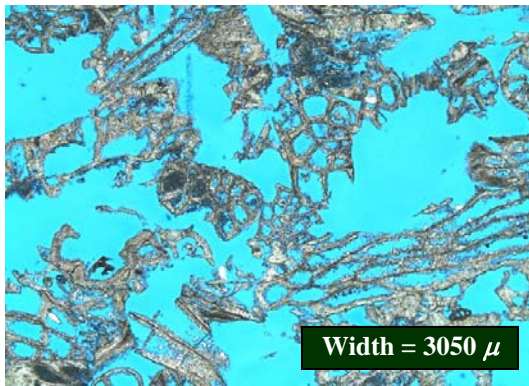


Fig. 2.2 Thin sections of Gambier limestone

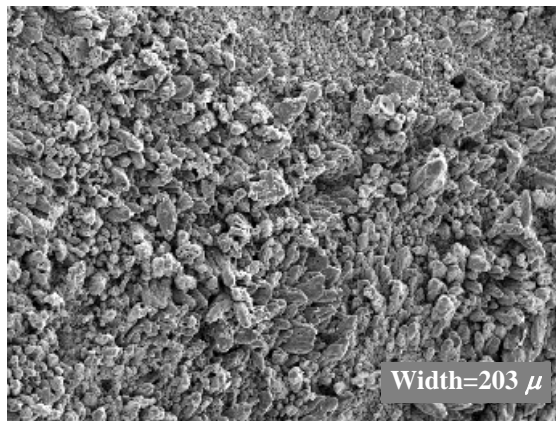
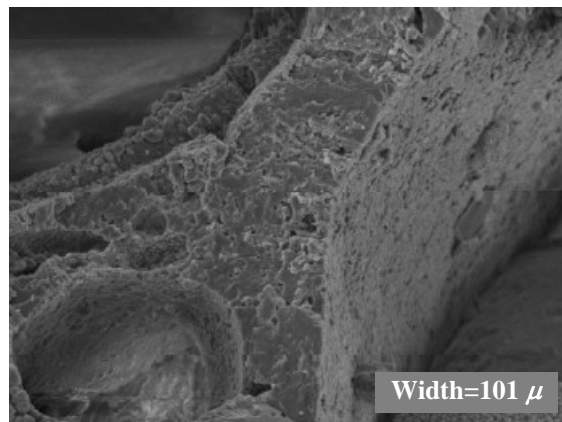
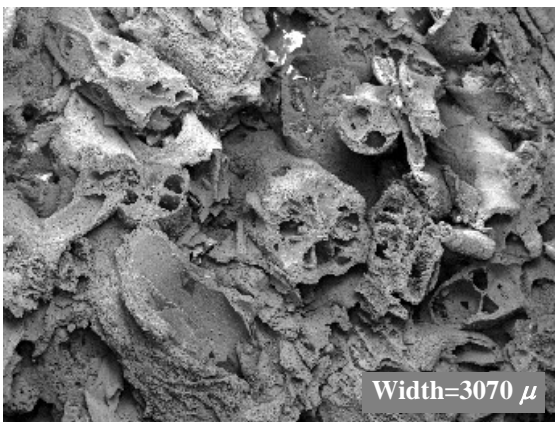


Fig. 2.3 SEM micrographs of Gambier limestone

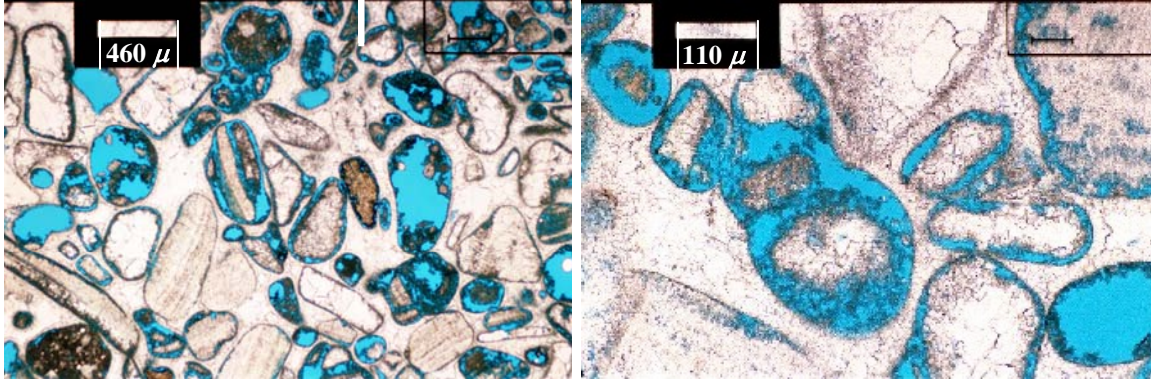


Fig. 2.4 Thin sections of Edwards (GC) limestone

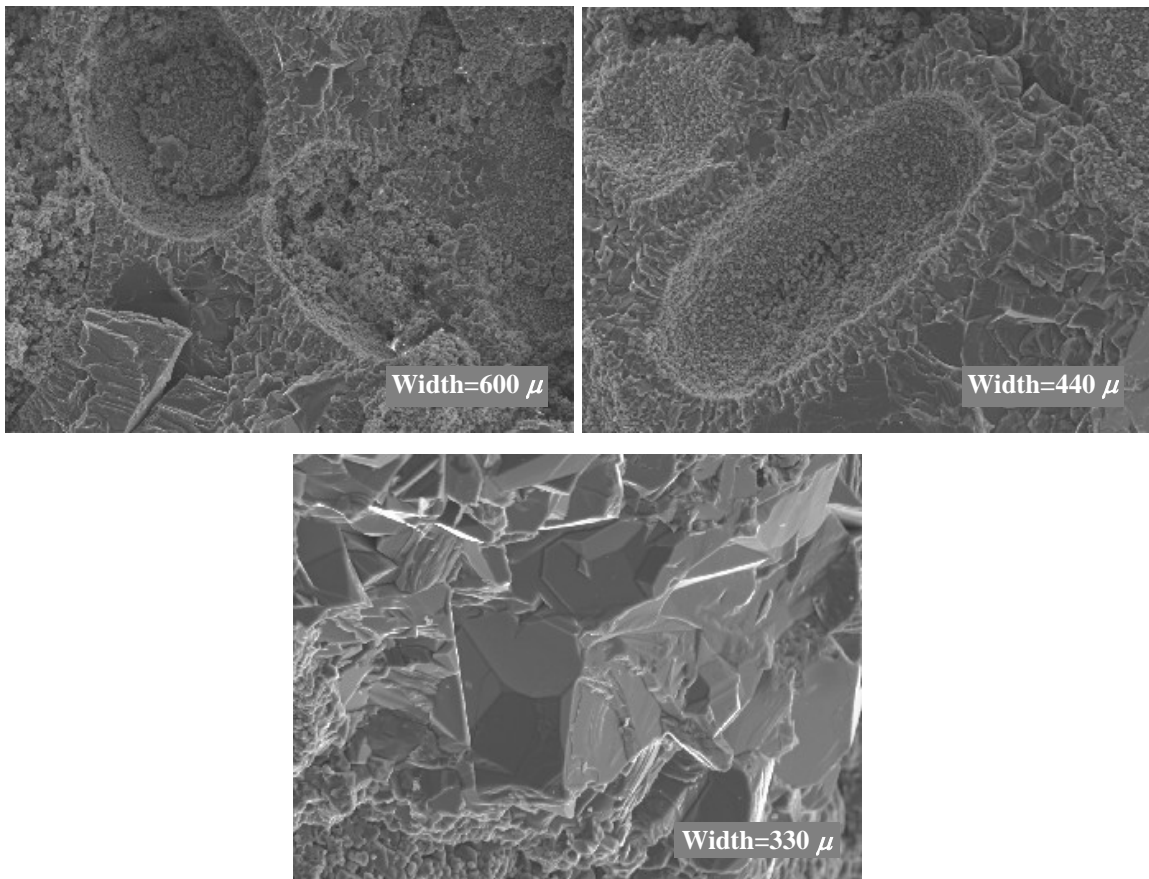


Fig. 2.5 SEM micrographs of Edwards (GC) limestone

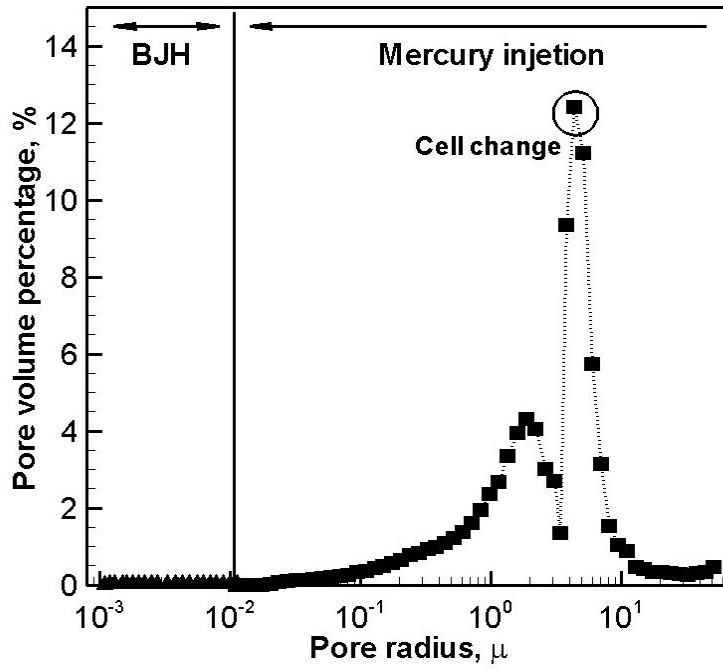


Fig. 2.6 Pore size distribution of Edwards (GC) limestone

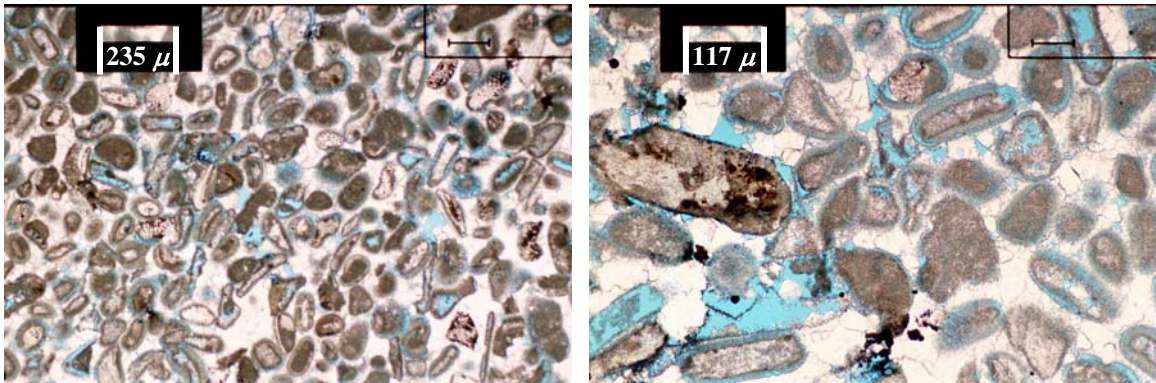


Fig. 2.7 Thin sections of Whitestone UZ limestone

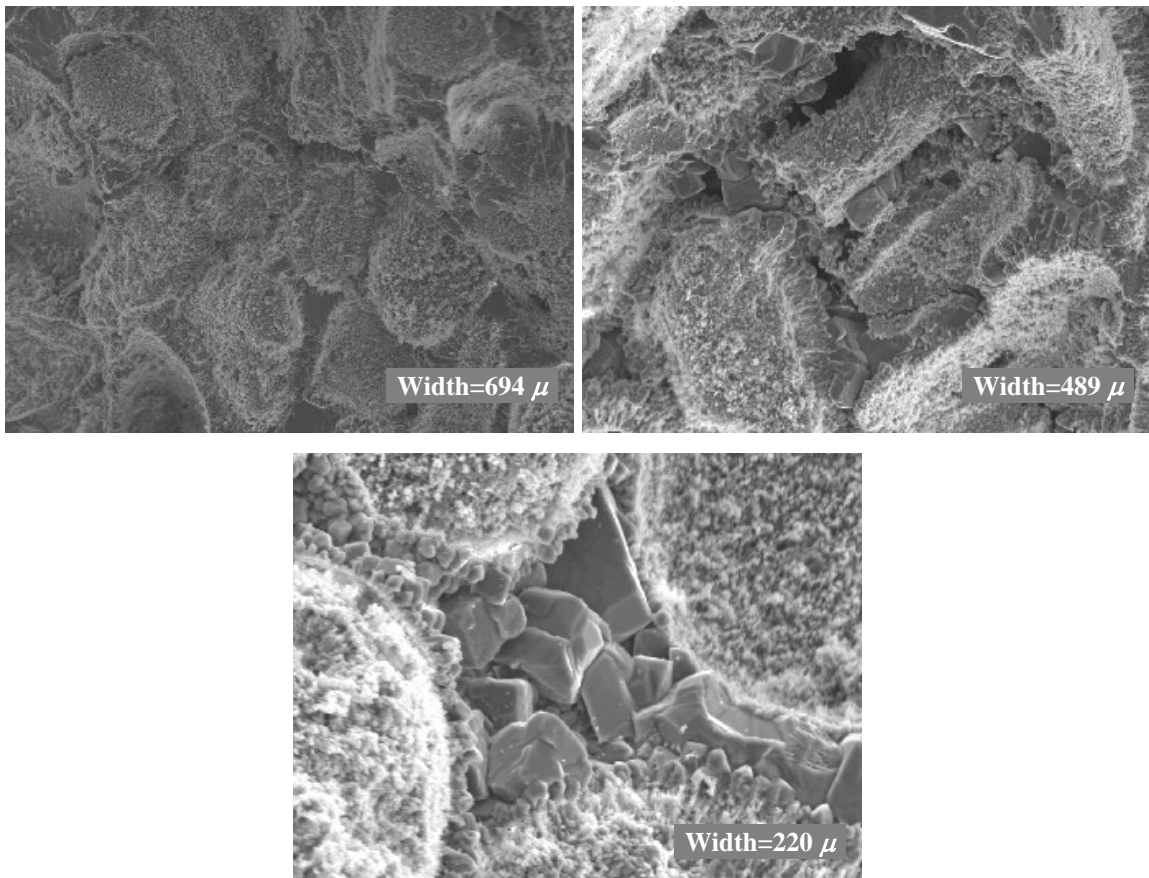


Fig. 2.8 SEM micrographs of Whitestone UZ limestone

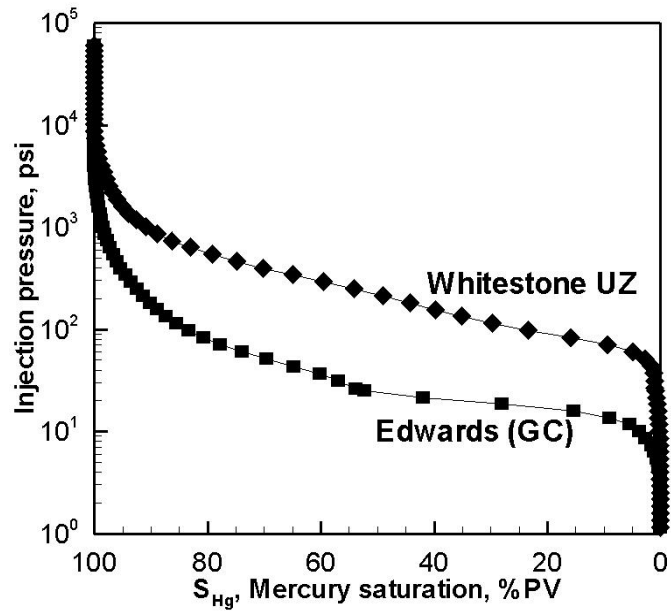


Fig. 2.9 Mercury injection for Whitestone UZ and Edwards (GC) limestones

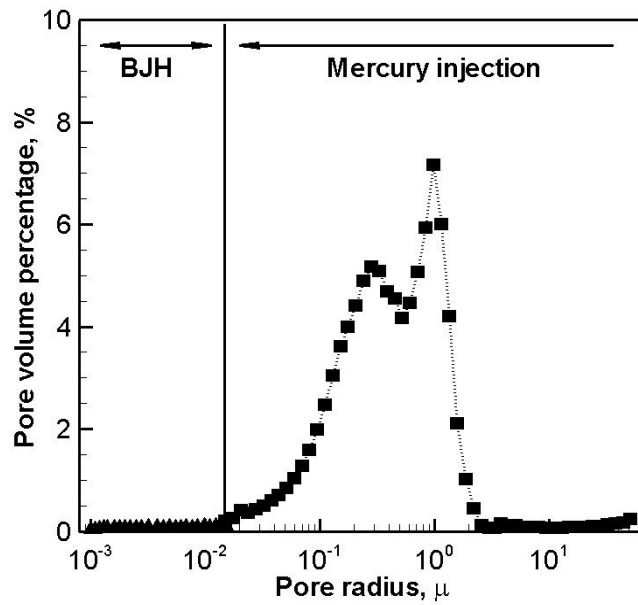


Fig. 2.10 Pore size distribution of Whitestone UZ limestones

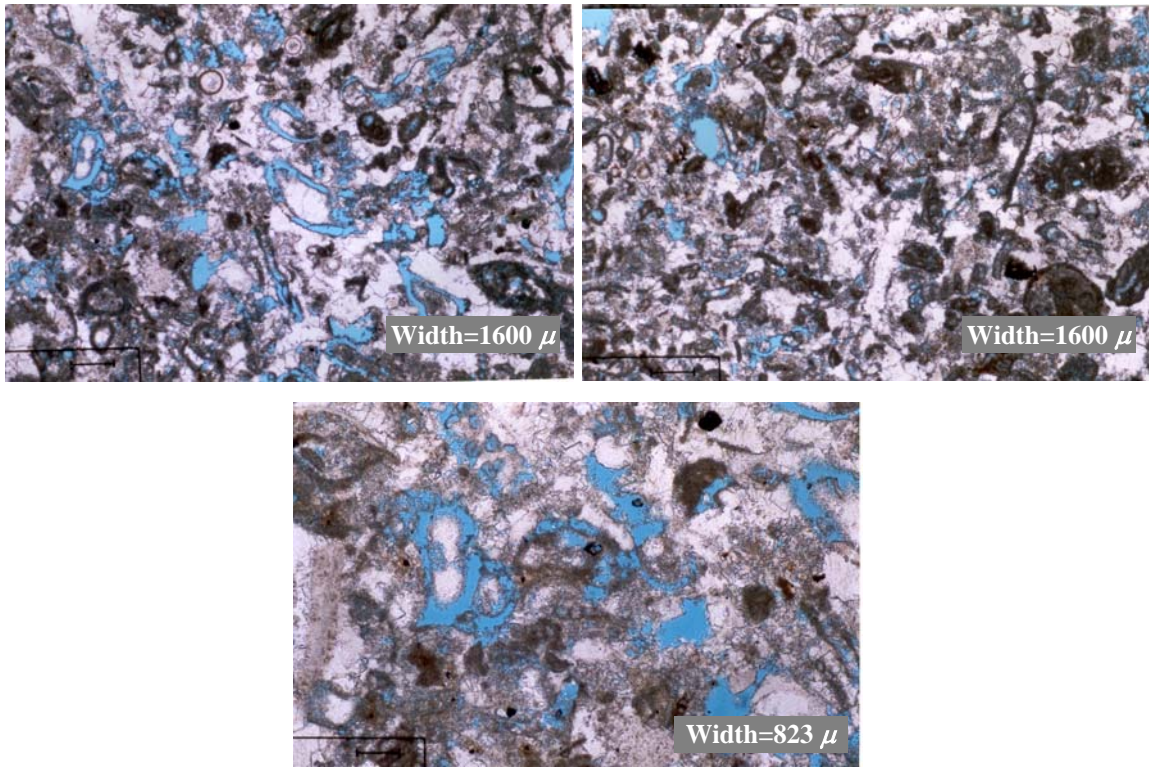


Fig. 2.11 Thin sections of Lueders limestone

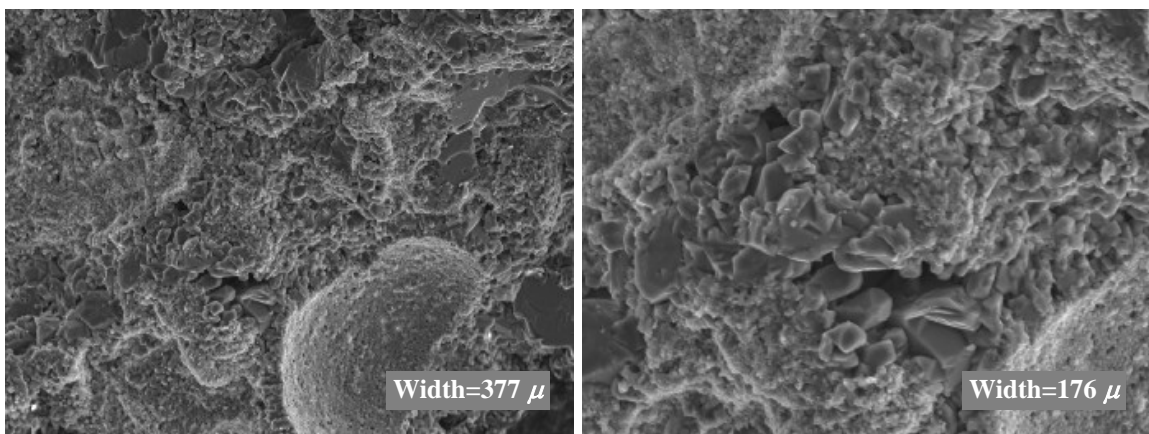


Fig. 2.12 SEM Micrographs of Lueders limestone

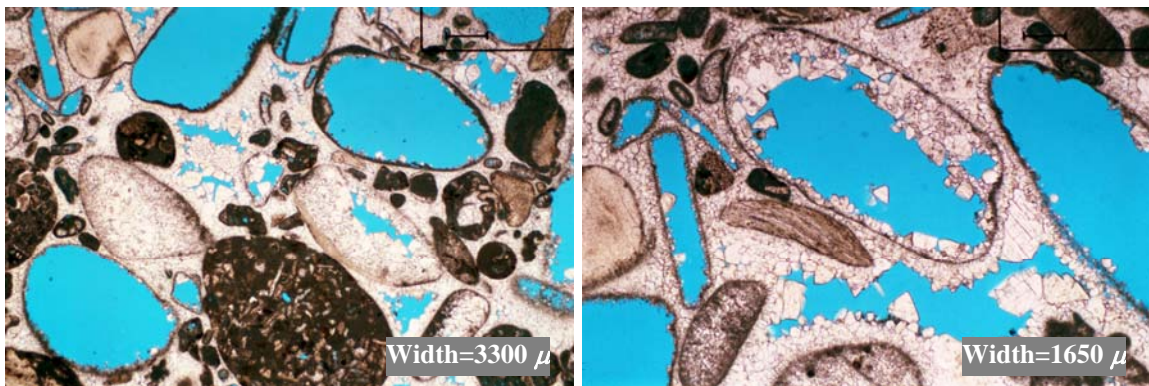


Fig. 2.13 Thin sections of Whitestone LZ limestone

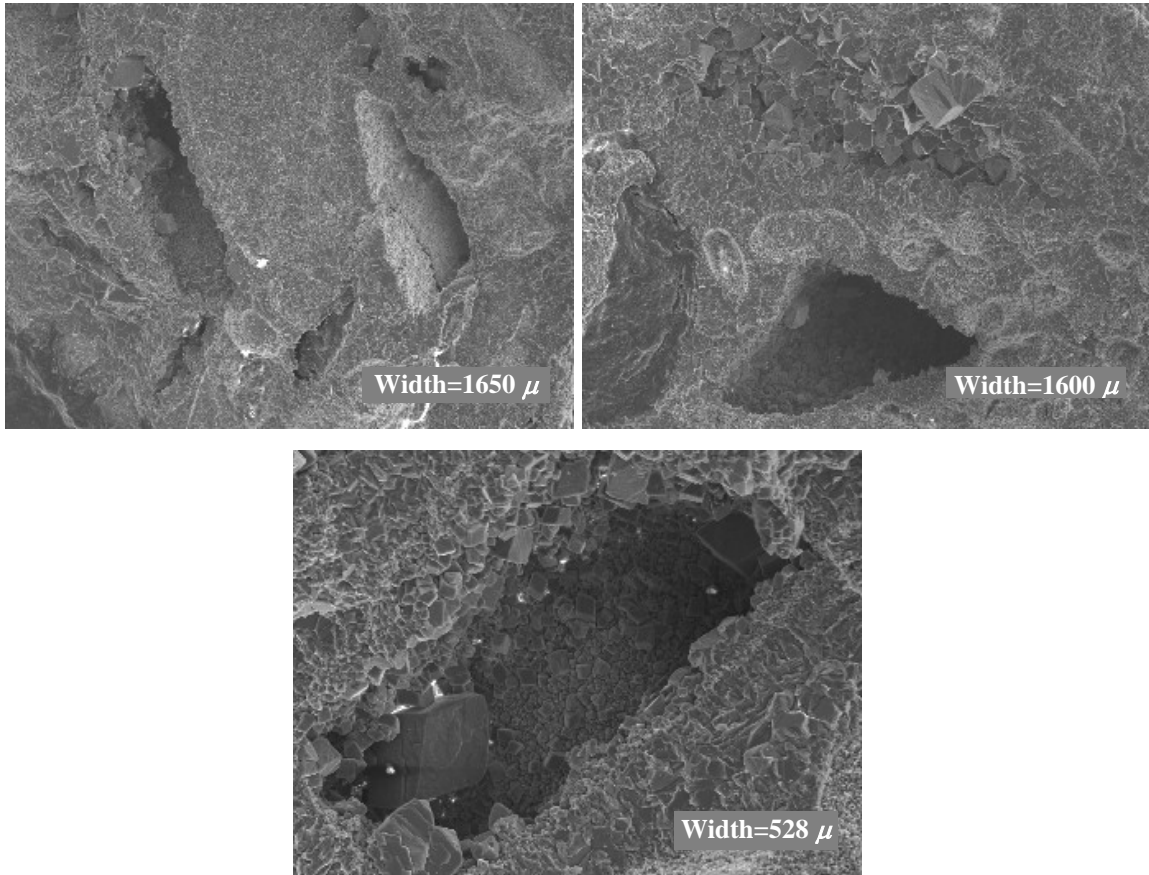


Fig. 2.14 SEM micrographs of Whitestone LZ limestone

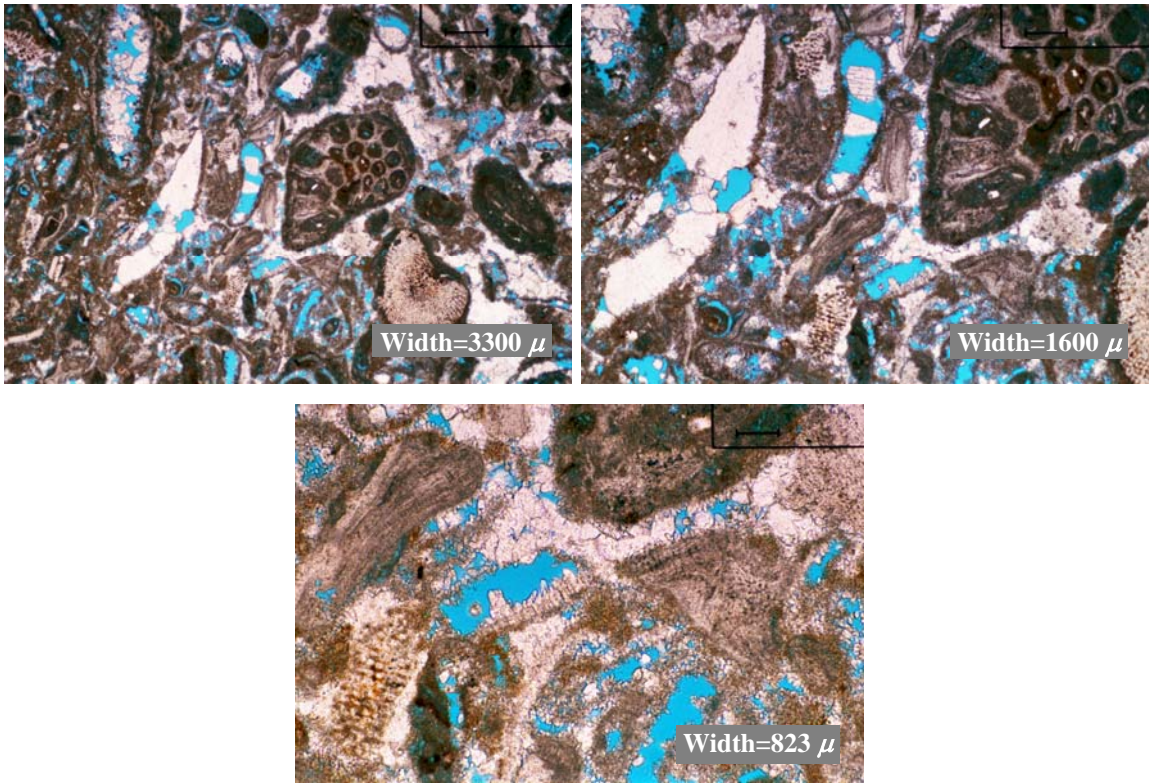


Fig. 2.15 Thin sections of Fort Riley limestone

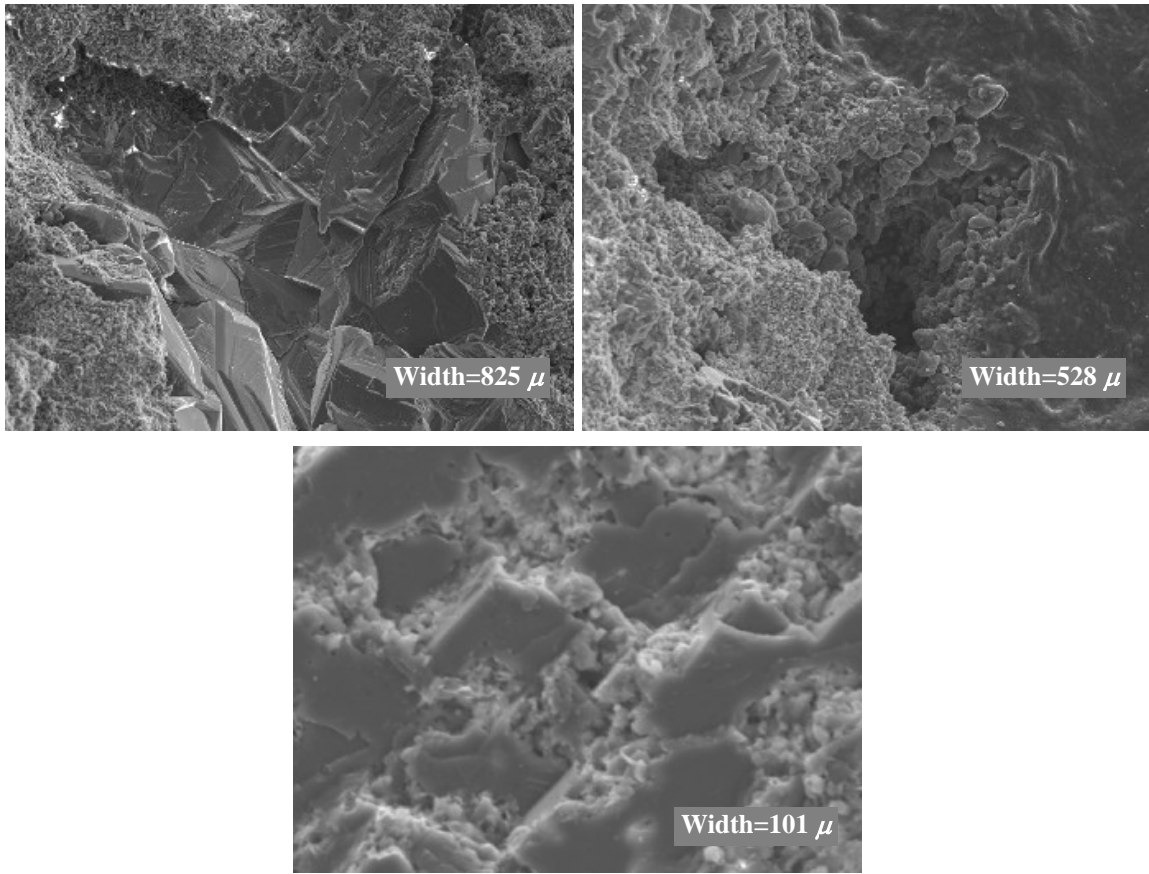


Fig. 2.16 SEM micrographs of Fort Riley limestone

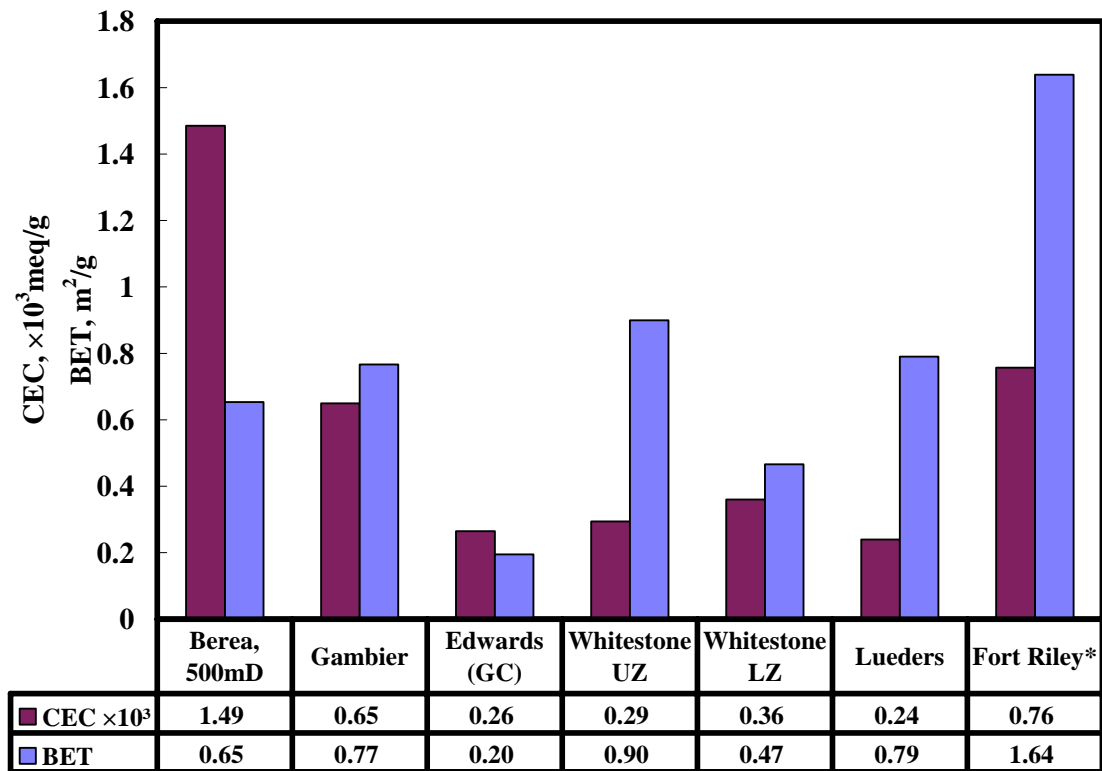


Fig. 2.17 BET surface area and CEC comparison of selected limestones and a Berea sandstone

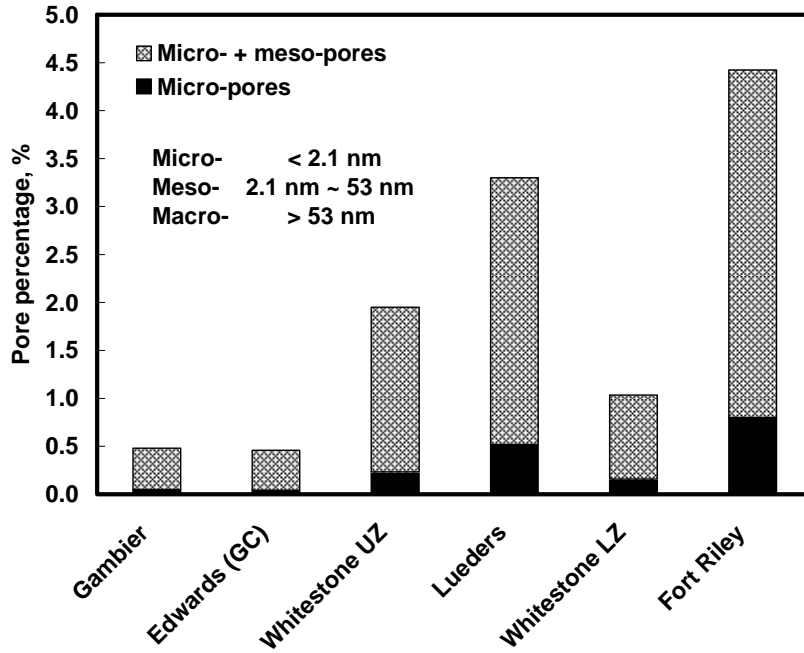


Fig. 2.18 Percentage of micro- and meso-porosity for all tested limestone rocks from water adsorption/desorption isotherms (Fischer *et al.*, 2005)

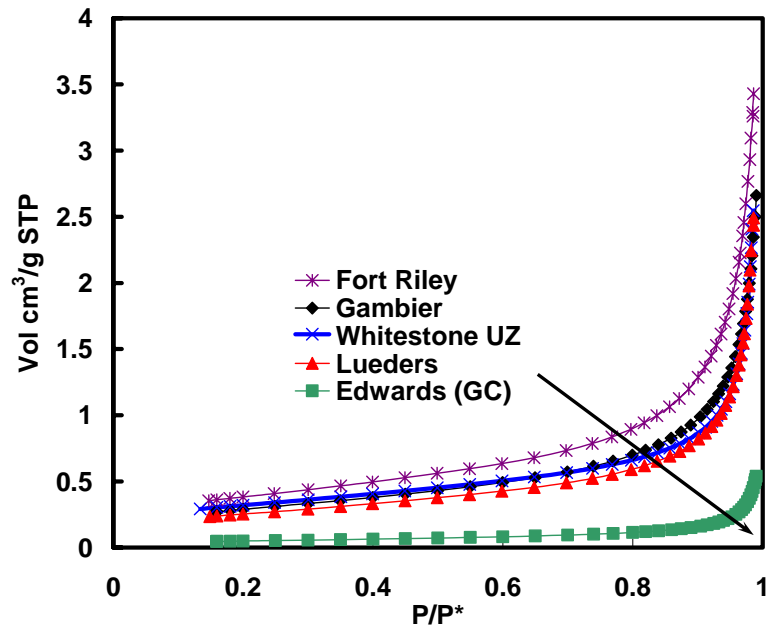


Fig. 2.19 Adsorbed volume versus relative pressure for five selected limestones from BJH analysis

Part II: Wettability Control

A useful approach to study of the effect of wettability on oil recovery behavior is to compare results for very strongly water-wet (VSWW) outcrop core samples with those obtained after wettability alteration. Many techniques, such as adsorption of well defined chemicals or adsorption from crude oil, have been used in the petroleum industry to obtain a spectrum of wettability conditions. In the present work, wettability alteration through adsorption from crude oil was investigated for variations in crude oil composition, initial water saturation, and aging time. Induced wettability states (MXW) were compared through spontaneous imbibition measurements. Wetting stability was tested for mixed-wet core samples prepared by adsorption of an organic film from crude oil (MXW-F). Preliminary measurements were made of the effect of oil viscosity on imbibition rates for cores prepared using two crude oil/brine/rock (COBR) combinations. However, the results did not show consistent trends.

Introduction

Wettability alteration through adsorption from crude oil is a widely used wettability control technique in the petroleum industry. Polar components in crude oil can be adsorbed onto rock surfaces when they are contacted by crude oil. Because of the positive charges on carbonate rock surfaces, carboxylic acids are more likely to attach to carbonate surfaces (Stumm and Morgan, 1970; Cram, 1972; Treiber *et al.*, 1972; Somasundaran, 1975; Cuiec, 1975, 1991; Anderson, 1986a; Buckley *et al.*, 1998). Reported experimental results on chalk samples showed that the acid number of a crude oil was closely related to the wetting alteration ability of the crude oil (Standnes and Austad, 2000). Many parameters such as crude oil properties, initial water saturation, aging time, aging temperature, core preparation procedure, etc., can be adjusted to achieve a spectrum of wettability (Zhou *et al.*, 2000; Xie and Morrow, 2001; Tie *et al.*, 2003).

After aging cores with crude oil, the crude oil can be replaced by a mineral oil so that the stability of the adsorbed film can be studied with the possibility of further adsorption eliminated. However, direct displacement of the crude oil with a low solvency mineral oil can result in destabilization and surface precipitation or deposition of the asphaltenes, which render the core less water-wet (Al-Maamari and Buckley, 2003; Tie *et al.*, 2003). Crude oil can be replaced by an intermediate solvent, e.g., toluene or decalin, in order to prevent precipitation (Morrow *et al.*, 1986; Graue *et al.*, 1999; Tong *et al.*, 2002 and 2003b). It has been reported that by the use of decalin as the intermediate solvent, stable wetting could be obtained on MXW-F cores (Graue *et al.*, 1999; Tong *et al.*, 2002 and 2003b). Tong *et al.* (2002) reported successful correlation of viscosity ratio by changing the probe (mineral) oil viscosity for MXW-F Berea sandstone cores.

In the present work, wettability alteration through adsorption from crude oil was investigated for two limestones. The effects of crude oil, initial water saturation, and aging time were tested. MXW-F Gambier cores were used in a study of the stability of

induced wetting states. Correlation of the effect of oil phase viscosity on imbibition rate was investigated for MXW-F Gambier and Edwards (GC) cores.

Experiments

Three crude oils were used to study wettability alteration through adsorption from crude oil. Details of brine and crude oil properties are listed in Table 2.1 and 2.2. Clean dry cores were first vacuum saturated with 5% CaCl₂ (Gambier) or synthetic sea water (Edwards (GC)) and immersed in brine at elevated temperature for 10 days to reach ionic equilibrium with the rock surface. Brine saturated cores were then flooded with crude oil (Edwards (GC)) or mineral oil (Gambier) to establish an initial water saturation. For the Gambier cores, the mineral oil was displaced by decalin followed by crude oil. The cores were then immersed in crude oil and aged in sealed containers at 75°C for 10 days. Spontaneous imbibition was then performed on aged core samples to assess the induced wettability. Cores so prepared were referred to as mixed-wet (MXW). The effects of crude oil composition, initial water saturation, and aging time, were tested on two different core types, Gambier and Edwards (GC). Selected core properties are listed in Tables 2.3 and 2.4.

If, as in the present work, the crude oil in a mixed-wet core was displaced by an intermediate solvent, i.e., decalin, and the solvent was then displaced by a clean mineral oil, e.g., Soltrol 220, to leave an absorbed film (F) on the rock surface, the achieved wetting state was referred to as MXW-F. MXW-F Gambier and Edwards (GC) cores were tested for wetting stability and the effect of probe oils of different viscosity on imbibition rate. Selected core properties are listed in Table 2.5.

Results and Discussion

Wettability Alteration

Wettability alteration through adsorption from crude oil is affected by numerous factors related to the crude oil/brine/rock interactions. In the present work, reproducibility of wettability alteration was tested for two cores prepared in parallel using the same experimental parameters (Fig. 2.20). Experimental observations for both limestones and sandstones showed that reproducibility were usually good for MXW cores.

Crude Oils

Gambier and Edwards (GC) limestone cores were tested for the effect of variation in crude oil composition through addition of alkanes (Fig. 2.21). The initial water saturation for each rock type was kept close to constant. For a given procedure for establishing initial water saturation, there will usually be significant differences between rock types because of distinct differences in the type of porosity and the pore structure.

For Gambier limestone, Cottonwood crude oil clearly rendered the rock less water-wet in comparison to the core prepared with Minnelusa crude oil, even though the Minnelusa crude oil has higher asphaltene content (see Fig. 2.21a). For Edwards (GC) cores, the core sample prepared using Ladybug crude oil showed almost no oil production after a month of imbibition while recovery from the core aged with Cottonwood crude was more than 20% (see Fig. 2.21b). Raising the imbibition temperature for the Ladybug core to

60°C resulted in very little additional oil recovery indicating that wettability was not influenced by wax deposition. It is widely accepted that the ability of a crude oil to alter wettability is related to the asphaltene content, acid number, base number, or some combination of the three. From the experimental observations for the two carbonate rocks, it can be seen that the acid number of the crude appears to be a dominant factor. The asphaltene content provides an indication of the total amount of polar components in the crude oil but showed opposite trends to the wetting alteration ability of the crude oil for the two tested limestones. However, the wetting alteration of the Minnelusa and the Cottonwood crude oils on Berea sandstone cores (Fig. 3.16c) showed that even though the Cottonwood crude oil has lower base number than the Minnelusa oil, it caused greater wettability change towards reduced water-wetness. So, it appears that the ratio of the acid/base number to the asphaltene content of the crude oil, which represents the relative concentration of the effective wetting alteration (polar) compounds in a crude oil, rather than the acid/base number or the asphaltene content alone, may provide a better indication of the wetting alteration ability of the crude oil. More comparisons between carbonates and sandstones are needed before the properties of a specific crude oil can be used to predict the oil's wettability alteration capability.

Initial Water Saturation

The saturation and distribution of the initial water control the amount of the rock surface accessible to adsorption of polar components and therefore the wetting alteration that provides mixed wettability. As the initial water saturation decreases, an increasing fraction of the rock surface is overlain by crude oil and the water-wetness of the MXW rocks decreases (Xie and Morrow, 2001). The effect of initial water saturation was investigated with two crude oil/brine/rock (COBR) combinations, Minnelusa/5% CaCl₂/Gambier and Cottonwood/Sea water/Edwards (GC) (Fig. 2.22). For both of the tested combinations, clear trends of reduced water-wetness with decrease in the initial water saturation were observed.

For the Minnelusa/5% CaCl₂/Gambier COBR system, a reduction of only ~2% in the initial water saturation (28% to 26.2%) resulted in reduction of the scaled imbibition by almost a whole log cycle (see Fig. 2.22a). For the Cottonwood/Sea water/Edwards (GC) COBR system, a reduction in the initial water saturation from 16.0% to 12.3% resulted in almost complete suppression of imbibition (see Fig. 2.22b). Therefore, for individual rocks, it is important to keep the initial water saturations as close to constant as possible when examining other parameters that affect wettability and oil recovery behavior. An additional set of experiments was conducted for the Ladybug/Sea water/Edwards (GC) system. However, due to the strong capability of the Ladybug crude oil to alter wettability, no oil recovery was observed during over a month for cores with 16.5%, 18.8%, and 24.5% initial water saturation.

Aging Time

Increase in aging time can result in increased adsorption of polar components onto the rock surfaces. Zhou *et al.* (2000) showed that with increase in the aging time, the scaled spontaneous imbibition became slower indicating decreased water-wetness. Four cores were used to test the effect of aging time. Results are shown in Fig. 2.23. It can be seen

that even at very low initial water saturation (~5.5%) a significant amount of oil (>10% OOIP) was recovered from the two cores aged for only 1.5 and 3 days. Doubling the aging time from 1.5 to 3 days did not cause significant reduction in spontaneous imbibition behavior. When the aging time was increased to 10 days, the spontaneous imbibition was greatly suppressed even at a somewhat higher initial water saturation (8.9%). If the aging time was further increased to 20 days, no oil production was observed after one month for a core with an initial water saturation of 16.4%. Therefore, aging time is one of the most important parameters in wetting alteration of carbonates and needs careful attention in comparative wettability studies.

In summary, the effects of the three parameters, crude oil composition, initial water saturation, and aging time, depend significantly on the specific crude oil/brine/rock interactions. Prediction of oil recovery from specific properties of the crude oil, the brine, and the rock will be highly limited. Extreme caution should be taken in attempt to predict wetting behavior for different rock types.

Stability of Induced Wetting for Limestones

The stability of induced wetting states was investigated for MXW-F Gambier limestone cores prepared with Minnelusa crude oil. Mineral oils of different viscosities were used as probe oils. Results are shown in Fig. 2.24. It can be seen that the induced wettability state was stable for the two MXW-F cores with high viscosity mineral oils (90.1 cP and 173.6 cP) as the probe oils (Figs. 2.24d and 2.24e). For the MXW-F cores with relatively low viscosity mineral oils, 3.8 cP, 19.8 cP, and 44.9 cP, the second cycle of spontaneous imbibition was always faster than the first cycle (Figs. 2.24a, 2.24b, and 2.24c). A third cycle of imbibition was tested for cores prepared using 3.8 cP and 173.6 cP mineral oils. The spontaneous imbibition behavior of the core using 3.8 cP probe oil fell in between the first and second cycle indicating that there had been no removal of adsorbed material from the rock surface (Fig. 2.24a). The core tested using 173.6 cP mineral oil showed a similar trend, but the difference was only minimal indicating close-to-stable wetting. (Fig. 2.24e).

Correlation of Viscosity Ratio for MXW-F Cores

Correlation of viscosity ratio was tested for two MXW-F COBR systems, Minnelusa/5% CaCl₂/Gambier and Cottonwood/Sea water/Edwards (GC) (Figs. 2.25 and 2.26). For Gambier limestone, in the first cycle of imbibition, the scaled spontaneous imbibition of cores with different mineral oil viscosities were relatively close to that for the G05 core prepared with 44.9 cP mineral oil (Fig. 2.26a). Two core samples, G02 and G04 tested with lower viscosity mineral oils (3.8 cP and 19.8 cP respectively), exhibited a sudden increase in the oil recovery rate after t_D of 4×10^5 . For the second cycle of imbibition, two cores, G06 and G01 prepared with the most viscous mineral oils (90.1 cP and 173.6 cP respectively), were closely correlated and gave stable wetting (Figs. 2.25b and 2.26b). Other cores showed faster spontaneous imbibition with core G05 still giving the fastest scaled imbibition.

For the Cottonwood/Sea water/Edwards (GC) system, a clear induction time was observed for all the tested core samples (see Figs. 2.25c and 2.26c). Correlation of

spontaneous imbibition behavior was only obtained on cores prepared with 3.8 and 173.6 cP mineral oils. Other cores prepared with mineral oil viscosities between 3.8 and 173.6 cP showed lower oil recovery with the core prepared with 44.9 cP mineral oil exhibiting the lowest recovery at any given dimensionless time.

Based on the results obtained to date for two COBR systems with limestone rock, it is concluded that Ma *et al.*'s (1997) scaling group does not give reliable scaling for the effect of viscosity ratio for the two tested MXW-F limestones.

Table 2.1 Synthetic brine composition

Brine	NaCl (g/L)	KCl (g/L)	CaCl ₂ (g/L)	MgCl ₂ (g/L)	NaN ₃ (g/L)	pH	TDS (mg/L)
Sea water	28	0.935	2.379	5.365	0.1	6.6	36779
5% CaCl ₂	-	-	50	-	0.1	6.9	50100

Table 2.2 Selected properties of crude oil samples

Crude oil	ρ , g/ml	μ_o , 22°C, cP	n-C7 asphalt., wt%	Acid #, mg KOH/g oil	Base #, mg KOH/g oil
Minnelusa	0.9062	77.2	9.0	0.17	2.29
Cottonwood	0.8874	24.1	2.3	0.56	1.83
Ladybug	0.8699	13.5	0.07	1.57	0.59

Table 2.3 Gambier and Edwards (GC) cores tested for the effect of initial water saturation

No.	D	L	ϕ	k	μ_o	IFT	S_{wi}
	cm	cm	%	mD	cP	mN/m	%
Gambier limestone							
GA0	3.74	5.00	55.1	6050	56.1	25	0
GA3	3.73	4.97	54.7	5565	56.1	25	15.1
GB3	3.78	4.89	54.8	5610	62.8	25	26.2
GB2	3.77	4.88	55.1	5060	62.8	25	27.9
GB1	3.79	4.80	54.5	5600	62.8	25	28.0
GB4	3.78	5.22	54.6	5390	62.8	25	35.1
Edwards (GC) limestone							
6EGC28B	3.75	6.32	24.1	30.0	24.1	29.7	8.9
1EGC22A	3.73	6.42	21.1	12.9	24.1	29.7	12.3
1EGC05A	3.80	6.26	20.8	11.6	24.1	29.7	16.0

Table 2.4 Edwards (GC) cores tested for the effect of aging time for Cottonwood crude oil

No.	D	L	ϕ	k	$Aging\ time$	S_{wi}
	cm	cm	%	mD	days	%
6WTC26B	3.75	6.45	24.5	26.8	3	5.5
6WTC28A	3.74	6.39	24.8	32.9	1.5	5.6
6WTC28B	3.75	6.32	24.1	30.0	10	8.9
6WTC29A	3.74	6.30	24.0	26.8	20	16.4

Table 2.5 Gambier and Edwards (GC) MXW-F cores tested for wetting stability and the effect of oil phase viscosity

No.	D	L	ϕ	k	μ_o	S_{wi}
	cm	cm	%	mD	cP	%
Gambier						
G01	3.78	4.99	53.4	5790	173.6	28.4
G02	3.78	5.01	53.2	5420	3.8	28.5
G04	3.77	5.13	55.6	5530	19.8	28.8
G05	3.78	5.08	53.6	5170	44.9	28.3
G06	3.77	4.94	53.8	5080	90.1	28.9
Edwards (GC)						
1EGC06B	3.80	6.37	21.2	10.4	3.8	16.3
1EGC16A	3.73	6.33	20.4	10.9	90.1	16.6
1EGC16B	3.74	6.40	20.9	11.4	44.9	16.8
1EGC21A	3.73	6.30	21.0	13.6	173.6	16.8
1EGC21B	3.73	6.37	22.3	14.9	19.8	17.0

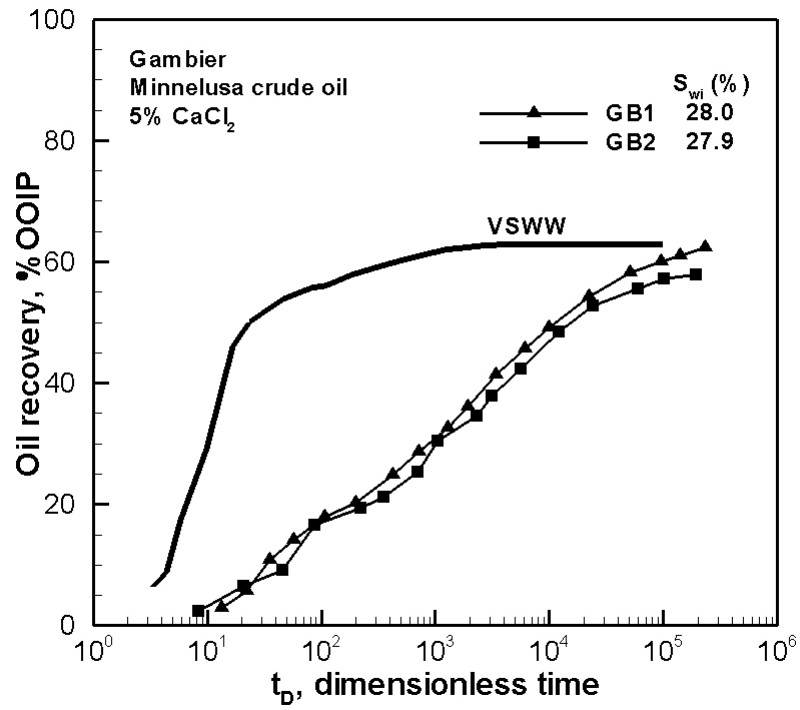
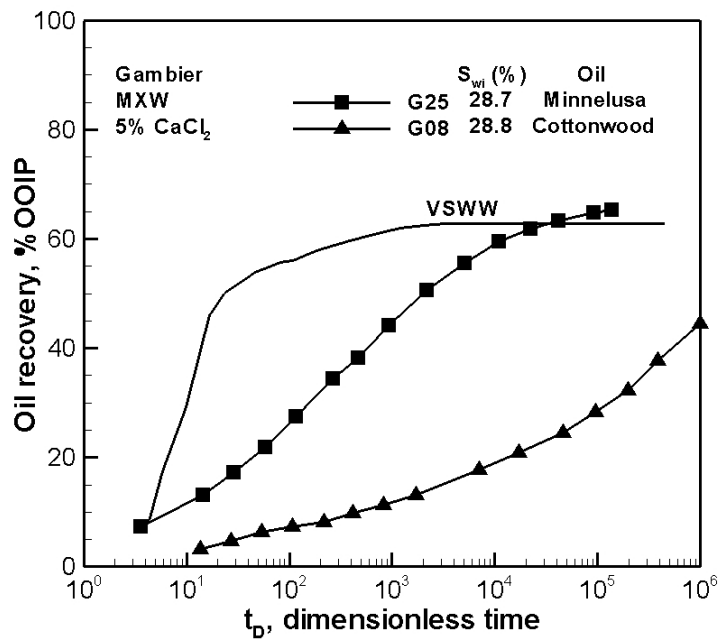
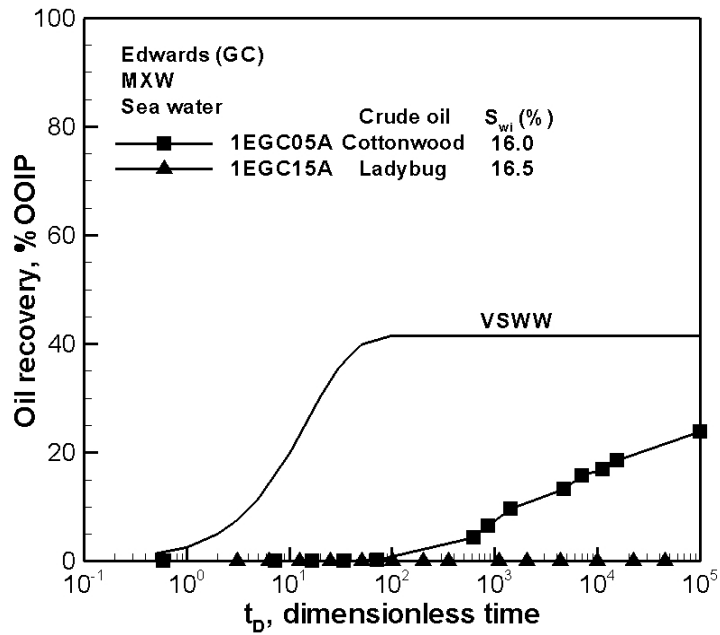


Fig. 2.20 Example of reproducibility of imbibition behavior for wettability alteration of duplicate core plugs.

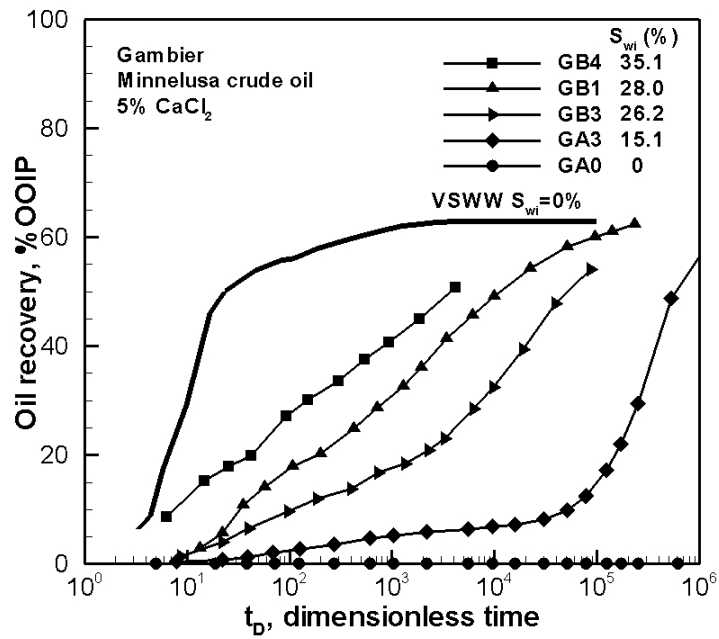


(a) Gambier (Tie et al., 2003)

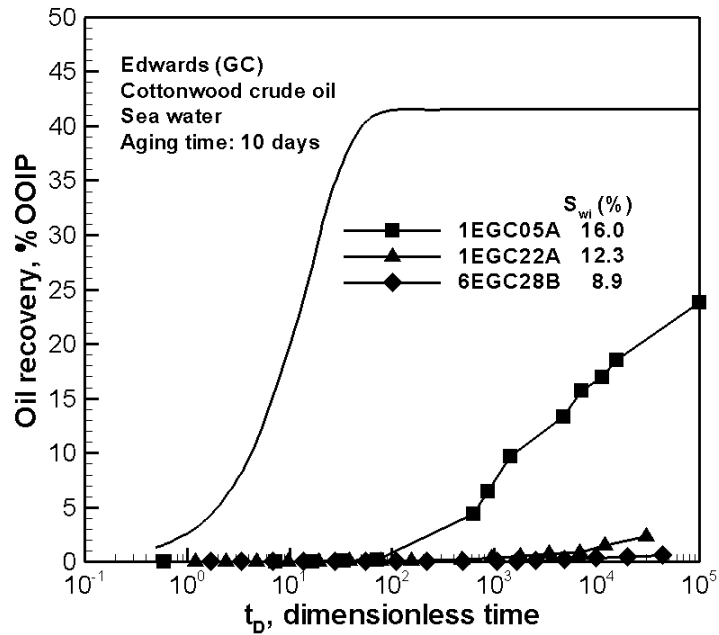


(b) Edwards (GC)

Fig. 2.21 The effect of crude oil composition on wettability alteration



(a) Minnelusa/5% CaCl_2 /Gambier



(b) Cottonwood/Sea water/Edwards (GC)

Fig. 2.22 The effect of initial water saturation on wettability alteration

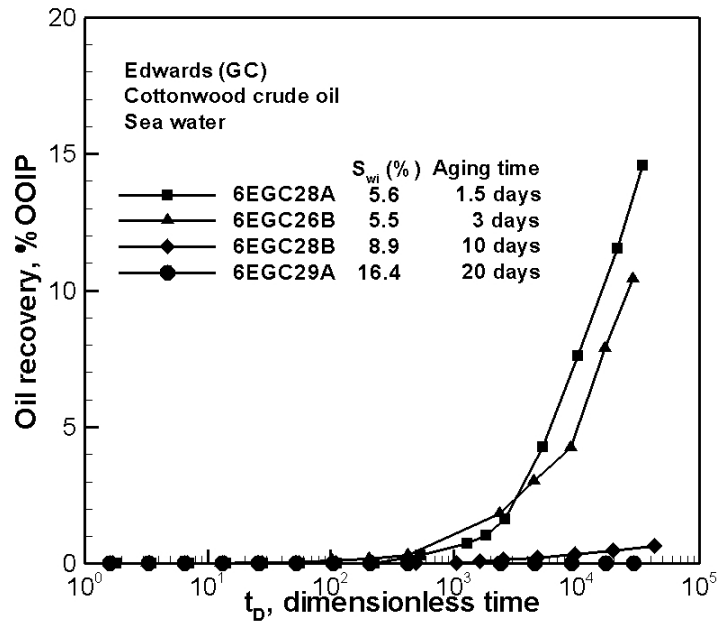
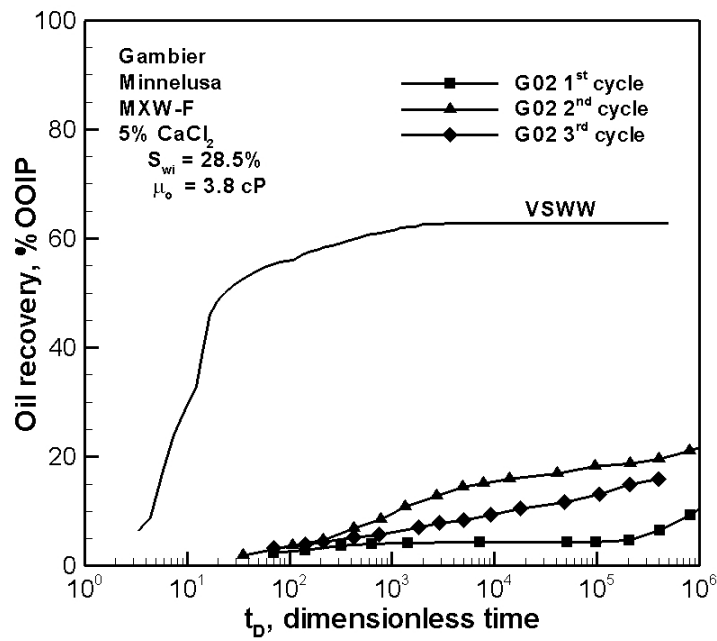
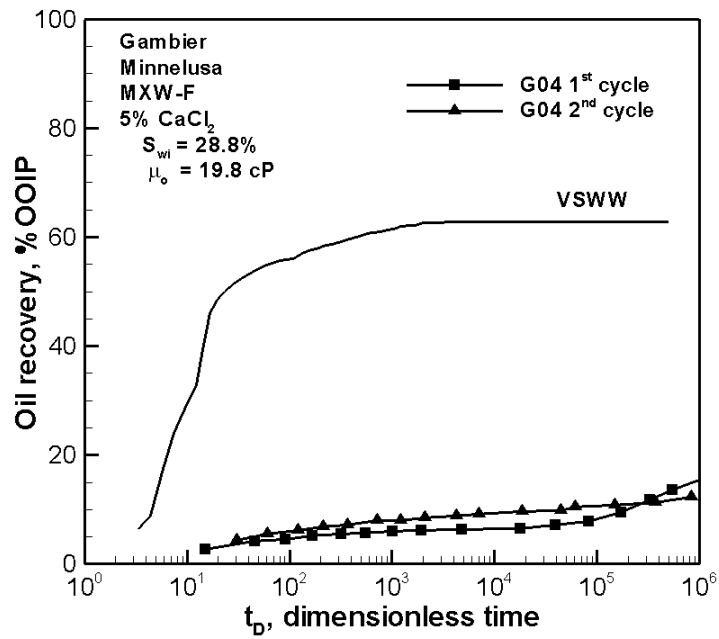


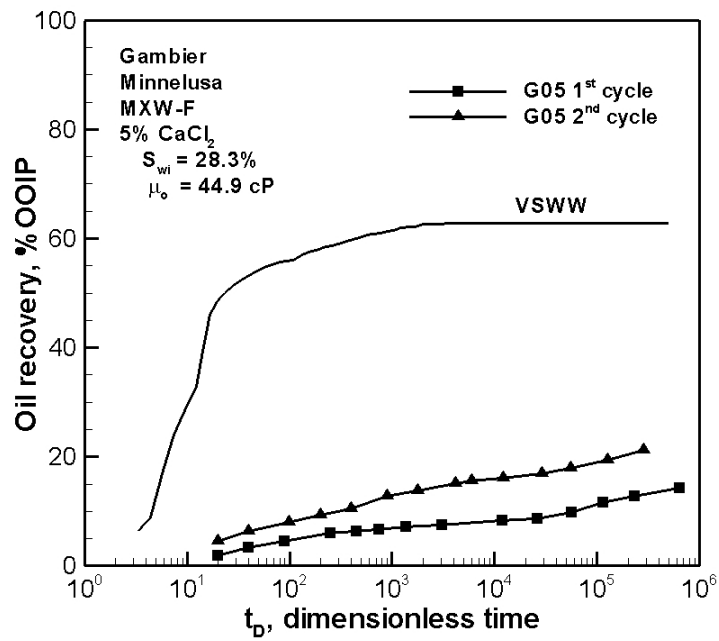
Fig. 2.23 The effect of aging time and initial water saturation on wettability alteration



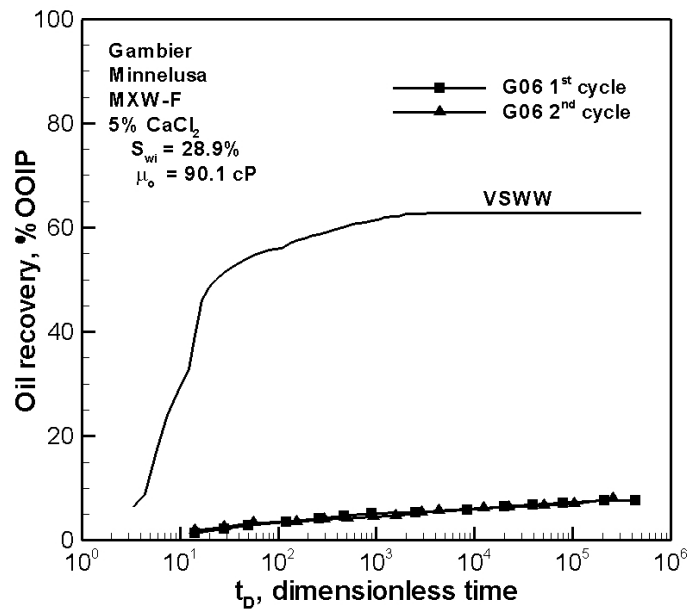
(a) G02 3.8 cP



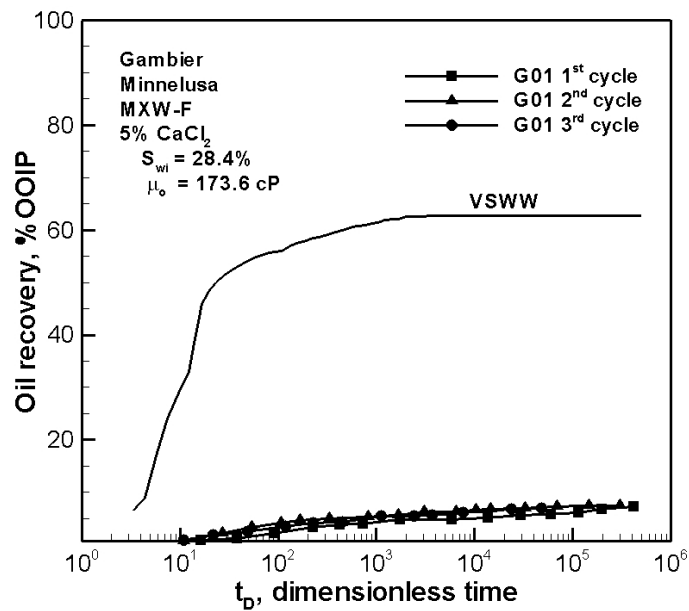
(b) G04 19.8 cP



(c) G05 44.9 cP

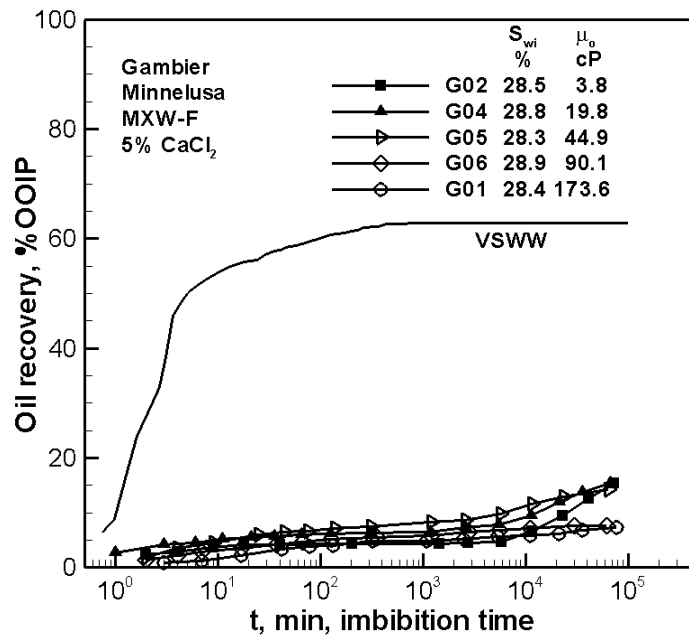


(d) G06 90.1 cP

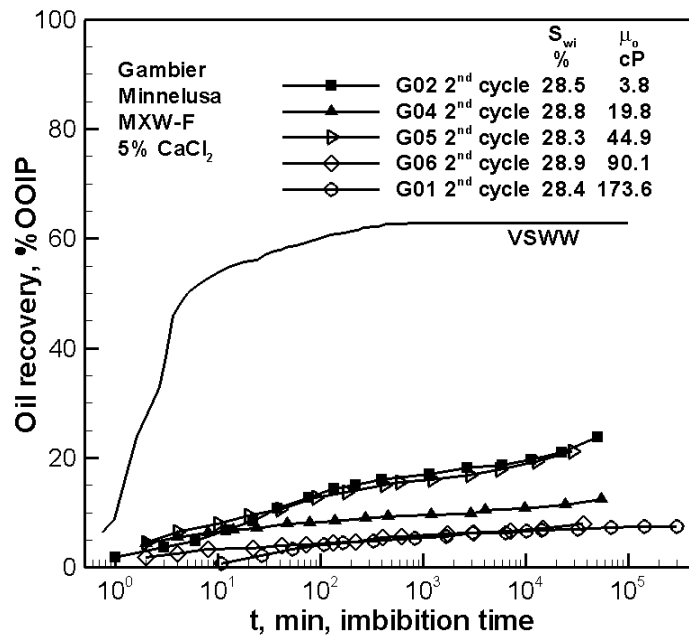


(e) G01 173.6 cP

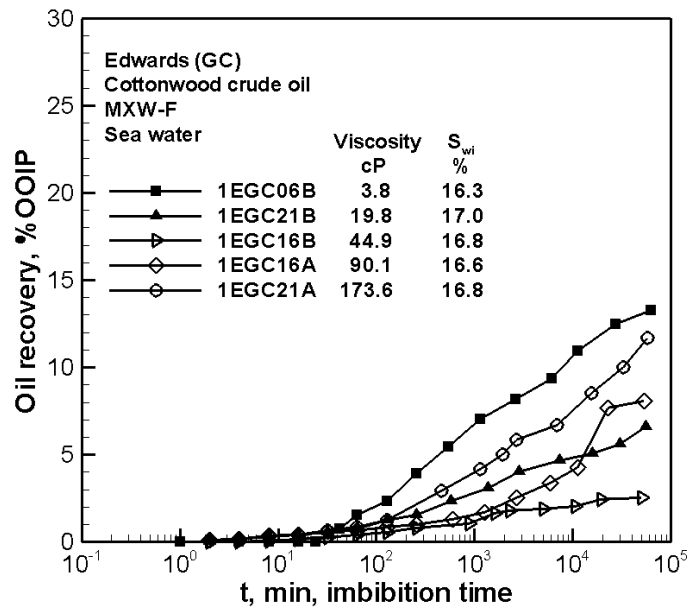
Fig. 2.24 Tests of stability of the induced wettability state for MXW-F wetting for five values of mineral oil viscosity.



(a) Gambier 1st cycle

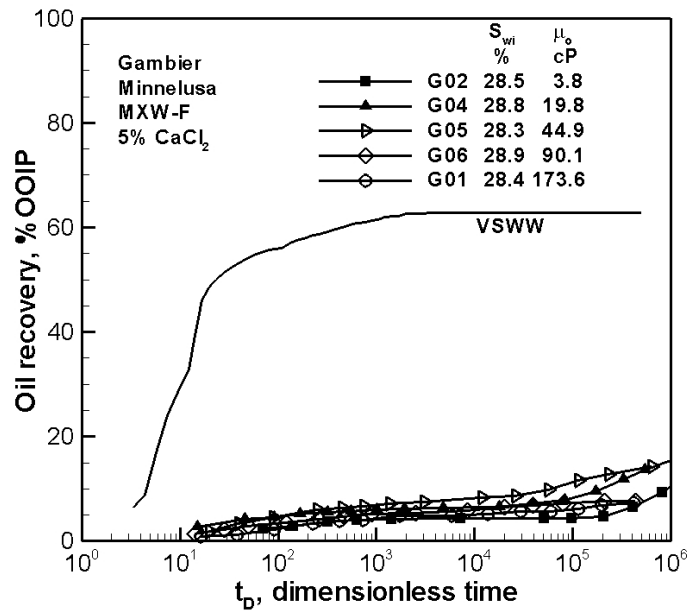


(b) Gambier 2nd cycle

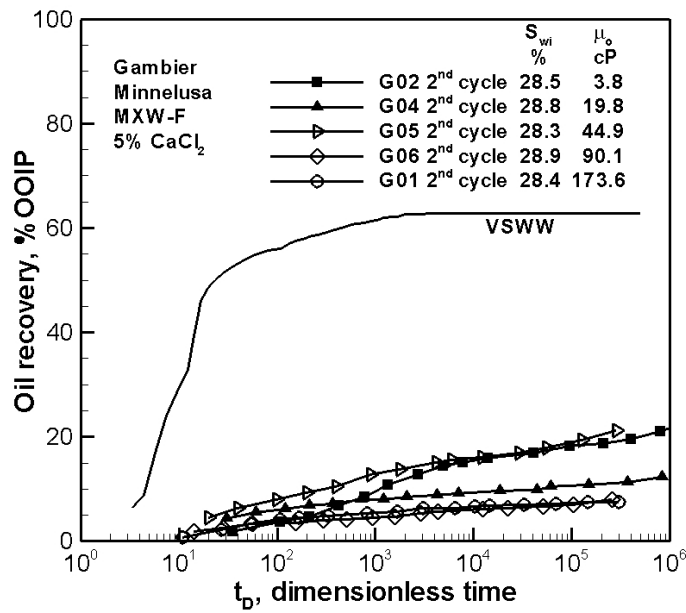


(c) Edwards (GC)

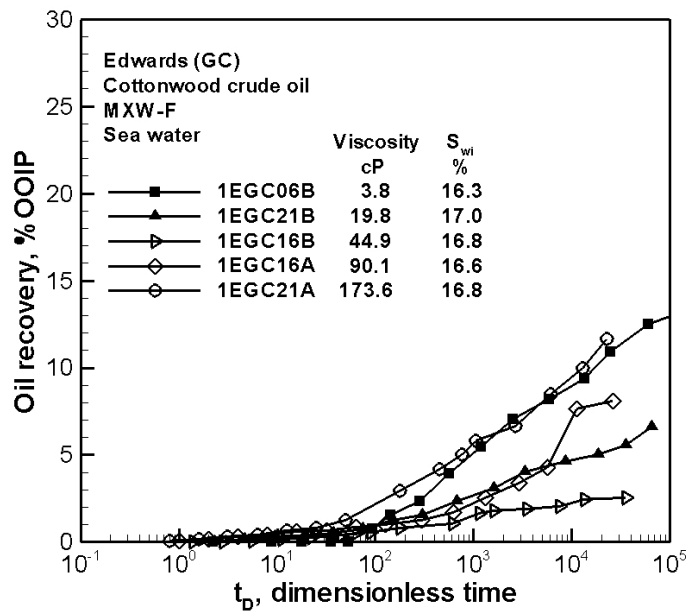
Fig. 2.25 Oil recovery vs. imbibition time for MXW-F Gambier and Edwards (GC) cores with different mineral oil viscosities



(a) Gambier 1st cycle



(b) Gambier 2nd cycle



(c) Edwards (GC)

Fig. 2.26 Oil recovery versus dimensionless time for MXW-F Gambier and Edwards (GC) cores with variation in viscosity of the probe mineral oil.

Task 3: Spontaneous imbibition

Hongguang Tie and Norman Morrow, Chemical & Petroleum Engineering, and Peigui Yin, Enhanced Oil Recovery Institute, University of Wyoming

Part I: Very Strongly Water-Wet (VSWW) Imbibition

Very strongly water-wet (VSWW) conditions provide an important reference state for wettability alteration and oil recovery studies. Spontaneous imbibition tests with clean mineral oil can be used as an evaluation method for determination of the wettability of outcrop carbonates as supplied. Six selected limestones were tested for spontaneous imbibition with zero initial water saturation (S_{wi}). Scaled results were compared with previously reported data for sandstone and other rock types. A homogeneous grainstone, Edwards (GC), was used to test the applicability of a widely adopted scaling group (Ma *et al.*, 1997) for different oil phase viscosities, core lengths, and boundary conditions. Successful correlations were obtained for variations in core properties, core length, and oil phase viscosity. For cores with different boundary conditions, comparisons between Edwards (GC) limestone and Berea 90 sandstone showed that correlation could only be achieved on cores with boundary conditions such that either radial or linear imbibition was dominant. Results showed that radial imbibition contributed less to oil recovery than linear imbibition. This was possibly caused by directional heterogeneity that resulted from diagenesis but further investigation is needed.

Introduction

Because spontaneous imbibition can be the dominant oil recovery mechanism for fractured reservoirs, there is growing interest in scaling of spontaneous imbibition. Ma *et al.* (1997) proposed a scaling group to correlate spontaneous imbibition behavior of very strongly water-wet Berea sandstone cores of different core porosities, permeabilities, lengths, shapes, boundary conditions, interfacial tensions, and viscosities of the oil phase.

$$t_D = t \sqrt{\frac{k}{\phi}} \frac{\sigma}{\sqrt{\mu_w \mu_o}} \frac{1}{L_c} \quad (3.1)$$

where t_D is the dimensionless time, t the actual imbibition time, k the permeability of the tested sample, ϕ the porosity, σ the interfacial tension, μ_w the aqueous phase viscosity, μ_o the oil phase viscosity, and L_c a characteristic length that was defined as:

$$L_c = \sqrt{\frac{V}{\sum_{i=1}^n \frac{A_i}{x_{A_i}}}} \quad (3.2)$$

where V is the bulk volume of the rock matrix, A_i the surface area for the i^{th} imbibition direction, x_{A_i} the normal distance from the i^{th} open imbibition surface to the no-flow boundary, and n the total number of surfaces open to imbibition.

Fischer and Morrow (2004, 2005) reported close correlation of VSWW spontaneous imbibition for Berea sandstone through the use of Equation (3.1) for matched viscosity between oil and water phases and for wide variations in aqueous phase viscosity by the use of glycerol as the viscosifying agent.

In the present work, comparison of spontaneous imbibition behavior was conducted on six selected limestones. Correlation of very strongly water-wet imbibition data for different core properties, core dimensions, oil phase viscosities, and boundary conditions, was investigated for Edwards (GC) limestone. Measurements were also made the effect of boundary conditions for Berea 90 sandstone cores.

Experiments

Six Limestones

Very strongly water-wet spontaneous imbibition experiments for six different outcrop limestones were performed starting at zero initial water saturation. Cores were first vacuum saturated with clean Soltrol 220 (or high viscosity mineral (WMO) oil for Gambier to avoid ultra-fast imbibition). Low permeability cores were also pressurized up to 1000 psi with N₂ to ensure complete saturation. After saturation, spontaneous imbibition of synthetic sea water (or 5% CaCl₂ for Gambier limestone) at room temperature was monitored using graduated glass imbibition cells. Brine properties are listed in Table 3.1.

Scaling of VSWW Imbibition

Three factors which affect spontaneous imbibition behavior, mineral oil viscosity, core length, and boundary conditions, were studied for Edwards (GC) limestone cores. A comparative study was made on Berea 90 sandstone cores at different boundary conditions. Viscosity variation in the probe oil (clean mineral oil) was obtained by mixing Soltrol 220 with high viscosity mineral oil (WMO) at several different volumetric ratios. Prior to experimental use, Soltrol 220 was purified by passage through a chromatographic column packed with silica gel and alumina to remove any polar impurities. The viscosity of clean Soltrol 220 was 3.8 cP @20°C and the interfacial tension (IFT) was ~50 mN/m against sea water. The high viscosity mineral oil was cleaned first by mixing with silica gel and alumina, followed by filtration. The viscosity of the high viscosity mineral oil was ~174 cP @20°C and the IFT was ~50 mN/m against sea water or 5% CaCl₂. The measured interfacial tensions were independent of mineral oil viscosities. Cores with different boundary conditions were prepared by sealing parts of core surfaces with epoxy resin (Devcon 5 Minute[®] Epoxy and Hardener). Selected core properties are listed in Tables 3.2, 3.3, and 3.4.

Results and Discussion

Spontaneous Imbibition of Clean Mineral Oil for Six Limestone Rocks

All cores were initially 100% oil saturated. Spontaneous imbibition results are shown in Fig. 3.1a. Most of the imbibition curves, except those for the Gambier and Whitestone LZ limestones, showed similar shape to that for Berea 90 sandstone. Even for viscous mineral oil, recovery from Gambier limestone was slightly faster than the other cores because of its high porosity (~54%) and permeability (>4 D). The final recovery for the six tested rocks varied from 28% for Whitestone LZ, which is likely caused by the abundance of large moldic pores inside the rock (see Fig. 3.2), to >60% for Gambier limestone (~63%). Scaled imbibition results using Equation (3.1) are shown in Fig. 3.1b. The correlation brought the spontaneous imbibition behavior of the Whitestone UZ limestone very close to that of the Berea 500. The highly heterogeneous Whitestone LZ

still exhibited markedly slower dimensionless times for imbibition behavior than other rocks.

If all the curves are normalized according final recovery (except for Whitestone LZ), and compared with the range of normalized imbibition obtained for a wide variety of rocks by Viksund *et al.* (1998) (see Fig. 3.1c), it can be seen that the curves for Gambier, Whitestone UZ, Edwards (GC) fall very close to each other and to the normalized spontaneous imbibition behavior for the Berea 500; they lie towards the lower values of dimensionless time of the Viksund *et al.* (1998) spread.. On the other hand, the normalized imbibition behavior of Lueders and Fort Riley limestones were essentially identical. They exhibited longer dimensionless times than the Viksund spread, and fell close to the average curve for Berea 90 (a batch of Berea sandstone with permeability around 90 mD with distinctly different character than the Berea 500).

From the spontaneous imbibition behavior (Fig. 3.1) and the petrophysical analysis shown in Chapter 2, it is concluded that all of the selected limestone rocks except Whitestone LZ are very strongly water-wet. Three limestone rocks, i.e., Gambier limestone, Edwards (GC), and Whitestone UZ, were selected for the present study on wettability and oil recovery based on the following experimental results and petrophysical analysis:

- (1) their scaled imbibition behavior is close to that for Berea 500 VSWW spontaneous imbibition;
- (2) they have distinctly different pore structures and porosity types;
- (3) they exhibit a wide range of final oil recoveries from VSWW spontaneous imbibition;
- (4) based on variation in permeability of plugs from individual quarried blocks, two of them, Gambier limestone and Edwards (GC), are homogeneous, and one, Whitestone UZ, heterogeneous.

VSWW Correlation

Edwards (GC), a homogeneous limestone, was selected to test the applicability of the scaling group (Ma *et al.*, 1997) to the correlation of VSWW spontaneous imbibition for a carbonate rock with variations in rock porosity and permeability, probe oil viscosity, core length, and boundary condition.

Correlation of Oil Viscosity

Rate of spontaneous imbibition by VSWW Edwards (GC) cores decreased with increase in the probe oil viscosity (Fig. 3.3a). Large decrease was observed when the mineral oil viscosity increased from 3.8 cP to 42.3 cP. Further increase in oil viscosity from 42.3 cP to 173.6 cP did not result in much change in the spontaneous imbibition behavior. After scaling by Equation (3.1), the imbibition behavior of cores with probe oil viscosities from 3.8 cP to 81.5 cP were closely correlated (Fig. 3.3b). Cores tested with oil viscosity of 173.6 cP exhibited a slightly slower scaled imbibition than the others, but the difference was small. Overall, the application of Ma *et al.*'s scaling group (1997) provided a satisfactory correlation of spontaneous imbibition data for VSWW Edwards (GC) limestone with different probe oil viscosities.

Comparison of the final oil recovery vs. the viscosity of the probe oil showed a tendency for oil recovery to increase with increase in probe oil viscosity (Fig. 3.3c) except for the 81.5 cP oil. Overall, final oil recovery increased by more than 4% with increase in mineral oil viscosity from 3.8 cP to 173.6 cP.

Correlation of Core Length

Ten 1½" diameter Edwards (GC) cores with the length ranging from 1.0 in to 3.0 in were tested for spontaneous imbibition with clean Soltrol 220 mineral oil at zero initial water saturation. L_c^2 varied from 0.82 to 1.55 cm². The increase in core length represents an increase in the relative area of core surface open to radial versus linear imbibition (Table 3.3). Recovery vs. time behavior is plotted in Fig. 3.4a. Further magnification of the portion of 1 to 100 minutes region of the plot with reduced y-axis is presented in Fig. 3.4b for better illustration. Although no clear trend of change in imbibition recovery with increase in core length was observed, application of the scaling group (Equation 3.1) significantly reduced separation between the original data (Fig. 3.4c).

Final oil recovery vs. core length indicates increase in reproducibility of residual saturation to spontaneous imbibition with increase in core length (Fig. 3.4d). When the core length was equal to or longer than 2.5", the differences between duplicate experiments were less than 1%. Differences as high as ~20% were observed for the two 1" core samples. This probably results from the increased effect of core scale heterogeneity with decrease in core length. Therefore, 2.5" length was adopted as an experimental standard for the current study to give reproducibility and for experimental convenience. Although close values of residual oil saturation were obtained for the 2.5" length cores, variation in recovery of up to 10% in laboratory waterflood experiments was still sometimes observed for cores of this length (see Chapter 8).

Fit of Aronofsky et al. (1958) Equation to Scaled Spontaneous Imbibition

Scaled imbibition results for variations in probe oil viscosity and core length were fitted with Aronofsky *et al.*'s (1958) equation to obtain a standard reference curve. Dimensionless time was used instead of the actual imbibition time, as in Equation (3.1), to account for changes in probe oil viscosity and core lengths for the Edwards (GC) limestone.

$$\frac{R}{R_{max}} = 1 - e^{-\alpha t_D} \quad (3.3)$$

where R is the oil recovery, R_{max} the final oil recovery, α the oil production decline constant, and t_D the dimensionless imbibition time.

A combination of correlated spontaneous imbibition for different probe oil viscosities and core lengths is shown in Fig. 3.5. An average final oil recovery from all the tested samples, 41.52%, for R_{max} and an α value of 0.055 gave a close fit. This value of α is close to the value of 0.05 used by Ma *et al.* (1997) to obtain a close fit to scaled VSWW spontaneous imbibition for the Berea 500 sandstone. In this work the reference VSWW spontaneous imbibition curve for the Edwards (GC) limestone is given by:

$$R = 41.52 \times (1 - e^{-0.055t_D}) \quad (3.4)$$

Correlation of Boundary Conditions

Five different boundary conditions, including one end open (OEO), two ends open (TEO), two ends closed (TEC), one end closed (OEC), and all faces open (AFO), were tested. Detailed information about the five boundary conditions, including core condition, flow regimes, and characteristic length, is shown in Fig. 3.6. Two of the most important boundary conditions for fundamental study are OEO, in which only linear countercurrent imbibition occurs, and TEC, in which imbibition is radial. Comparison of oil recovery vs. imbibition time (Fig. 3.7a) shows decreased imbibition rate with increase in the amount of sealed imbibition surfaces. Sealing one end of the core slowed down the early time spontaneous imbibition by more than 5 times compared to the AFO cases. One surprising observation is that although the curved surface area of the core is about 3.4 times the combined area of the two end surfaces and the normal distance from the open imbibition surface to the no-flow boundary is much longer from the ends than from the sides, TEC (sealing the two end surfaces) and TEO (sealing the side cylindrical surface) cores showed very close spontaneous imbibition behavior. After scaling by Equation (3.1) imbibition behavior of the two linear imbibition cases, OEO and TEO, almost overlapped with each other and were very close to the AFO cases (Fig. 3.7b). However, the AFO cases clearly show faster early imbibition than two linear imbibition cases and a different shape of recovery vs. t_D curve. Sealing the end faces of the core resulted in significantly slower than expected scaled spontaneous imbibition. These observations and the experimental results for cores of different lengths (see Fig. 3.4) indicate that linear imbibition is dominant for the Edwards (GC) limestone. Because almost all pores in the Edwards (GC) limestone are moldic pores that resulted from selective dissolution processes, there could be directional dependence on the properties of the rock that determine two phase flow behavior. This directional heterogeneity may be the reason why linear instead of radial flow dominates in oil recovery by imbibition for Edwards (GC) limestone as cut from the block. By adjusting the oil production decline constant, α , the shape of the oil recovery vs. t_D curves for TEO and OEO boundary conditions can be closely fitted by the Aronofsky *et al.*'s equation (1958).

If oil recovery is plotted against square root of imbibition time, there are clearly linear portions at the early time of imbibition for the two linear imbibition cases, OEO and TEO (Fig. 3.7d). The presence of the linear portions confirms that countercurrent imbibition is the dominant oil recovery mechanism (Li *et al.*, 2003; Li *et al.*, 2004). Close correlation between the TEO and OEO cases shows that the middle of the core acts as the no-flow boundary for the TEO core. Comparison of final oil recovery for all the tested boundary conditions (Fig. 3.7d) did not exhibit clear dependency of the final oil recovery on boundary condition except that the TEC core showed the lowest final recovery among all tested samples, but the difference is small.

Comparison of Berea 90 Sandstone and Edwards (GC) with Different Boundary Conditions

Experiments were run on four Berea 90 sandstone cores for the four different boundary conditions: OEO, TEO, TEC, and AFO. For the AFO sandstone core of significantly

greater length than radius, radial countercurrent imbibition is clearly the dominant mechanism. Excluding the linear component of imbibition by sealing the two end surfaces (TEC), causes only minimal reduction in rate of spontaneous imbibition (Fig. 3.8a). As expected, significant reduction in imbibition rate was observed for both the TEO and the OEO cores. Sealing the two ends resulted in a reduction in the surface area open to imbibition by about 25%. For attainment of 20% OOIP, the TEC core required 1.3 times the amount of time needed for the AFO core, whereas the time for the TEO core was slower by 14.4 times, and for the OEO core was slower by 61.3 times. It is clear that the contribution of linear imbibition to oil recovery is not proportional to the relative amount of rock surfaces involved in linear imbibition. Differences that relate to the distance from an open core face to a no flow boundary are expected to be compensated by the use of L_c , the characteristic length.

Application of Ma *et al.*'s (1997) scaling group gave close correlation for the TEC and the AFO boundary conditions and the OEO and TEO cases. However, close correlation was not obtained between linear and radially dominated imbibition results. If compared with results obtained for Edwards (GC) limestone, it appears that Equation (3.1) is only able to give satisfactory correlation of the all faces open results for boundary conditions in which imbibition is controlled by the dominant flow mechanism under the conditions of the test.

Plots of oil recovery against the square root of imbibition time (Fig. 3.8c) showed the expected linear relationship until late time for OEO and TEO cores. About 2% OOIP higher oil recovery was obtained for the AFO and TEC cores.

Table 3.1 Synthetic brine composition

Brine	NaCl (g/L)	KCl (g/L)	CaCl₂ (g/L)	MgCl₂ (g/L)	NaN₃ (g/L)	pH	TDS (mg/L)
Sea water	28	0.935	2.379	5.365	0.1	6.6	36779
5% CaCl₂	-	-	50	-	0.1	6.9	50100

Table 3.2 Edwards (GC) cores tested with different mineral oil viscosities

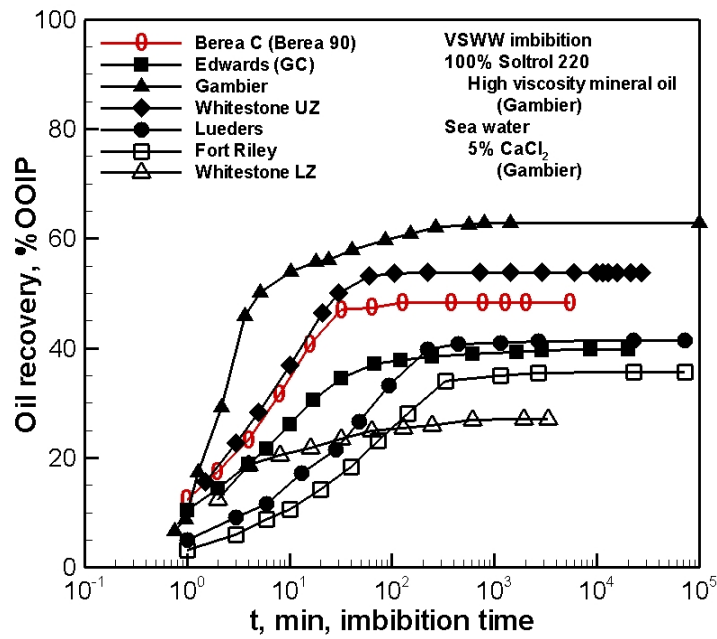
No.	D	L	ϕ	k_g	μ_o	L_c	$\sqrt{\frac{k}{\phi}} \frac{\sigma}{\sqrt{\mu_o \mu_w}} \frac{1}{L_c^2}$
	<i>cm</i>	<i>cm</i>	<i>%</i>	<i>mD</i>	<i>cP</i>	<i>cm</i>	<i>1/min</i>
1EGC01A	3.80	6.36	21.3	11.1	3.8	1.238	2.292
1EGC02A	3.80	6.06	21.6	14.5	3.8	1.228	2.644
1EGC03A	3.80	6.54	21.7	13.2	18.7	1.242	1.109
1EGC03B	3.80	6.53	21.7	10.8	42.3	1.242	0.667
1EGC04A	3.80	6.32	21.2	10.5	81.5	1.236	0.484
1EGC01B	3.80	6.21	22.1	11.5	173.6	1.232	0.342
1EGC02B	3.80	6.16	22.2	12.3	173.6	1.231	0.354

Table 3.3 Edwards (GC) cores tested for the effect of variation in core length ($\mu_o = 3.8\text{cP}$)

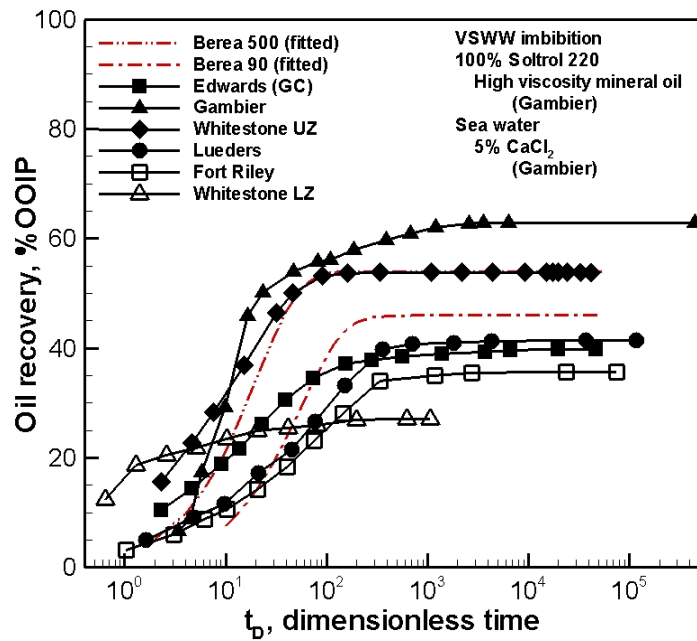
No.	D	L	ϕ	k_g	L_c	$\sqrt{\frac{k}{\phi}} \frac{\sigma}{\sqrt{\mu_o \mu_w}} \frac{1}{L_c^2}$	L	A_{side}/A_{end}
	<i>cm</i>	<i>cm</i>	<i>%</i>	<i>mD</i>	<i>cm</i>	<i>1/min</i>	<i>in</i>	
1EGC27C	3.74	2.54	19.8	14.0	0.92	4.902	1.0	1.4
1EGC28C	3.74	2.50	20.5	8.1	0.91	3.716	1.0	1.3
1EGC29A	3.74	3.77	19.0	7.5	1.08	2.616	1.5	2.0
1EGC29B	3.74	3.80	21.1	9.2	1.08	2.742	1.5	2.0
1EGC27B	3.73	5.02	22.0	13.2	1.17	2.766	2.0	2.7
1EGC28B	3.74	5.11	20.7	9.8	1.17	2.439	2.0	2.7
1EGC01A	3.80	6.36	21.3	11.1	1.24	2.300	2.5	3.3
1EGC02A	3.80	6.06	21.6	14.5	1.23	2.644	2.4	3.2
1EGC27A	3.73	7.64	20.7	13.2	1.25	2.503	3.0	4.1
1EGC28A	3.73	7.54	20.8	12.3	1.24	2.419	3.0	4.0

Table 3.4 Edwards (GC) and Berea 90 sandstone cores tested for correlation of different boundary conditions

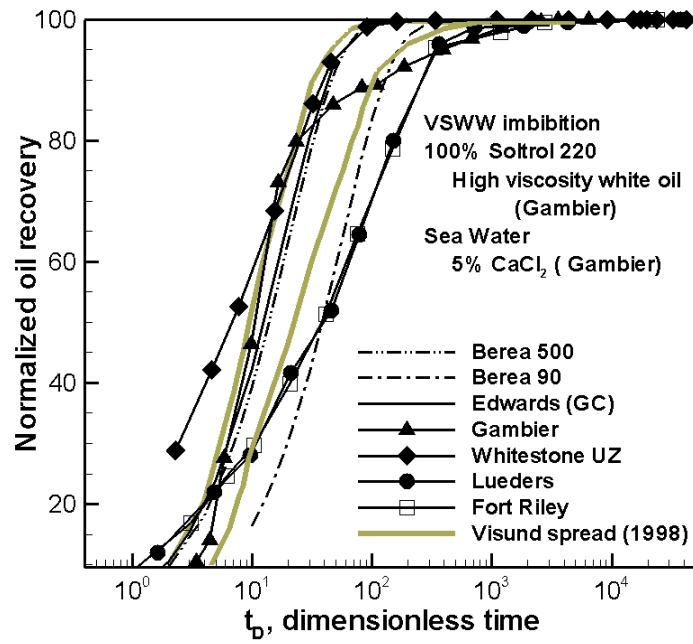
No.	D	L	ϕ	k_g	L_c	$\sqrt{\frac{k}{\phi}} \frac{\sigma}{\sqrt{\mu_o \mu_w}} \frac{1}{L_c^2}$	Boundary condition
	cm	cm	%	mD	cm	1/min	
Edwards (GC) limestone							
1EGC17B	3.74	6.49	20.5	10.3	6.49	0.0818	OEO
1EGC18B	3.74	6.38	20.1	9.1	6.38	0.0804	OEO
1EGC19A	3.74	6.38	21.2	13.2	3.19	0.3779	TEO
1EGC19B	3.74	6.47	21.0	12.2	3.24	0.3550	TEO
1EGC17A	3.73	6.40	20.6	12.1	1.32	2.1399	TEC
1EGC18A	3.73	6.38	20.5	9.2	1.32	1.8707	TEC
1EGC20A	3.74	6.36	21.2	12.7	1.29	2.2542	OEC
1EGC20B	3.74	6.45	21.0	11.2	1.29	2.1234	OEC
1EGC01A	3.80	6.36	21.3	11.1	1.24	2.2924	AFO
1EGC02A	3.80	6.06	21.6	14.5	1.23	2.6439	AFO
Berea sandstone							
2C02B	3.75	5.52	17.07	68.5	5.52	0.320	OEO
2C01B	3.75	5.50	16.44	67.9	2.75	1.308	TEO
2C02A	3.74	6.34	17.07	70.7	1.32	5.672	TEC
2C01A	3.75	6.23	17.49	71.3	1.22	6.621	AFO



(a) Recovery vs. time



(b) Recovery vs. t_D

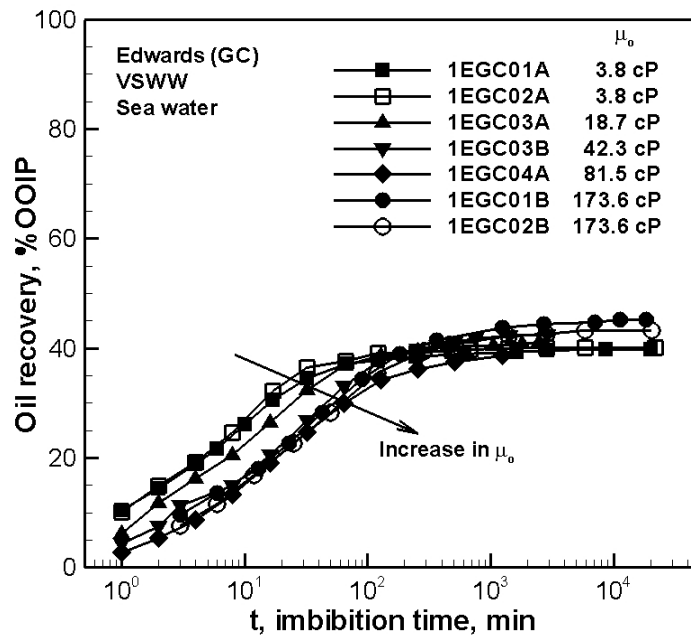


(c) Normalized comparison

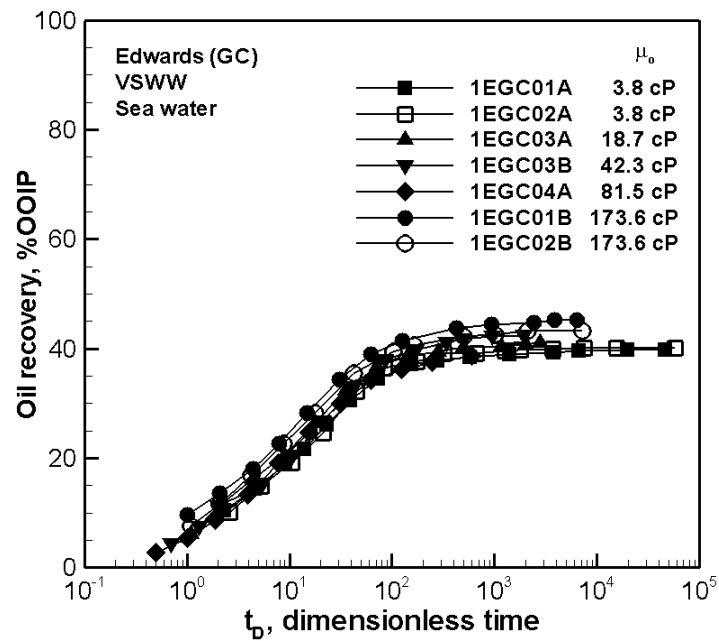
Fig. 3.1 Spontaneous imbibition behavior of six selected limestones



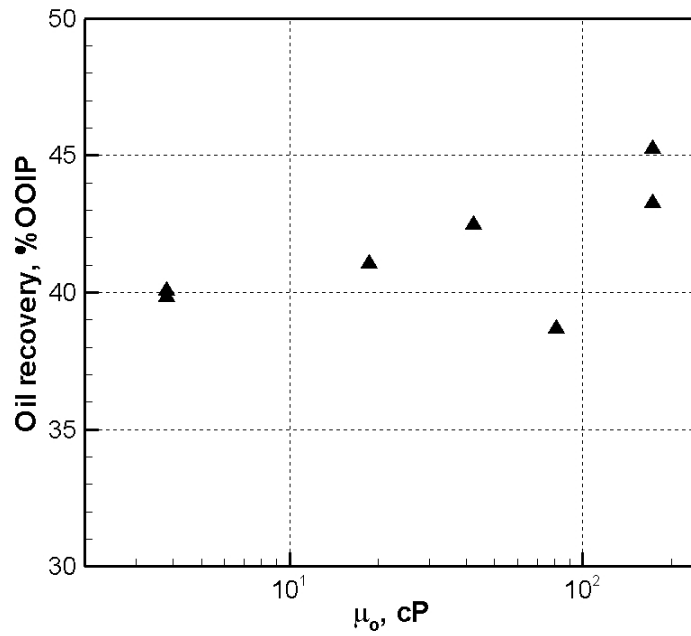
Fig. 3.2 Vugs in Whitestone LZ Cores (1.5" diameter core)



(a) Recovery vs. time

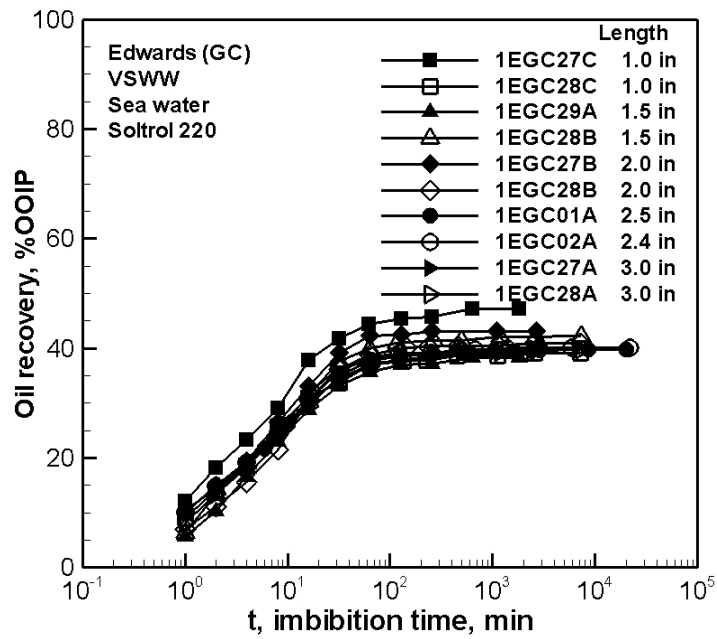


(b) Recovery vs. t_D

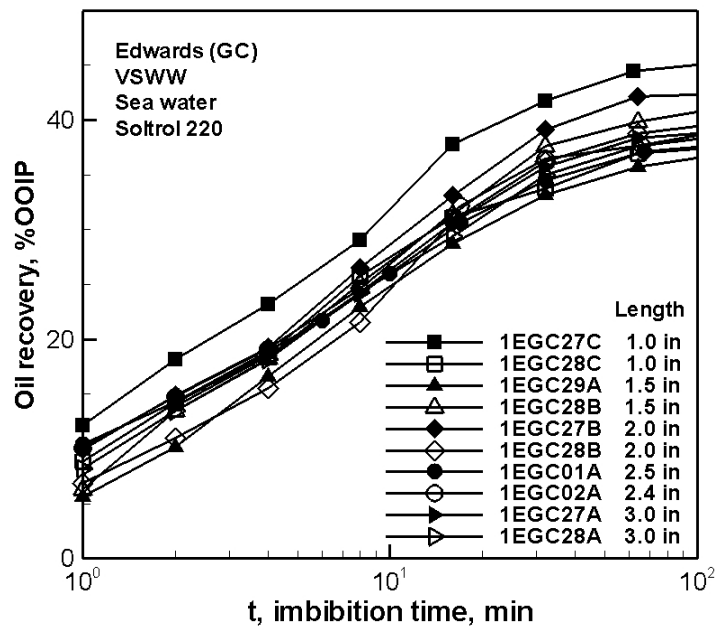


(c) Final recovery vs. oil viscosity

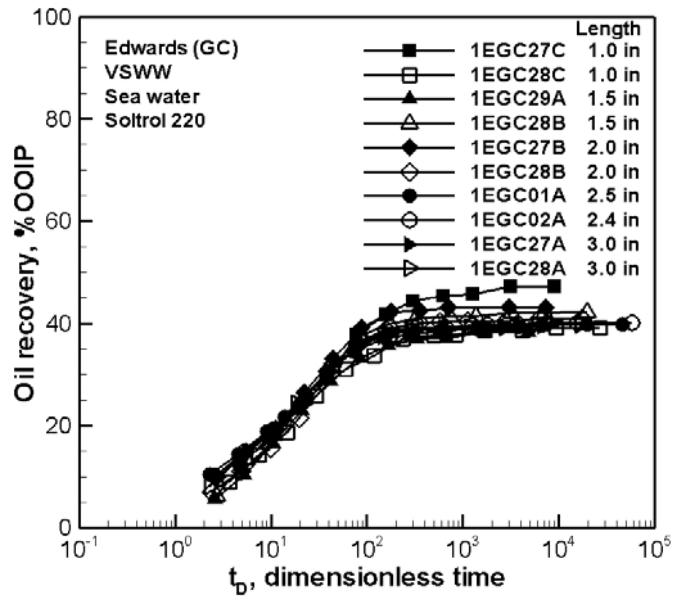
Fig. 3.3 Spontaneous imbibition behavior of VSWW Edwards (GC) AFO cores with different probe oil viscosities



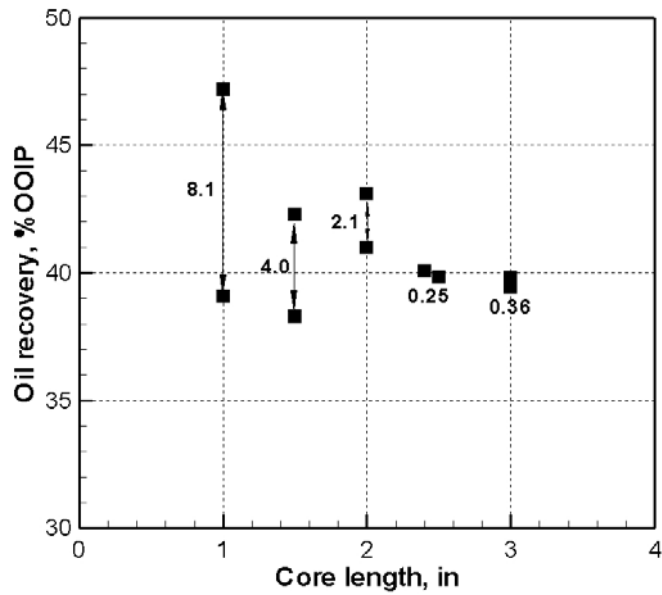
(a) Recovery vs. time



(b) Recovery vs. time portion



(c) Recovery vs. t_D



(d) Final recovery vs. core length

Fig. 3.4 Spontaneous imbibition behavior of VSWW Edwards (GC) cores of different lengths

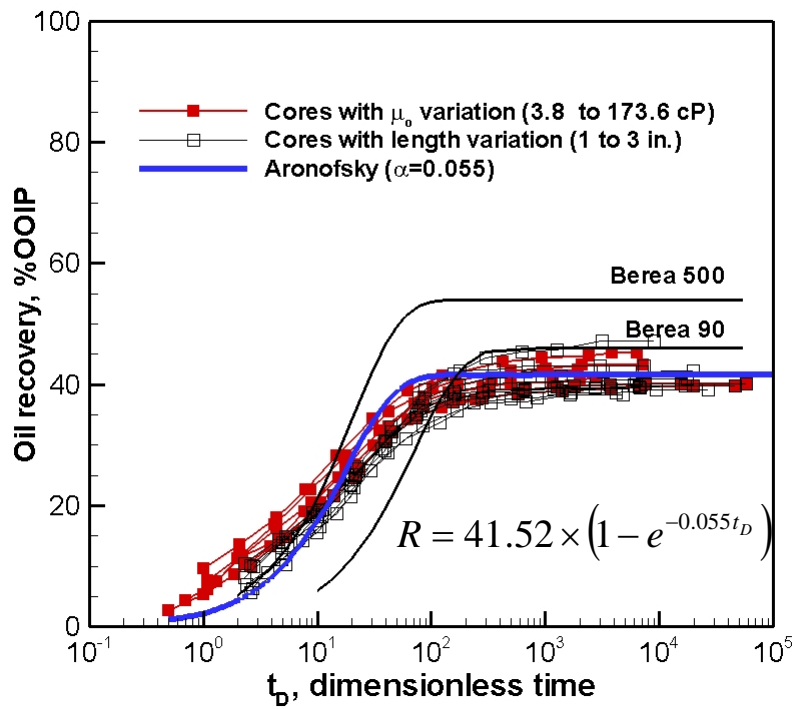


Fig. 3.5 Correlated VSWW Edwards (GC) spontaneous imbibition for different core lengths and probe oil viscosities and fit to Aronofsky *et al.* (1958) equation

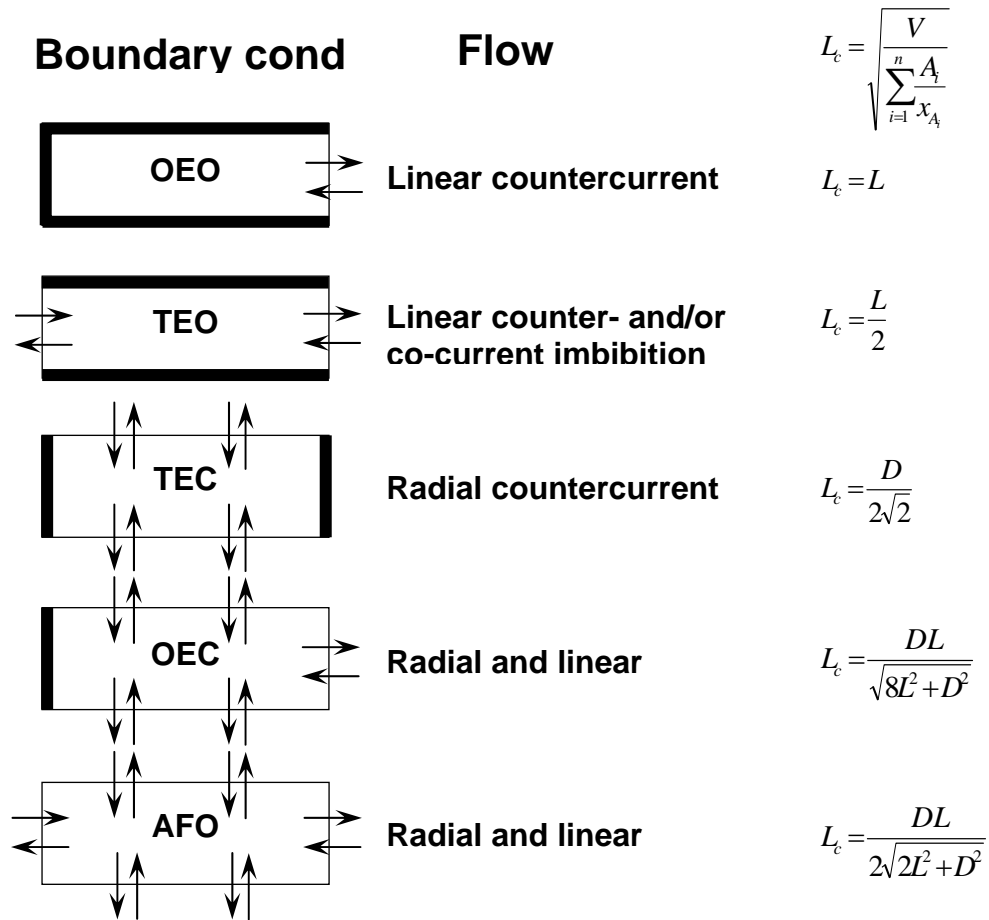
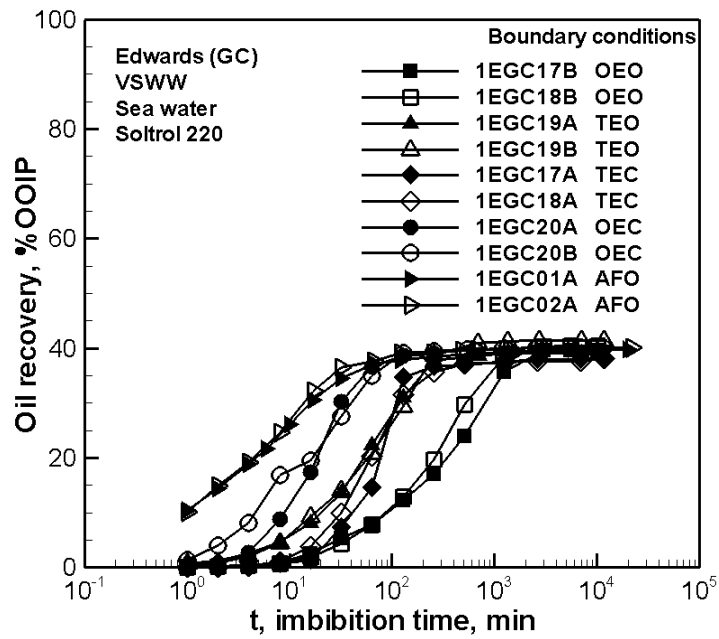
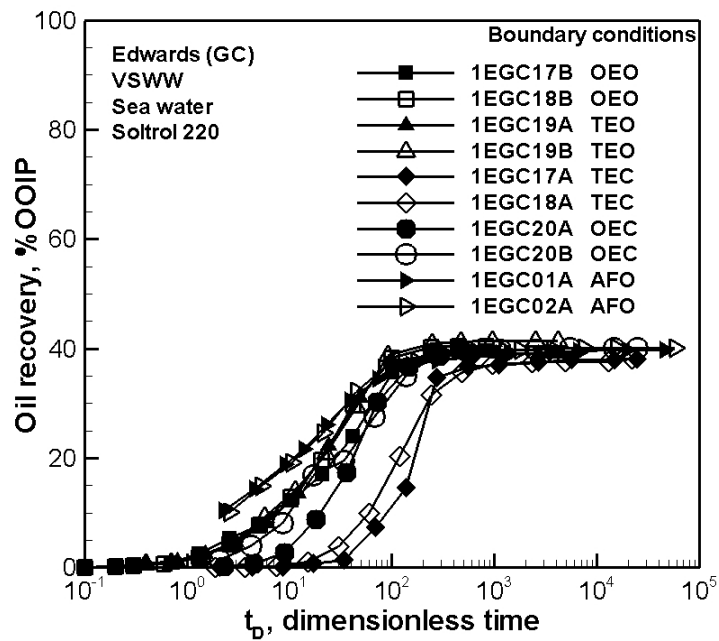


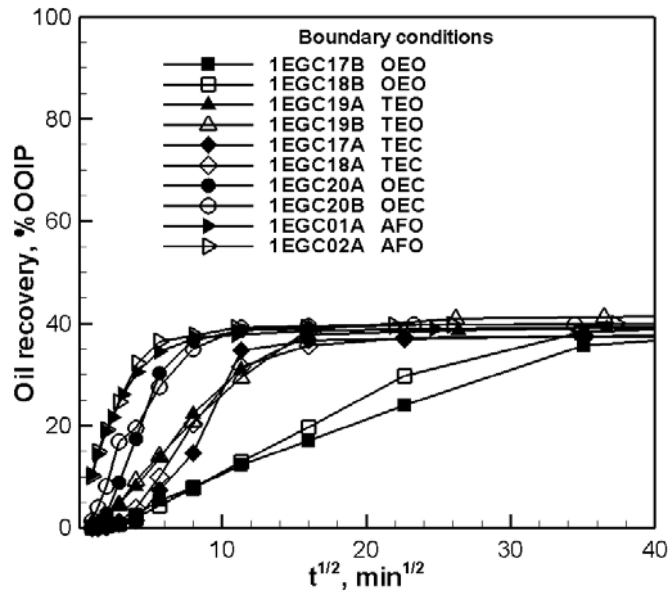
Fig. 3.6 Different boundary conditions, flow regimes, and characteristic length



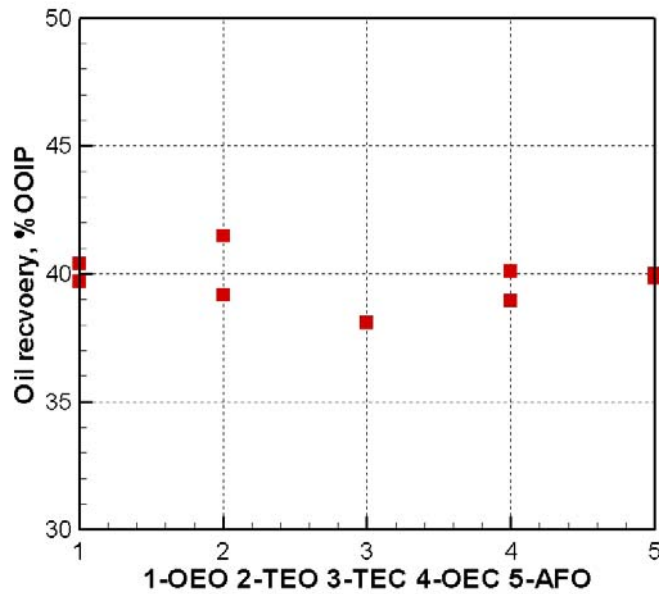
(a) Recovery vs. time



(b) Recovery vs. t_D

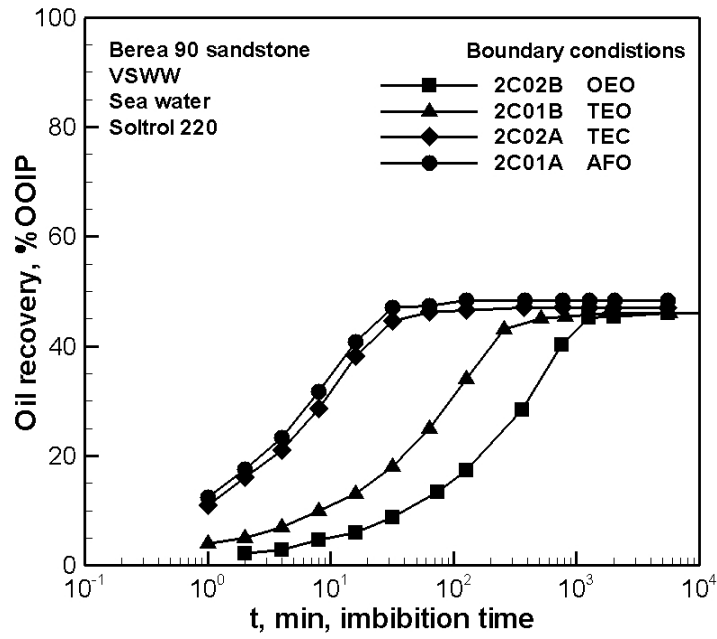


(c) Recovery vs. \sqrt{t}

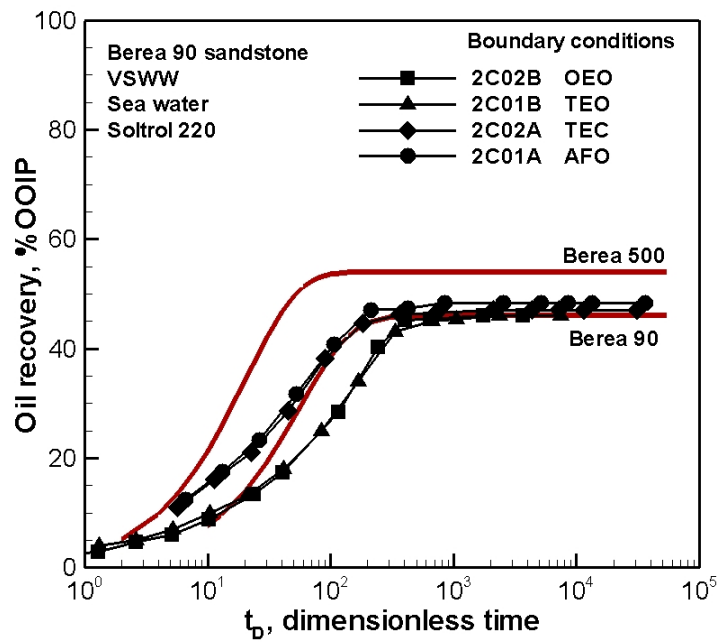


(d) Final recovery vs. boundary condition

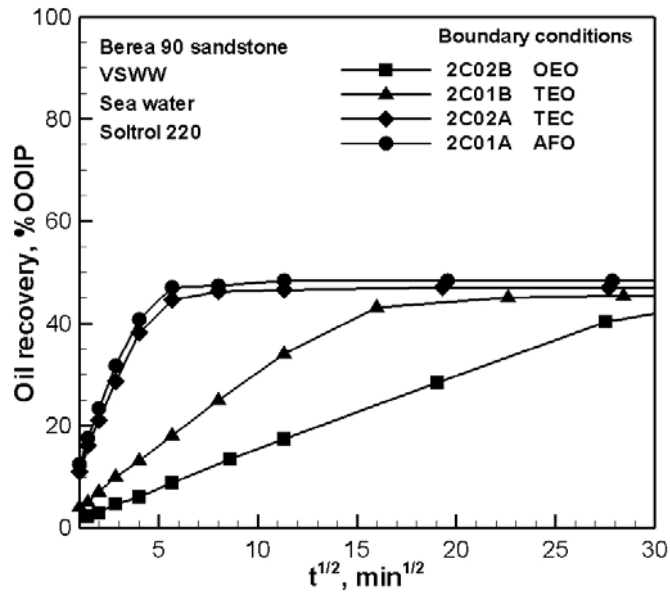
Fig. 3.7 Spontaneous imbibition behavior of VSWW Edwards (GC) cores with different boundary conditions



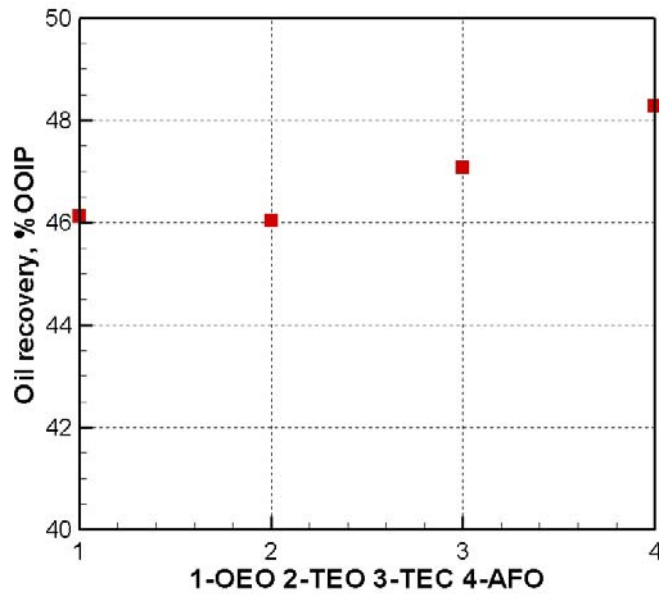
(a) Recovery vs. time



(b) Recovery vs. t_D



(c) Recovery vs. \sqrt{t}



(d) Final recovery vs. boundary condition

Fig. 3.8 Spontaneous imbibition behavior of VSWW Berea 90 cores with different boundary conditions

Part II: The Effect of Different Crude Oil/Brine/Rock (COBR)

Combinations on Wettability through Spontaneous Imbibition

Wettability depends on crude oil/brine/rock interactions. The presence of initial water saturation can determine the areas of rock pore surface where such interactions result in adsorption of polar components from crude oil to give a condition described as mixed wettability (MXW). If crude oil is removed to leave an organic film (F) on the rock surface, the condition is referred to as MXW-F. MXW and MXW-F wetting states are compared through spontaneous imbibition measurements for crude oil/brine/rock combinations that include one sandstone and one limestone with each rock type exposed to an asphaltic and a moderately asphaltic crude oil. The solvency of the crude oils for the asphaltenes was decreased by addition of n-decane with volumetric ratio ranging from 14% to 30%. The limestone exhibited greater sensitivity to crude oil solvency than the sandstone. Whatever the crude oil or its composition, rates of recovery of refined oil by spontaneous imbibition from MXW-F cores were slower than for the corresponding MXW cores.

Introduction

Although about one half of world oil reserves are held in carbonate formations, the number of laboratory studies of oil recovery from carbonate rocks are far fewer than for sandstone. Denekas *et al.* (1959) found both acidic and basic components of crude oil could change the wettability of sandstone, while the basic nitrogenous components mainly affected limestone. Somasundaran (1975) noted that quartz surfaces are more sensitive to basic components in crude oil while carbonate surfaces are more sensitive to acidic components. Buckley *et al.* (1998) pointed out that one mechanism for wettability alteration induced by contacting a mineral surface with crude oil is by nonspecific attraction between oppositely charged surface sites. Specific interactions, ion binding, and chelation may all contribute to crude oil/brine/rock interactions (Buckley *et al.*, 1998). Near neutral pH, silica is negatively charged, whereas calcite is positively charged. Because of such effects, it has often been suggested that the oil recovery mechanisms controlled by adsorption from crude oil for sandstone differ from those for carbonate. For example, it has often been suggested that carbonates are more likely to be oil wet (Anderson, 1986a).

Al-Maamari and Buckley (2003) pointed out that the stability of asphaltenes could be a dominant factor that overrides the various ionic interaction mechanisms and makes the surfaces oil-wet through asphaltene precipitation. One approach to investigation of the potential reservoir wetting changes caused by such effects during production is to run laboratory tests at reservoir pressure and temperature using reconstituted live oil. However, such tests are expensive. It may be possible to design simplified laboratory tests that are relevant to reservoir conditions. For example, if the solvency of the live crude oil is matched through addition of n-decane, rather than hydrocarbon gases (mainly methane), to the dead crude oil, the effect of wettability on reservoir performance might be modeled satisfactorily simply by running tests at elevated temperature but ambient pressure.

In previous work, Xie *et al.* (2002) showed that the stability of wetting changes induced on smooth quartz surfaces by adsorption from crude oil depended on its chemical properties. Oil with moderate (~2%) to high asphaltene content (~9%) and high base numbers generally gave films that were stable to movement of the three phase line of contact back and forth across the surface. For sandstones, a series of investigations were performed on correlation of MXW and MXW-F imbibition behavior that included, the effects of initial water saturation, wetting stability, and crude oil composition (Xie and Morrow, 2002; Tong *et al.*, 2002; Tong *et al.*, 2003a; Tong *et al.*, 2003b).

In this work, exploratory studies are reported on the effect of different crude oil/brine/rock combinations on the wettability of MXW and MXW-F cores through spontaneous imbibition measurements. Limestone outcrop samples were obtained from Mt. Gambier, Australia, and Berea sandstone was supplied by Cleveland Quarries, Ohio. These rocks were chosen mainly because of availability and the distinct difference in their surface mineralogy. An asphaltic crude oil from a sandstone reservoir and a moderately asphaltic crude oil from a carbonate reservoir were used to induce wettability changes. The effect of decrease in solvency of the crude oils on wettability alteration was investigated through addition of alkane.

Experimental Materials and Procedures

Cores

Limestone

Fourteen cores, nominally of 3.8 cm diameter and 5.0 cm length, were cut from Mt. Gambier limestone (Australia). The air permeabilities of the cores ranged from 3750 md to 5420 md with twelve of the cores in the range 4000 to 4500 md. Porosities were all in the range $54.0 \pm 1.4\%$. One reason for use of this high permeability rock in this exploratory study was to ensure that imbibition could be measured within reasonable times even at close-to-neutral wettability. The limestone is composed of coral fossil fragments, with a minor amount of coarse sparry calcite. It is very porous and interparticle and intraparticle pores are abundant (see Figs. 3.9a (i) and (ii)).

Sandstone

Seventeen cores, nominally of 3.8 cm diameter and 7.6 cm length, were cut from blocks of Berea sandstone referred to as Berea 90 (Tong *et al.*, 2002). Air permeabilities ranged from 80 to 123 md with 15 of the cores in the range 90 to 113 md. Porosities were all within $18.4 \pm 0.6\%$. This rock sample is subarkose with framework mainly composed of quartz, feldspar, and lithic fragments. Minor amounts of sparry dolomite cement and kaolinite and chlorite clays exist. Porosities are dominated by intergranular pores (see Figs. 3.9a (iii) and (iv)). From X-ray diffraction analysis, the ratio of chlorite to kaolinite for Berea 90 was higher than typically observed for Berea sandstone of higher permeability.

Individual core properties are listed in Tables 3.5 and 3.6. Surface areas from nitrogen adsorption (BET) and cation-exchange capacities are included in Table 3.7.

Crude Oil

One crude oil from a Wyoming sandstone reservoir of Permian/Lower Permian age (Gibbs Field, Minnelusa formation) and one from a Wyoming dolomite reservoir of Permian age (Cottonwood Creek, Phosphoria dolomite) were selected. The Cottonwood crude oil was sparged with nitrogen to remove H₂S. Asphaltene content, acid and base numbers, viscosities and densities of the two crude oils are presented in Table 3.8.

Crude Oil with Reduced Solvency (CO/Reduced Solvency)

The solvency of the dead Minnelusa crude oil for its asphaltene was reduced by addition of n-decane 14% and 22% by volume to provide solvencies above and below the onset of precipitation (Wang, 2002). Tests on Cottonwood crude oil were run after addition of either 20% or 30% by volume of n-decane.

Brine

A 5% CaCl₂ brine was used for displacement tests of the limestone rock in order to limit dissolution (Graue *et al.*, 1994). Simulated Minnelusa reservoir brine was used for the tests on sandstone/Minnelusa oil combinations. Sea water was used in tests on sandstone/Cottonwood oil combinations. NaN₃ (0.10 g/L) was added as a biocide to all brines in order to prevent bacterial growth. Brine compositions are listed in Table 3.9.

Mineral Oil

Mineral oils (Soltrol 220 mineral oil, 3.8 cp, and a heavy mineral oil of about 175 cp), with polar components removed by exposure to silica gel and alumina, were used in core preparation and imbibition tests.

Oil/Brine Interfacial Tension

Interfacial tensions (IFT), measured by drop volume tensiometer (Krüss DVT-10), were 27.0 mN/m for Minnelusa/Minnelusa brine, 25.1 mN/m for Minnelusa/5% CaCl₂, 29.7 mN/m for Cottonwood/sea water, and 27.2 mN/m for Cottonwood/5% CaCl₂. IFT values of this magnitude provide indication that the oil is not contaminated by oil field chemicals such as corrosion inhibitors (Hirasaki and Zhang, 2004). Refined oil/brine interfacial tensions were ~50 mN/m.

Establishment of Initial Water Saturations Prior to Aging

Initial water saturations were established by displacing brine with either crude oil or heavy mineral oil. The core samples were first saturated with, and then soaked in, the selected brines for at least 10 days to attain ionic equilibrium. Two different procedures were adopted in reaching target values of S_{wi} : (1) for sandstone samples with Minnelusa crude oil, S_{wi} of about 25% was established by displacing reservoir brine directly with crude oil at 45°C at 0.2 ml/min to 5.0 ml/min (about 0.72 to 18.75 PV/hr). (2) For limestone samples and sandstone cores treated with Cottonwood crude oil, S_{wi} was attained by displacing brine with heavy mineral oil followed by displacement of mineral oil with 5 PV decalin. The decalin was then displaced with 5 PV of the crude oil at elevated temperature (T_f). The heavy mineral oil floods of sandstone samples were performed at 0.15 ml/min to 0.50 ml/min (about 0.6 PV/hr to 2 PV/hr). A rate of 0.20 ml/min was used for the subsequent decalin and crude oil displacements. For the

limestone samples, heavy mineral oil was injected at 0.25 ml/min to 5.0 ml/min (about 0.5 to 10 PV/hr) to give S_{wi} of about 28.5%. Subsequent decalin and crude oil displacements were run at 0.25 ml/min (about 3 ft/day, 0.5 PV/hr). In all tests, the flow direction was reversed and 1 PV of the displacement oil was injected to even out the water saturation along the length of the core.

Initial water saturation is a critical parameter of wetting and imbibition (Xie and Morrow, 2001; Tong *et al.*, 2002) that deserves to be investigated in its own right for carbonates. However, attempts to obtain a close match of the initial water saturations of the limestone and sandstone would not serve much purpose. The fraction of water retained by fine pores and microporosity can be expected to differ significantly between the two rock types.

Aging in and Replacement of the Crude Oil and CO/Reduced Solvency

Cores containing crude oil or CO/Reduced Solvency mixtures at S_{wi} were submerged in the selected oil and aged in sealed pressure vessels for 10 days at 75°C (T_a). If the cores are then tested with these oils, they are referred to as MXW cores.

In preparation of MXW-F cores, crude oil or modified crude oil was displaced by 5 PV of decalin at 3 ft/day (about 0.72 PV/hr for the sandstone, and about 0.5 PV/hr for the limestone) at 50°C. Decalin was then displaced with 5 PV of Soltrol 220 at ambient temperature. The effect of contact of the mineral oil with crude oil on wettability was tested by omitting the intermediate solvent (decalin) displacement so that the crude oil was displaced directly by the mineral oil.

Spontaneous Imbibition

The prepared MXW and MXW-F core samples were set in glass imbibition cells filled with the selected brine. Oil volume produced by imbibition of brine, expressed as percentage of original oil in place (%OOIP), versus time was recorded. All of the imbibition tests were performed at ambient temperature (T_m).

Amott Indices

After brine imbibition, some of the MXW and MXW-F cores were selected for measurement of Amott wettability indices (Amott, 1959). The cores were flushed with the test brine at rates up to 48 ft/day (for sandstone) and 60 ft/day (for limestone) ft/day (2.4 ml/min and 5.0 ml/min respectively). The flow direction was reversed and one additional PV of brine was injected to even out the fluid distribution along the length of the core. Then the core was immersed in oil and recovery of brine by spontaneous imbibition was recorded. After completion of the imbibition step, the cores were flooded with oil at rates equal to those used in the corresponding brine flood to determine the amount of brine recovered by forced displacement.

Results and Discussion

Previous studies showed that a semi-empirical scaling group initially developed for strongly water-wet conditions (Ma *et al.*, 1997), can be used to compare changes in imbibition rate as a result of changes in wettability for a variety of MXW (Xie and

Morrow, 2001) and MXW-F (Tong *et al.*, 2002) wetting conditions. The following scaling group is used in the present work to assess changes in wettability from spontaneous imbibition behavior.

$$t_D = t \sqrt{\frac{k}{\phi}} \frac{\sigma}{\sqrt{\mu_o \mu_w}} \frac{1}{L_c^2} \quad (3.5)$$

where t_D is dimensionless time, t is time, k is permeability, ϕ is porosity, σ is the interfacial tension, and μ_o and μ_w are the oil and brine viscosities. L_c is a characteristic length that compensates for sample size, shape and boundary conditions (Ma *et al.*, 1997).

Mixed-wet cores often do not exhibit clear-cut imbibition end points. In the present work the imbibition recovery, $V_{o,imb}$ for oil and $V_{w,imb}$ for brine, used in calculation of Amott indices was operationally determined by the recovery at a cutoff dimensionless time of 10^5 (This corresponds to imbibition time ranging from about 3 days for the Mt. Gambier limestone MXW-F cores to about 80 days for Berea sandstone MXW cores). The largest value of $V_{o\varepsilon,imb}$ (see Table 3.10, Core 5B8) was obtained after 12 months. Post-cutoff recovery, if any, by spontaneous imbibition, $V_{o\varepsilon,imb}$ and $V_{w\varepsilon,imb}$, was added to the recoveries obtained by force displacement, $V_{o,f}$ for oil recovery and $V_{w,f}$ for brine recovery to obtain Amott indices from the following equations (Cuiec, 1991).

$$I_w = \frac{V_{o,imb}}{V_{o,imb} + V_{o\varepsilon,imb} + V_{o,f}} \quad (3.6)$$

$$I_o = \frac{V_{w,imb}}{V_{w,imb} + V_{w\varepsilon,imb} + V_{w,f}} \quad (3.7)$$

$$I_{w-o} = I_w - I_o \quad (3.8)$$

Comparison of Imbibition by Limestone and Sandstone MXW Cores

MXW Cores – Recovery of Minnelusa and Cottonwood Crude Oils

Fig. 3.9b presents scaled imbibition data for MXW limestone cores for Minnelusa and Cottonwood crude oils. Results for sandstone cores are presented in Fig. 3.9c. The rate of recovery for Cottonwood oil is less than for the Minnelusa oil for both the sandstone and limestone cores. One contributing reason for this behavior is that, although the Minnelusa crude oil has higher asphaltene content than Cottonwood oil (9.0% vs. 2.3%), the ratio of acid and base number to asphaltene content of the Cottonwood oil is comparatively high.

Imbibition rates (normalized with respect to rates for very strongly water-wet (VSWW) conditions) vs. oil recovery for the two oils and two rocks are shown in Fig. 3.9d. For the same fraction of oil recovery, the relative rate of recovery for the sandstone falls between the relative rates measured for the limestone.

Minnelusa Crude Oil Plus Alkane

MXW imbibition rates for limestone samples decrease with addition of n-decane (see Fig. 3.10a). For the sandstone cores, Fig. 3.10b, noticeable decrease was only achieved when 22% of n-decane was added to the crude oil. Also, an obvious induction time was observed for Minnelusa crude oil containing 22% of n-decane.

Cottonwood Crude Oil Plus Alkane

In MXW (Cottonwood) limestone cores, imbibition rates decrease significantly with the increase in the added volume of n-decane (Fig. 3.10c). For sandstone cores, Fig. 3.10d, decreases in imbibition rates were also observed but were small relative to those observed for the limestone. No significant differences were observed in imbibition behavior between cores prepared with 20% and 30% of n-decane added to the crude oil except after long imbibition time.

Comparison of Imbibition for Limestone and Sandstone MXW-F Cores

Direct Displacement of Crude Oil by Mineral Oil

For both limestone and sandstone core samples, and either Minnelusa or Cottonwood crude oil, the MXW-F samples prepared by direct flush of crude with 5 PV of Soltrol 220 mineral oil (MO) show very low imbibition rate and recovery (see Figs. 3.11a and 3.11b). The likely cause of the large change in wetting is surface precipitation of asphaltenes (Al-Maamari and Buckley, 2003). Conditions for surface precipitation propagate through the core as the injected refined oil mixes with the crude oil to give a composition that results in surface precipitation. This composition is close to that for the onset of asphaltene precipitation (Al-Maamari and Buckley, 2003).

MXW-F for Different Crude Oils

Comparison of imbibition results for MXW-F limestone and sandstone cores are presented in Fig. 3.11a and Fig. 3.11b respectively. Compared to MXW results, the rate and extent of imbibition for MXW-F cores were consistently lower for all tests. For example, the recovery from Cottonwood MXW-F cores is about 10% for limestone and 11% for sandstone, while the recovery from Cottonwood MXW cores is 28% for limestone and 33% for sandstone. (cf. Figs. 3.9b, 3.9c and 3.11a, 3.11b respectively). For sandstone samples, the imbibition rate for MXW-F (Minnelusa) cores is faster than for MXW-F (Cottonwood) cores. Except at early time, the scaled imbibition rates of MXW-F (Cottonwood) cores are almost the same for both limestone and sandstone cores.

Minnelusa Oil Plus Alkane

For both limestone and sandstone MXW-F (Minnelusa plus alkanes) core samples respectively, the imbibition rates are dramatically suppressed compared to the results for MXW (Fig. 3.11c and Fig. 3.11d). For limestone core samples, the imbibition rates for MXW-F cores prepared with 14% and 22% of n-decane in Minnelusa crude oil were low and showed no significant differences. (The MXW-F core prepared with Minnelusa crude oil even showed slightly lower imbibition rate and recovery.) For sandstone MXW-F cores, no differences in the imbibition behavior were observed for cores prepared with 0%, 14%, and 22% n-decane added to Minnelusa crude oil.

Cottonwood Oil Plus Alkane

In MXW-F (Cottonwood), for both limestone and sandstone core samples (cf. Figs. 3.11e, 3.11f and Figs. 3.10c, 3.10d respectively), the imbibition rates are suppressed compared to corresponding MXW combinations (Figs. 3.10c and 3.10d). For both rock types, addition of alkanes had essentially no effect on imbibition behavior.

Amott Indices

For both limestone and sandstone, Table 3.10, the Amott index of MXW cores lay in the water-wet range (0.3 to 1) by Cuiec's classification (Cuiec, 1987 and 1991). For the MXW-F cores, all the values of I_{w-o} fell in the range of intermediate-wet (-0.3 to 0.3). Moreover, limestone MXW-F cores all had neutral wettability (-0.1 to 0.1).

The largest change in wettability from the original VSWW state was observed for an MXW-F limestone core prepared by direct displacement of Minnelusa crude oil with mineral oil ($I_w = 0.05$, $I_o = 0.93$, $I_{w-o} = -0.88$). This provides strong evidence for wettability alteration by asphaltene precipitation, a mechanism which was first identified through contact angle behavior (Al-Maamari and Buckley, 2003).

Table 3.5 Minnelusa crude oil

Core	L cm	D cm	k md	ϕ	S_{wi} %	μ_o cP	σ mN/m	Recovery of oil (imbibition)
Berea sandstone								
5B2	7.745	3.784	92.5	0.179	24.6	77.2	27.0	Crude
5B3	7.506	3.783	97.9	0.180	25.0	3.8	49.5	mineral oil
5B8	7.394	3.785	103.7	0.185	24.6	77.2	27.0	crude
5B32	7.668	3.782	94.3	0.185	25.7	3.8	49.5	mineral oil
5B33	7.719	3.782	99.0	0.187	25.2	3.8	49.5	mineral oil
3B3	8.118	3.799	99.3	0.184	25.8	19.1	22.1	14 (v)% decane + crude
3B4	7.776	3.799	92.3	0.183	25.5	3.8	49.5	mineral oil
3B5	7.878	3.798	93.7	0.182	26.1	3.8	49.5	mineral oil
3B6	7.854	3.798	94.2	0.182	25.6	14.5	25.1	22 (v)% decane + crude
3B20	7.827	3.798	123.3	0.188	25.3	3.8	49.5	mineral oil
Mt Gambier limestone								
G25	5.334	3.765	4530	0.550	28.7	70.6	25.1	crude
G02	5.006	3.782	5420	0.532	28.5	3.8	49.5	mineral oil
G07	4.961	3.776	4220	0.541	28.4	3.8	49.5	mineral oil
G12	4.917	3.778	4090	0.528	28.6	3.8	49.5	mineral oil
G13	5.055	3.778	4420	0.554	28.6	19.1	25.1	14 (v)% decane + crude
G26	5.181	3.774	4270	0.530	28.4	3.8	49.5	mineral oil
G15	5.017	3.770	3990	0.533	28.6	14.5	25.4	22 (v)% decane + crude

Table 3.6 Cottonwood crude oil

Core	L cm	D cm	k md	ϕ	S_{wi} %	μ_o cP	σ mN/m	Recovery of oil (imbibition)
Berea sandstone								
3B11a	7.050	3.798	113.6	0.190	24.6	3.8	49.5	mineral oil
3B12a	7.261	3.798	107.1	0.190	25.6	3.8	49.5	mineral oil
3B13a	7.158	3.798	109.2	0.190	25.2	9.2	28.6	20 (v)% decane + crude
3B15a	7.038	3.798	103.7	0.188	24.6	24.1	29.7	crude
3B16a	7.279	3.784	100.0	0.187	25.5	3.8	49.5	mineral oil
3B16b	7.064	3.785	80.7	0.182	24.2	3.8	49.5	mineral oil
3B17a	7.061	3.788	101.4	0.186	25.2	6.4	28.9	30 (v)% decane + crude
Mt Gambier limestone								
G08	5.103	3.772	4350	0.542	28.8	24.1	27.2	crude
G10	4.897	3.773	4140	0.548	28.2	3.8	49.5	mineral oil
G11	5.087	3.780	4160	0.526	28.4	3.8	49.5	mineral oil
G16	4.948	3.770	4060	0.531	28.5	3.8	49.5	mineral oil
G17	4.904	3.770	3750	0.538	28.7	9.2	27.0	20 (v)% decane + crude
G18	5.056	3.767	4170	0.550	28.5	3.8	49.5	mineral oil
G19	5.050	3.764	4120	0.544	28.4	6.4	26.9	30 (v)% decane + crude

Table 3.7 Selected properties of sandstone and limestone cores

Cores	BET, m ² /g	CEC, meq/100g
Berea sandstone	1.2	0.30
Mt. Gambier limestone	0.77	0.065

Table 3.8 Selected properties of crude oil samples

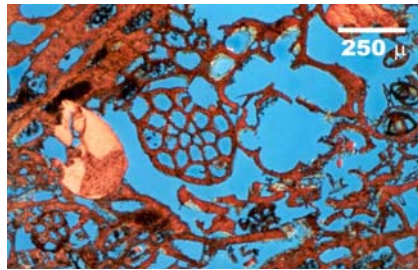
Crude oil	Density, g/ml	μ_o at 22°C, cP	n-C7 asphalt., wt%	Acid #, mg KOH/g oil	Base #, mg KOH/g oil
Minnelusa	0.9062	77.2	9.0	0.17	2.29
Cottonwood	0.8874	24.1	2.3	0.56	1.83

Table 3.9 Synthetic brine composition

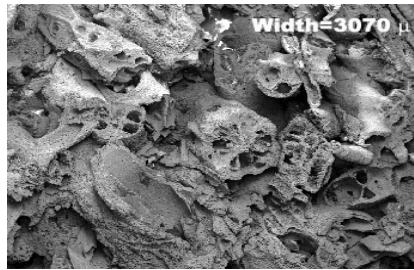
Brine	NaCl	KCl	CaCl ₂	MgCl ₂	MgSO ₄	Na ₂ SO ₄	NaN ₃	pH	TDS
	g/L	g/L	g/L	g/L	g/L	g/L	g/L		mg/L
Minnelusa	29.8	-	2.1	-	0.394	5.903	0.1	6.8	38297
Sea water	28	0.935	2.379	5.365	-	-	0.1	6.6	36779
5% CaCl₂	-	-	50	-	-	-	0.1	6.9	50100

Table 3.10 Amott Indices

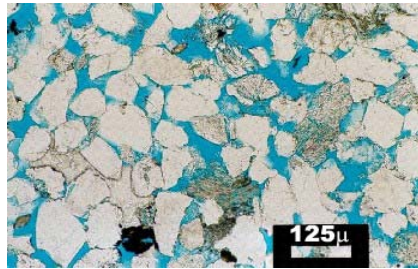
Core	$V_{o,imb}$	$V_{oe,imb}$	$V_{o,f}$	I_w	$V_{w,imb}$	$V_{w\&,imb}$	$V_{w,f}$	I_o	I_{w-o}	Wetting State
	mL	mL	mL		mL	mL	mL			
Mt. Gambier limestone										
G07	0.43	0.17	8.40	0.05	6.80	0.55	0	0.93	-0.88	MXW-F (Minnelusa Direct Flood)
G12	2.03	0.67	10.54	0.15	1.45	0.10	9.70	0.13	0.02	MXW-F (14% Decane + Minnelusa)
G08	6.26	3.54	3.15	0.48	0.10	0	12.50	0.01	0.48	MXW (Cottonwood Crude)
G11	1.00	0.03	10.80	0.08	1.37	0.03	8.70	0.14	-0.05	MXW-F (Cottonwood Direct Flood)
G10	2.23	0.72	10.90	0.16	2.20	0.40	9.40	0.18	-0.02	MXW-F (Cottonwood)
Berea sandstone										
5B8	4.15	0.35	1.20	0.73	0	-	-	0	0.73	MXW (Minnelusa)
3B3	4.50	2.90	0.05	0.6	0	-	-	0	0.60	MXW (22% Decane + Minnelusa)
3B12b	2.07	0.41	5.03	0.28	0.28	0	6.42	0.04	0.24	MXW-F (Minnelusa)
3B15a	3.80	0.65	0.85	0.72	0	-	-	0	0.72	MXW (Cottonwood)
3B13a	4.60	2.00	0	0.70	0	-	-	0	0.70	MXW (20% Decane + Cottonwood)
3B16b	0.42	0.16	7.13	0.05	0.65	0.07	6.30	0.09	-0.04	MXW-F (Cottonwood Direct Flood)
3B12a	1.30	0.37	7.00	0.16	0.30	0.10	7.50	0.04	0.12	MXW-F (Cottonwood)



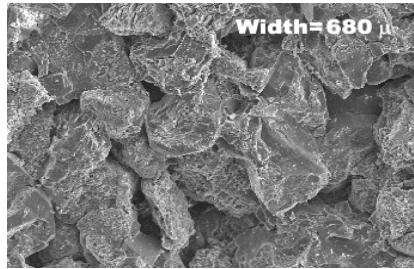
i. Thin section, limestone



ii. SEM, limestone

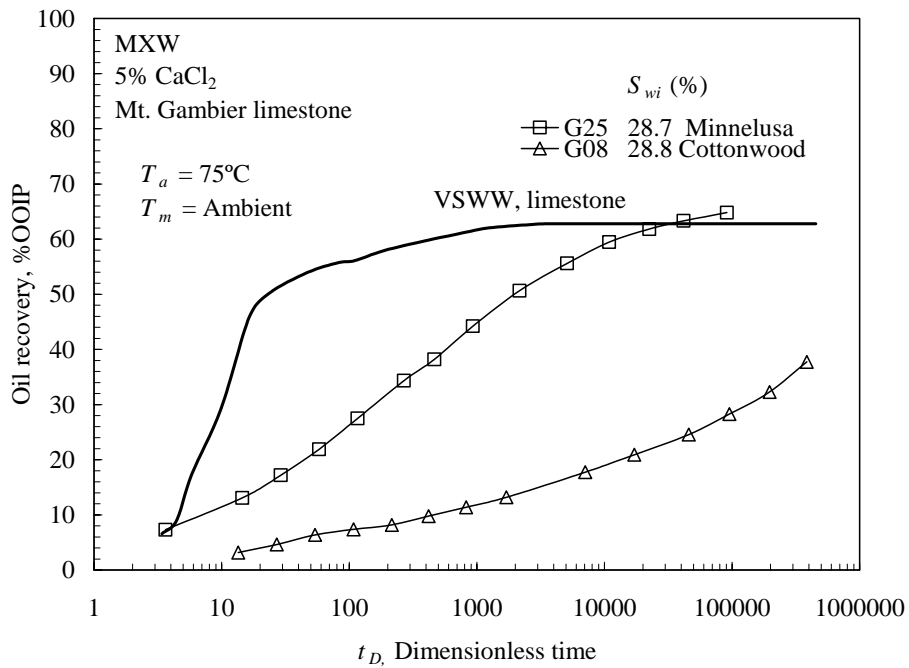


iii. Thin section, sandstone

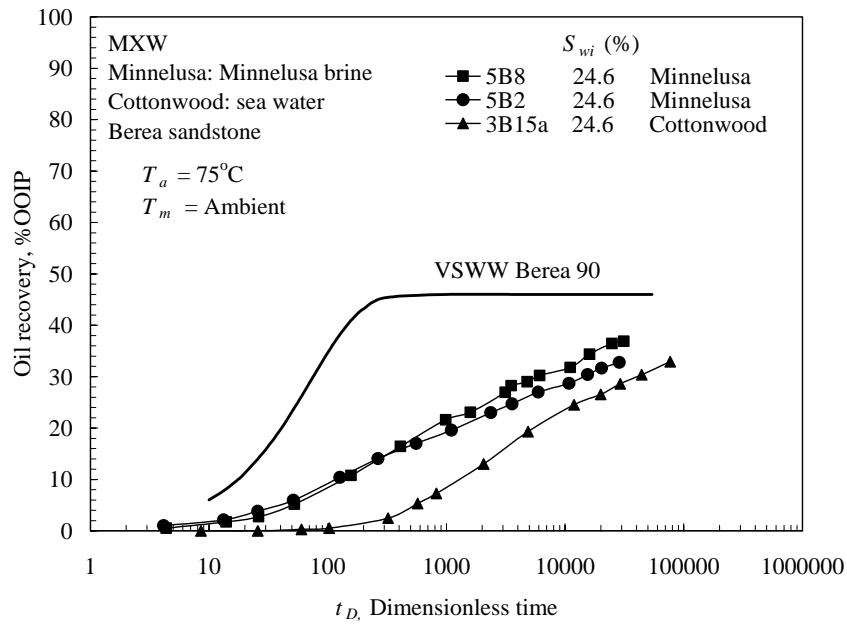


iv. SEM, sandstone

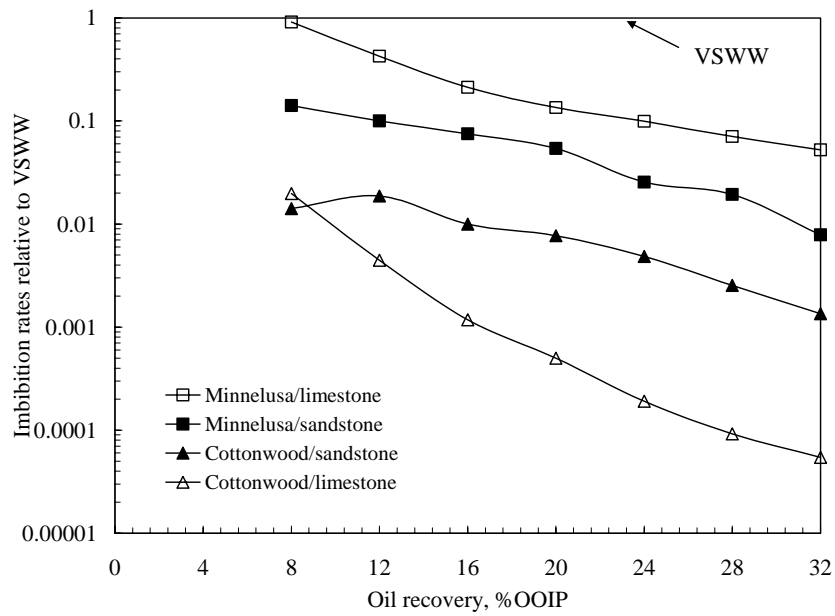
(a) Thin section and SEM photos



(b) Limestone

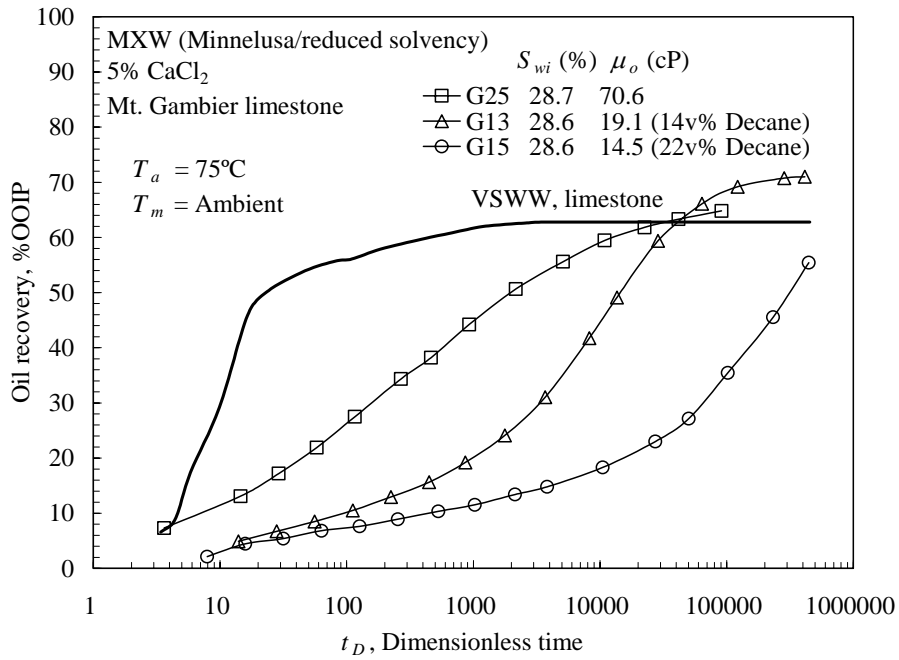


(c) Sandstone

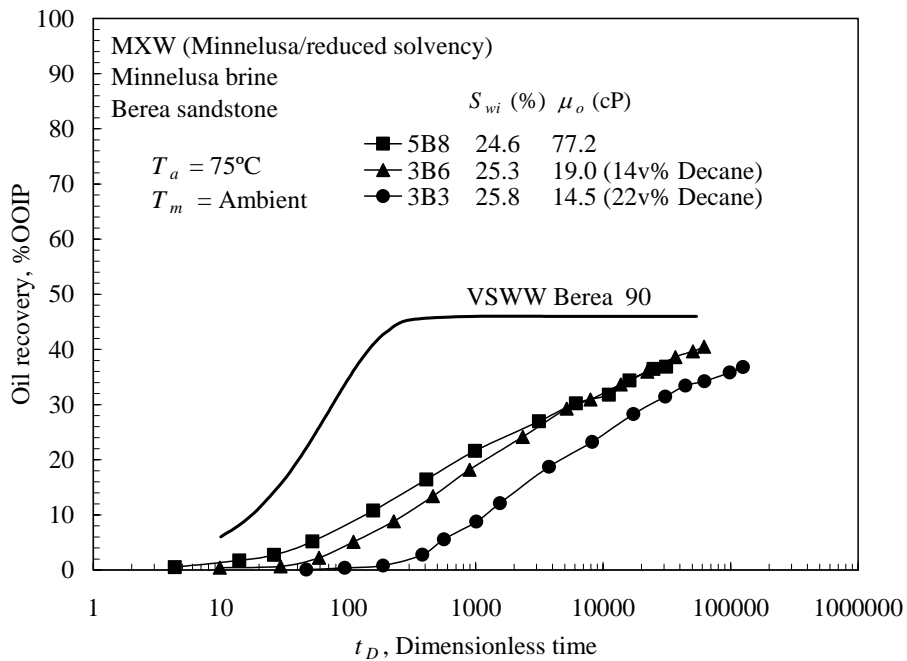


(d) Relative reduction in imbibition rates

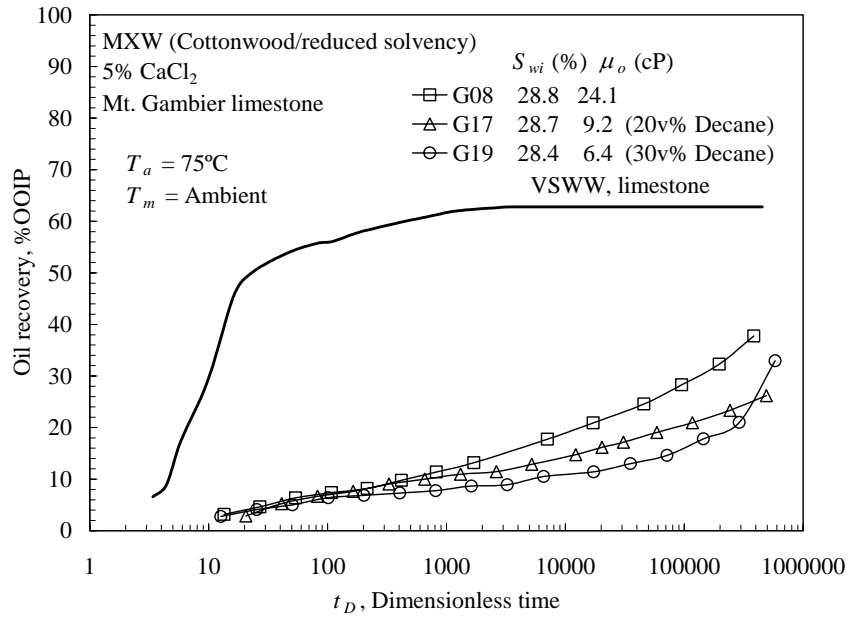
Fig. 3.9 Thin section and SEM photos and recovery of crude oil from MXW limestone and sandstone by spontaneous imbibition.



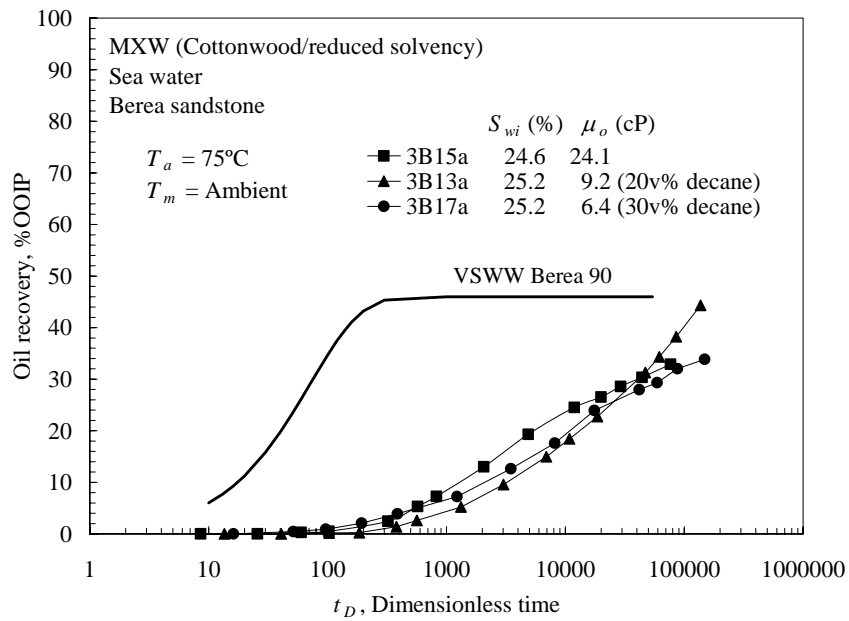
(a) Minnelusa/limestone



(b) Minnelusa/sandstone

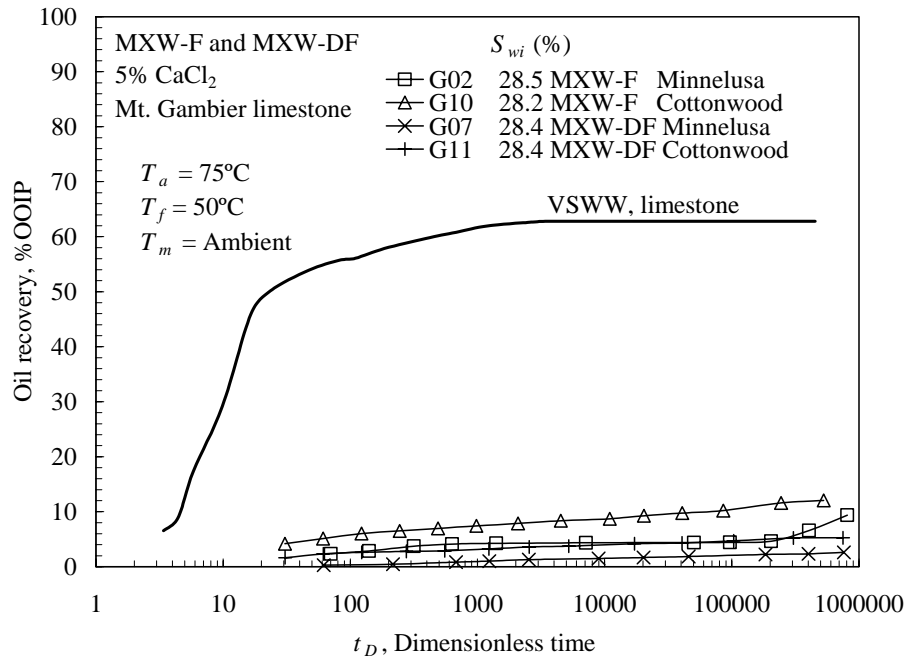


(c) Cottonwood/limestone

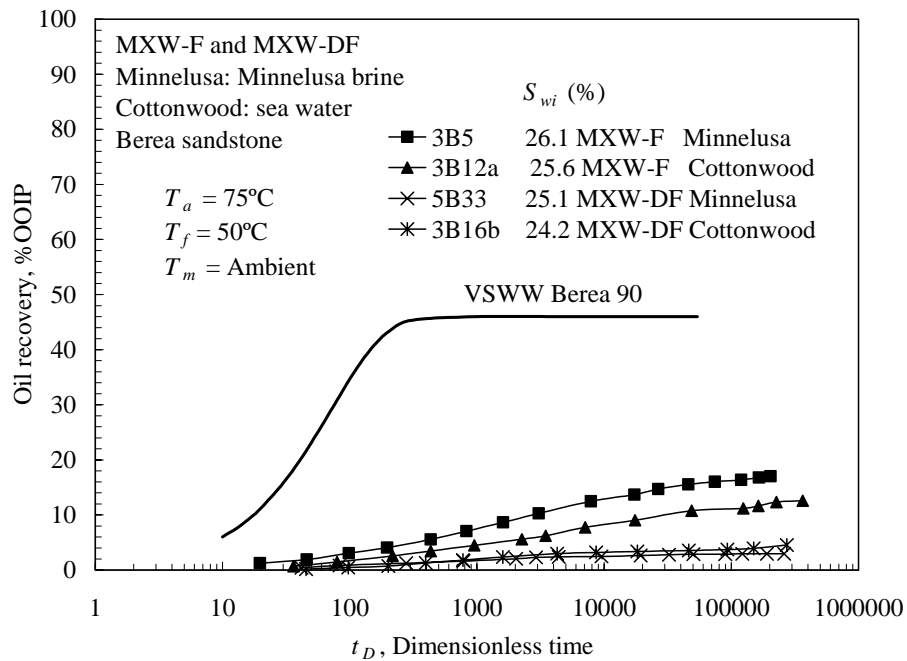


(d) Cottonwood/sandstone

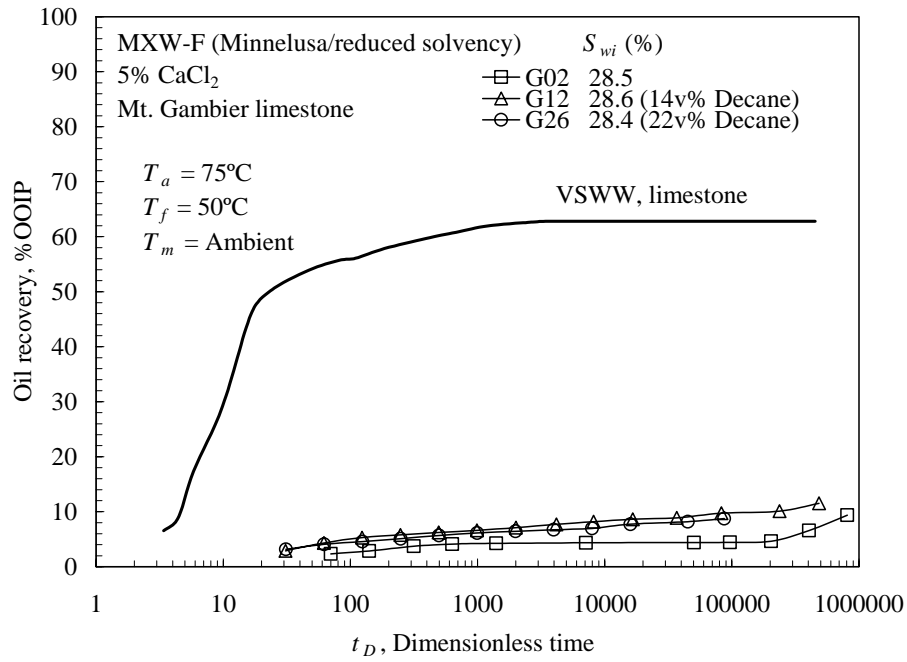
Fig. 3.10 Recovery of crude oil from MXW (CO/reduced solvency) limestone and sandstone by spontaneous imbibition.



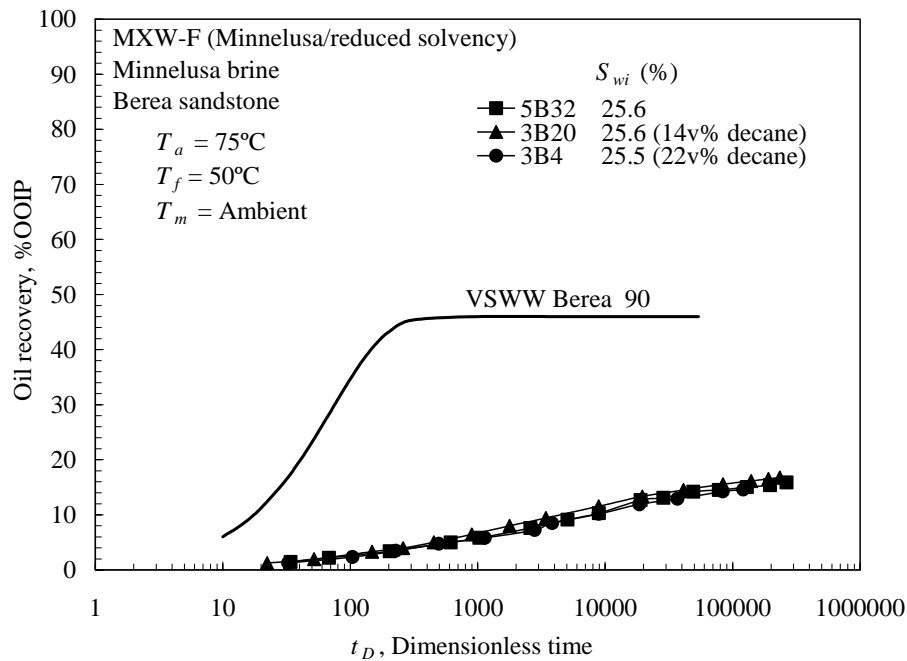
(a) Limestone



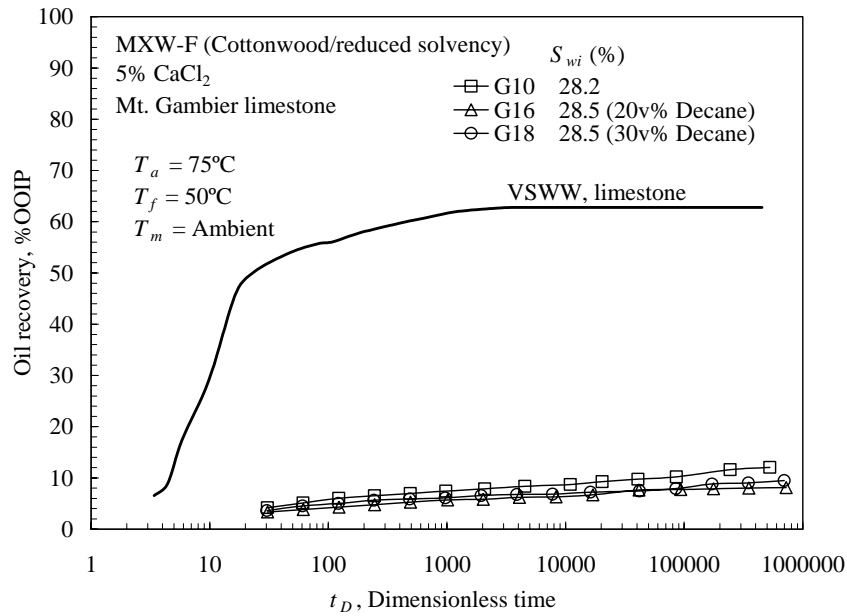
(b) Sandstone



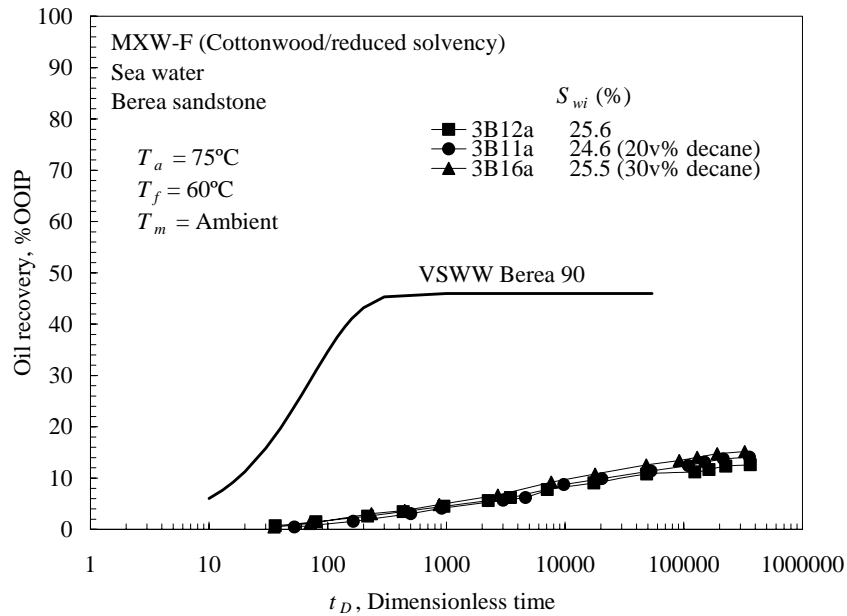
(c) Minnelusa/limestone



(d) Minnelusa/sandstone



(e) Cottonwood/limestone



(f) Cottonwood/sandstone

Fig. 3.11 Recovery of mineral oil from MXW-F, MXW-F (CO/reduced solvency), and MXW-DF limestone and sandstone by spontaneous imbibition.

Part III: Oil Recovery by Spontaneous Imbibition before and after Wettability Alteration of Three Carbonate Rocks by A Moderately Asphaltic Crude Oil

Carbonate rocks can exhibit great morphological complexity at the pore, core, and reservoir scale. Cores ranging in permeability from 7 to 4000 md were cut from three outcrop limestones (two grainstones and a reef boundstone). One of the grainstones was homogeneous at the core scale and the other was distinctly heterogeneous. The rocks were characterized by permeability and porosity, thin section, scanning electron microscopy, BET surface area, and cation exchange capacity (CEC). Scaled data for the three types of outcrop limestone at very strongly water-wet conditions (VSWW) agreed well with correlated results for a wide range of other rock types. Mixed-wet rocks (MXW) were prepared, in the presence of initial water saturation, by adsorption from Cottonwood Creek crude oil, a moderately asphaltic crude. The crude oil was displaced by an intermediate solvent which was in turn displaced by refined oil to leave an adsorbed film (F) of polar crude oil components on the rock surface. This wetting state is referred to as MXW-F. In other experiments, the crude oil was directly displaced by refined oil to obtain wetting states by surface precipitation of asphaltenes referred to as MXW-DF. The wetting states induced in the three carbonate rocks by the above methods were compared through measurements of spontaneous imbibition of brine and oil. Recoveries by forced displacement were measured to obtain Amott indices to oil and water. For all three rock types, MXW cores gave significantly higher rate and extent of imbibition than the MXW-F cores. MXW-DF cores showed the greatest wettability change. All of the MXW-F and MXW-DF cores exhibited intermediate wettability.

Introduction

Carbonate reservoirs hold about one-half of the world's oil reserves. Reported studies of oil recovery behavior from carbonate rocks are much fewer than for sandstone. Berea sandstone has been used as a model rock in by far the majority of studies on oil recovery from sandstones. To date, no comparable model rock has been adopted widely for study of carbonates. Indiana limestone, which, for example, has sometimes been employed in past studies, exhibits a large degree of macroscopic heterogeneity at the core scale (Churcher *et al.*, 1991). In the present work, change in wettability induced by adsorption from crude oil was investigated for three selected outcrop limestones: a reef boundstone from Mt. Gambier, Australia, and two grainstones from Texas.

In wettability studies, very strongly water-wet cores provide the reference condition for identifying changes resulting from wettability alteration. A distinct advantage of using clean outcrop carbonates is that they are very strongly water-wet whereas, as yet, there are no reliable core cleaning techniques for restoration of reservoir carbonates to very strongly water-wet states. Several mechanisms can contribute to wettability alteration by crude oil. Non-specific interaction between oppositely charged surface sites is believed to

be one of the most important factors (Buckley *et al.*, 1998). Near neutral pH, carbonate surfaces are positively charged. Negatively charged components, such as carboxylic acids, can be expected to attach to the surface and alter the wetting (Block and Simms, 1967; McCaffery and Mungan, 1970; Lowe *et al.*, 1973; Somasundaran, 1975; Cuiec, 1984). Al-Maamari and Buckley (2003) pointed out that displacement of crude oil by a precipitant for asphaltenes could result in surface deposition which overrides various ionic interactions and render the rock surface strongly oil-wet.

From advancing contact angle measurements on calcite and quartz surfaces for a series of crude oils representing a wide variety of carbonate and sandstone reservoirs, Treiber *et al.* (1972) and Chilingar and Yen (1983) concluded that carbonate reservoirs tend more towards oil wetness than sandstones. However, Tie *et al.* (2003) showed that by aging either carbonate or sandstone cores with crude oil (at 75°C for 10 days), the wettability, assessed from recovery of crude oil by spontaneous imbibition and by Amott wettability indices, still remained in the water-wet region.

In this work, spontaneous imbibition behavior is compared for three well characterized limestones, before and after inducing mixed wettability by adsorption from crude oil in the presence of an initial water saturation. Cottonwood Creek crude oil, a moderately asphaltic crude oil, from a producing carbonate reservoir, was used to induce wetting change. Three distinct forms of wetting alteration from VSWW that depend on the method of treatment are compared for each rock type.

Experimental

Rock Characterization

Three limestone rocks selected for study are Whitestone Upper Zone (Whitestone UZ or WUZ), Edwards (Garden City) (Edwards (GC) or EGC), and Gambier (G). The limestones characterized using various petrophysical observations and measurements. BET surface area and cation exchange capacity (CEC) results are listed in Table 3.11. Desorption/adsorption isotherms for water have also been reported (Fischer *et al.*, 2005). From thin sections (see Fig. 3.12), according to Dunham's classification (Dunham, 1962), both Whitestone UZ and Edwards (GC) are grainstones. Gambier rock is a reef boundstone. SEM micrographs are included in Fig. 3.12.

Cores

Whitestone UZ, also known as Texas Crème, quarried from the upper bench of the Whitestone Member of the Lower Cretaceous Walnut Formation, Texas, is a grainstone composed mostly of calcite. Air permeabilities and porosities varied significantly for cores cut from a 12 by 12 by 6 inch block. Air permeabilities of individual cores varied by more than an order of magnitude (<1 md to ~14 md) and porosities ranged from 18.9% to 26.4%. On the basis of this variation, Whitestone UZ is referred to as a heterogeneous limestone. In this study of comparative wetting change, three Whitestone

UZ core samples of 6 md permeability were selected to avoid extreme differences in core properties (see Table 3.12).

Edwards (GC), which is also known as West Texas Crème, Cedar Hill Cream, or Valencia Ivory building stone, is an outcrop Cretaceous limestone from West Texas. The rock is quarried from a member of the Edwards Formation. Petrophysical property measurements on samples cut from individual 12 by 12 by 6 inch blocks showed only modest variation. Air permeabilities are around 13 md and porosities are about 21%. The rock is mainly composed of calcite crystals, which can be identified both in the bulk of the rock matrix and at pore walls (see Fig. 3.12b). Water adsorption isotherms show that only about 0.5% of the pore space is in the micropore (0 to 2.1 nm) to mesopore (2.1 to 53.0 nm) range (Fischer *et al.*, 2005).

Gambier limestone is an Oligocene-age outcrop quarried from Mount Gambier, Australia. Air permeabilities are about 4000 md and porosities about 54%. Abundant coral fossil fragments can be readily identified from thin section (Fig. 3.12a) and SEM (Fig. 3.12b). A minor amount of sparry calcite can be seen in the rock matrix (Fig. 3.12a). Interparticle and intraparticle pores are abundant. Gambier has high CEC compared to Whitestone UZ and Edwards (GC) and abundant macro and microporosity.

Brine

In initial studies of Gambier limestone (Tie *et al.*, 2003), 5% CaCl₂ was adopted to limit dissolution as recommended by Graue *et al.* for chalk (Graue *et al.*, 1994). Further testing indicated that consistent results for limestone could be obtained with synthetic sea water. Synthetic sea water (Table 3.13) was subsequently adopted as a standard brine, partly because of its widespread use as an injection brine, and used in the present work for tests with Whitestone UZ and Edwards (GC). 100 ppm NaN₃ was added to the brine to prevent bacterial growth.

Crude Oil

A moderately asphaltic crude, Cottonwood Creek crude oil, from a Wyoming dolomite reservoir of Permian age (Cottonwood Creek, phosphoria dolomite), was employed in this work. The oil was sparged with nitrogen to remove H₂S; the density and viscosity at room temperature ($T_m = \sim 22^\circ\text{C}$) after N₂ sparging were 0.8874 g/cm³ and 24.1 cp respectively. The crude oil is moderately asphaltic with the n-C7 asphaltene content being 2.3 wt%. Acid and base numbers are 0.56 and 1.83 mg KOH/g oil respectively. Interfacial tensions (IFT) were measured by a drop volume tensiometer (Krüss DVT-10). The IFT of Cottonwood crude oil was 29.7 mN/m to sea water and 27.2 mN/m to 5% CaCl₂. Hirasaki and Zhang proposed that IFT values of this magnitude can be taken as an indication that the crude oil is not likely to be contaminated by oil field chemicals such as corrosion inhibitors (Hirasaki and Zhang, 2004).

Mineral Oils

Two oils were used in this work. Soltrol® 220, with viscosity of 3.8 cp, was used in some imbibition experiments as the probe oil. Before use, polar impurities were removed by passing the oil through a chromatographic column packed with silica gel and alumina. After cleaning, the Soltrol 220/brine interfacial tensions were ~50 mN/m.

Heavy mineral oil, with viscosity around 180 cp, was used to establish initial water saturation for the Gambier limestone samples. This oil was cleaned first by making a suspension of silica gel and alumina to remove any polar impurities followed by filtration.

Intermediate Solvent

Decalin, decahydronaphthalene (C₁₀H₁₈), was used as an intermediate solvent in preparation of MXW-F samples to prevent destabilization of asphaltenes by direct contact between mineral oil and crude oil.

Core Preparation

Very Strongly Water-Wet (VSWW) Cores ($S_{wi} = 0\%$)

All VSWW imbibition reference curves were obtained for core samples initially 100% saturated with mineral oil by vacuum. Soltrol 220 was used in tests with Whitestone UZ and Edwards (GC). Heavy mineral oil was used for tests on the highly permeable Gambier cores in order to avoid ultra fast imbibition. Whitestone UZ and Edwards (GC) cores were pressurized up to 900 psi under oil to ensure complete saturation.

MXW Cores

Core samples were first saturated with, and soaked in, the selected brine for at least 10 days to attain ionic equilibrium. Then, for Whitestone UZ and Edwards (GC) cores, S_{wi} was established by displacing synthetic brine with crude oil at 50°C at an initial flooding rate of 0.60 PV/hr (about 3 ft/day). Details of preparation of Gambier cores are given in Tie *et al.* (2003). In all tests, the direction of oil flow was reversed and a further PV of the oil was injected to even out the water saturation along the length of the core.

Cores at S_{wi} were submerged in stock crude oil (oil taken directly from the sample stock) and aged in sealed pressure vessels for 10 days at 75°C (T_a). For imbibition tests performed with cores using crude oil directly as the probe oil, the wetting states of the core samples are referred to as MXW.

Mixed-Wet with Film (MXW-F and MXW-DF) Cores

Imbibition experiments were also performed with cores using mineral oil (Soltrol 220) instead of crude oil as the probe oil. If the crude oil was displaced first with 5 PV of decalin to avoid destabilization of asphaltenes, and then 5 PV of clean mineral oil (Soltrol

220), the samples are referred to as MXW-F. If the crude oil was directly displaced with mineral oil, the cores are referred to as MXW-DF samples. All displacements of one oil by another were performed at 3 ft/day.

Spontaneous Imbibition

The prepared VSWW, MXW, MXW-F, and MXW-DF core samples were set in glass imbibition cells filled with the selected brine. Oil volume, expressed as percentage of original oil in place (%OOIP), was recorded vs. time. All imbibition tests were performed at ambient temperature (T_m).

Amott Indices

After brine imbibition tests, Amott index measurements (Amott, 1959; Cuiec, 1987 and 1991) were performed on all core samples. Forced displacement tests were performed for core samples after brine imbibition at rates ranging from 3 ft/day up to 50 ft/day for Whitestone UZ limestone, 3 ft/day up to 25 ft/day for Edwards (GC) limestone, and 2 ft/day up to 50 ft/day for Gambier limestone. One additional pore volume of brine was injected with the flow direction reversed to even out the fluid distribution along the core. After determining the Amott index to water, oil imbibition was followed by forced displacement with oil to determine the Amott index to oil.

Results and Discussion

Ma *et al.* (1997) used a semi-empirical scaling group to correlate spontaneous imbibition behavior of VSWW media over a wide range of conditions.

$$t_D = t \sqrt{\frac{k}{\phi}} \frac{\sigma}{\sqrt{\mu_o \mu_w}} \frac{1}{L_c^2} \quad (3.9)$$

where t_D is dimensionless time, t is time, k is permeability, ϕ is porosity, σ is the interfacial tension, and μ_o and μ_w are the oil and brine viscosities. L_c is a characteristic length that compensates for sample size, shape and boundary conditions.

Use of this scaling group to compare the spontaneous imbibition rate of cores with wetting states other than VSWW (MXW (Xie and Morrow, 2001), MXW-F (Tong *et al.*, 2002)) provides an indication of the degree of wetting change.

Measurement of Amott wettability indices involves spontaneous imbibition tests. It is sometimes stated that imbibition of either brine or oil should be allowed to reach equilibrium (Anderson, 1986b). However, imbibition by mixed-wet cores does not usually give clear cut end points. Reported Amott indices in this work were based on an operational end point definition given by a dimensionless imbibition time, t_D , of 10^5 (Tie *et al.*, 2003).

VSWW Imbibition

All the VSWW imbibition experiments were carried out with 0% initial water saturation. In contrast to MXW cores, the presence of initial water saturation has only moderate effect on VSWW imbibition behavior (Viksund *et al.*, 1998; Xie and Morrow, 2001). Scaled spontaneous imbibition results of the three chosen carbonate samples are compared in Fig. 3.13a. The final oil recoveries of the three limestones show significant differences, 62.8%, 53.8%, 41.5% for Gambier, Whitestone UZ, and Edwards (GC) respectively. Thus trapped oil varies by a factor of 1.5. The low recovery from Edwards (GC) is ascribed to the numerous small vugs of about 200 μ diameter formed by selective dissolution of fossils (see Figs. 3.12a and 3.12b).

If all the curves are normalized by final recovery, as shown in Fig. 3.13b, it can be seen that they fall into a narrow range and are close to the correlated results for Berea 500 sandstone (Zhang, et al., 1996) and a wide range of other rock types (Viksund *et al.*, 1998). Whitestone UZ showed slightly faster imbibition at early time; this could be related to the inherent heterogeneity. The agreement between scaled imbibition behavior of three tested limestones and many other outcrop rocks is strong indication that the three selected outcrop limestones are free of organic contaminants.

Comparison of Imbibition for Different Rock Types

Initial water saturation (S_{wi}) is a key factor in the development of mixed wettability. It controls the amount of rock surface exposed to adsorption from crude oil (Salathiel, 1973). Xie and Morrow (2001) showed that mixed-wet cores become increasingly less water-wet, as indicated by orders of magnitude decrease in scaled imbibition rate, with decrease in initial water saturation established prior to aging in crude oil. Therefore, the initial water saturation for experiments performed with the same rock type should be kept constant when investigating other aspects of crude oil/brine/rock interactions. However, for different rock types with distinct difference in pore structure and size distribution, as in the present work, attempting to bring all cores to the same S_{wi} would serve little purpose. The S_{wi} values for each rock types were ~28.7% for Whitestone UZ, ~16.1% for Edwards (GC), and ~28.5% for Gambier. These values represent a compromise between rock petrophysical properties and technical convenience. For example, S_{wi} for Whitestone UZ and Edwards (GC) was established by essentially the same displacement conditions, whereas injection of heavy mineral oil was needed to attain an S_{wi} of ~28.5% for Gambier cores.

Figs. 3.14a and 3.14b present, respectively, the scaled imbibition results for Whitestone UZ and Edwards (GC) cores for MXW, MXW-F, and MXW-DF wetting states. For both of these grainstones, at any given dimensionless imbibition time, excluding induction time, MXW cores gave the highest rate and recovery of oil by spontaneous imbibition and MXW-DF cores showed the least. The same sequence of rate and recovery was given by the Gambier samples (Fig. 3.15a) (Tie *et al.*, 2003). As shown in Table 3.14, Amott

index measurements also confirmed decrease of water wetness in the sequence MXW, MXW-F, and MXW-DF for all the three tested rock types. The same sequence was obtained for Berea sandstone (Tie *et al.*, 2003).

Spontaneous Imbibition of Oil by Gambier Cores – Cottonwood and Minnelusa Crudes

After forced displacement of oil by water in the Amott test, cores were tested for imbibition of oil. From the Amott wettability index measurements in Table 3.14, it is seen that only Gambier MXW-F and MXW-DF cores showed some recovery of water by spontaneous imbibition of oil. Fig. 3.15b presents the oil imbibition curves for Gambier cores at the three tested wetting states given by Cottonwood crude oil. Oil imbibition results for a core prepared with Minnelusa crude oil (Tie *et al.*, 2003) are also included. The high degree oil wetness may be related to asphaltene content of crude oil (9% for Minnelusa vs. 2.3% for Cottonwood) used in preparation of the core sample. The value of I_o of 0.93 for Gambier core prepared by direct displacement of asphaltic Minnelusa crude oil by mineral oil is the highest value of I_o yet seen for an outcrop rock after exposure to crude oil. In fact, no additional recovery of water was measured for forced displacement of oil. The value of I_o of 0.93, rather than 1, is based on a cut-off at $t_D = 10^5$. An I_{w-o} of -0.6 for MXW-F Edwards (GC) after aging with a North Sea crude oil at an S_{wi} of ~17% has been observed (Graue, 2005).

MXW Imbibition

Fig. 3.16a presents a comparison of the scaled MXW imbibition data for the three limestones. The Whitestone UZ core exhibited the fastest scaled imbibition behavior of the three rock types; Gambier imbibed slightly faster than Edwards (GC). The Whitestone UZ sample was more water-wet, $I_{w-o} = 0.63$, than Edwards (GC) and Gambier ($I_{w-o} = 0.44$ and 0.48 respectively). All three MXW rocks had values of I_{w-o} in the water-wet range [1.0, 0.3] according to Cuiec's classification (Cuiec, 1987 and 1991).

MXW-F and MXW-DF Imbibition

Figs. 3.16b and 3.16c present scaled spontaneous imbibition data for MXW-F and MXW-DF cores for the three selected rock types. It can be seen clearly that for all three rock types, MXW-DF cores gave slower scaled imbibition than MXW-F cores. The slow imbibition of MXW-DF cores is ascribed to surface precipitation of asphaltenes resulting from direct displacement of crude oil by mineral oil (Al-Maamari and Buckley, 2003). But even with almost complete suppression of brine imbibition, I_{w-o} for the three MXW-DF cores is still very close to zero (-0.05 to -0.09).

Induction Time

From Figs. 3.16a, 3.16b and 3.16c, for MXW, MXW-F, and MXW-DF cores, Edwards (GC) and Whitestone UZ cores all showed induction times prior to noticeable imbibition. For Edwards (GC), the induction time for MXW and MXW-F cores was about 30 mins,

while that for Whitestone UZ cores was under 5 mins. The Gambier cores showed no delay in brine imbibition behavior for all tested samples.

Oil Recovery

Final oil recovery by a combination of spontaneous imbibition followed by forced displacement is compared for Whitestone UZ and Edwards (GC) rocks at all the tested wettability states (see Fig. 3.16d). It can be seen that for the conditions tested, highest recovery of the probe oil was obtained for MXW-F grainstones that are weakly water-wet. (The wetting category which exhibits maximum recovery is expected to shift with decrease in initial water saturation.) Recovery from VSWW, MXW, MXW-F, MXW-DF Gambier boundstone did not match the trend obtained for the grainstones.

Oil Wetness of Carbonate Rocks

In general, carbonate reservoir rocks are widely reported to be less water-wet than sandstones. However, for the three rocks of the present work, MXW cores exhibited extensive imbibition of water (I_w from 0.44 to 0.63) with Cottonwood crude oil at the tested initial water saturations.

Several possible factors may contribute to this overall difference. Reservoir connate water and wettability can be difficult to re-establish in the laboratory. Reservoir carbonates often have lower initial water saturation than the values used in this work. In general, the lower the initial water saturation, the higher the fraction of rock surface that is exposed to adsorption from crude oil. Factors governing the retention of water by capillarity in the reservoir, for example, change in the free water level, could also change over geologic time.

Restored state procedures are commonly used to reestablish reservoir wettability in the laboratory. Cleaning usually involves solvent flow or extraction using a series of organic solvents, such as chloroform, methanol, toluene, tetrahydrofuran, etc. So-called clean cores are observed to be neutral-wet. The problem of cleaning carbonates to the very strongly water-wet state exhibited by the outcrop limestones used in this study is well known. The traditional rock cleaning process includes Dean-Stark extraction with toluene. The high boiling point of toluene (110.6°C) will cause removal of connate water before extracting the crude oil so that areas of rock previously overlain by bulk water may become exposed to adsorption from crude oil (Hirasaki *et al.*, 1990). This may compromise the restored state procedure.

Model Limestone

A search some fifty years ago for a readily available sandstone led to adoption of Berea sandstone as a model rock for oil recovery and a wide variety of other topics. Results of the present study indicated that Edwards (GC) is well suited for use as a model limestone. The rock has low BET surface area, is low in microporosity, and meets criteria that are

sometimes used to describe sandstone as clean. Cores from a single block have been found to be uniform in permeability and porosity (about 11 md and 21% for the tested block). The high residual saturation (~60%) at VSWW and reduction of residual to 30% of OOIP at intermediate wettability is of special value to parametric studies such as determining relationships between oil recovery and wettability.

Table 3.11 Selected properties of three rocks

Cores	BET, m ² /g	CEC, meq/100g
Whitestone UZ	0.90	0.00029
Edwards (GC)	0.20	0.00026
Gambier	0.77	0.00065

Table 3.12 Cores

Sample No.	<i>L</i> cm	<i>D</i> cm	<i>k_g</i> md	ϕ	<i>S_{wi}</i> %	μ_o cp	σ mN/m	Wetting
Whitestone UZ								
3WUZ02A	3.74	6.30	7.42	0.26	28.7	24.1	29.7	MXW
3WUZ01A	3.75	6.05	6.90	0.25	28.7	3.8	49.6	MXW-F
3WUZ01B	3.75	6.36	7.58	0.24	28.8	3.8	49.6	MXW-DF
Edwards (GC)								
1EGC05A	3.80	6.26	11.6	0.21	16.0	24.1	29.7	MXW
1EGC06B	3.80	6.37	10.4	0.21	16.3	3.8	49.6	MXW-F
1EGC06A	3.80	6.38	12.9	0.21	16.3	3.8	49.6	MXW-DF
Gambier (Tie <i>et al.</i> , 2003)								
G08	5.10	3.77	4350	0.54	28.8	24.1	27.2	MXW
G10	4.90	3.77	4140	0.55	28.2	3.8	49.5	MXW-F
G11	5.09	3.78	4160	0.53	28.4	3.8	49.5	MXW-DF

Table 3.13 Synthetic brine composition

Brine	NaCl (g/L)	KCl (g/L)	CaCl ₂ (g/L)	MgCl ₂ (g/L)	NaN ₃ (g/L)	pH	TDS (mg/L)
Sea water	28	0.935	2.379	5.365	0.1	6.6	36779

Table 3.14 Amott indices

Sample No.	$V_{o, imb}$ mL	$V_{oe, imb}$ mL	$V_{o, f}$ mL	I_w	$V_{w, imb}$ mL	$V_{we, imb}$ mL	$V_{w, f}$ mL	I_o	I_{w-o}	Wetting
Whitestone UZ										
3WUZ02A	4.70	0	2.72	0.63	0	-	-	-	0.63	MXW
3WUZ01A	2.35	0.08	5.50	0.30	0	-	-	-	0.30	MXW-F
3WUZ01B	0.53	0.09	7.07	0.07	1.20	0	5.80	0.17	-0.10	MXW-DF
Edwards (GC)										
1EGC05A	2.95	0	3.70	0.44	0	-	-	-	0.44	MXW
1EGC06B	1.65	0.52	6.90	0.18	0	-	-	-	0.18	MXW-F
1EGC06A	0	0	6.95	0.00	0.78	0.05	7.70	0.09	-0.09	MXW-DF
Gambier (Tie <i>et al.</i> , 2003)										
G08	6.26	3.54	3.15	0.48	0.10	0	12.50	0.01	0.48	MXW
G10	2.23	0.72	10.90	0.16	2.20	0.40	9.40	0.18	-0.02	MXW-F
G11	1.00	0.13	10.80	0.08	1.37	0.03	8.70	0.14	-0.05	MXW-DF

Note: $V_{o, imb}$ and $V_{w, imb}$ are oil and water recovery from brine and oil imbibition tests at the chosen 10^5 cut-off dimensionless time. $V_{oe, imb}$ and $V_{we, imb}$ are oil and water production after $t_D = 10^5$. $V_{o, f}$ and $V_{w, f}$ are forced displacement recovery of oil and water.

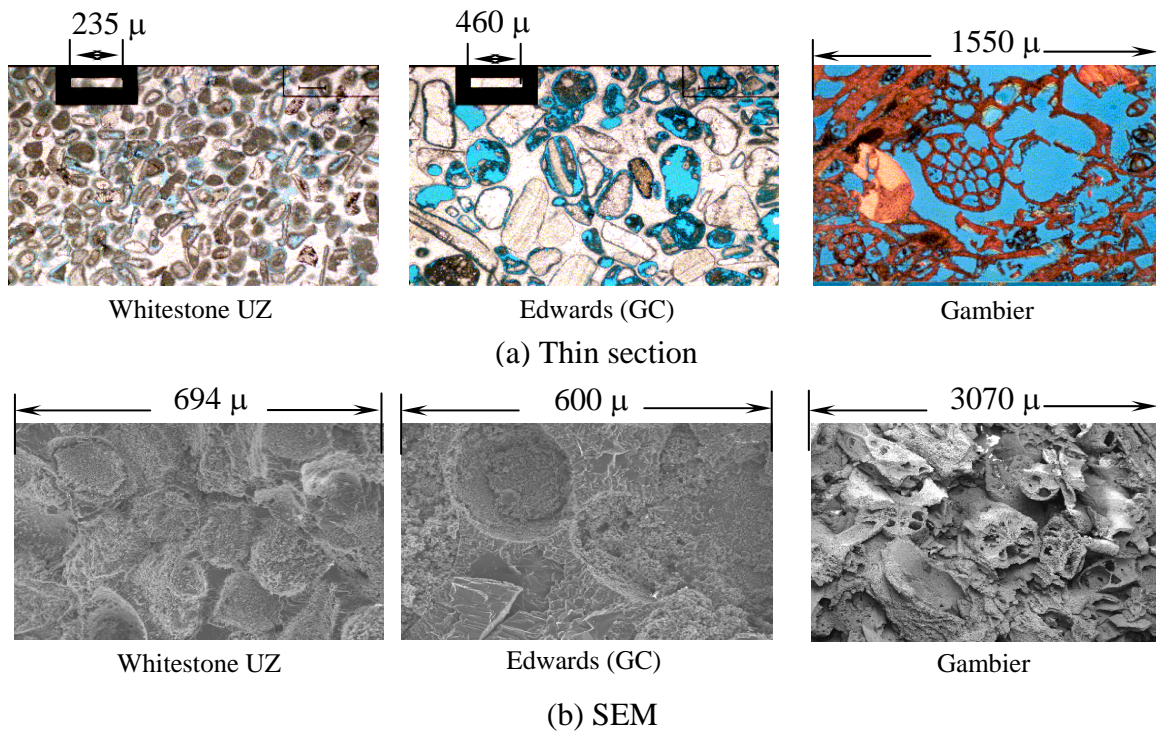
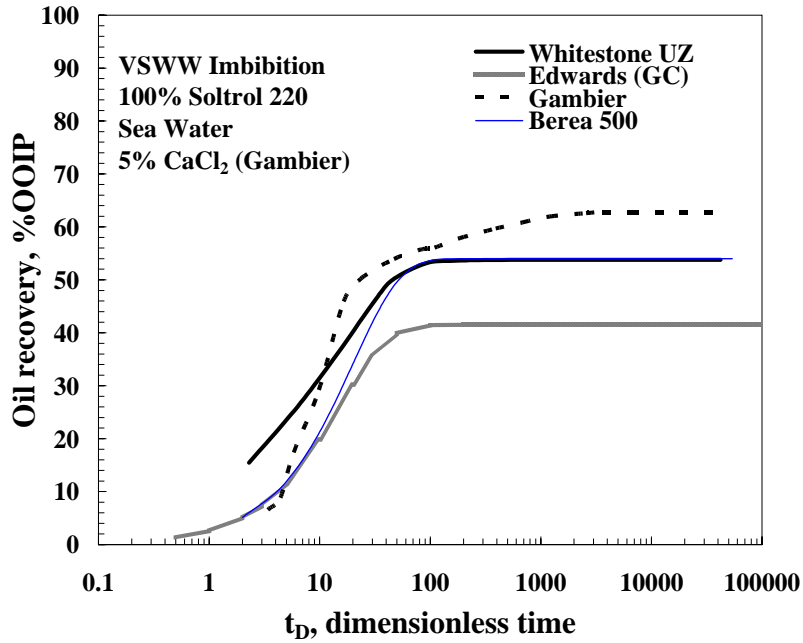
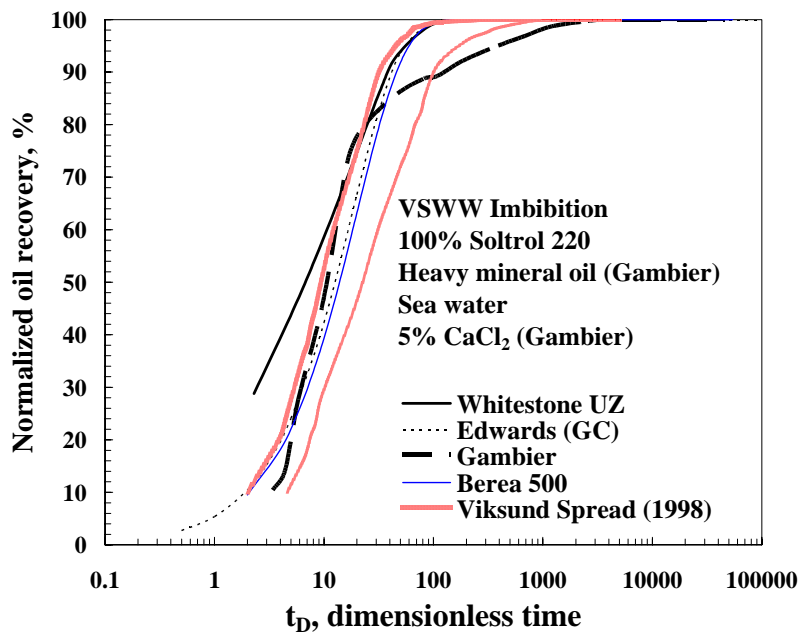


Fig. 3.12 Thin section and SEM photos

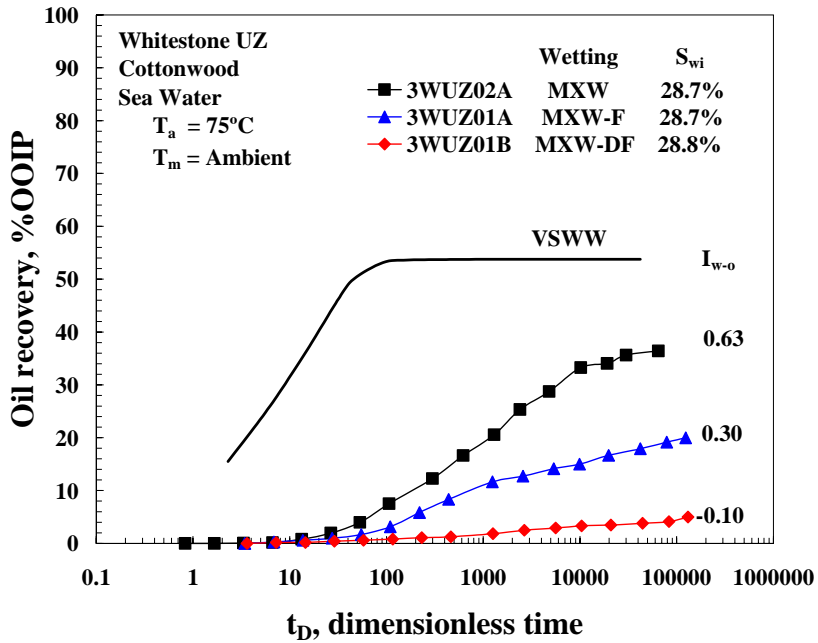


(a) Correlated MXW Imbibition

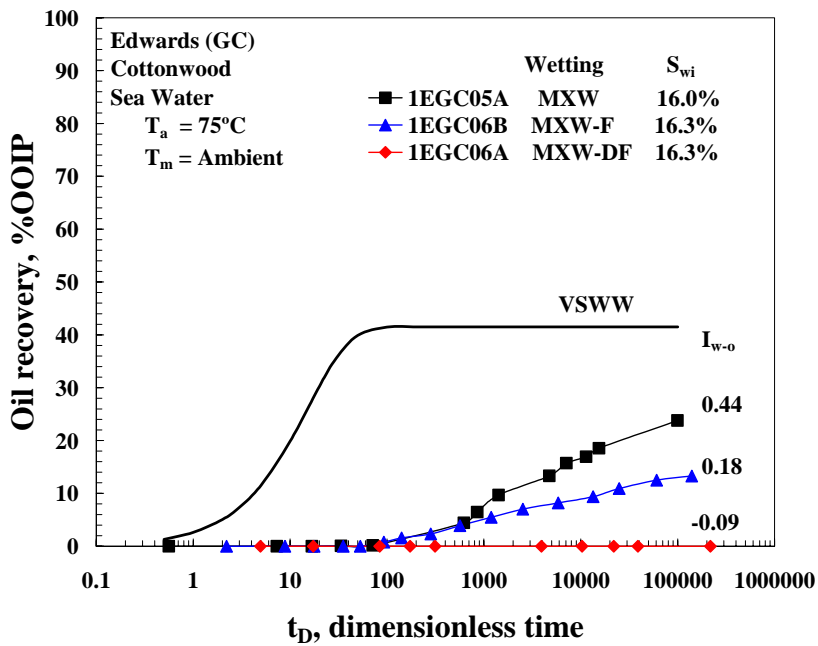


(b) Normalized to final recovery

Fig. 3.13 (a) Scaled VSWW imbibition results for the three limestones and Berea sandstone, and (b) comparison with range of normalized results for a variety of rock types.

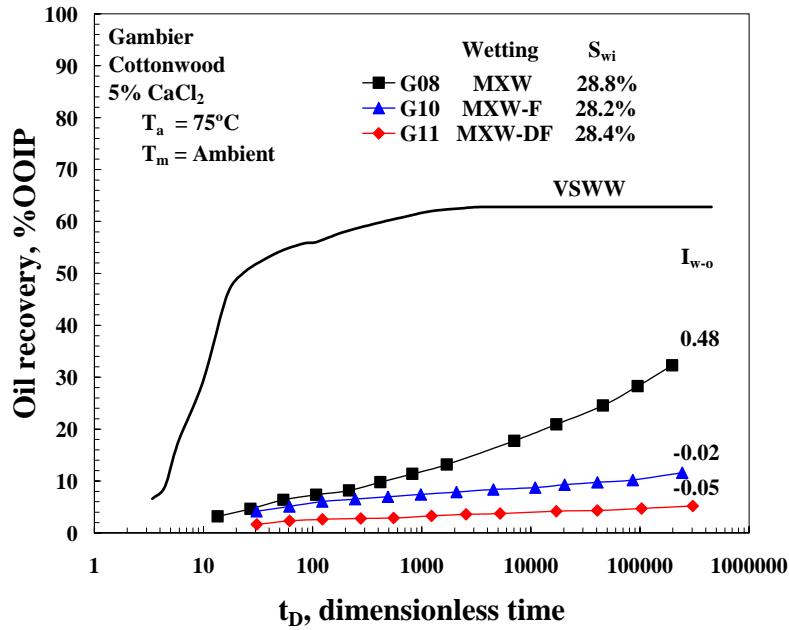


(a) Whitestone UZ cores

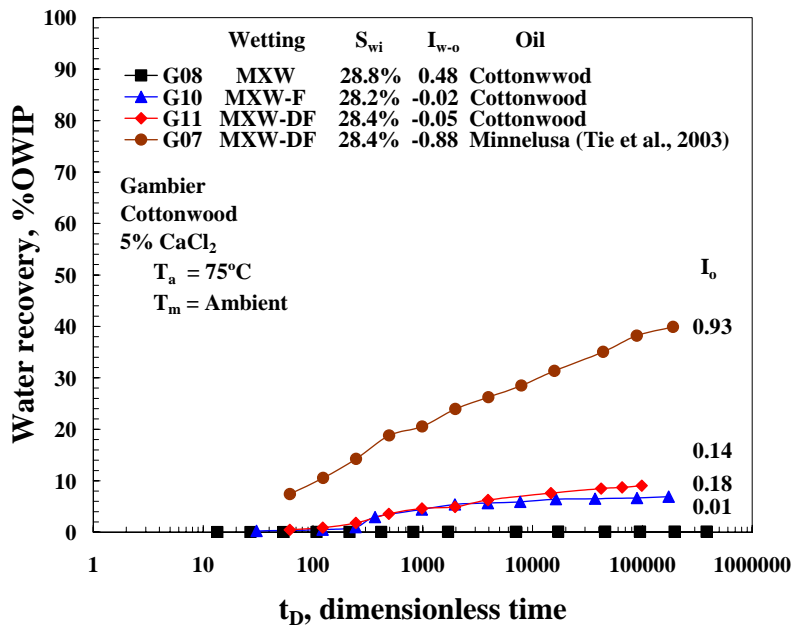


(b) Edwards (GC) cores

Fig. 3.14 Comparison of spontaneous imbibition for two grainstones with MXW, MXW-F, and MXW-DF wetting states induced by Cottonwood crude oil

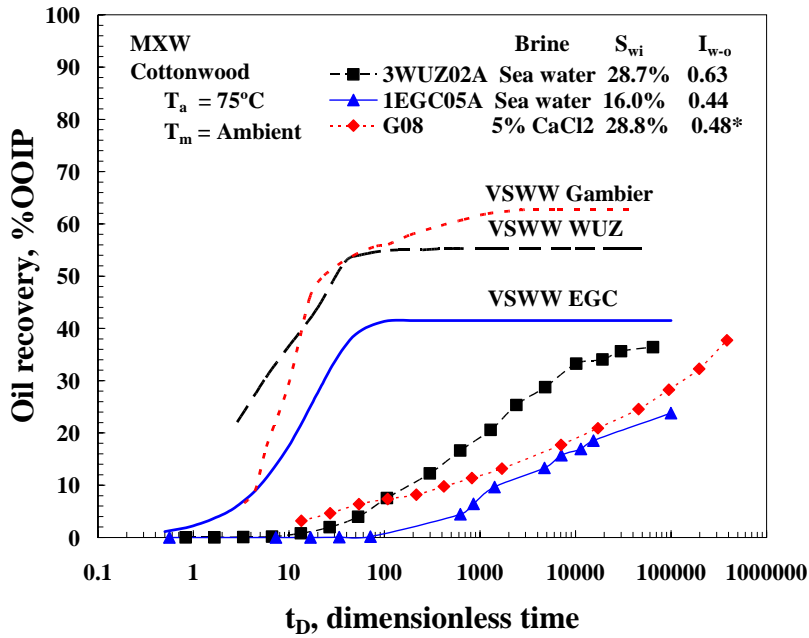


(a) Brine imbibition

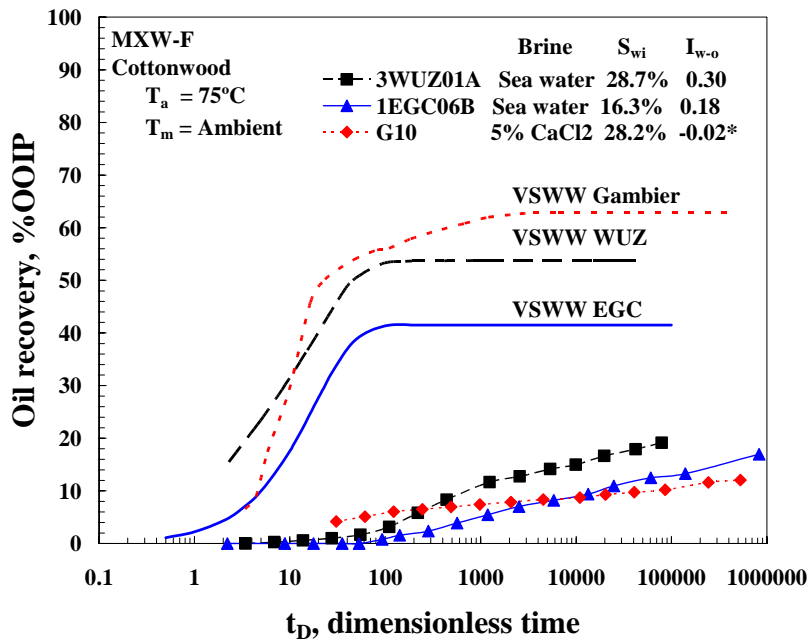


(b) Oil imbibition

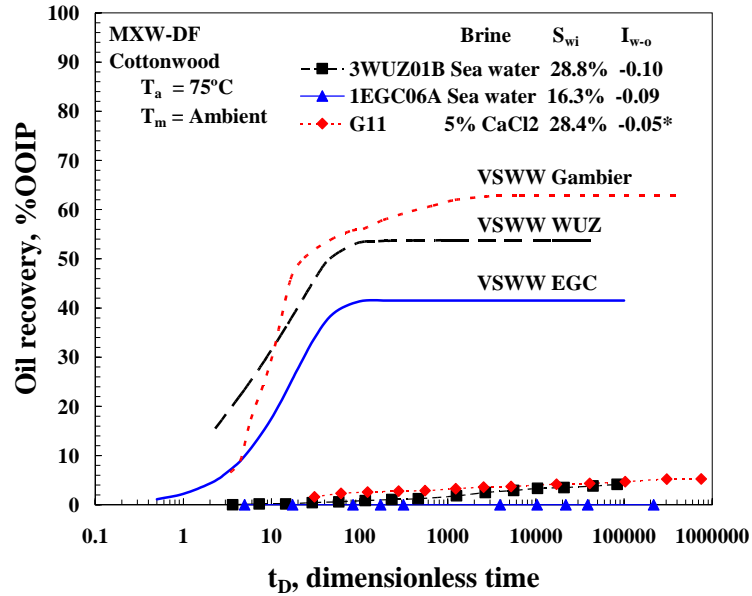
Fig. 3.15 Comparisons of (a) spontaneous imbibition of brine for Gambier cores with MXW, MXW-F, and MXW-DF wetting states induced by Cottonwood crude oil (Tie *et al.*, 2003) and (b) spontaneous imbibition of oil after forced displacement (MXW-DF for Gambier and Minnelusa crude oil is included)



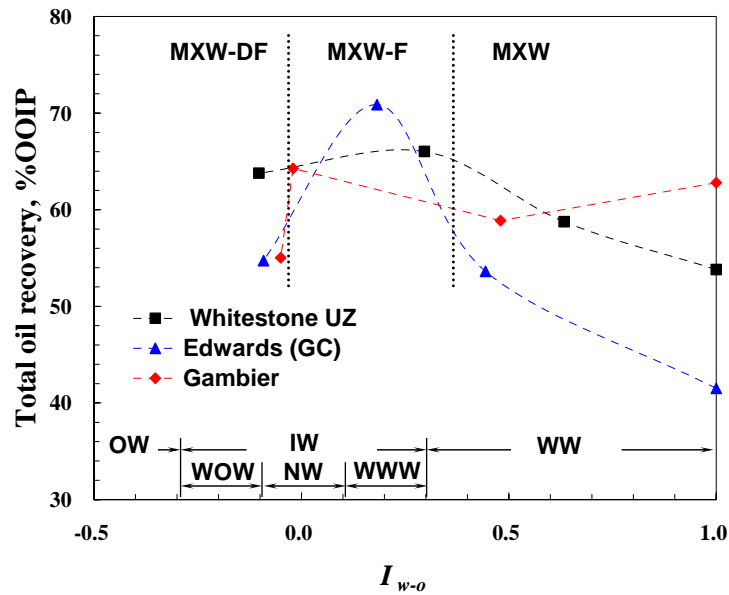
(a) Scaled MXW imbibition



(b) Scaled MXW-F imbibition



(c) Scaled MXW-DF imbibition



(d) Total recovery vs. wettability

Fig. 3.16 Comparison of recovery of oil with VSWW for (a) MXW, (b) MXW-F, (c) MXW-DF by spontaneous imbibition for three carbonate rocks, and (d) total oil recovery (spontaneous imbibition plus forced displacement) versus Amott-Harvey wettability index. (WW – water-wet, WWW – weakly water-wet, NW – neutral wet, WOW – weakly oil-wet, IW – intermediate wetting, OW – oil-wet (Cueic, 1991)) (* Tie *et al.*, 2003)

Task 4: Oil recovery by waterflooding

Hongguang Tie, Zhengxin Tong and Norman R. Morrow, Chemical & Petroleum Engineering, University of Wyoming

Carbonate reservoirs commonly exhibit great morphological complexity from pore to field scale. Interpretation of laboratory waterfloods is often problematic because of unexpected sensitivity of oil recovery to flood rates comparable to field values. The circumstances under which rate sensitivity occurs need to be further identified. In this work, three outcrop limestones with distinct differences in petrophysical properties were selected for investigation of the combined effect of pore structure and wettability on residual saturations. The rocks were tested at very strongly water-wet conditions followed by preparation of mixed-wet states. A comparative study of waterflood recovery was made for mixed wettability with crude oil or mineral oil as the test oil. Mineral oil was tested after either direct displacement of crude oil or first displacing crude with an intermediate solvent to avoid surface precipitation of asphaltenes. Flooding rates ranged from below or near field rates to well above with increase in capillary number achieved by increase in flood rate. Reduction of residual oil saturation with increase in flood rate ranged from slight for a homogeneous grainstone to highly significant for both a heterogeneous grainstone and a boundstone of very high porosity and permeability.

Introduction

The magnitude of the ratio of viscous to capillary forces is usually expressed as capillary number. In waterflood experiments, capillary number represents the ratio of viscous driving forces to capillary retaining forces that control the retention of residual oil in waterflood experiments. Taber (1981) listed the numerous expressions used for this ratio and many of them are equivalent (Larson *et al.*, 1981). The following definition for capillary number is employed in this paper.

$$N_c = \frac{v\mu}{\sigma} \quad (4.1)$$

where v is the Darcy velocity, μ is the viscosity of the displacing phase, and σ is the IFT.

Early laboratory studies of rate effects, usually related to tertiary oil recovery by surfactant flooding, examined the mobilization of trapped oil blobs or ganglia from very strongly water-wet (VSWW) sandstones and unconsolidated media. (Ojeda *et al.*, 1953; Paez *et al.*, 1954; Moore and Slobod; 1956; Wagner and Leach, 1966; Taber, 1969; Foster, 1973; Chatzis *et al.*, 1988; Morrow *et al.*, 1988) The entrapment of nonwetting phase during waterflooding is caused by capillary action. The majority of the trapped nonwetting phase results from snap-off to give either isolated blobs held in individual pore bodies or more complex blobs that branch over two or more pores. (Chatzis *et al.*, 1983; Morrow, 1984; Chatzis *et al.*, 1988) Laboratory studies demonstrated that when the driving viscous forces exceeded the retaining capillary force, the trapped oil became mobile. However, in order to achieve a high enough ratio of viscous to capillary forces for oil production, a critical capillary number of the order of 10^{-5} must be reached for rocks such as Berea sandstone which has a relatively narrow range of pore size distribution. For rocks with a wider pore size distribution, decrease of residual oil

saturation spanned a wider range of capillary number. (Stegemeier, 1977; Lake, 1984) For both cases, extremely low interfacial tensions must be achieved for mobilization of the trapped oil at field flood rates. Observations on mixed-wet Berea sandstone also indicated that high capillary numbers were needed to achieve significant tertiary oil recovery. (Morrow *et al.*, 1986)

Laboratory core analysis of oil recovery behavior from carbonate rocks is usually of great uncertainty due to core plug variability in morphology and wettability. McCaffery *et al.* (1978) reported large variations of waterflood residual oil saturation ranging from 15% to 40%. Values depended on the amount of secondary porosity, the initial water saturation, and other conditions. Furthermore, in many reported instances, waterflood tests on reservoir core samples do not yield well-defined residual oil saturations even with very low flooding rates comparable to field values. In contrast to sandstones, Morrow found continuous decrease of waterflood residual saturation over a wide range of capillary number for Caddo reservoir carbonates whereas recovery from outcrop Baker dolomite was consistent with sandstone behavior. (Morrow, 1984) deZabala and Kamath (1995) and Kamath *et al.* (2001) studied waterflood oil recovery behavior of several heterogeneous reservoir limestones. All the tested samples showed dependency of waterflood residual saturation on flood rate. Furthermore, it was shown that the behavior could not be attributed to capillary end effects. The highest reduction of residual saturation was from 60 to 32% PV with increase in capillary number from 2×10^{-8} to 4×10^{-7} . Network modeling under various scenarios indicated that core scale heterogeneity could result in increased regions of invasion with increase in flow rate. (Kamath *et al.*, 1996; Xu *et al.*, 1999) These observations raise the intriguing question of whether significant enhanced oil recovery would result from even modest reductions in interfacial tension by use of surfactants. (Morrow, 1984; Kamath *et al.*, 2001)

A problem in the study of reservoir carbonates is that cores generally have poorly defined wetting states. A well recognized problem in the restoration of carbonate reservoir wettability is the difficulty of first cleaning the carbonate cores to a very strongly water-wet condition. In investigation of rate effects, base line studies at very strongly water-wet conditions are needed to assess the combined contributions of pore structure and wettability. Rate sensitivity effects have therefore been investigated for three outcrop limestones. Two of these were grainstones, one being identified as homogeneous at the core scale and the other, from variation in standard petrophysical properties, heterogeneous. The third was a high porosity/permeability boundstone. The effect of flood rate on recovery has been examined for very strongly water-wet, and three types of mixed wettability state generated by adsorption from a moderately asphaltic crude oil.

Experiments

Rock Characterization

Three outcrop limestones were selected for study, Edwards (Garden City) ((Edwards (GC) or EGC), Whitestone Upper Zone (Whitestone UZ or WUZ), and Gambier (G). Based on Dunham's classification (Dunham, 1962), both Edwards (GC) and Whitestone UZ are grainstones and Gambier is a boundstone. Thin section and SEM micrographs are presented in Fig. 4.1. In addition to standard petrophysical properties, the three

limestones were characterized by a variety of other methods. BET surface area and cation exchange capacity (CEC) results are listed in Table 4.1. Mercury injection and BJH pore structure analysis were used to obtain pore structure data for each rock type (Fig. 4.2). Fractions of micro-, meso-, and macro-porosity (pore radius <2.1nm, 2.1 to 53nm, and >53nm, respectively) have been identified from desorption/adsorption isotherms. (Fischer *et al.*, 2005)

Rocks

Edwards (GC) from West Texas, is also known as West Texas Crème, Cedar Hill Cream, or Valencia Ivory building stone. The rock is quarried from a member of the Edwards Formation close to Garden City, Texas. Petrophysical property measurements on samples cut from individual 12 by 12 by 6 inch blocks were homogeneous in that the air permeabilities and porosities of the cores fell in the range of 12.1 ± 1.7 md and $21.0 \pm 0.3\%$ respectively (Table 4.2). This rock is composed mostly of calcite minerals both inside the rock matrix and at the pore walls (see Fig. 4.1). Hardly any fine pore structure can be identified by SEM. BET surface area and micro- and meso-porosity are significantly lower than for the other two rock types. Mercury injection analysis showed low entry pressure (about 10 psi). Pore structure analysis using combined results from mercury injection (for the larger pores) and BJH pore structure analysis (for very small pores) showed a relatively narrow pore size distribution and almost no pore throats of less than 30 nm radius (see Fig. 4.2b). A peak in pore throat diameter is indicated at around 5μ by mercury injection. The secondary peak is probably artifact because it coincides with change in the mercury injection cell at 30 psi.

Whitestone UZ, also known as Texas Crème building stone, quarried from the upper bench of the Whitestone Member of the Lower Cretaceous Walnut Formation, Texas, is a grainstone composed mostly of calcite (see Fig. 4.1). Although uniform in appearance to the naked eye, Whitestone UZ rock was consistently heterogeneous at the core scale within individual blocks and from one block to another, as indicated by standard petrophysical properties. The air permeabilities and porosities of the tested cores ranged from 3.9 to 13.7 md and 19.1 to 26.4% respectively (Table 4.2). Selectivity was exercised in obtaining four cores with permeabilities in the range of 7.25 ± 0.35 md. BET measurements indicated comparatively high surface areas. Mercury injection data did not exhibit a plateau. Pore throat frequency analysis (see Fig. 4.2c) showed a wider pore size distribution compared to Edwards (GC) limestone. Pore throat sizes range from 10 nm to 2μ with peaks at 300 nm and 1μ .

Gambier limestone is an Oligocene-age outcrop quarried from Mt. Gambier, Australia. Air permeabilities and porosities of the cores fell in the range of 4245 ± 105 md and $53.7 \pm 1.1\%$ respectively (Table 4.2). The limestone is composed of readily identifiable coral fossil fragments, with a minor amount of coarse sparry calcite. Interparticle and intraparticle pores are abundant (see Fig. 4.1). Mercury injection data for this rock are not yet available. The BET surface area is close to that of Whitestone UZ limestone. Desorption/adsorption isotherms for water indicated that even though the BET surface area is comparatively high, the percentage of micro-pores to meso-pores in Gambier

limestone is about .5% and is close to that of the Edwards (GC) limestone. (Fischer *et al.*, 2005)

Properties of the core used in this work are listed in Table 4.2.

Crude Oil

Several 5 gallon containers of Cottonwood crude oil, a moderately asphaltic crude from a Wyoming dolomite reservoir of Permian age (Cottonwood Creek, phosphoria dolomite), were obtained for this work. H₂S was removed by sparging the crude oil with nitrogen. Asphaltene content, acid and base numbers, viscosity and density, are listed in Table 4.3.

Brine

The test brine was either synthetic sea water or 5% CaCl₂. NaN₃ (100 ppm) was added as a biocide to prevent bacterial growth. Brine viscosity was 1 cP at room temperature. Brine compositions are listed in Table 4.4.

Mineral Oil

Mineral oil (Soltrol 220, 3.8 cP), with polar components removed by flowing the oil through a chromatographic column packed with silica and alumina, was used in core preparation and waterflood tests.

Decalin, decahydronaphthalene (C₁₀H₁₈), was used as an intermediate solvent for displacement of crude oil during core preparation in order to avoid surface precipitation of asphaltenes by direct contact between crude oil and mineral oil.

Oil/Brine Interfacial Tension

Crude oil/brine interfacial tensions (IFTs), measured by drop volume tensiometer (Krüss DVT-10), were 29.7 mN/m (seawater) and 27.2 mN/m (5% CaCl₂) at room temperature. IFT values of this magnitude provide indication that the crude oil is not contaminated by oil field chemicals such as corrosion inhibitors. (Hirasaki and Zhang, 2004) Refined oil/brine interfacial tension was 50 mN/m at room temperature.

Core Preparation

VSWW core samples were prepared without the presence of initial water saturation by vacuum saturation with Soltrol 220. Core samples prepared with an initial water saturation (S_{wi}) were first saturated with, and then soaked in, the selected brine for at least 10 days to attain ionic equilibrium. Two different procedures were adopted in reaching target values of S_{wi} . For Edwards (GC) and Whitestone UZ samples, S_{wi} was established by displacing reservoir brine directly with crude oil at 50°C at 3 ft/day (about 0.60 PV/hr). Details of preparation of Gambier samples are described in earlier work. (Tie *et al.*, 2003) In all tests, the flow direction was reversed and 1 PV of the displacement oil was injected to even out the water saturation along the length of the core.

Cores containing crude oil at S_{wi} were submerged in stock crude oil (oil taken directly from the sample stock) and aged in sealed pressure vessels for 10 days at 75°C (T_a). If crude oil was used as the probe oil, cores so prepared are referred to as MXW.

In preparation of mixed-wet cores with mineral oil as the probe oil, for one type of wettability, crude oil was first displaced by 5 PV of decalin at 3 ft/day at 50°C to avoid destabilization of asphaltenes. Decalin was then displaced with 5 PV of Soltrol 220 at ambient temperature to give mixed-wet film (MXW-F) cores. If the intermediate solvent (decalin) displacement step was omitted, so that the crude oil was displaced directly by the mineral oil to intentionally induce surface precipitation of asphaltenes, the wetting state of the cores is referred to as mixed wettability, direct flood (MXW-DF).

Waterflood

Two approaches were taken to investigation of rate sensitivity. In the first, waterflood tests were performed at ambient temperature with synthetic seawater. Flooding rates ranged from 0.6 to 49.4 ft/day for Edwards (GC), and 0.7 to 48.6 ft/day for Whitestone UZ. Flooding at a particular rate was continued until production of oil was observed to have essentially ceased over one pore volume of brine injection. These tests are referred to as high PV waterfloods.

In a second, less time consuming approach, waterflood studies were performed on core samples prepared as described above followed by measurements of spontaneous imbibition to characterize wettability (Tie *et al.*, 2003; Tie and Morrow, 2005). Waterflooding was started from $S_{wi}(imb)$ and oil recovery given by injection of 2PV brine was measured, followed by a step increase in rate and injection of a further 2PV and so on. Flooding rates in these tests ranged from 2.9 to 48.1 ft/day for Edwards (GC), 3.0 to 26.6 ft/day for Whitestone UZ, and 2.0 to 40.0 ft/day for Gambier. These tests are referred to as 2 PV waterflood tests.

Pore Casts

Pore structure was examined through preparation of pore casts. Thin slices of core were vacuum saturated with a mixture of epoxy resin and hardener (composition was listed in Table 4.5) and then pressured up to 900 psi to ensure complete saturation of the pore space. After wiping off any excess epoxy at the rock surfaces, samples were set in an oven at 75°C for over 24 hours to solidify the resin. The rock slices were then immersed in 10% hydrochloric acid. A stereoscopic microscope was used to examine the location of revealed pore space after dissolving away most of the rock, and to examine the shapes of individual pores and arrays of pores after gentle mechanical separation.

Results and Discussion

Oil Recovery for VSWW Cores

Characterization of different rock types involves the question of what value of initial water saturation should be used. For VSWW rocks, variation in initial water saturation has only moderate effect on spontaneous imbibition. Furthermore, whether the rate of imbibition increases or decreases with increase in initial water saturation appears to depend on a delicate balance between reduction in capillary driving force versus increase in transmissibility of the invading wetting phase. (Viksund *et al.*, 1998; Baldwin and Spinler, 2002) Use of an initial saturation of 0% provides a convenient common starting point for comparison of recovery of mineral oil from VSWW rocks.

Waterflood results for Edwards (GC) and Whitestone UZ cores (duplicate tests for each rock), initially 100% saturated with mineral oil (Soltrol 220), are shown in Fig. 4.3. Final recoveries at low flood rates are comparable to those obtained by VSWW spontaneous imbibition (Tie and Morrow, 2005), so the Amott wettability index to water (Amott, 1959;

Cuiec, 1987 and 1991), defined as $I_w = \frac{V_{o,imb}}{V_{o,imb} + V_{o,f}}$, of both of these outcrop samples

was close to 1. For the Edwards (GC) cores, 98% of the final recovery occurred before breakthrough at less than 0.7 PV of brine injected. Final recovery was reached within 1 PV of brine injection. Residual saturations were high and even though the Edwards (GC) is comparatively homogeneous at the core scale, the residual oil saturations for the duplicate cores differed by about 10%.

For both of the Whitestone UZ cores, recovery at breakthrough was less than 50% of the final recovery; more than 2 to 5 PV of additional brine was needed to reach final recovery. Even though the Whitestone UZ rock is heterogeneous at the core scale and early breakthrough is consistent with heterogeneous pore structure, the residual saturations for the two tested plugs were in close agreement.

The final recovery for Edwards (GC) was much lower than for Whitestone UZ. Much of the pore space in the Edwards (GC) is in the form of small vugs, of about 200 μ diameter, formed by selective dissolution of fossils; the vugs are connected by narrow throats of about 5 μ radius (from Hg injection). The high pore-body-to-throat ratio results in a large portion of oil being trapped inside the vugs as isolated blobs. Whitestone UZ showed greater response to increase in capillary number than Edwards (GC) even though the Edwards (GC) had much higher residual oil saturation. For the Edwards (GC), increase in capillary number by a factor of 8 only decreased the residual oil saturation by about 2% OOIP whereas for Whitestone UZ, residual saturation was reduced by 3.2% OOIP with increase in capillary number by a factor of 4.

High PV Waterfloods of MXW Cores

Initial water saturation is an important factor in controlling wetting states of cores that contain crude oil, because the presence and distribution of connate water governs how much of the rock surface is exposed to adsorption. (Salathiel, 1973) Mixed-wet cores become increasingly less water-wet with decrease in initial water saturation (Xie and Morrow, 2001). In establishing initial water saturation values, several considerations arise. For tests designed to reproduce reservoir conditions, there is no doubt that the reservoir connate water saturation should be targeted. For comparison between rock types with extreme differences in pore structure, as in the present work, besides the technical difficulties and arbitrary nature of the choice, there is no pressing case for setting the same initial water saturation for all rocks. The main requirements are that the level of connate water saturation should be as uniform as possible and that the mobility of the water phase is extremely low. The initial water saturation for each particular rock type (see Table 4.2) represents a compromise between these considerations and technical convenience.

Waterflood oil recovery results for MXW Edwards (GC) and Whitestone UZ samples are presented in Fig. 4.4. The Edwards (GC) samples showed difference in residual saturation of over 10% OOIP. The sample that gave lower residual saturation, 1EGC24A, was aged at an initial water saturation of 16.8% versus 19.8% for the companion sample. Another possible contributing factor was that after the adopted standard of 10 days aging at 75°C, the sample was stored for one month at ambient temperature simply because of test scheduling. However, for both Edwards (GC) limestone cores, the dependency of waterflood recovery on flooding rate was only slight. As waterflood rates increased from 0.6 ft/day to 49.4 ft/day, the total additional oil recovery was less than 2.7% OOIP. Furthermore, most of this increase was achieved at rates of less than 1.5 ft/day.

For the MXW Whitestone UZ cores, oil recovery behavior was comparable for two cores that differed in permeability by almost a factor of 2 (see Fig. 4.4). The dependency of oil recovery on flood rate was significantly higher over a wide range of capillary number. For 3WUZ04A, MXW residual oil was reduced from 42 to 36 % OOIP with increase in capillary number from 1.8×10^{-7} to 1.4×10^{-6} .

Comparison of VSWW and MXW results for Edwards (GC) and Whitestone UZ are presented in Figs. 4.5a and 4.5b respectively. For both Edwards (GC) and Whitestone UZ MXW cores, residual oil saturation at any tested capillary number was always lower than for VSWW cores. However, the decrease in residual oil for MXW was far greater for Edwards (GC) than for Whitestone UZ (Fig. 4.5). Tie and Morrow showed that MXW cores prepared by methods comparable to that of the present work had Amott wettability indices falling between 0.3 to 1. (Tie and Morrow, 2005) This range is classified as water-wet. (Cuiec, 1987 and 1991) Thus, reduction of water-wetness within the water-wet range can greatly increase oil recovery. The large reduction in oil trapping for Edwards (GC) with wetting change from VSWW to MXW is ascribed to the reduction of snap-off and associated increased recovery from vugs.

2PV Waterfloods

Unlike production from VSWW rock, mixed-wet rocks often feature continuous production of oil with continued injection of water. (Salathiel, 1973) Thus, there may not be a readily defined ultimate residual oil and the time required to reach reasonably definitive residual oil saturations at low injection rates can be excessive. It has also been found that oil recovery often does not reach a constant value with respect to time by spontaneous imbibition. For purposes of comparison and practical reasons, from examination of the character of a large body of data, a cut off dimensionless time of 10^5 was adopted for operational definition of oil recovery by spontaneous imbibition. (Tie *et al.*, 2003; Tie and Morrow, 2005) Beyond this value, very long times are required for significant further production.

Similarly, the times and pore volumes required to attain stable residual oil saturations as for the data shown in Fig 4.4, even as operationally defined, are excessive. Further measurements of the effect of flood rate on oil recovery were based on injection of 2PV of brine, starting at the residual oil saturation achieved by spontaneous imbibition. Considerations that went into this choice were that the imbibition data provide

characterization of wettability, 2PV injection well exceeds typical field injection volumes, and the amount of oil recovery given by 2PV injection usually far exceeds that recovered after say a further 20 PV. The adopted compromise of injecting 2PV at each injection rate probably captures the essential features of the effect of rate on oil recovery at low flooding rates.

This approach was applied to Edwards (GC), Whitestone UZ (cores 3WUZ01A and B and 3WUZ02A were selected for closeness in permeability and porosity, see Table 4.2), and to the very high porosity and permeability Gambier reef boundstone. Results for the three distinctly different wetting states, MXW, MXW-F, and MXW-DF, are presented in Figs. 4.6a, b, and c, respectively. For all three rock types, after 2PV injection, the lowest residual oil saturation was always given by MXW-F. Clearly, oil recovery shows a wide range of dependency on flood rate for at all three wettability states. For MXW wettability (crude oil is the probe oil), all of the rock types showed distinct sensitivity to flooding rate. The slopes of recovery versus $\log N_c$ were comparable with Whitestone UZ giving the lowest residuals (Fig. 4.6a). For MXW-F (mineral oil as the probe oil), the Gambier boundstone showed by far the highest sensitivity to flood rate with residual oil at high rate approaching the relatively low values of residual oil exhibited by Edwards (GC) and Whitestone UZ (Fig 4.6b). For MXW-DF (crude oil directly displaced by the mineral oil (probe oil)), sensitivity to rate was significant for Whitestone UZ and Gambier but only minor for Edwards (GC) (Fig. 4.6c). Residual saturations were lowest for Whitestone UZ and, as for Gambier, showed consistent significant decrease with increase in flood rate.

Comparison for each rock of the three induced wettability states is presented in Fig. 4.7. Overall, the Edwards (GC) core showed the least dependency on capillary number; the greatest reduction in residual oil (8.9%OOIP) was obtained for MXW wetting when the capillary number was increased by a factor of 16 (Fig. 4.7a). Residual oil decreased at all levels of capillary number in the sequence VSWW, MXW, MXW-F, and then increased for MXW-DF. This behavior is qualitatively consistent with recovery being optimum at some intermediate wetting state, probably close to neutral, as observed for sandstone. (Jadhunandan and Morrow, 1995) Residual saturation for MXW-F cores was about half of the average measured for VSWW cores.

Whitestone UZ results exhibited the same sequence as Edwards (GC) of decreasing residual oil for the MXW, MXW-DF, and MXW-F floods. However, the overall reduction in residual oil for Whitestone UZ was distinctly higher than for Edwards (GC) (cf. Figs. 4.7a and 4.7b).

Gambier limestone exhibited the greatest change in residual oil with rate for all three wetting states. The difference between the two extreme wettability states, MXW and MXW-DF, was relatively minor. The lowest residual saturations and the highest sensitivity to rate were observed for the MXW-F cores. However, although the residual saturations for MXW-F were much lower than for MXW-DF, the Amott indices for were both very close to zero.

For MXW-DF wetting, the two grainstones gave distinctly higher residual saturation in waterflood experiments compared to the MXW wetting state. Comparison of combined recovery from spontaneous imbibition and waterflooding for four distinctly different wetting states are plotted against Amott-Harvey indices in Fig. 4.8. (Tie and Morrow, 2005) Division of VSWW, MXW, MXW-F, and MXW-DF for all of the data are indicated. As reported previously for sandstones (Jadhunandan and Morrow, 1995), optimum recovery was obtained at weakly water-wet to neutral-wet wettability (Tie and Morrow, 2005). For these examples the optimum was given by MXW-F for all three rock types.

Sensitivity of Residual Oil to Flood Rate

Fig. 4.9a shows the reduction in residual for the high PV waterfloods at each capillary number. The results given by 2 PV sequential waterflooding (after spontaneous imbibition) are shown in Fig. 4.9b. It can be clearly seen that for all of the tested wetting states, with both high PV and 2PV waterfloods, all of the three tested rock types showed some degree of dependency of final oil recovery on waterflood rate, even though the capillary number was still well below the critical capillary number for mobilization of residual oil in sandstones. Overall, Edwards (GC) limestone was the least rate sensitive and Gambier the most.

From examination of the mercury injection data and the derived pore size distributions, Edwards GC clearly has the narrowest pore size distribution of the three limestones. Lake showed a schematic diagram of the effect of pore size distribution on the capillary desaturation curve and pointed out that decrease of non-wetting phase residual saturation occurred over a wider range for rocks with a wide pore size distribution. (Lake, 1984) For the three limestones investigated in the present work, sensitivity of residual oil saturation to flow rate at very low capillary numbers has been observed for four distinct wetting states (VSWW, MXW, MXW-F, and MXW-DF). Two of the limestones (Whitestone UZ and Gambier) consistently showed more sensitivity than the other (Edwards (GC)) for all four wetting states at the core scale. It is concluded that different degrees of heterogeneity of pore structure together with related change in sweep efficiency is the underlying cause of such rate sensitivity.

Photographs of the prepared pore casts for the three tested limestones are presented in Fig. 4.10. Pores in the Edwards (GC) are almost all moldic pores that resulted from diagenetic dissolution processes (Fig. 4.10a). Interconnections between different pores are poor and the aspect ratio of this rock, from pore throat size, given by mercury injection pressure, and body size, given by thin section or pore cast, is very high (50 to 60). During preparation of the pore cast, individual pores were easily separated from each other confirming weak interconnections at throats. Once the oil snaps off or is bypassed by the injected brine under very strongly water wet conditions, high capillary numbers (beyond the tested range, $>4 \times 10^{-6}$) are probably needed for remobilization of the residual oil. This is consistent with the lack of observed sensitivity of residual oil to increase in flood rate.

It can be seen from Fig. 4.10b that the Whitestone UZ contains mainly somewhat spherical moldic pores that resulted from dissolution of fossils and some irregularly shaped interparticle pores formed by partial cementation. Individual pores were harder to separate from each other than Edwards (GC) indicating better interconnection between pores even though the sizes of the throats are small (Fig. 4.10b). Whitestone UZ also had lower aspect ratio than Edwards (GC). Experimentally observed moderate rate sensitivity of this rock possibly resulted from the wide variety of pore shapes and sizes.

In the Gambier limestone, the main pores formed by an individual fossil are parallel chambers that have one large and two small dimensions (see Fig. 4.10c). Clusters of these long skinny fossil chamber pores are oriented according to fossil fragment orientation. Interconnections of these fossil chamber pores within a single fossil depend on much smaller sized intraparticle pores within the skeletal structure of the fossil. Access for drainage of fossil chambers can occur independently of other chambers in the same fossil (S. Seth, 2005, personal communication). Interparticle pores (between the fossils) are of various sizes and are more irregularly shaped. This wide variety of pore sizes and types are believed to be the cause of the relatively huge sensitivity of oil recovery to flow rate measured for this rock.

Table 4.1 Selected properties of sandstone and limestone cores

Cores	BET, m ² /g	CEC, meq/100g
Edwards (GC)	0.20	0.026
Whitestone UZ	0.90	0.029
Gambier	0.77	0.065

Table 4.2 Core properties

Core	L	D	k	ϕ	S_{wi}	σ	Wetting state
	cm	cm	mD		%	mN/m	
Edwards (GC) (EGC)							
1EGC25A	3.74	6.41	11.3	0.206	0	50	VSWW
1EGC25B	3.74	6.45	10.9	0.212	0	50	VSWW
1EGC23B	3.74	6.24	11.4	0.213	19.8	29.7	MXW
1EGC24A	3.73	6.39	13.7	0.210	16.1	29.7	MXW
1EGC05A	3.80	6.26	11.6	0.208	16.0	29.7	MXW
1EGC06B	3.80	6.37	10.4	0.212	16.3	29.7	MXW-F
1EGC06A	3.80	6.38	12.9	0.210	16.3	29.7	MXW-DF
Whitestone UZ (WUZ)							
3WUZ07A	3.75	6.36	3.9	0.233	0	50	VSWW
3WUZ07B	3.75	6.45	1.4	0.191	0	50	VSWW
3WUZ04A	3.75	6.25	7.5	0.256	24.3	29.7	MXW
3WUZ04B	3.75	6.41	13.7	0.264	25.8	29.7	MXW
3WUZ02A	3.74	6.30	7.4	0.257	28.8	29.7	MXW
3WUZ01A	3.75	6.05	6.9	0.252	28.7	29.7	MXW-F
3WUZ01B	3.75	6.36	7.6	0.242	28.8	29.7	MXW-DF
Gambier (G)							
G08	5.10	3.77	4350	0.542	28.8	27.2	MXW
G10	4.98	3.77	4140	0.548	28.2	49.5	MXW-F
G11	5.09	3.78	4160	0.526	28.4	49.5	MXW-DF

Table 4.3 Selected properties of crude oil samples

Crude oil	Density, g/ml	μ_o at 22°C, cp	n-C7 asphalt., wt%	Acid #, mg KOH/g oil	Base #, mg KOH/g oil
Cottonwood	0.8874	24.1	2.3	0.56	1.83

Table 4.4 Synthetic brine composition

Brine	NaCl (g/L)	KCl (g/L)	CaCl ₂ (g/L)	MgCl ₂ (g/L)	NaN ₃ (g/L)	pH	TDS (mg/L)
Sea water	28	0.935	2.379	5.365	0.1	6.6	36779
5% CaCl ₂	-	-	50	-	0.1	6.9	50100

Table 4.5 Composition of epoxy resin and hardener for pore casts

Epoxy	Weight
ERL 4221	20.2 g
DER 736	8.4 g
NSA	52.3 g
Hardener	
DMAE	0.6 g

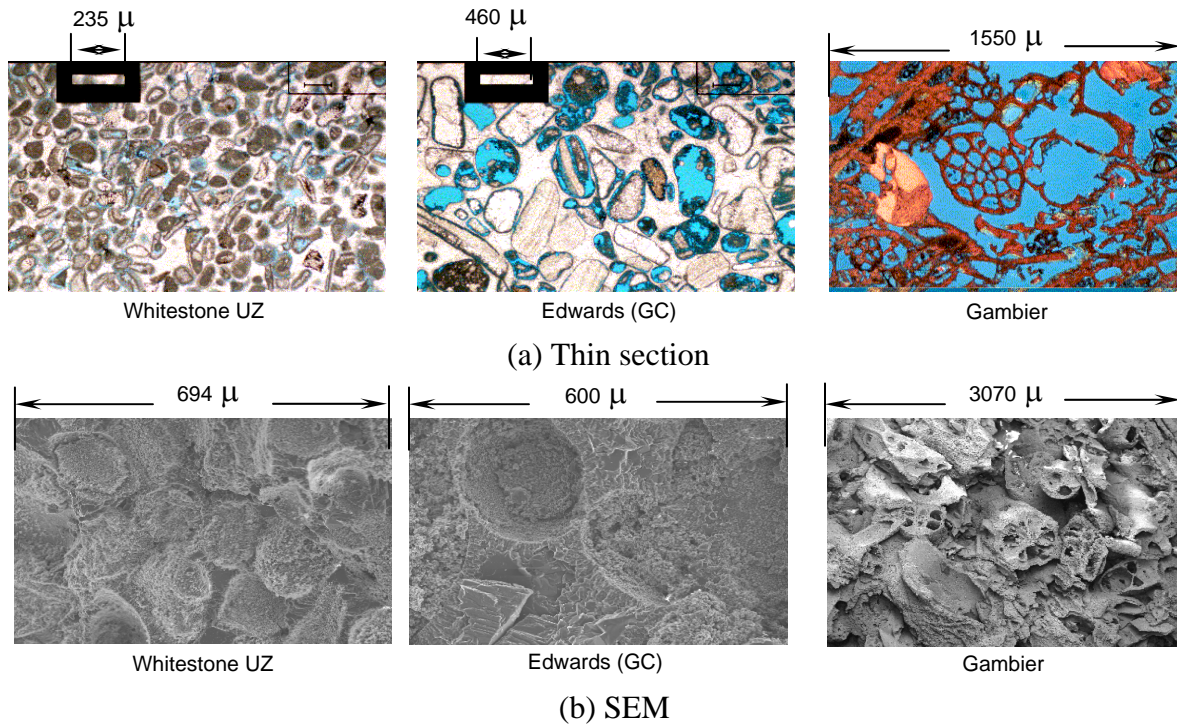
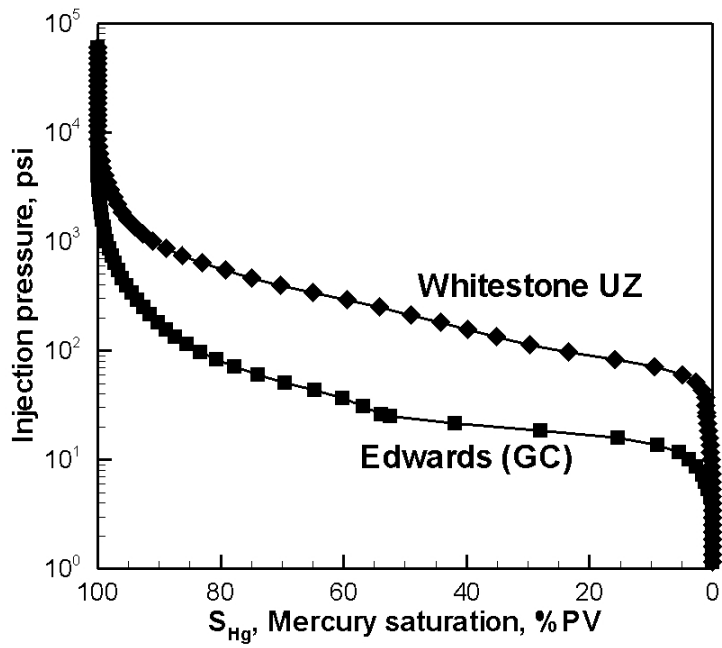
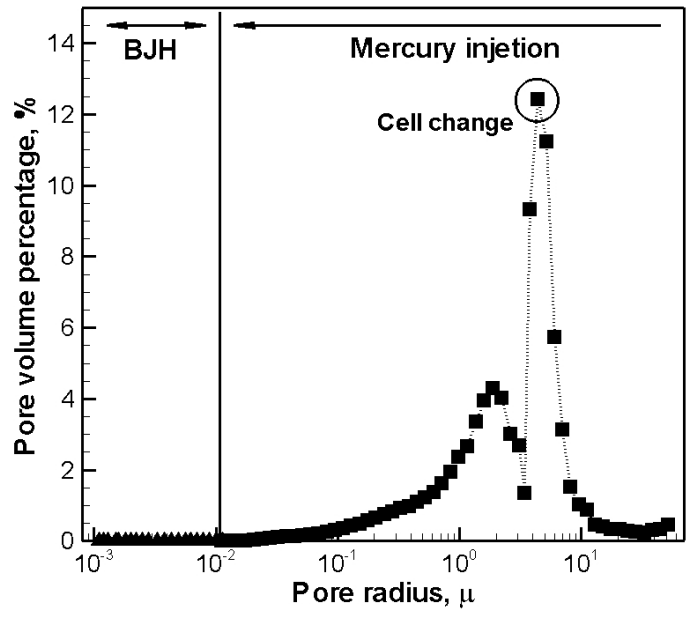
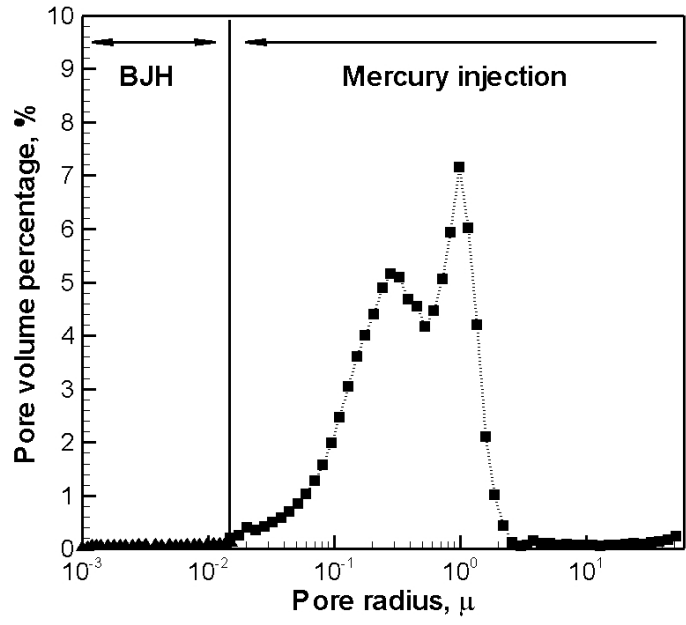


Fig. 4.1 Thin section and SEM





(b) Edwards (GC) pore structure



(c) Whitestone UZ pore structure

Fig. 4.2 Mercury injection and pore structure

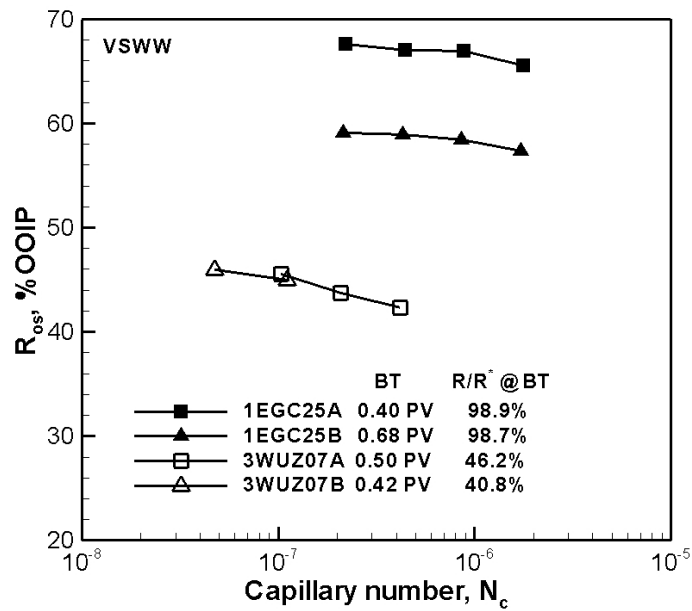


Fig. 4.3 Waterflood residual saturation for VSWW Edwards (GC) and Whitestone UZ rocks (BT: Breakthrough, R: oil recovery, R* : oil recovery at lowest flooding rate)

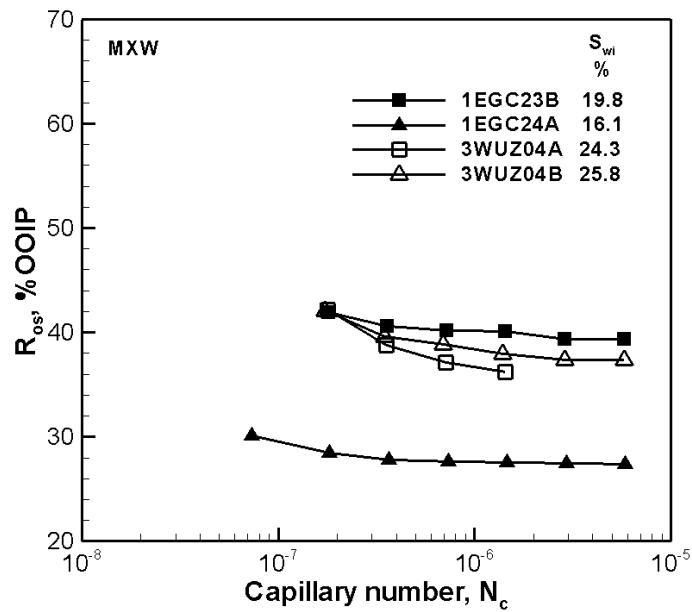
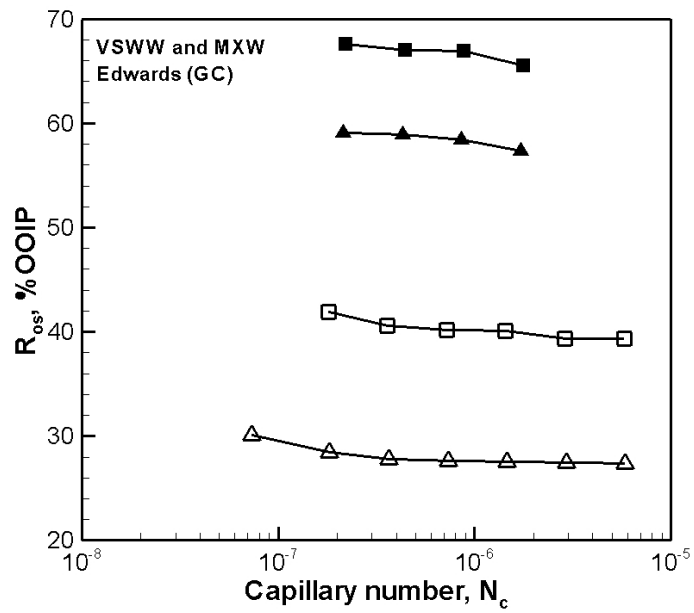
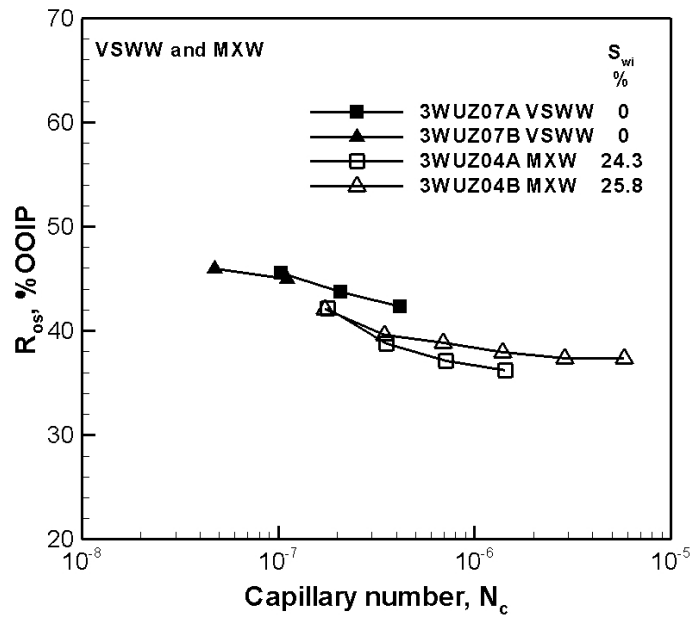


Fig. 4.4 Waterflood residual saturation for MXW Edwards (GC) and Whitestone UZ rocks

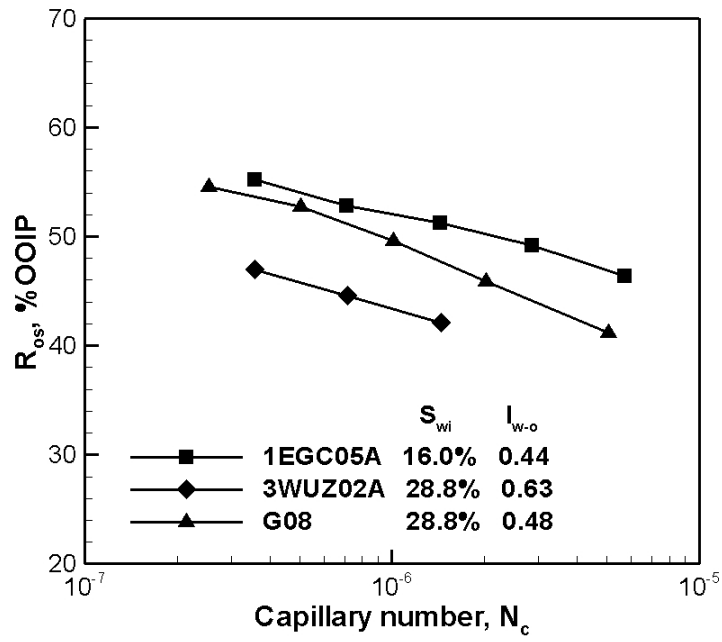


(a) Edwards (GC)

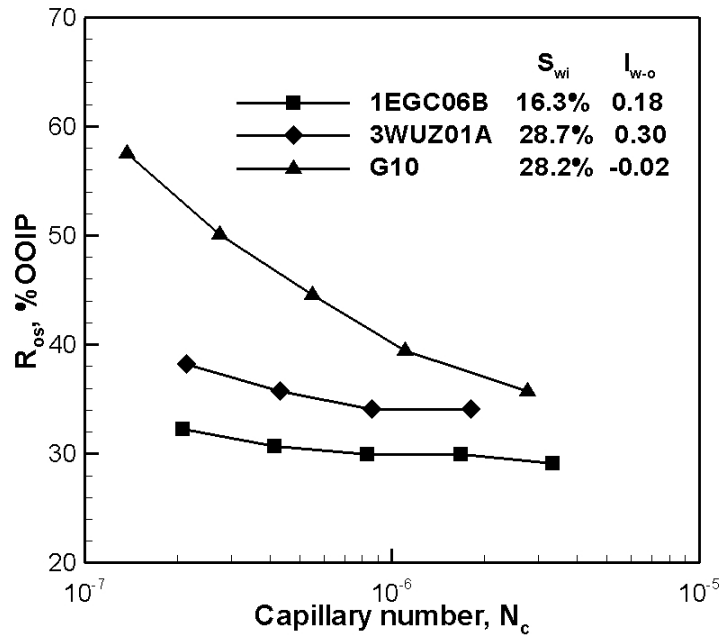


(b) Whitestone UZ

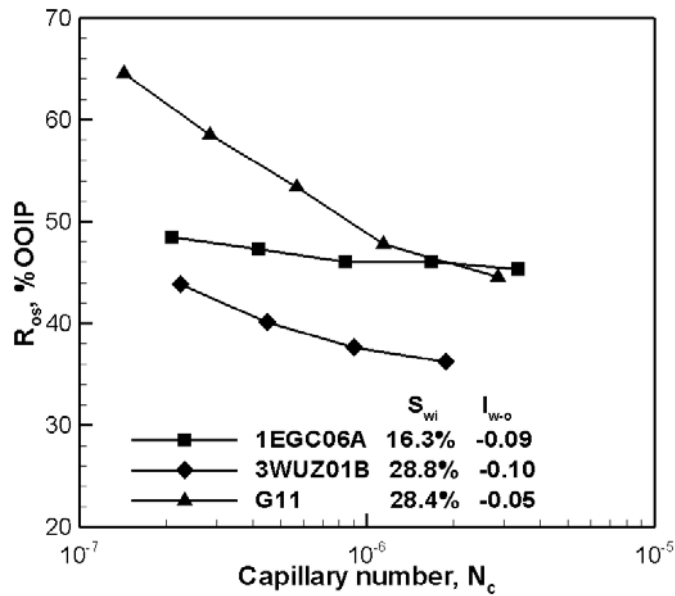
Fig. 4.5 Waterflood residual saturation for Edwards (GC) and Whitestone UZ rocks with VSWW and MXW wetting states.



(a) MXW

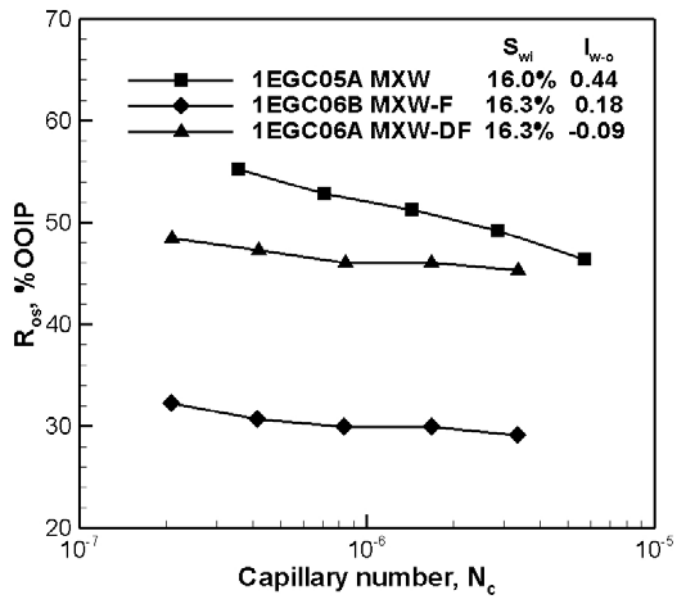


(b) MXW-F

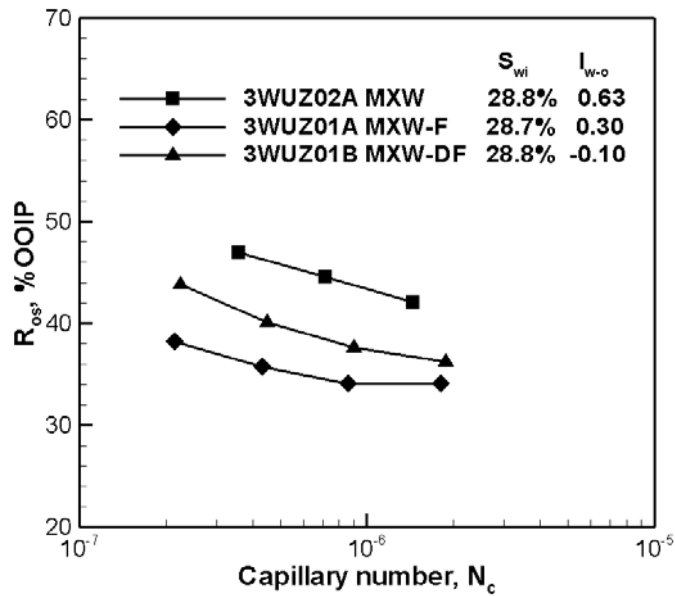


(c) MXW-DF

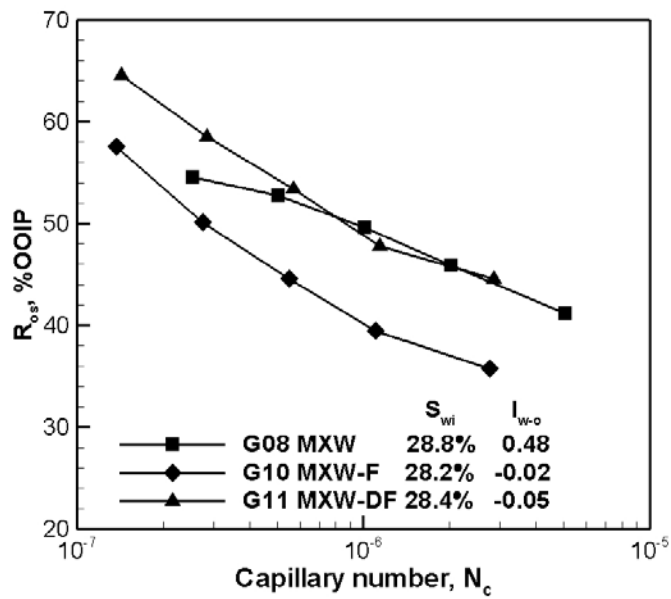
Fig. 4.6 Waterflood residual saturation for Edwards (GC), Whitestone UZ, and Gambier limestone for various rates (2PV at each rate): (a) MXW, (b) MXW-F, and (c) MXW-DF wetting states.



(a) Edwards (GC)



(b) Whitestone UZ



(c) Gambier

Fig. 4.7 Waterflood residual saturation vs capillary number (2PV injected at each rate) for MXW, MXW-F, and MXW-DF wetting states: (a) Edwards (GC), (b) Whitestone UZ, and (c) Gambier limestones.

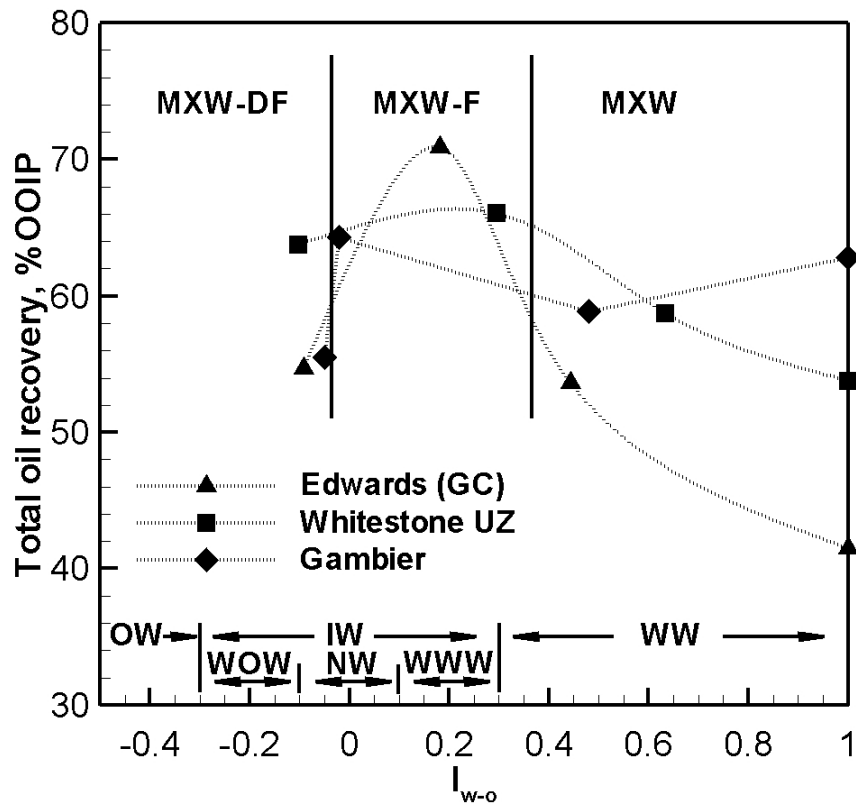
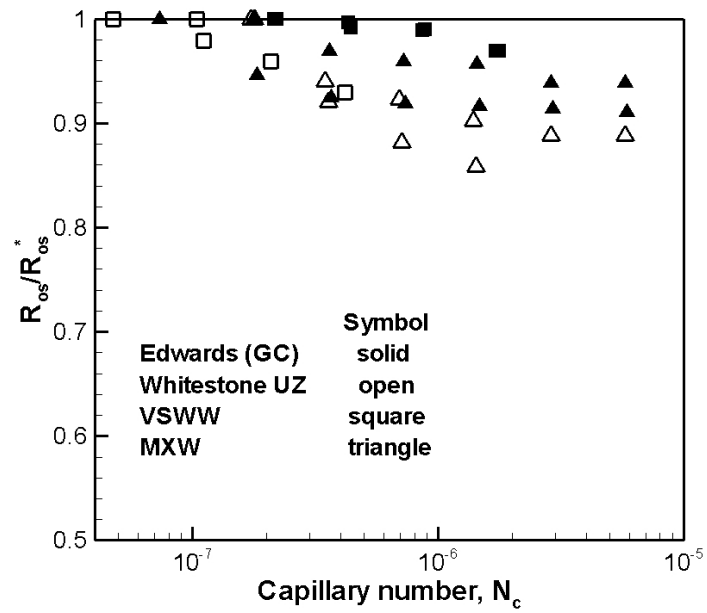
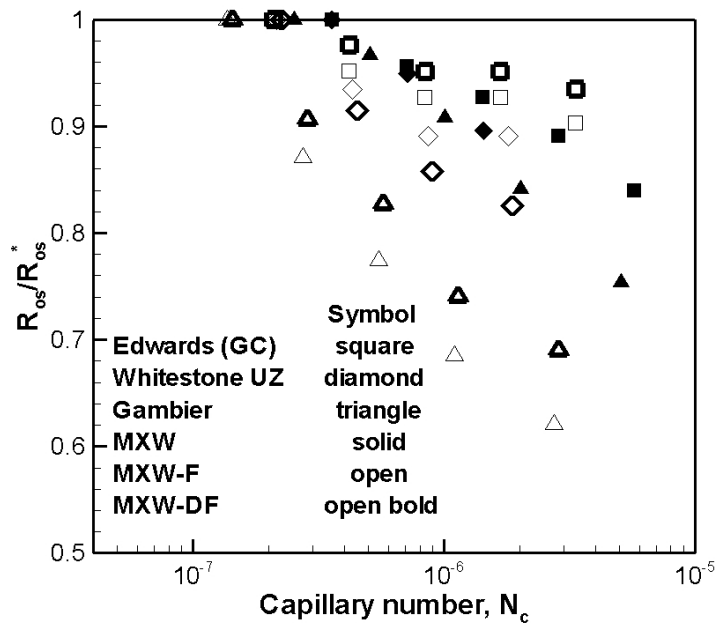


Fig. 4.8 Comparison of total oil recovery (spontaneous imbibition plus forced displacement) versus Amott-Harvey wettability index (Tie and Morrow, 2005). (WW – water-wet, WWW – weakly water-wet, NW – neutral wet, WOW – weakly oil-wet, IW – intermediate wetting, OW – oil-wet (Cuiec, 1991))

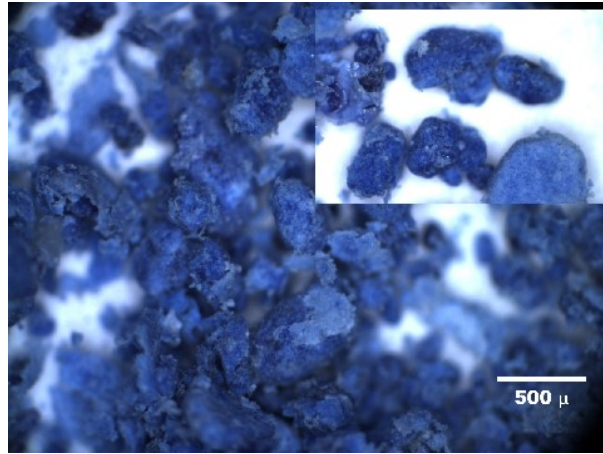


(a) High volume waterfloods

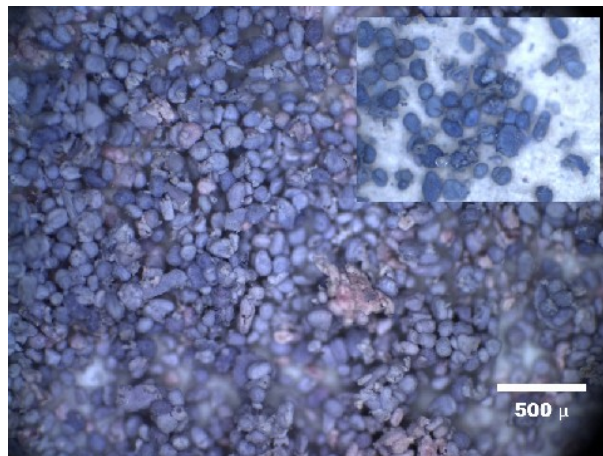


(b) 2PV waterflood

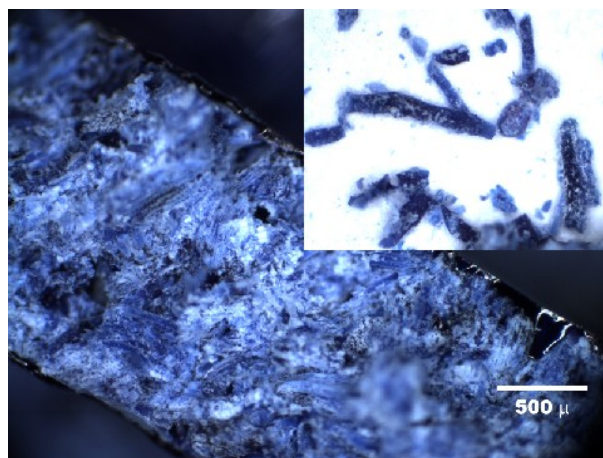
Fig. 4.9 Relative reduction in residual oil saturation with increase in capillary number for all tested samples at all the tested wetting states. (R_{os}^* - residual oil at lowest flood rate)



(a) Edwards (GC)



(b) Whitestone UZ



(c) Gambier

Fig. 4.10 Pore casts for the three tested limestones

Conclusions

Task1

1. Roughness and/or steps on calcite surfaces contribute to uncertainty in contact angle measurements. Freshly cleaved Iceland spar was used for most experiments. Polishing calcite did not improve repeatability of measurements. Results on polished marble were comparable to those on freshly cleaved Iceland spar.
2. AFM showed steps on calcite surfaces. Adsorbed material was more stable under water than in air. In most cases, increased imaging forces could be used to clear a portion of the surface so that an estimate of thickness of the adsorbed layer could be made. Longer aging times produced thicker adsorbed layers.
3. Three different methods of surface preparation have been investigated. Resulting, in each case, in contact angle measurements. The surface preparations and results can be summarized as follows:
 - a. **Adhesion of a drop of crude oil on a clean, brine-covered calcite surface.** There are clear differences between different crude oils, but much smaller, less consistent differences due to brine composition. In general, oils with higher asphaltene contents have lower contact angles in adhesion type tests. Selection of smooth areas of surface can avoid surface roughness problems. Tests are limited in duration (2-15 min); pinning of the contact line is often a problem.
 - b. **Adhesion of drops of crude oil after calcite has been aged in oil, excess oil removed from the surface by floatation with brine.** Aging time was limited to at most one day because the floatation technique was unable to remove crude oil reproducibly from surfaces aged for longer periods of time. It was also necessary to coat the bottom of the aging cell with water to facilitate subsequent floatation, which had the effect of minimizing the distinction between dry and pre-wetted surfaces. Drops may tend to be retained on the rough surfaces, causing problems with reproducibility of this method.
 - c. **Adsorption of crude oil components on dry and pre-wetted calcite.** The effects of aging time were similar to those reported previously for mica surfaces. Contact angles on pre-wetted surfaces increased with increased aging time; those on initially dry surfaces were constant with aging time. Differences were greatest between different oils; less distinction could be seen between different pre-treatment brines. The effects of aging temperature and removal of the asphaltene fraction were tested using this approach.
4. Correlations with selected oil properties were found for all three methods of surface preparation. Larger molecules correlated with lower contact angles, perhaps because they have slower interaction kinetics. Acid and base numbers are involved in the correlations, as were previous results on mica.

Task 2

5. Six selected limestone rocks were characterized. Based on permeability measurements on 1½"×2½" core plugs cut from 12"×12"×6" blocks, three of them, Gambier, Edwards (GC), and Lueders, are homogeneous and the other three, Whitestone UZ, Whitestone LZ, and Fort Riley, are heterogeneous. Five of the tested limestones are grainstones based on Dunham's carbonate rock classification (1962). Gambier is a boundstone. For all the selected limestones, despite the distinct differences in pore structure for the six tested limestones, all pore walls are covered by calcite crystals of various sizes.
6. Edwards (GC), Gambier, and Whitestone UZ, two of which are homogeneous and one heterogeneous, showed distinct differences in porosity, permeability, and pore structure and sizes. The three rocks were selected for study of wettability alteration and oil recovery.
7. Five of the six selected outcrop limestones were very strongly water wet as supplied. Three of them, Edwards (GC), Gambier, and Whitestone UZ, showed scaled spontaneous imbibition behavior close to that of a wide variety of rocks and synthetic porous media.
8. The wetting alteration ability of the three tested crude oils was directly related to acid number, but showed an inverse trend with respect to asphaltene content.
9. Initial water saturation and aging time are important for wetting alteration of limestone cores and need special attention with respect to comparative studies of wettability and oil recovery behavior.
10. Stable wetting with respect to cyclic spontaneous imbibition tests was achieved for MXW-F Gambier limestone cores when high viscosity mineral oil ($\mu_o > 90$ cP) was used as the probe oil.
11. Ma *et al.*'s (1997) scaling group did not provide satisfactory correlation for variation of mineral oil viscosity for MXW-F limestone cores.

Task 3

12. The dimensionless time proposed by Ma *et al.* (1997) gave satisfactory results on VSWW Edwards (GC) limestone cores for correlation of probe oil viscosity, core length, but not for boundary conditions.
13. For VSWW Edwards (GC) cores, higher probe oil viscosity resulted in higher final oil recovery when all the other conditions were the same. For fixed diameter, longer cores showed better experimental reproducibility.

14. Linear imbibition was the dominant oil recovery mechanism for the Edwards (GC) limestone cores. For the tested Berea sandstone with a length to radius ratio of 3 the radial imbibition appeared to be the dominant oil recovery mechanism. Further testing for the effects of directional heterogeneity is needed.
15. For the two ends open boundary condition (TEO), setting a no-flow boundary in the middle of the core resulted in close correlation with data for one end open for both Edwards (GC) limestone and Berea 90 sandstone. Results for all faces open (AFO) did not always fall on this correlation.
16. A crude oil with intermediate asphaltene content (Cottonwood, 2.3%) but high acid and base number relative to asphaltene content caused larger reduction in imbibition rate than a high asphaltene content oil (Minnelusa, 9.0%) for both sandstone and limestone cores.
17. Modification of both Cottonwood and Minnelusa crude oil composition through addition of increasing fraction of alkane resulted in systematic decrease in rate of oil recovery from limestone by spontaneous imbibition. For sandstones, the overall changes, if any, in wetting with addition of alkanes were small except for the Minnelusa oil above the onset of precipitation.
18. For any combination of Cottonwood oil and Minnelusa oil and sandstone or limestone, direct displacement of crude oil by mineral oil resulted in almost complete suppression of spontaneous imbibition. The behavior is ascribed to generation of strongly oil-wet surfaces by surface precipitation resulting from destabilization of asphaltenes.
19. Comparison of crude oil recovery at MXW conditions with recovery of mineral oil for MXW-F conditions generated by the corresponding parent crude oil, showed the latter to be distinctly less water-wet for any of the tested combinations.
20. Three selected outcrop limestones, Edwards (GC), Whitestone UZ, and Gambier, were very strongly water-wet (unlike fresh or cleaned carbonate cores from oil reservoirs) and provide a definitive initial condition for study of wettability change caused by adsorption from crude oil.
21. Wettability alteration from VSWW conditions by commonly used core preparation techniques resulted in a consistent pattern of wettability change indicated by three distinct spontaneous imbibition curves. Rate and recovery was highest with crude oil as the probe oil (MXW), less if crude oil was displaced by a solvent followed by mineral (probe) oil (MXW-F), and least for direct displacement of crude oil by mineral (probe) oil (MXW-DF).
22. Total oil recovery from grainstones given by a combination of spontaneous imbibition followed waterflooding was highest at slightly water-wet conditions.

Task 4

23. Three distinct types of outcrop limestones, two grainstones (one relatively heterogeneous as indicated by several petrophysical properties including a wider pore size distribution and the other referred to as homogeneous) and a very high permeability/porosity boundstone were all VSWW, a wettability condition that has not yet been achieved by cleaning reservoir carbonates.
24. For all three limestones, some degree of sensitivity of residual oil saturation to rate, at capillary numbers much lower than measured for mobilization of oil from VSWW sandstones, was observed for VSWW conditions and for three types of mixed wettability induced by adsorption from a moderately asphaltic crude oil.
25. For the two grainstones, the homogeneous grainstone exhibited far greater reduction in residual oil with change to mixed wettability but much less sensitivity to rate than the heterogeneous grainstone at all wettability states. The boundstone was the most rate sensitive.
26. For the two grainstones, oil recovery was highest for mixed wettability states on the water wet side of neutral wettability.
27. Inspection of pore casts showed that differences in rate sensitivity of the three tested limestones could be attributed to the pore structure.

References

- Al-Maamari, R.S.H. and J.S. Buckley, "Asphaltene Precipitation and Alteration of Wetting: the Potential for Wettability Changes during Production," SPE 59292, 2000 SPE/DOE IOR Symposium, Tulsa, OK, U.S.A., 2-5 Apr.; SPE REE (Aug. 2003) 210-14.
- Amott, E., "Observations Relating to the Wettability of Porous Rock," *Trans.*, AIME (1959) **216**, 156-62.
- Anderson, W.G., "Wettability Literature Survey – Part 1: Rock/Oil/Brine Interactions and the Effects of Core Handling on Wettability," *JPT* (Oct. 1986a) 38, **11**, 1125-44.
- Aronofsky, J.S., L. Masse, and S.G. Natanson, "A Model for the Mechanism of Oil Recovery from the Porous Matrix due to Water Invasion in Fractured Reservoirs," *Trans. AIME*, (1958) **213**, 17-9.
- ASTM D664-01: "Standard Test Method for Acid Number of Petroleum Products by Potentiometric Titration," *ASTM* (2001).
- ASTM D2896-98: "Standard Test Method for Base Number of Petroleum Products by Potentiometric Perchloric Acid Titration," *ASTM* (1998).
- Baldwin, B. A., and E.A. Spinler, "In-Situ Saturation Development during Spontaneous Imbibition," *JPSE*, (Jul. 2002), **35**, No.1, 23-32.
- Barrett, E. P., L.G. Joyner, and P.P. Halenda, "The Determination of Pore Volume and Area Distribution in Porous Substance. I. Computations for Nitrogen Isotherms," *J. Am. Chem. Soc.* (1951), **73**, 373-80.
- Bassiouni, Z., *Theory, Measurement, and Interpretation of Well Logs*, SPE textbook series vol. 4, SPE, Richardson, TX, 1994.
- Basu, S. and Sharma, M.M.: "Characterization of Mixed Wettability States in Oil Reservoirs by Atomic Force Microscopy," SPE 35572, 1996.
- Block, A. and B.B. Simms, "Desorption and Exchange of Adsorbed Octadecylamine and Stearic Acid on Steel and Glass," *J. Colloid Interface Sci.*, (1967) **25**, 514-18.
- Boneau, D. F. and R.L. Clampitt, "A Surfactant System for the Oil-Wet Sandstone of the North Burbank Unit," *JPT* (May, 1977), 501-6.
- Brantley, S. L. and N.P. Mellot, "Surface Area and Porosity of Primary Silicate Minerals," *American Mineralogist* (2000), **85**, 1767-83.
- Brunauer, S., P.H. Emmett, and E. Teller, "Adsorption of Gases in Multimolecular Layers," *J. Am. Chem. Soc.* (1938) **60**, 309-19.
- Buckley, J.S., Y. Liu, and S. Monsterleet, "Mechanisms of Wetting Alteration by Crude Oils," *SPEJ* (Mar. 1998) **3**, 54-61.
- Buckley, J.S. and Fan, T.: "Crude oil/Brine Interfacial Tension," SCA 2005 P017.
- Buckley, J.S. and Wang, J.X.: "Crude Oil and Asphaltene Characterization for Prediction of Wetting Alteration," *J. Pet. Sci. Eng.* (2002) **33**, 195-202.

- Chatzis, I., M.S. Kuntamukkula, and N.R. Morrow, "Effects of Capillary Number on the Microstructure of Residual Oil in Strongly Water-Wet Sandstones," *SPE RE* (Aug. 1988), **3**, 902-12.
- Chatzis, I., N.R. Morrow, and H.T. Lim, "Magnitude and Detailed Structure of Residual Oil Saturation," *SPEJ* (Mar.-Apr. 1983), **23**, 311-26.
- Chilingar, G. V. and T.F. Yen, "Some Notes on Wettability and Relative Permeability of Carbonate Reservoir Rocks, II," *Energy Sources* (1983) **7**, No. 1, 67-75.
- Choquette P. W. and L.C. Pray, "Geological Nomenclature and Classification of Porosity in Sedimentary Carbonates," *AAPG Bull.* (1970), **54**, 2, 207-50.
- Choquette, P. W. and N.P. James, "*Diagenesis 12: Diagenesis in Limestones-3. The Deep Burial Environment*," *Geoscience Canada* (1987), **14**, 3-35.
- Churcher, P. L., P.R. French, J.C. Shaw, and L.L. Schramm, "Rock Properties of Berea Sandstone, Baker Dolomite, and Indiana Limestone," SPE 21044, presented at the SPE International Symposium on Oilfield Chemistry, Anaheim, CA, U.S.A., Feb. 20-22, 1991.
- Cram, P. J., "Wettability Studies with Non-Hydrocarbon Constituents of Crude Oil," Petroleum Recovery Research Inst., research report RR-17 (Dec. 1972).
- Cuiec, L.E., "Restoration of the Natural State of Core Samples," SPE 5634, the SPE Annual Technical Conference and Exhibition, Dallas, TX, Sept. 28-Oct. 2, 1975.
- Cuiec, L. E., "Rock/Crude-Oil Interactions and Wettability: An Attempt to Understand Their Interrelation," SPE 13211 presented at the 1984 SPE Annual Technical Conference and Exhibition, Houston, TX, U.S.A., Sept. 16-19.
- Cuiec, L. E., "Wettability and Oil Recoveries," *North Sea Oil and Gas Reservoirs*, © The Norwegian Institute of Technology, Ed. J. Keppe *et al.*, Graham and Trotman Ltd., UK, (1987), 193-207.
- Cuiec, L. E., "Evaluation of Reservoir Wettability and Its Effect on Oil Recovery", *Interfacial Phenomena in Petroleum Recovery*, Ed. N.R. Morrow, Marcel Dekker, Inc., New York, (1991), 319-75.
- Cuiec, L. E., D. Longeron, and J. Pacsirszky, "On the Necessity of Respecting Reservoir Conditions in Laboratory Displacement Studies," SPE 7785, Middle East Tech. Conf., Manama, Bahrain, Mar. 25-29, 1979.
- Denekas, M. O., C.C. Mattax, and G.T. Davis, "Effects of Crude Oil Components on Rock Wettability," *Trans.*, AIME (1959) **216**, 330-3.
- deZabala, E. F. and J. Kamath, "Laboratory Evaluation of Waterflood Behavior of Vugular carbonates," SPE 30780, presented at the 1995 SPE Annual Technical Conference and Exhibition, Dallas, TX, U.S.A., Oct. 22-25.
- Dubey, S.T. and Doe, P.H.: "Base Number and Wetting Properties of Crude Oils," *SPERE* (Aug. 1993) **8**, 195-200.

- Dunham, R. J., "Classification of Carbonate Rocks According to Depositional Texture," Ed. W.E. Ham *Classification of Carbonate Rocks. Memoir 1*, AAPG, 1962, 108-21.
- Fan, T. and Buckley, J.S.: "Rapid and Accurate SARA Analysis of Medium Gravity Crude Oils," *Energy and Fuels* (2002) **16**, 1571-1575.
- Fischer, H., and N.R. Morrow, "Scaling of Oil Recovery by Spontaneous Imbibition for Wide Variation in Aqueous Phase Viscosity with Glycerol as the Viscosifying Agent", paper presented at the 8th International Symposium on Reservoir Wettability, May 16-18th, 2004, Houston, TX., JPSE in press.
- Fischer, H., and N.R. Morrow, "Spontaneous Imbibition with Matched Liquid Viscosities", paper SPE 96812, the 2005 SPE Annual Technical Conference and Exhibition, Dallas, TX, U.S.A., 9-12 Oct., 2005.
- Fischer, H., N.R. Morrow, and G. Mason, "Application of Water Desorption/Adsorption Isotherms Data to Characterization of Micro- and Meso-porosity in Sandstone and Carbonate Rocks," presented at the 7th International Symposium on the Characterization of Porous Solids, COPS VII, Aix-en-Provence, France, May 26-28, 2005.
- Foster, W. R., "A Low-Tension Waterflooding Process," *JPT* (Feb. 1973), **25**, 205-10.
- Gant, P. L. and W.G. Anderson, "Core Cleaning for Restoration of Native Wettability," *SPEFE* (Mar. 1988), 131-8.
- Gaudin, A.M., Witt, A.F., and Decker, T.G.:" Contact angle Hysteresis - Principles and Application of Measurement Methods," *Trans.,AIME* (March 1963) 107-112.
- Goddard, W.A. and Tang, Y.: "Screening Methods for Selection of Surfactant Formulations for IOR from Fractured Carbonate Reservoirs," Topical report, DOE Contract DE-FC26-04NT15521.
- Gomari, K.A.R. and Hamouda, A.A.: "Effect of Fatty Acids, Water Composition and pH on the Wettability Alteration of Calcite Surface," *Journal of Petroleum Science and Engineering*, (2006) **50**, Issue 2, 140-150.
- Graue, A., E. Tonheim, and B. Baldwin, "Control and Alteration of Wettability in Low-Permeability Chalk", Proceedings of the 3rd International Symposium on Evaluation of Reservoir Wettability and Its Effect on Oil Recovery, Ed. N.R. Morrow, Laramie, WY, U.S.A., Sept. 21-23, 1994.
- Graue, A., B.G. Viksund, and B.A. Baldwin, "Reproducible Wettability Alteration of Low-Permeable Outcrop Chalk," 1998 SPE/DOE improved Oil Recovery Symposium, Tulsa OK, Apr. 19-22; *SPEREE*, (Apr. 1999) **2**, 2, 134-40.
- Halley, R. B., "Burial Diagenesis of Carbonate Rocks," R.B. Halley and R.K., Mathews, *Carbonate Depositional Environments, Modern and Ancient, Part 6: Diagenesis 2. Quart. Colo. School of Mines* (1987), 82 (1), 1-15.
- Hirasaki, G.J., "Wettability: Fundamentals and Surface Forces," *SPEFE*, (1991) **6**, 217-226.

- Hirasaki, G. J., J.A. Rohan, and S.T. Dubey, "Wettability Evaluation during Restored-States Core Analysis," SPE 20506 presented at the 1990 SPE Annual Technical Conference and Exhibition, New Orleans, LA, U.S.A., Sept. 23-28.
- Hirasaki, G. J., and D.L. Zhang, "Surface Chemistry of Oil Recovery from Fractured, Oil-Wet, Carbonate Formation," *SPEJ* (Jun. 2004), 151-62.
- Jadhunandan, P., and N.R. Morrow, "Effect of Wettability on Waterflood Recovery for Crude Oil/Brine/Rock Systems," *SPE* (Feb. 1995), **10** (1), 40-6.
- James, N. P., and P.W. Choquette, "Diagenesis 9. Limestones - The Meteoric Diagenetic Environment," *Geoscience Canada* (1984), **11**, 161-94.
- Kamath, J., B. Xu, S.H. Lee, and Y.C. Yortsos, "Pore Network Modeling of Laboratory Experiments on Heterogeneous Carbonates," SPE 36681, presented at the 1996 SPE Annual Technical Conference and Exhibition, Denver, CO, U.S.A., Oct. 6-9.
- Kamath, J., R.F. Meyer, and F.M. Nakagawa, "Understanding Waterflood Residual Oil Saturation of Four Carbonate Rock Types," SPE 71505, presented at the 2001 SPE Annual Technical Conference and Exhibition, New Orleans, Sept. 30 – Oct. 3, 2001.
- Kazemi, H., J.R. Gilman, and A.M. El-Sharkaway, "Analytical and Numerical Solution of Oil Recovery from Fractured Reservoirs Using Empirical Transfer Functions," *SPE* (May 1992), **7**, 219-27.
- Lake, L. W., "A Technical Survey of Micellar Polymer Flooding," presented at Enhanced Oil Recovery, a Symposium for the Independent Producer, Southern Methodist University, Dallas, TX, Nov. 1984.
- Larson, R. G., H.T. Davis, and L.E. Scriven, "Displacement of Residual Nonwetting Phase from Porous Media," *Chem. Eng. Sci.* (1981) **36** (1), 75-85.
- Legens, C., Palermo, T., Toulhoat, H., Fafet, A., and Koutsoukos, P.: "Carbonate Rock Wettability Changes Induced by Organic Compound Adsorption," *Journal of Petroleum Science and Engineering*, (1998)20, Issues 3-4, 277-282.
- Li, Y., Morrow, N. R. and Ruth, D.: "Similarity solution for linear countercurrent spontaneous imbibition" *JPSE* (2003) **39** (3-4), 309-26.
- Li, Y., D. Ruth, G. Mason, and N.R. Morrow, "Pressure Acting in Counter-Current Spontaneous Imbibition," proceedings of the International Symposium on Reservoir Wettability and its Impact on Oil Recovery, Austin, Texas, USA, July 2004; *JPSE* in press
- Lichaa, P.M., Alpustun, H., Abdul, J.H., Nofal, W.A., and Fuseni, A.B.: "Wettability Evaluation of a Carbonate Reservoir Rock," Proc. Advances in Core Evaluation, III Reservoir Management, European Core Analysis Symposium, p.327 (1993).
- Liu, L. and Buckley, J.S.: "Alteration of Wetting of Mica Surfaces," *Journal of Petroleum Science and Engineering*, (1999)**24**, 75-83.
- Liu, Y. and Buckley, J.S.: "Evolution of Wetting Alteration by Adsorption from Crude Oil," *SPE FE*, (1997) **12** (1), 5-11.

- Lord, D.L., and Buckley, J.S.: "An AFM Study of Morphological Features that Affect Wetting at Crude Oil-Water-Mica Interfaces," *Colloids and Surfaces A* (2002) **206**, 531-546.
- Lowe, A. C., M.C. Phillips, and A.C. Riddiford, "On the Wetting of Carbonate Surfaces by Oil and Water," *J. Cdn. Pet. Tech.* (Apr.-Jun. 1973), **12** (44), 33-40.
- Lucia, F. J., "Petrophysical Parameters Estimated from Visual Description of Carbonate Rocks: A Field Classification of Carbonate Pore Space," *JPT* (Mar. 1983), 626-37.
- Lucia, F. J., "Rock Fabric/Petrophysical Classification of Carbonate Pore Space for Reservoir Characterization," *AAPG Bull.* (1995), **79** (9), 1275-300.
- Ma, S., N.R. Morrow, and X. Zhang, "Generalized Scaling of Spontaneous Imbibition Data for Strongly Water-Wet Systems," *JPSE*, (1997), **18**, 165-78.
- Madsen, L. and Lind, I.: "Adsorption of Carboxylic Acids on Reservoir Minerals from Organic and Aqueous Phase," *SPERE*, (1998)1, Issue 1, 47-51.
- Mattax, C. C., and J.R. Kyte, "Imbibition Oil Recovery from Fractured, Water-Drive Reservoir," *SPEJ* (Jun. 1962), 177-84.
- McCaffery, F. G. and N. Mungan, "Contact Angle and Interfacial Tension Studies of Some Hydrocarbon-Water-Solid Systems," *J. Cdn. Pet. Tech.* (Jul.-Sept. 1970) **9** (3), 185-96.
- McCaffery, F. G., P.M. Sigmund, and N.C. Wardlaw, "A Treatise on Hydrocarbon Recovery from Carbonate Reservoirs," Research Report RR-36, Petroleum Recovery Institute, Edmonton, Alberta, Canada, Dec. 1978.
- Moore, C. H., *Carbonate Diagenesis and Porosity, Developments in Sedimentology* 46, *Elsevier Publ. Co., 1989.*
- Moore, T. F. and R.L. Slobod, "The Effect of Viscosity and Capillarity on the Displacement of Oil by Water," *Prod. Monthly* (Aug. 1956), **20**, 20-30.
- Morrow, N. R., "Measurement and Correlation of Conditions for Entrapment and Mobilization of Residual Oil," Final Report to the U.S. Dept. of Energy, DOE/BC/10310-34, (Oct., 1984).
- Morrow, N. R., H.T. Lim, and J.S. Ward, "Effect of Crude-Oil-Induced Wettability Changes on Oil Recovery," *SPE FE* (Apr. 1986), **1**, 89-103.
- Morrow, N. R., I. Chatzis, and J.J. Taber, "Entrapment and Mobilization of Residual Oil in Bead Packs," *SPE RE* (Aug. 1988), **3**, 927-34.
- Morse, J.W.: "The surface chemistry of calcium carbonate minerals in natural waters: an overview," *Marine Chemistry*, (1986)20, 91-112.
- Moulin, P. and Roques, H.: "Zeta Potential Measurement of Calcium Carbonate," *Journal of Colloid and Interface Science*, (2003)261, 115-126.
- Ojeda, E., F. Preston, and J.C. Calhoun, "Correlations of Oil Residuals Following Surfactant Floods," *Prod. Monthly* (Dec. 1953), **18**, 20.

- Paez, J., P. Reed, and J.D. Calhoun Jr., "Relationships between Oil Recovery, Interfacial Tension and Pressure Gradient in Water-Wet Porous Media," *Bull., Penn State U., Mineral Ind. Exp. Sta.* (1954) No. 64, 115.
- Pierre, A., Lamarche, J.M, Mercier R., and Foissy, A.: "Calcium as Potential Determining Ion in Aqueous Calcite Suspensions," *Journal of Dispersion Science and Technology*, (1990) 11, No.6, 611-635.
- Salathiel, R. A., "Oil Recovery by Surface Film Drainage in Mixed-Wettability Rocks," *JPT* (Oct. 1973) 1216-24; *Trans., AIME*, **255**.
- Scholle, P. A. and D.S. Ulmer-Scholle, *A Color Guide to the Petrography of Carbonate Rocks: Grains, Textures, Porosity, Diagenesis*, AAPG Memoir 77, Tulsa, OK, 2003.
- Seethepalli, A., Adibhatla, B., and Mohanty, K. K.: "Wettability Alteration during Surfactant Flooding of Carbonate Reservoir," paper SPE 89423 presented at the SPE/DOE Fourteenth Symposium on Improved Oil Recovery held in Tulsa, Oklahoma, U.S.A., 17-21 April 2004.
- Shedid, A.S. and Mamdouh, T.G.: "Factors Affecting Contact Angle Measurement of Reservoir Rocks," *Journal of Petroleum Science and Engineering*, (2004)**44**, 193-203.
- Somasundaran, P., "Interfacial Chemistry of Particulate Flotation," *Advances in Interfacial Phenomena of Particulate/Solution/Gas Systems; Applications to Flotation Research*, P. Somasundaran and R.B. Grieves (Eds.), AIChE Symposium Series (1975) **71**, No. 150, 1-15.
- Somasundaran, P. and Agar, G.E.: "The Zero Point of Charge of Calcite," *Journal of Colloid Interface Science*. (1967) 24, 433-440.
- Standnes, D. C. and T. Austad, "Wettability Alteration in Chalk 1. Preparation of Core Material and Oil Properties," *JPSE (2000a)* **28**, 111-21.
- Standnes, D.C. and Austad, T.: "Wettability Alteration in Chalk 2. Mechanism for Wettability Alteration from Oil-Wet to Water-Wet using Surfactants," *Journal of Petroleum Science and Engineering*, (Nov. 2000b) 28, No.2, 123-143.
- Stegemeier, G. L., "Mechanisms of Entrapment and Mobilization of Oil in Porous Media," *Improved Oil Recovery by Surfactant and Polymer Flooding*, Ed. D.O. Shah and R.S. Schechter, Academic Press Inc., New York City (1977), 55-91.
- Strand, S., Høgnesen, E.J., and Austad, T.: "Wettability Alteration of Carbonates – Effects of Potential Determining Ions (Ca^{2+} and SO_4^{2-}) and Temperature," *Colloids and Surfaces A – Physicochemical and Engineering Aspects*, (Mar. 2006) 275, No.11-3, 1-10.
- Stumm, W. and J.J. Morgan, *Aquatic Chemistry*, J. Wiley and Sons, New York, 1970.
- Taber, J. J., "Dynamic and Static Forces Required To Remove a Discontinuous Oil Phase from Porous Media Containing Both Oil and Water," *SPEJ* (Mar. 1969), **9** (1), 3-12.

- Taber, J. J., "Research on Enhanced Oil Recovery, Past, Present, and Future," *Surface Phenomena in Enhanced Oil Recovery*, Ed. D. O. Shah, Plenum Press, New York City (1981), 13-52.
- Thomas, M.M., Clouse, J.A., and Longo, J.M.: "Adsorption of Organic Compounds on Carbonate Minerals 1. Model Compounds and Their Influence on Mineral Wettability," *Chemical Geology*, (1993a)109, 201-213.
- Thomas, M.M., Clouse, J.A., and Longo, J.M.: "Adsorption of organic compounds on carbonate minerals 3. Influence on dissolution rates," *Chemical Geology*, (1993b) 109, 227-237.
- Thompson, D.W. and Pownall, P.G.: "Surface Electrical Properties of Calcite," *Journal of Colloid and Interface Science*, (Aug. 1989)131, No 1, 74.
- Tie, H., and N.R. Morrow, "Oil Recovery by Spontaneous Imbibition Before and After Wettability Alteration of Three Carbonate Rocks by a Moderately Asphaltic Crude Oil," presented at the 2005 International Symposium of Society of Core Analysis, Toronto, Canada, Aug. 21-25.
- Tie, H., Z. Tong, and N.R. Morrow, "The Effect of Different Crude Oil/Brine/Rock Combinations on Wettability through Spontaneous Imbibition," presented at the 2003 International Symposium of Society of Core Analysis, Pau, France, Sept. 22-25.
- Tong, Z., X. Xie, and N.R. Morrow, "Scaling of Viscosity Ratio for Oil Recovery by Imbibition From Mixed-Wet Rocks," *Petrophysics*, (Jul.-Aug. 2002) **43** (4), 338-46.
- Tong, Z., N.R. Morrow, and X. Xie, "Spontaneous Imbibition of Mixed-Wettability States in Sandstones Induced by Adsorption from Crude Oil," *JPSE*, (2003a) **39**, (3 - 4), 351-61.
- Tong, Z., X. Xie, and N.R. Morrow, "Crude Oil Composition and the Stability of Mixed Wettability in Sandstones," *Petrophysics*, (Jul.-Aug. 2003b) **44** (4), 233-42.
- Treiber, L. E., D.L. Archer, and W.W. Owens., "A Laboratory Evaluation of the Wettability of Fifty Oil-Producing Reservoirs," *SPEJ*, (Dec. 1972), 531-40.
- Viksund, B. G., N.R. Morrow, S. Ma, W. Wang, and A. Graue, "Initial Water Saturation and Oil Recovery From Chalk and Sandstone by Spontaneous Imbibition," *Proceedings of the 1998 International Symposium of Society of Core Analysis*, the Hague, The Netherlands, Sept.
- Wagner, O. R. and R.O. Leach, "Effect of Interfacial Tension on Displacement Efficiency," *SPEJ* (Dec. 1966), 335-44.
- Wang, J.X.: "Predicting Asphaltene Flocculation in Crude oil," Ph.D. Thesis, NMIMT, Socorro, Apr. (2000).
- Xie, X., Morrow, N.R., and Buckley, J.S.: "Crude Oil/Brine Contact Angles on Quartz Glass," paper SCA-9712 presented at the 1997 SCA International Symposium, Calgary, 8-10 Sept.

- Xie, X., and N.R. Morrow, "Oil Recovery by Spontaneous Imbibition from Weakly Water-Wet Rocks," *Petrophysics*, (Jul.-Aug. 2001) **42** (4), 313-22.
- Xie, X., N.R. Morrow, and J.S. Buckley, "Contact Angle Hysteresis and the Stability of Wetting Changes Induced by Adsorption from Crude Oil," *JPSE* (2002), **33**, 147-59
- Xu, B., J. Kamath, Y.C. Yortsos, and S.H. Lee, "Use of Pore-Network Models to Simulate Laboratory Corefloods in a Heterogeneous Carbonate Sample," *SPEJ* (Sept. 1999), **4** (3), 179-86.
- Yang, L., Wang, J.X., Fan, T., and Buckley, J.S.: "Wetting Estimates from Crude Oil Chemical Properties," paper SCA 2003-01 presented at the 2003 SCA Symposium, Pau, 21-24 Sept.
- Zhang, P. and Austad, T.: "The Relative Effects of Acid Number and Temperature on Chalk Wettability," paper SPE 92999 presented at the 2005 SPE International Symposium on Oilfield Chemistry, Houston, Texas, February 2 – 4.
- Zhang, X., N.R. Morrow, and S. Ma, "Experimental Verification of a Modified Scaling Group for Spontaneous Imbibition," *SPE RE*, (Nov. 1996), **11** (4), 280-5.
- Zhou, X., N.R. Morrow, and S. Ma, "Interrelationship of Wettability, Initial Water Saturation, Aging Time and Oil Recovery by Spontaneous Imbibition and Waterflooding," *SPEJ* (Jun. 2000), **5** (2), 199-207.